

IN THE MATTER OF

The Resource Management Act 1991

AND

IN THE MATTER OF

applications for resource consents in relation to
Te Ahu a Turanga; Manawatū Tararua Highway
Project

BY

NEW ZEALAND TRANSPORT AGENCY
Applicant

TE AHU A TURANGA: TECHNICAL ASSESSMENT D
HYDROLOGICAL ASSESSMENT

Contents

INTRODUCTION	1
Qualifications and experience.....	1
Code of conduct	3
Purpose and scope of assessment.....	3
Context (relationship with other technical assessments).....	4
EXECUTIVE SUMMARY	5
Introduction	5
Design rainfalls.....	6
Climate change	6
Design events	7
Manawatū River Bridge (BR02).....	7
Central alignment.....	8
Mangamanaia Stream Bridge (BR07).....	9
Eastern Roundabout	11
Conclusion on Project effects	11
PROJECT DESCRIPTION.....	11
EXISTING ENVIRONMENT.....	12
Geomorphic setting	12
Fluvial setting	15
Project sub-catchments.....	18
Hydrological processes	22
Runoff generation	24
Runoff hydrograph.....	28
Streamflow generation	29
METHODOLOGY	31
Background.....	31
Design rainfalls.....	33
Flow regimes.....	37
Manawatū - Upper Gorge	38
Pohangina River	42
Manawatū River at Teachers' College	43
'Stream 7'	45
Mangamanaia Stream.....	47
Design flows for 'small' catchments	57
Allowance for climate change	59
Interaction of floods in the Manawatū and Pohangina Rivers	62
HYDRAULIC MODELLING	64
Manawatū River Bridge (BR02).....	65
Results	69
Scour	78
Conclusions on Manawatū River Bridge (BR02)	80
Mangamanaia Bridge (BR07)	81
Results	86
Conclusions on the Mangamanaia Stream Bridge (BR07)	96
Eastern Roundabout	96

Results	97
Conclusions on Eastern Roundabout.....	101
Existing backwater flooding	101
ASSESSMENT OF POTENTIAL EFFECTS.....	103
Manawatū River Bridge (BR02).....	104
Central alignment	105
Mangamanaia Stream Bridge (BR07).....	106
Eastern Roundabout	107
SUMMARY	108
APPENDICES.....	109

Glossary

Term	Definition
Accretion	The gradual enlargement of an area of land through the natural accumulation of sediment deposited by a river, lake or sea.
Active channel	A channel of a stream subject to change by prevailing discharges.
Aggradation	Accumulation of sediment on the channel bed or floodplain.
Annual exceedance probability (AEP)	The probability of a given flood event occurring in any year, usually expressed as a percentage.
Antecedent gorge	A drainage system which has maintained its general direction across an area of localised uplift.
Areal Reduction Factor	An adjustment factor applied to point estimates of rainfall to account for the effect of catchment area. The ARF effectively reduces the rainfall estimated from gauge data.
Artificial drains	Drains installed across the floodplain to support land use.
Average recurrence interval (ARI)	The average number of years that it is predicted between events of a given magnitude occurs. Also known as the return period.
Backwater effects	The effect which a dam, inflow, lake, coast or any obstruction has in raising the surface, and reducing the velocity of flow upstream.
Bankfull discharge	The flow that completely fills the channel and above which overbank flow will occur (i.e. the point at which the river is about to spill onto the floodplain). This is generally regarded to be the approximate 2.33-year ARI event.
Bar	The ridge-like accumulation of sand, gravel, or other alluvial material formed in the channel, along the banks, or at the mouth of a stream where a decrease in velocity induces deposition.
Baseflow	The flow in a channel derived from the slow drainage of soil water or groundwater. Maintains flow in a stream or river during periods between surface runoff events.
Bathymetry	The elevation and form of the bed of a river, lake or ocean.
Bedload	Coarse material that is transported along the bed of a river during floods. Excludes finer material that may be suspended within the water column. Moves at a rate significantly slower than the velocity of the water.
Bow-wave	A wave or system of waves caused by the interaction of the flow with the base of a structure.
Bluff	A high bank or bold headland, with a broad, precipitous, sometimes rounded cliff face overlooking a plain or body of water, especially on the outside of a stream meander.
Capillary forces	The forces that hold moisture within the pores of a soil or regolith. The strength of the force generally increases as the pores get smaller.
Constructed wetland	An artificial wetland constructed to treat wastewater, greywater or stormwater runoff.
Degradation	The wearing down or away and the general lowering of the land/channel surface by natural processes of weathering and erosion.
Delayed Flow	See baseflow.
Depression storage	These are small low points in the topography of the land which can store precipitation that would otherwise become runoff.
Direct channel precipitation	The first to arrive is direct channel precipitation, or rain that falls onto the river. While this is usually a very small proportion of the precipitation, it arrives very quickly and can increase

	significantly during longer storms, when the surface area of the stream, and any wetlands or ponds may increase markedly.
Direct runoff	Water which arrives rapidly after the onset of precipitation; also called storm runoff. Also see Storm flow and quickflow.
Drainage density	The length of potential drainage lines divided by catchment area. Areas with a high drainage density are generally associated with high flood peaks, variable flow regimes, and high sediment loads.
Dry weather flow	See baseflow.
DTM	Digital Terrain Model, often used interchangeably with DEM which is a Digital Elevation Model. A DTM is a digital representation of the landscape allowing 3D analyses.
Ephemeral streams	Generally, a small stream or upper reaches of a stream that flows only in direct response to precipitation.
Erosion	The process where rock and soil are removed, transported, and repositioned by the action of running water, ice, wind, waves, currents, and mass wasting.
Floodplain	A relatively flat alluvial landform created largely by the contemporary flow regime of the river. The floodplain is inundated by flows greater than bankfull discharge and therefore subject to the periodic deposition of sediment and debris.
Freshes	Higher flow events between baseflow (lower threshold) and bankfull flows (upper threshold).
Gravel bar	A free-forming depositional feature, in this case made-up of gravel. Also see bar.
HEC-HMS	Hydrologic Engineering Centre-Hydrologic Modelling System. HEC-HMS is designed to simulate hydrologic processes of watersheds. The software includes many traditional hydrologic analysis procedures such as event infiltration, unit hydrographs, and hydrologic routing.
HEC-RAS	Hydrologic Engineering Centre-River Analysis System. HEC-RAS allows the user to perform one-dimensional steady flow, one and two-dimensional unsteady flow calculations, sediment transport/mobile bed computations, and water temperature/water quality modelling.
Hortonian overland flow	Flow over the ground surface that occurs when rainfall intensity exceeds the infiltration capacity of the soil and any depression storage is full. Generally rare in forested terrain with a temperate climate.
Hydrograph	The changes in flow (either water level or volume) over time.
Hyetographs	The changes in rainfall intensity over the duration of an event.
Infiltration capacity	The maximum rate of infiltration that can be sustained once any soil storage is saturated. Varies as a function of soil type and hydraulic properties.
Interfluve	The boundary between adjacent catchments; theoretically the region of not lateral water flow.
Intermittent stream	A stream that ceases to flow for periods of the year but has a well-defined channel where the bed and banks can be distinguished.
Land cover database (LCDB)	A multi-temporal, thematic classification of New Zealand's land cover.
Loess	Fine grained sediment that has been deposited by the wind generally under glacial conditions when sea levels were lower.
Macropores	Large pores (>1mm) within a soil or regolith that allow water to flow through them under the influence of gravity. Can act as 'pipes'.

Manning's n	The roughness coefficient used in Manning's formula to calculate flow in open channels.
Orographic enhancement	The increase in rainfall caused by an increase in elevation. Generally, areas of higher elevation receive greater rainfall because air is forced to rise when encountering a mountain or hill.
Overbank flooding/flow	Occurs at flows above bankfull discharge when the channel can no longer contain the volume of runoff. Floodwater spills over the banks and starts to flow across the floodplain.
Overflow channel	A watercourse that is generally dry but conducts flood water that have overflowed the banks of a river. Generally, only flow during larger flood events.
Overland flow	Water that flows over the ground surface. May be caused either by the soil/regolith being saturated or when rainfall intensity exceeds the infiltration capacity. See also Hortonian overland flow and saturated overland flow.
Overland flow paths	The path taken by overland flow.
Paleochannels	Old, abandoned, and generally inactive channels found on a floodplain.
Perched water table	A local, unconfined aquifer at a higher elevation than the regional groundwater system. Generally, form during rainstorm events when there is a permeability discontinuity in the soil profile e.g. when a more permeable soil/regolith overlies relatively impermeable bedrock.
Perennial stream	A stream or reach of a stream that flows continuously throughout the year.
PMP (Probable Maximum Precipitation)	Theoretically the greatest depth of precipitation for a given duration that is meteorologically possible over an area at a particular time.
Quickflow	Runoff generated by rainfall that takes a rapid pathway to the stream channel. This is the runoff that generates the rising limb of a flood hydrograph. Also see Storm flow and Direct runoff.
Rational method	A simple empirical procedure for determining runoff from small catchments.
Regional flood estimation (RFE)	Method based on work carried out by McKerchar & Pearson (1989) for estimating the magnitude of design floods in ungauged catchments. The method is based on long-term flow records from throughout the country which are related in terms of their catchment area, and the relationship between catchment area and the mean annual flood.
Regolith	Unconsolidated material that overlies the bedrock. Includes any soil and weathered bedrock above the competent bedrock.
Representative Concentration Pathways	Representative pathways (scenarios) providing time-dependent projections of atmospheric greenhouse gas (GHG) concentrations, developed by the IPCC for the 5 th assessment report.
Runoff	Water flowing under the influence of gravity either across the ground surface or in open channels.
Runoff coefficients	The proportion of rainfall that becomes runoff. Depends on both the intensity of the rainfall and catchment characteristics.
Saturated overland flow	Overland flow that occurs because the soil is saturated and acting as if the surface is sealed.
SCS curve number	The SCS curve number method is a simple, widely used and efficient method for determining the approximate amount of runoff from a rainfall even in a particular area. The curve number is based on the area's hydrologic soil group, land use, land condition and hydrologic condition.

Sediment load	The material that is eroded and transported by a stream. Total load consists of dissolved load, suspended load, and bedload.
Sediment transport	The movement of sediment through a river system. See also bedload and suspended load.
Serviceability limit state (SLS)	The state beyond which a structure becomes unfit for its intended use through deformation, vibratory response, degradation or other operational inadequacy.
Soil moisture content	The water held in soil layers above the level at which groundwater occurs.
Streamflow	Comprises the movement of water under the influence of gravity in open channels of various sizes.
Storm runoff	Water which arrives rapidly after the onset of precipitation is termed storm runoff. Also see quickflow and direct runoff.
Subsurface flow	The flow of water beneath earth's surface as part of the water cycle.
Suspended load	Finer material that is transported within the water column and moves at approximately the speed of flow. Moves more often, faster and further than bedload.
Thalweg	The line of deepest flow and generally highest velocity within a river or stream.
Time of Concentration (ToC)	The time taken for water to travel from the catchment boundary to the catchment outlet i.e. the minimum duration of a rainstorm necessary so that all parts of the catchment are contributing to runoff.
Throughflow	Water that infiltrates the soil surface and then moves laterally through the regolith to the stream channel. Movement can occur either as unsaturated flow (particularly through macropores such as root channels or cracks within the soil) or as a saturated layer.
True right/left bank	The right/left bank of a river when looking downstream.
Type-hydrograph	The characteristic shape of hydrographs during large flood events. Used to model the runoff during design events by scaling the peak discharge.
Ultimate Limit State (ULS)	The state beyond which the strength or ductility capacity of the structure is exceeded, or when it cannot maintain equilibrium and becomes unstable.

INTRODUCTION

1. My full name is Dr John (Jack) Allen McConchie. I am currently employed as the Technical Principal (Hydrology & Geomorphology) by WSP. I have been engaged by the Transport Agency to provide expert technical support in the areas of hydrology and hydraulics in relation to the Te Ahu a Turanga; Manawatū Tararua Highway Project (the “**Project**”).

Qualifications and experience

2. I have the following qualifications and experience relevant to this assessment. I hold a Bachelor of Science degree with First Class Honours (from Victoria University of Wellington) and a PhD (also from Victoria University of Wellington).
3. I am a member of several professional and relevant associations including the:
 - (a) New Zealand Hydrological Society;
 - (b) American Geophysical Union;
 - (c) New Zealand Geographical Society;
 - (d) Australia-New Zealand Geomorphology Group; and
 - (e) Environment Institute of Australia and New Zealand.
4. I am an Environmental Commissioner (2011-present) and have been an Independent Professional Adviser to Waka Kotahi New Zealand Transport Agency (the “**Transport Agency**”) since 2011.
5. I was the New Zealand Geographical Society representative on the Joint New Zealand Earth Science Societies' Working Group on Geopreservation. This Working Group produced the first geopreservation inventory; published as the New Zealand Landform Inventory.
6. Prior to the start of 2008, I was an Associate Professor with the School of Earth Sciences at Victoria University of Wellington. I taught undergraduate courses in hydrology and geomorphology, and a postgraduate course in hydrology and water resources.
7. For more than 40 years my research and professional experience has focused on various aspects of hydrology and geomorphology, including: slope and surface water hydrology (including water quality), hydrometric analysis, groundwater dynamics, landscape evolution, and natural hazards. Within

these fields I have edited one book. I have written, or co-authored, 10 book chapters and over 50 internationally-refereed scientific publications; including several papers focused specifically on the flow regimes of rivers, erosion and sediment transport, and the potential effects of land use and climate change.

8. I prepared a range of technical reports and expert evidence to support a change to Taupō District Council's District Plan to recognise the extent and magnitude of the flood hazard. The flood hazard from Lake Taupō and its six major tributaries was assessed. I also provided technical evidence to the Environment Court in respect of Taupō District Council's Plan Change 20 to re-zone land use adjacent to the Kuratau River.
9. I have extensive experience responding to natural hazards; particularly flooding and slope instability. This includes: Cyclone Alison in the Ruahine Range (1975); the Hutt Valley rainstorm (1976); extensive landsliding in Wairarapa (1978); Cyclone Bola (1988); Waikato floods (1998) and the Manawatū floods (2004). Most recently I assisted with the North Canterbury Transport Infrastructure Recovery (NCTIR) and the Flaxbourne-Ward community response to the effects of the Kaikoura Earthquake (2016).
10. I worked on the *Climate Change Impacts for Flood Hazard*¹ in the Wellington region and led the Hutt^{2&3} and Waikanae^{4,5&6} River's *Erosion and Sediment Transport Studies*.
11. I have considerable experience working on major infrastructure projects including the Hamilton North Bypass; Western Link Road; Kopu Bridge; Tauranga Eastern Link Road; Basin Bridge; Transmission Gully; Peka Peka to Otaki Expressway; Petone-Grenada Link Road, and the realignment of SH3 at both Mt Messenger and Awakino Gorge. This experience gives me an in-depth understanding of climate, hydrology, flooding, and erosion and sediment transport processes as they interact with infrastructure.

¹ Edwards, S.; McConchie, J.A. & Maas, F. 2012. *Greater Wellington Region Climate Change Impacts Study Stage 1. Scoping Report*. Report prepared for Greater Wellington Regional Council. Project No. 351044.00.

² McConchie, J.A. 2010. Hutt River Sediment Transport - source to beach. Report prepared for Greater Wellington. Regional Council. Project No 350763.00. 28p.

³ McConchie, J.A.; Webby, M.G.; Morrow, F.J.; Maas, F.J.; & Cox, J.E. 2011. Quantification and validation of a sediment budget for the lower Hutt River, Wellington, New Zealand. *Journal of hydrology (NZ)* 50(1): 241-256.

⁴ McConchie, J.A.; Morrow, F.J. & Ward, H. 2012. Waikanae River Sediment Transport Study. Stage 1 - Scoping Study. Report prepared for Greater Wellington Regional Council. Project No. 353001.00. 96p.

⁵ McConchie, J.A.; Webby, M.G.; Ferguson, R. & Smith, H. 2012. Waikanae River Sediment Transport. Phase 2A – Sediment Budget. Report prepared for Greater Wellington Regional Council. Project No. 353043.00. 88p.

⁶ McConchie, J.A.; Webby, M.G.; Ferguson, R. & Smith, H. 2012. Waikanae River Sediment Transport. Phase 2B - Sediment Management Options. Report prepared for Greater Wellington Regional Council. Project No. 353043.00. 31p.

12. Finally, I provided technical evidence on behalf of the Transport Agency to *Hearing Stream 4 – Water quality and stormwater*, in regard to Wellington Regional Council's proposed Natural Resources Plan.

Code of conduct

13. I confirm that I have read the Code of Conduct for expert witnesses contained in the Environment Court Practice Note 2014. This assessment has been prepared in compliance with that Code, as if it were evidence being given in Environment Court proceedings. In particular, unless I state otherwise, this assessment is within my area of expertise and I have not omitted to consider material facts known to me that might alter or detract from the opinions I express.

Purpose and scope of assessment

14. This assessment:
 - (a) Describes the Project, with particular focus on those elements that are relevant to hydrological and hydraulic processes;
 - (b) Describes the hydrological features and processes of the existing environment within which the Project will be constructed;
 - (c) Describes the methodology that I have applied to assess the effects of the Project on those features and processes and vice versa, including:
 - (i) Assessing the "design rainfalls" in the Project area (that is, the rainfall that is assumed in the Project area to inform the design of stormwater management devices);
 - (ii) Assessing the flow regimes of the Manawatū River and its tributaries to understand the flood hazard in these catchments;
 - (iii) Considering the potential effects of climate change;
 - (iv) Assessing the potential interaction of floods from the Manawatū and Pohangina Rivers and the Mangamanaia Stream;
 - (d) Summarises the results of hydraulic modelling carried out in relation to the Project's two bridges and the Eastern Roundabout;
 - (e) Based on the above, provides an overall assessment of the effects of the Project from a hydrological and hydraulics perspective, including describing how the Project will interact with the various rivers and

streams within the Project area, and the constraints that the rainfall and runoff processes impose on the Project's design and construction; and

- (f) Provides my conclusion on the actual and potential effects of the Project from a hydrological and hydraulics perspective.

Context (relationship with other technical assessments)

15. The role of rainfall, runoff and water is integral to several of the Projects' workstreams including:
 - (a) Hydrology, including rainfall, runoff and streamflow generation, hydraulic design, and flood hazard mitigation (covered in this assessment);
 - (b) Water quality, including erosion and sediment entrainment, transport and deposition (covered by **Mr Keith Hamill's** technical assessment – **Technical Assessment C**);
 - (c) Ecology and in-stream services, including consideration of the effects of highway construction and operation (covered by **Ms Justine Quinn's** technical assessment – **Technical Assessment G**);
 - (d) Erosion and sediment control, to isolate, localise and mitigate any potential effects during construction (covered by **Mr Campbell Stewart's** technical assessment – **Technical Assessment A**); and
 - (e) Stormwater management, to control, mitigate and remediate any effects on runoff generation following completion of the Project (covered by **Mr David Hughes'** technical assessment – **Technical Assessment B**).
16. While these workstreams each involve a discrete suite of investigations, the hydrology and hydrological processes provide key interconnections and constraints. Managing these interactions is critical to ensure a consistent, robust, and integrated approach in the technical reports, and the assessment of environmental effects.
17. Many of the potential environmental effects of the Project relate to its interaction with the rainfall-runoff relationships which exist within the Project area. In particular, the hydrological processes which occur between precipitation within the catchment and runoff to the Manawatū River affect: stormwater and erosion and sediment control management and design; water quality and ecology; the hydraulic design of the bridges; and the flood hazard within the potentially affected catchments.

18. Consideration of the hydrology and rainfall-runoff relationships within the Project area therefore underpins and connects various other inputs and investigations relating to the Project and its potential effects.
19. The emphasis of this hydrological and hydraulic assessment is therefore to provide a robust environmental baseline against which the potential effects of the Project, both during and following construction, can be assessed.

EXECUTIVE SUMMARY

Introduction

20. Many of the potential environmental effects of the Project relate to its interaction with the rainfall-runoff relationships which exist within the Project area.
21. While there are good hydrometric data for the Manawatū River and its large tributary the Pohangina River, there are few rainfall and flow data for the Project area. Consequently, a comprehensive review of rainfall data from the wider area was used to derive robust design rainfalls for use in the design of stormwater treatment devices and erosion and sediment control management.
22. Despite the relatively large scale of the Project, its actual and potential effects on the hydrology of the area are minor. There are a number of reasons for this:
 - (a) The magnitudes of any potential effects are small relative to the size and existing dynamics of the receiving environment. For example, the entire area potentially impacted by the Project (not just the footprint) represents less than 0.3% of the Manawatū catchment (if the upper Mangamanaia sub-catchment is excluded).
 - (b) The area has already been subject to significant land cover and land use change. Any changes as a result of the Project will be extremely small relative to those that have occurred in the past.
 - (c) Any actual and potential effects of the Project will be strictly avoided, managed and mitigated through the proposed stormwater management and erosion and sediment control measures. This is different to many of the permitted land use activities which currently occur throughout the area.

Design rainfalls

23. All data from rain-gauges in the wider vicinity of the Project was analysed as part of a hydrometric review. The review included comparison of the empirical data with data derived from HIRDS v4 (High Intensity Rainfall Design developed by NIWA), and consideration of the spatial variability of rainfall and the most appropriate temporal rainfall distributions. This analysis ensures that the most representative rainfall data has been used in the design of the Project.
24. The results of this comprehensive rainfall analysis are provided in a technical report prepared for the Project which is attached as **Appendix D.1: Design Rainfalls – Analysis and Recommendations**.

Climate change

25. If predicted global climate change eventuates, it may cause more than just a rise in the world's temperature. Warmer temperatures mean that more water vapour will enter the atmosphere, while also increasing the air's ability to hold moisture.
26. How potential climate change has been incorporated into the design, and the assessment of actual and potential effects of the Project, is discussed in detail in **Appendix D.1**.
27. To ensure resilience of the Project, climate change over the 100-year life of the infrastructure (i.e. to 2120) was considered.
28. Consequently, when considering stormwater-related infrastructure, the design rainfalls were adjusted for the potential effects of climate change to 2120. The design rainfalls were applied as 'lumped totals', or 'temporally distributed totals' for any sub-catchment larger than approximately 100ha.
29. The design of bridge crossings over larger streams and rivers followed a different approach when considering the potential effects of climate change to that for the stormwater infrastructure. While various methods have been adopted nationally, case studies provide mixed results in terms of the increase in flood magnitude relative to the projected increase in rainfall when applying calibrated rainfall/runoff models. However, the assumption of a linear relationship between projected increases in rainfall and peak flood discharge is reasonable.
30. Therefore, in considering the effects of future climate change to 2120 on bridge design a simple factoring approach was adopted. This factoring approach

assumes that the projected increases in flood magnitude approximate the projected increases in rainfall (i.e. the increase in temperature times the percentage increase in rainfall per degree of warming).

Design events

31. Two sets of design events were used: one set for construction; and one set for the life of the Project.
32. During construction, a range of design events were adopted assuming the current climate.
33. However, in the design of Project infrastructure the various design events were adjusted for the potential effects of climate change over the expected life of the Project (i.e. 100-years). The primary design event was therefore the 1% AEP⁷ rainfall or flood event adjusted for the potential effects of climate change to 2120.

Manawatū River Bridge (BR02)

34. The crossing of the Manawatū River will involve placing one pier within the active channel (“**Pier 2**”) and a pier on each bank. A computational hydraulic model allowed the potential effects of the proposed bridge across the Manawatū River to be quantified during a range of design events, including the SLS⁸ and ULS⁹.
35. The model shows that any effects of Pier 2 are both extremely small and extremely localised. The ‘bow-wave’ upstream of Pier 2 results in a local water level increase of up to 1.4m in the design event; however, this effect dissipates rapidly upstream. Downstream, and in the lee of Pier 2, there is a slight reduction in water level; up to 0.25m.
36. Any significant change in velocity is restricted to three locations. The greatest change is an increase in velocity, up to 1.5m/s, within the centre of the active channel. There is also a small increase in velocity at the entrance to the ‘Parahaki bypass channel’ on the true left of the Manawatū River. The other change is a reduction in velocity in the lee of Pier 2.
37. The construction of the bridge and piers will have no adverse effects on Parahaki Island. There will be a slight reduction in water level, up to 0.25m,

⁷ Annual exceedance probability.

⁸ Serviceability limit state.

⁹ Ultimate limit state.

but this is generally restricted to the upstream gravel bar and the left bank of the Manawatū River. There is no change to the flow velocity across Parahaki Island because of the relatively shallow depth of flooding and good vegetation cover. There is, however, a decrease in velocity along the edge of the gravel bar at the upstream end of Parahaki Island. This could potentially lead to the deposition of sediment and accretion of this zone of the gravel bar.

38. The proposed scour protection will further mitigate any potential adverse effects to Parahaki Island; it is not required for the protection of the pier.

Central alignment

39. The majority of the highway over the Ruahine Range will cross only ephemeral streams and the upper reaches of small perennial streams. These catchments are already highly modified by vegetation clearance and current land use activities. Consequently, the natural runoff processes are already highly modified.
40. This area is characterised by thin regolith¹⁰, generally rolling slopes, and the presence of loess (i.e. silty) soils. This means that the existing infiltration and percolation rates are low and slow, and the moisture holding potential of the regolith is low. The regolith therefore has only a limited potential to moderate and attenuate the effect of rainfall on the slopes.
41. The removal of the natural forest cover from most of these slopes has further limited the natural ability of the regolith to moderate and attenuate the effect of rainfall.
42. As a result, runoff is diffuse, and the flow regimes of these small drainage lines is intimately connected to rainfall. There is only a very limited capacity for moisture in the regolith to sustain streamflow for any significant period once rainfall ceases. This is why the small perennial streams tend to terminate at a distance downstream of the interfluvium¹¹ i.e. there is insufficient moisture storage to sustain baseflow once rainfall ceases.
43. It is likely that the regolith can only moderate and attenuate the effects of relatively small rainstorm events (i.e. events smaller than 10% AEP even under the current climate). During larger and longer rainstorms, the regolith behaves

¹⁰ Regolith is the unconsolidated material that overlies bedrock.

¹¹ The interfluvium is the catchment boundary or the ridge that separates sub-catchments.

at though it is sealed and saturated (i.e. it behaves as though it is a paved surface).

44. The construction of the Project will affect only a small proportion of the various catchments intersected by the highway. Any effects will consequently also be very small relative to the catchment runoff processes. Any effects will also be extremely localised.
45. In addition, for the reasons discussed above, any potential effects of the Project will only occur during relatively small rainstorms when the regolith properties provide some limited moisture storage capacity. For events larger than 10% AEP, there will be no difference in the rainfall-runoff behaviour of the regolith under existing conditions and following completion of the Project.
46. These small effects during small rainstorms will be minimised, mitigated, moderated and attenuated by the proposed stormwater treatment design and management. The stormwater treatment devices will intercept and treat runoff from the Project during all rainstorms up to the 10% AEP event. During larger rainstorms, any runoff from the Project will behave in the same manner as the existing slopes. Furthermore, runoff from the Project will be a small proportion of the total runoff and hence any potential effects will be so small that they could not be identified and quantified.
47. In my opinion therefore, any effects of the Project along the 'central alignment' will be minor. It is unlikely that they could be measured. Furthermore, runoff from the Project will be treated, attenuated and moderated which does not happen under the current land use management regime.

Mangamanaia Stream Bridge (BR07)

48. Following construction of the bridge, there is a small increase in water depth immediately upstream and against the foundation on which the Project will be constructed during the design event (i.e. the 1% AEP flood adjusted for the potential effects of climate change to 2120). Much of the area where the depth of flooding increases by more than 0.5m is within a constructed wetland. There will also be a significant area, upstream and on the true right bank, where water depths will reduce by up to 0.5m as a result of the construction of the bridge.
49. Downstream of the bridge, and adjacent to the highway, there is also a significant area where the depth of flooding will decrease by more than 0.5m.

50. Overall, the construction of the bridge will cause water levels to increase by more than 0.5m over approximately 4600m² (or 0.46ha) and decrease by more than 0.5m over 5700m² (or 0.57ha). Therefore, the net effect is that water levels during the design event will decrease by more than 0.5m over approximately 0.11ha. This is a relatively small change, and all these changes are within the existing floodplain of Mangamanaia Stream.
51. There will also be small changes in the velocity of floodwaters. Again, the effects of the construction of the bridge are relatively small and limited to the immediate vicinity of the bridge. There is a slight increase, by up to 0.6m/s, through the bridge and in the overflow channel immediately upstream back into the main channel. There is also a slight increase in velocity immediately downstream of the bridge as a result of the improved hydraulic efficiency of the channel. The majority of the overbank flooding actually experiences a reduction in velocity; by up to 0.6m/s.
52. Overall, the construction of the bridge will cause velocities to increase by up to 0.6m/s over approximately 1900m² (or 0.19ha) and decrease by up to 0.6m/s over 5400m² (or 0.54ha). The net effect therefore is that the velocity of floodwaters will decrease by up to 0.6m/s over approximately 0.34ha.
53. The construction of the bridge over Mangamanaia Stream will therefore result in relatively minor changes to flooding and the flood hazard even during the 1% AEP design event; increased to allow for the potential effects of climate change to 2120. All these changes will be in close proximity to the bridge. Overall, the construction of the Mangamanaia Bridge is likely to result in a slight reduction in the existing flood hazard.
54. Inundation of the floodplain of the Mangamanaia Stream during the same 1% AEP design event following construction of the bridge lasts for about 5-hours. However, flooding exceeds 0.3m in this location for only 2.2-hours.
55. This area floods currently during a 1% AEP flood even under the current climate. Therefore, the effect of the bridge, in the area where any effects are likely to be greatest, will be to increase the duration of inundation by a maximum of 2-hours. Obviously, any effect during smaller events will be significantly less.
56. In my professional opinion, the effects of constructing the proposed bridge over Mangamanaia Stream will be extremely small, and overall are likely to be

positive; although it is difficult to weigh changes in depth against changes in velocity.

Eastern Roundabout

57. The Eastern Roundabout will be constructed on an active floodplain. The raising of the ground for the Project will displace some floodwater, but any effects of the roundabout are extremely localised (i.e. mostly within 10-20 metres from the roundabout) and are limited to areas of pasture.
58. A greater area will have reduced flooding after construction of the Project than will experience deeper flooding. Increases in the depth of inundation are generally less than 0.5m, except within constructed wetlands associated with the Project. Even during the extreme design event modelled (i.e. the 1% AEP event increased to allow for the potential effects of climate change to 2120) flooding exceeding 0.3m will persist for less than 4-hours. This is likely to be very similar to, and potentially of shorter duration, than in the current environment because of improved drainage as a result of the Project.
59. SH2 west of Woodville is currently affected by infrequent but persistent flooding caused by the backwater effect upstream of the Manawatū Gorge. The new road alignment and roundabout will avoid this existing flood hazard.
60. The effects of the proposed Roundabout will therefore generally be positive. Any adverse effects will be extremely localised and of short duration.

Conclusion on Project effects

61. In my professional opinion, the Project will have an effect on the hydrology of the area which is almost certainly no more than minor. In fact, I believe that the Project will result in a number of environmental benefits; particularly relating to the continuity of streamflow generation and flood hazard mitigation.

PROJECT DESCRIPTION

62. Te Ahu a Turanga; Manawatū Tararua Highway Project (the Project) comprises the construction, operation and maintenance of approximately 11.5km of State highway connecting Ashhurst and Woodville via a route over the Ruahine Range. The purpose of the Project is to replace the indefinitely closed existing State Highway 3 (SH3) through the Manawatū Gorge.

The Project comprises a median separated carriageway that includes two lanes in each direction over the majority of the route and will connect with State

Highway 57 (SH57) east of Ashhurst and SH3 west of Woodville (via proposed roundabouts). A shared use path for cyclists and pedestrians is proposed, as well as a number of new bridge structures; including a bridge crossing over the Manawatū River.

63. The design and detail of each of the elements of the Project are described in:
 - (a) Section 3 of the Assessment of Environmental Effects (contained in Volume I);
 - (b) The Design and Construction Report (DCR) (contained in Volume II); and
 - (c) The Drawing Set (contained in Volume III).

64. The works that are the subject of this assessment are:
 - (a) The design rainfalls that underpin the design of the stormwater-related infrastructure and the erosion and sediment control measures;
 - (b) The hydraulic design and potential hydrological and hydraulic effects of the Manawatū Bridge;
 - (c) The hydraulic design and potential hydrological and hydraulic effects of the Mangamanaia Bridge; and
 - (d) The potential effects of the Eastern Roundabout on the existing flood hazard.

EXISTING ENVIRONMENT

Geomorphic setting

65. The geomorphology of the Manawatū region, in which the Project area is located, is dominated by incised-valleys, a prograding coastal plain, and aggrading/degrading floodplains. The landforms in the area are relatively young and composed predominantly of sedimentary rock overlain with newer alluvial and marine deposits.

66. The Manawatū River flows through an antecedent gorge, the nature of which is dictated by the course of the River despite movement of the surrounding topography.

67. Before the formation of the Tararua and Ruahine ranges, the Manawatū River ran roughly along its present course, uninterrupted by significant landforms, to

the west coast. For a period of time, the area now occupied by the Manawatū Gorge was part of the sea-bed, leading to the deposition of marine sediments on top of basement rock.¹²

68. Approximately 1.5-million years ago, uplift began along a series of NE-SW trending faults (i.e. the Wellington, Ruahine and Mohaka Faults) initiating the formation of the central ranges. This regional scale movement led to the diversion of many smaller water courses into the Manawatū River. Consequently, the Manawatū River gained the drainage from the entire eastern side of the uplifting range. Where the Manawatū River crossed the low point of the uplifting ranges, it continued to erode through the marine sediments and then the basement rock, keeping pace with the rate of uplift. Smaller, abandoned streams were uplifted with the ranges.
69. This process has led to the present-day approximately 1km wide and 6km long Manawatū Gorge. The geomorphological nature of the Gorge can be defined by three distinct zones; the river, the Gorge slopes and the broad flat-topped ridge crest (Figure D.1).

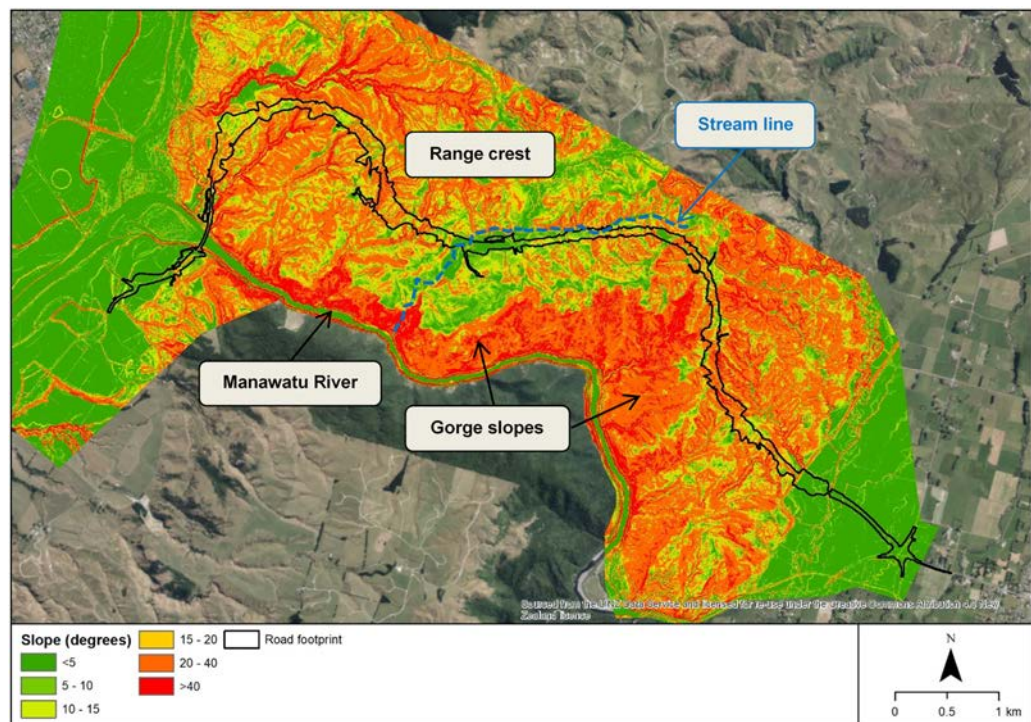


Figure D.1: Slope angles of the Manawatū Gorge and adjacent Ruahine Range.

70. The River is bound on both sides by slopes which rise 250-300m and are generally steep (35° - 45°) to very steep ($>45^\circ$). There are localised zones of near vertical bluffs (Figure D.1). The slopes are comprised of alternating

¹² Stevens, G.R., 1974: Rugged Landscape: The geology of central New Zealand, including Wellington, Wairarapa, Manawatū and the Marlborough Sounds. AH & AE Reed, Wellington.

sandstone and mudstone but also commonly contain sheared dark argillite, minor basalt, chert and limestone blocks.¹³

71. The steep Gorge slopes are differentiated from the top of the Ruahine Range by a distinct break in slope (Figure D.1). A profile of a tributary on the northern side of the Gorge (sub-catchment 4) highlights the relatively gentle slope along the flat-topped ridge crest, which at the break of slope drops steeply into the Manawatū Gorge (Figure D.2).

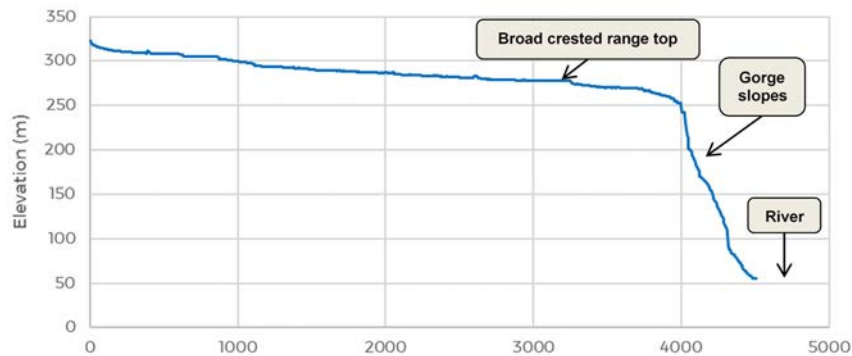


Figure D.2: Stream profile showing the distinctive break of slope. Much of the Project will be constructed on the range crest.

72. Above the steeply inclined Gorge slopes, the top of the Ruahine Range is characterised by broad, relatively smooth surfaces. These represent an ancient erosional surface upon which Pliocene and early Quaternary marine and alluvial deposits are preserved. These deposits consist of massive to poorly bedded, concretionary blue-grey mudstone with minor calcareous sandstone, coquina limestone, rhyolitic tephra and conglomerate (Figure D.3).

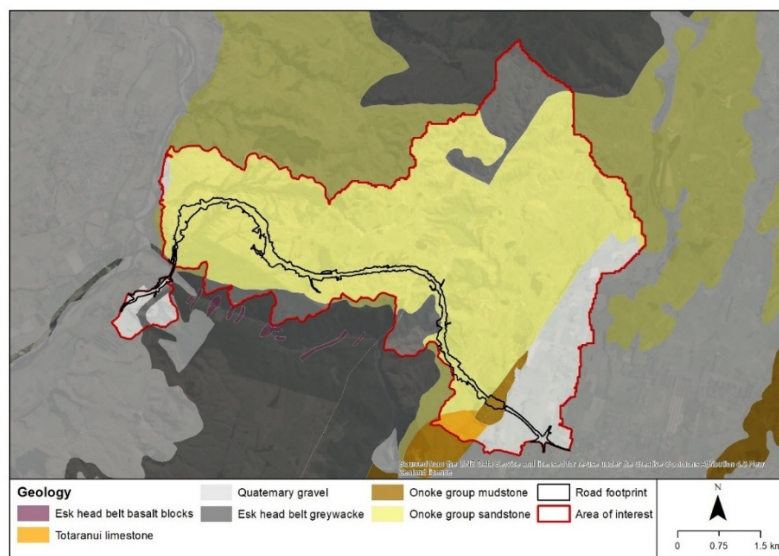


Figure D.3: Geology of the Project area.

¹³ Lee, J.M. and Begg, J.G. (compilers) 2002: Geology of the Wairarapa area. Institute of Geological and Nuclear Sciences 1:250 000 geological map 11. 1 sheet + 66 p. Lower Hutt, New Zealand. Institute of Geological and Nuclear Sciences Limited.

73. The soils within the Project area are formed in loess (i.e. fine silt) and are 'poorly' or 'imperfectly' drained (Figure D.4). The poor drainage of the soils means that they saturate rapidly and behave as though the soil has an impermeable surface (i.e. these surfaces are akin to the paved surface of the proposed highway). This means that it is unlikely that activities associated with the Project will have a significant effect on hydrological processes and runoff.

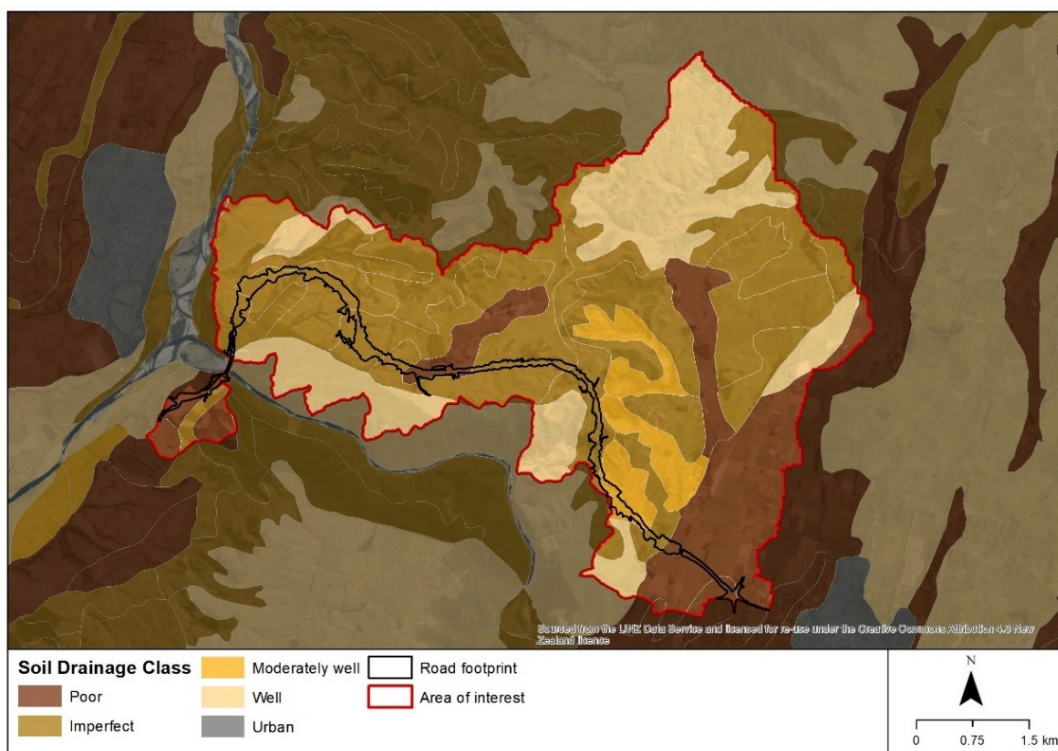


Figure D.4: Drainage properties of the soils within the Project area.

74. Much of the Project will be constructed on the range crest which has relatively diffuse drainage. The streams on the ridge crest include the smaller, abandoned valleys that were uplifted with the ranges.

Fluvial setting

75. The Manawatū River is 235km long and drains a catchment area of approximately 5,890km². The catchment has a number of large tributaries including the Oroua, Mangatainoka, Mangahao, Pohangina and Tiraumea (Figure D.5 & Table D.1). The smaller Mangamanaia catchment, also a tributary of the Manawatū River, is traversed by the Project towards its eastern extent.
76. The headwaters of the Manawatū River are located in the Ruahine Range, northwest of Norsewood. The river is unique in New Zealand in that it begins on the eastern side of a main divide and winds its way to the Tasman Sea on the western side of the range, at Foxton Beach.

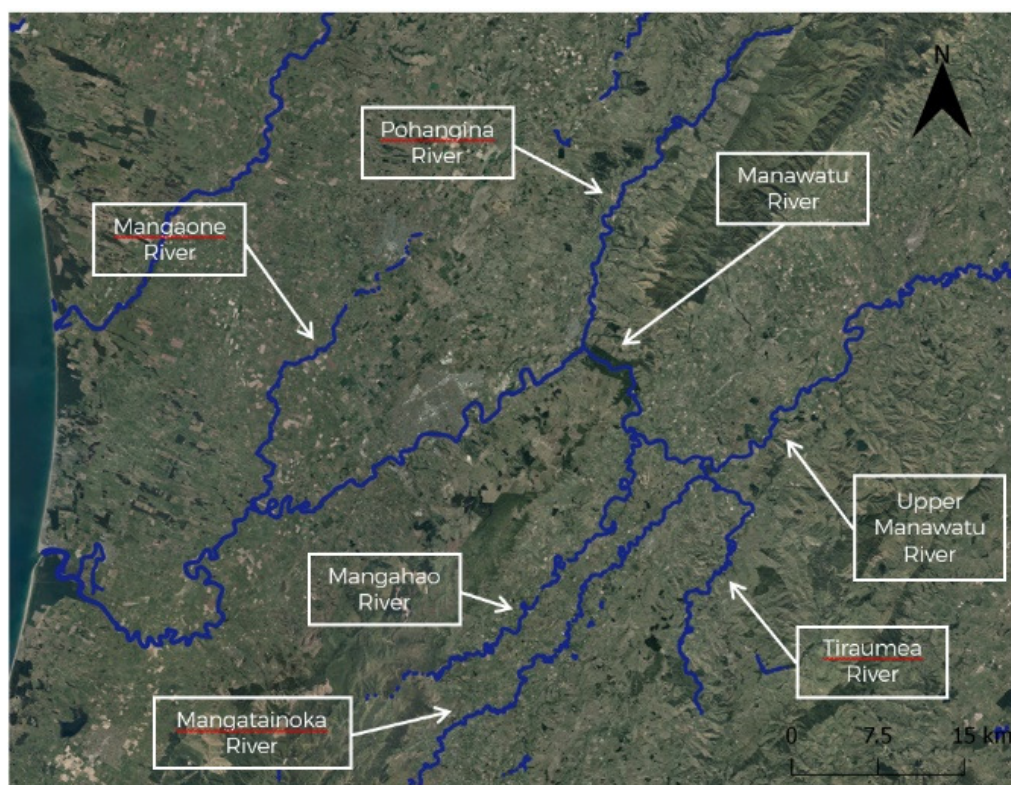


Figure D.5: Major rivers and tributaries of the Manawātū.

Table D.1: Catchment areas and current indicative sediment loads for the Manawātū River and its various tributaries.

River	Catchment area (km ²)	Estimated sediment load (Mt/year) ¹⁴
Upper Manawātū River	1300	0.81
Tiraumea River	1358	1.33
Mangatainoka River	481	0.23
Mangahao River	329	7.04
Pohangina River	551	0.76
Mangaone River	183	7.04
Oroua River	903	0.50
Manawātū River	5868	3.74

77. The confluence of Pohangina River is approximately 600m downstream of the western extent of the project area (Figure D.6). The Manawātū River then flows across the Manawātū plains, being augmented by the Mangaone and Oroua Rivers before discharging into the sea.

¹⁴ Booker, D.J., Whitehead, A.L. (2017). NZ River Maps: An interactive online tool for mapping predicted freshwater variables across New Zealand. NIWA, Christchurch. <https://shiny.niwa.co.nz/nzrivermaps/>



Figure D.6: Confluence of the Pohangina and Manawatū Rivers is about 600m downstream of the proposed bridge.

78. The major rivers of the area are typically single thread and gravel bedded, with the majority of coarse sediment consisting of greywacke. The river valleys themselves have considerable quantities of gravel stored as river terraces and floodplain deposits, with the size of the gravel decreasing gradually downstream. This decrease is such that the Manawatū River has two distinct bed phases; upstream of Opiki the riverbed is gravel while downstream it is predominantly sand and/or silt. Fine material constitutes the majority of total sediment load and is the product of the weathering of the softer Tertiary rocks. The transport of fine material in the Manawatū and its tributaries can be the result of even minor freshes (i.e. small floods) which mobilise material stored in riverbanks and on floodplains. Movement of larger sediment (i.e. bedload) requires larger flows with sufficient energy to overcome the resistance of the particles.
79. As expected for a relatively large river draining a steep mountainous and hill country catchment, the Manawatū River is prone to flooding. The interaction of the gravel bed of the River with large floods means that the channel is naturally dynamic and subject to significant, and often dramatic, changes in form and position (Figure D.7).



Figure D.7: The collapse of the Ashhurst Bridge in 1885.

Project sub-catchments

80. The Project traverses the upper portions of a number of small catchments that drain directly to the Manawatū Gorge. Consequently, the Project will interact with, and potentially affect, the hydrological and runoff process operating within these catchments. To identify the potential effects of the Project, and to avoid or mitigate any adverse effects, it is necessary to understand the existing characteristics of these catchments, particularly those that affect hydrological processes and runoff behaviour.
81. Above the steep slopes adjacent to the Manawatū Gorge, the top of the Ruahine Range is characterised by broad, relatively smooth surfaces. These represent an ancient erosional surface upon which Pliocene and early Quaternary marine and alluvial deposits are preserved. Much of the Project will be constructed on the range crest.
82. There is limited information regarding potential overland flow paths, drainage lines, and rivers and streams within the Project area. Consequently, a 1m resolution, hydrologically-correct DTM was generated from LiDAR. Using various spatial analysis tools, all potential overland flow paths and the increase in 'flow' downslope were derived. The threshold used to identify those areas where concentrated flow might occur was 4,000 cells or 0.4ha (Figure D.8). It should be noted that these are areas where concentrated flow might be expected, not the location of actual streams or permanent watercourses.

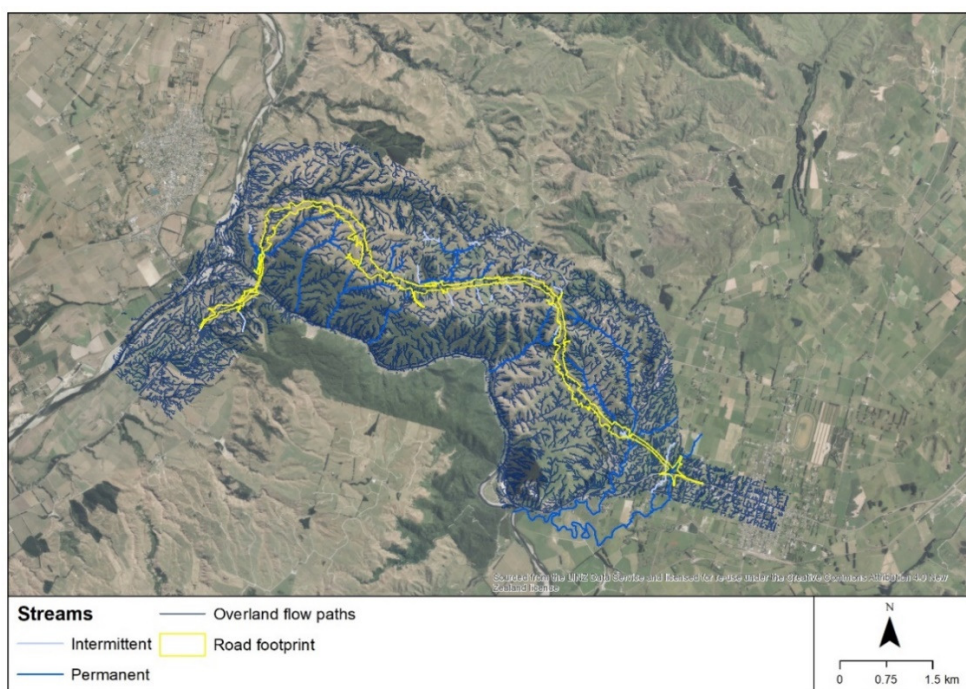


Figure D.8: Modelled overland flow paths and drainage network within the Project area, and those stream mapped in the field.

83. Using these drainage lines, and a flow accumulation of 30,000 cells (i.e. 3ha), the various sub-catchments with a potential to interact with the Project were identified, delineated, and their areas determined (Figure D.9). It is considered that a flow accumulation threshold of 3ha for the potential formation of permanent watercourses is likely to be more realistic than the threshold of 0.4ha discussed previously. It should be noted that both these thresholds are based solely on professional judgement. They have not been validated in the field as this would involve traversing the length of each stream under a range of conditions.
84. The sub-catchments potentially affected by the Project have a maximum combined area of approximately 34km², and more than half of this area is upstream of any potential works in the Mangamanaia catchment (Catchment 2 in Figure D.9). This means that the Project will affect a maximum of only approximately 0.6% of the area of the Manawatū catchment, or 0.3% if the upper Mangamanaia is excluded.

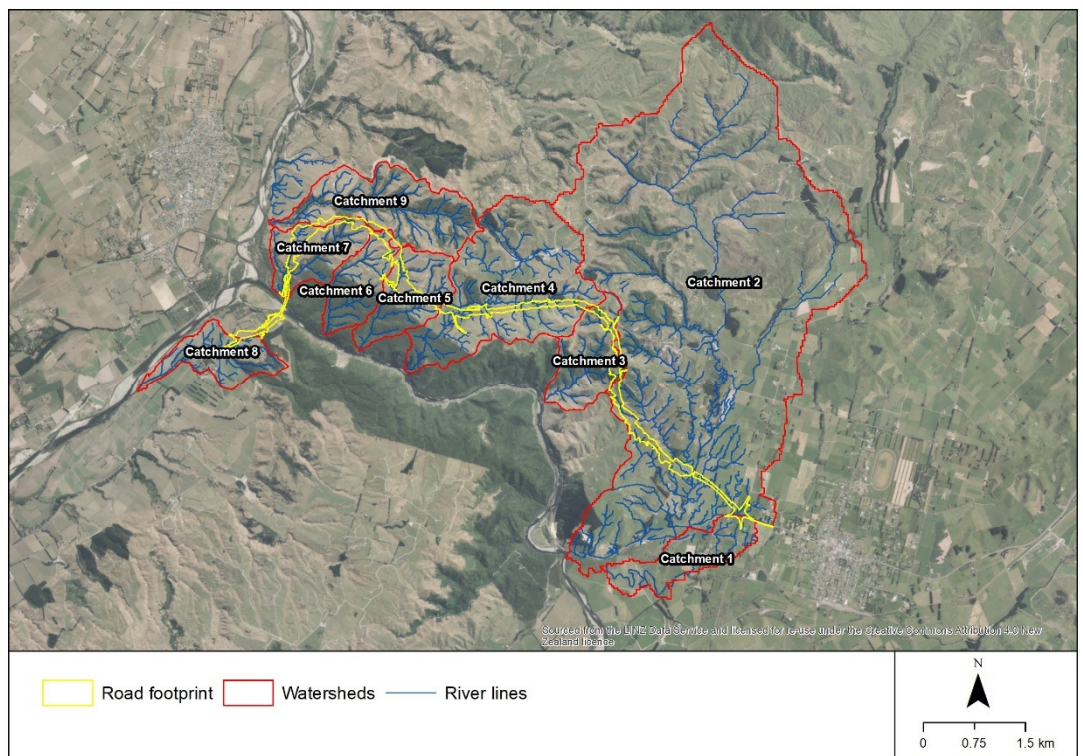


Figure D.9: Various sub-catchments potentially affected by the Project.

85. It should be noted, however, that only a very small percentage of these catchments will actually be affected by the Project, and considerable efforts will be made to avoid, mitigate or offset any potential adverse effects on those catchments. It should also be noted that only about 30% of the slopes draining directly to the Gorge will be potentially affected by the project; 70% of the slopes will be completely unaffected.

86. The majority of works associated with the Project will occur on the broad-crested ridge to the north of the Manawatū Gorge. There will be almost no effect on the steep, largely natural, forested slopes draining directly to the Gorge.
87. A detailed assessment of the habitat types potentially affected by the Project is provided in **Technical Assessment F**. However, at a catchment scale the national LCDB 4¹⁵ provides a valuable overview. The vast majority of the works will take place on land classified in the LCDB as 'High Producing Exotic Grassland (Pasture)'. Only very small areas of 'Indigenous Forest' will be potentially affected (Figure D.10). Consequently, the majority of the Project will traverse a landscape that has already been heavily modified.

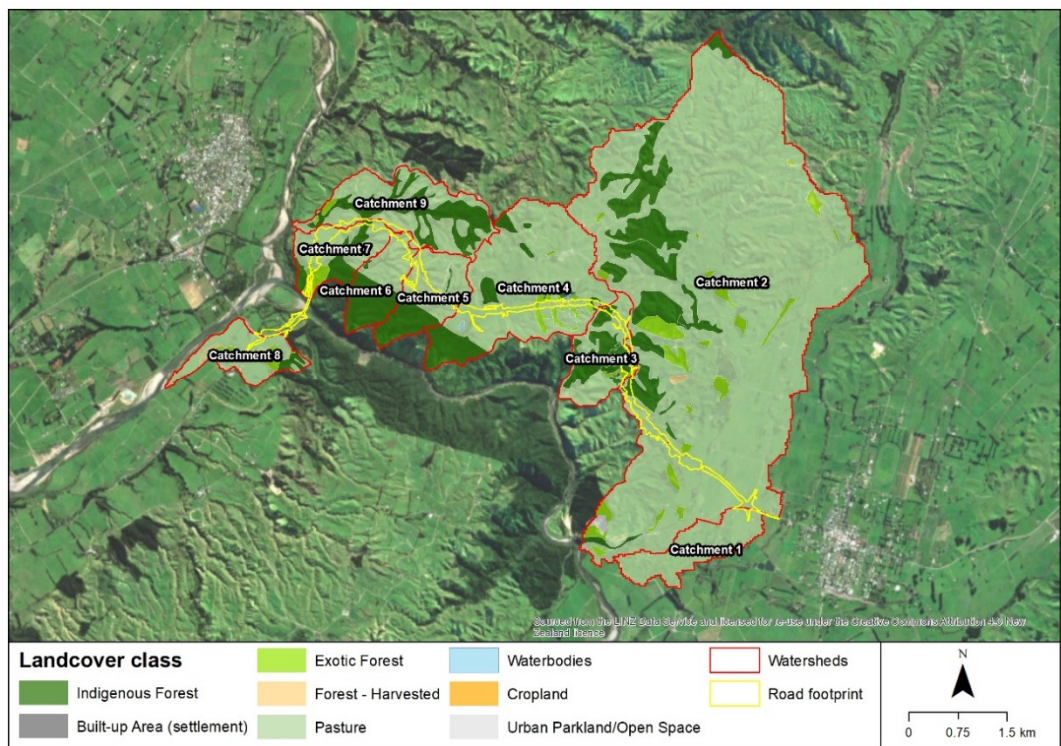


Figure D.10: Landuse in those catchments potentially affected by the Project.

88. Each of the sub-catchments is small, with the majority being less than about 2km². The exception is Catchment 2 (Mangamanaia) with an area of 20.55km²; however, the Project has the potential to affect only a small portion of the lower reaches of this catchment (Table D.2). It should be noted that these catchment areas are measured for the entire area upstream of their confluence with the Manawatū River. Consequently, these areas are extremely conservative (i.e. high) with respect to the area potentially affected by the Project.

¹⁵ LCDB v4.0 - Land Cover Database version 4.0, Mainland New Zealand. <http://www.lcdb.scinfo.org.nz/>

Table D.2: Landuse and sub-catchment parameters obtained from LCDB 4 and GIS analyses.

	Sub-catchment								
	1	2	3	4	5	6	7	8	9
	LCDB v4 Land use classes (2012)								
Broadleaved Indigenous Hardwoods	0%	5%	10%	12%	33%	53%	28%	0%	0%
Deciduous Hardwoods	0%	0%	0%	0%	0%	0%	0%	1%	0%
Exotic Forest	0%	4%	3%	0%	0%	0%	0%	11%	1%
Forest - Harvested	0%	0%	0%	0%	0%	0%	0%	3%	0%
Gorse and/or Broom	0%	0%	0%	4%	0%	0%	10%	0%	0%
High Producing Exotic Grassland	100%	84%	52%	79%	65%	47%	62%	78%	57%
Indigenous Forest	0%	0%	27%	3%	0%	0%	0%	7%	38%
Low Producing Grassland	0%	1%	0%	2%	2%	0%	0%	0%	3%
Manuka and/or Kanuka	0%	6%	9%	0%	0%	0%	0%	0%	0%
	Catchment parameters								
Catchment area (km ²)	1.17	20.55	1.23	4.12	1.20	0.95	1.10	1.01	2.20
Drainage length (km)	7.08	87.14	9.08	30.58	9.13	7.91	8.50	11.62	17.53
Drainage density (km/km ²)	6.041	4.241	7.356	7.431	7.629	8.300	7.703	11.559	7.960

89. For each of the sub-catchments, the drainage density (length of potential drainage lines divided by catchment area) was derived. This measure of the texture of dissection is associated with various geomorphic and hydrologic conditions. Areas with a high drainage density are generally associated with high flood peaks, variable flow regimes, and high sediment loads.
90. Sub-catchment 1 has an area of approximately 1.17km². However, as this catchment largely drains a flat, low-lying floodplain, with significant lengths of artificial drains and modified channels, there is some uncertainty regarding the exact area. This sub-catchment is entirely under pasture and being on a low-lying floodplain the drainage density is slightly lower than the average for those sub-catchments potentially affected by the Project.
91. Sub-catchment 2, the Mangamanaia catchment, is the largest catchment potentially affected by the Project (20.55km²). The catchment has two distinct physiographic units, the steeper dissected hill country to the west and north, and the generally flat low-lying floodplain to the east. The drainage density is one of the lowest in the Project area (4.24km/km²). Approximately 85% of the catchment is under pasture, with small areas of broadleaved indigenous hardwoods (5%) and manuka and kanuka (6%).
92. Sub-catchments 3-7 are all very similar in area; except for sub-catchment 4 which is larger at 4.12km². A greater proportion of sub-catchment 4 is also above the Gorge scarp which therefore has flatter slopes. This is reflected in

the greater percentage of high producing pasture in this catchment. Sub-catchments 3 and 6 have the smallest proportions of their catchments above the Gorge scarp. Consequently, these sub-catchments have a smaller proportion of pasture, and a larger proportion of natural forest. As expected for sub-catchments that are affected by the same rainfall regime, are composed of the same geology, and have the same topography, the drainage densities are all very similar (approximately 7.5km/km²).

93. Sub-catchment 8, another very small catchment (1.01km²), is different to the other sub-catchments in that it drains to the Manawatū River downstream of the Pohangina confluence (Figure D.9). The majority of this catchment is under pasture, but there is also a significant proportion under exotic forestry. The drainage density is the highest of all the sub-catchments but likely reflects the artificial drains installed across the floodplain to support the existing land use.
94. Sub-catchment 9, is the third largest of the sub-catchments (i.e. 2.20km²) but will generally only be affected by the enabling works. This catchment has the highest proportion of indigenous forest (38%), with about 60% under pasture. Since this sub-catchment is affected by the same rainfall regime, is composed of the same geology, and has the same slopes as sub-catchments 3-7, the drainage density is also similar (7.96km/km²).
95. The size of the various sub-catchments, their existing land use, and physical characteristics provide the context when assessing the hydrological processes operating in the area and the potential interaction of the Project with these processes.

Hydrological processes

96. As discussed above in the “context” section of my Introduction, many of the potential environmental effects of the Project relate to its interaction with the rainfall-runoff relationships which exist within the Project area. In particular, the hydrological processes which occur between precipitation within the catchment and runoff into the Manawatū River affect: stormwater and erosion and sediment control management and design; water quality; ecological health; recreational services; the hydraulic design of the bridges; and the flood hazard within the potentially affected catchments.

97. Consideration of the hydrology and rainfall-runoff relationships within the Project area is therefore critical to a range of inputs and investigations relating to the Project and its potential effects.
98. Precipitation, predominantly in the form of rainfall, provides the source and ultimate variability of all water within those sub-catchments potentially affected by the Project. Rainfall tends to vary as a function of elevation and these differences are exacerbated by the topography which can either disperse or concentrate any rainfall. This results in differences in runoff, streamflow and the potential for erosion and sediment transport within the various sub-catchments.
99. Much of this precipitation, however, never reaches the ground surface because it is intercepted by vegetation. Some moisture is stored on the leaf surfaces, some is evaporated back into the atmosphere, and the remainder falls to the ground. For the moisture that reaches the ground, the soil, acting as a filter, determines the path this water takes to reach a stream channel and eventually leave the catchment.
100. On reaching the ground, some of the precipitation infiltrates the soil surface and is held within the soil by capillary forces. The rest will first fill any depressions on the surface and then start to flow downslope to the drainage network. Depending on conditions, the soil moisture content may increase to a level at which gravity overcomes the capillary forces and the water will then start to percolate either laterally through the regolith until it reaches a stream, or vertically to the groundwater zone. This longer and slower flow path through the groundwater zone into streams, ponds or wetlands maintains streamflow during dry weather. Not all the moisture that passes through the soil surface, however, reaches a stream. Some is held as soil moisture and is returned to the atmosphere either by evaporation or by transpiration from the leaves of plants.
101. The paths taken by water as it moves through a catchment are important because they determine many of the characteristics of a landscape, the nature and generation of storm runoff, the risk and magnitude of any erosion and sediment transport processes, and the strategies required to mitigate any potential adverse environmental effects (Figure D.11).
102. Runoff or streamflow comprises the movement of water under the influence of gravity in open channels of various sizes. The quick response of streamflow following the onset of precipitation indicates that some of this precipitation

takes a rapid pathway to the stream channel (i.e. quickflow). The continuity of flow through dry periods indicates that some of the precipitation takes longer, or slower, pathways (i.e. baseflow). However, in larger river systems the various lag effects, and the multiple contributions from tributary streams, complicate this pattern. Furthermore, large variations in hydrologic characteristics, and therefore runoff processes, can occur over small, apparently homogeneous areas.

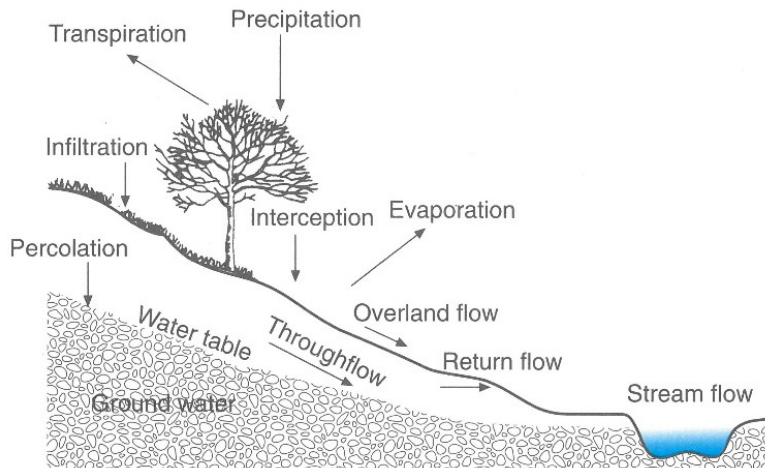


Figure D.11: The hydrological cycle, showing the continuous movement of water through various storages and pathways.

Runoff generation

103. The temporal and spatial variability of streamflow response to precipitation can be explained by the various flow paths that water takes in reaching the stream channel (Figure D.12).

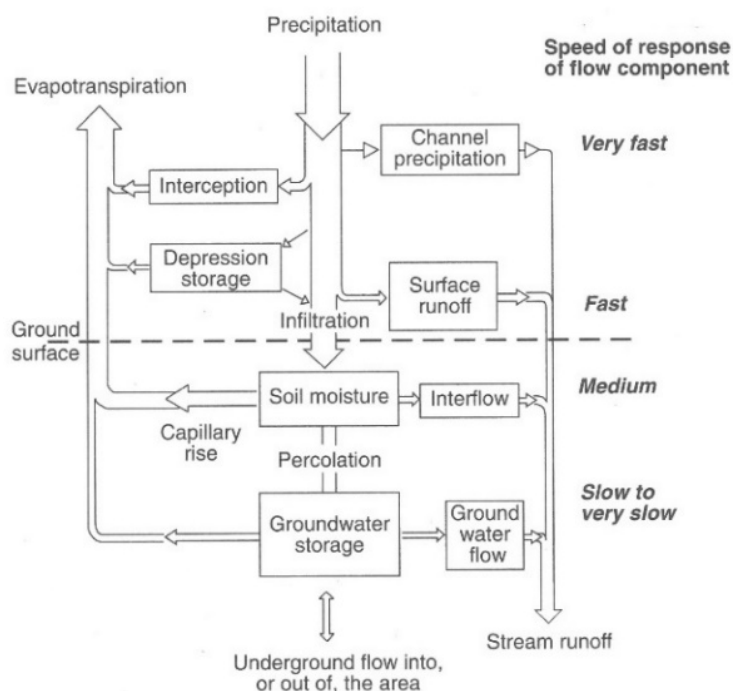


Figure D.12: Various linkages and flow paths between precipitation and streamflow.

104. This is because streamflow at a particular point in time, and at a particular point in a drainage system, integrates all the hydrologic processes and the condition of all the water stores and flow paths upstream. Water can arrive in the channel via a number of pathways. The first to arrive is direct channel precipitation, or rain that falls onto the river. While this is usually a very small proportion of the precipitation, it arrives very quickly and can increase significantly during longer storms, when the surface area of the stream, and any wetlands or ponds may increase markedly. Overland flow also arrives in the channel quickly, as the water flows over the ground rather than infiltrates the surface. The speed of overland flow depends on the surface roughness which can be affected by various land use practices; including earthworks and road construction. Overland flow can occur either because the rainfall intensities exceed the rate water can infiltrate the soil (Hortonian overland flow), or because the soil is already saturated and cannot hold any more water (saturated overland flow).
105. Hortonian overland flow only contributes to streamflow when rainfall intensity exceeds the infiltration capacity of the soil and any depression storage is full. Hortonian overland flow as a result of high rainfall intensities is unlikely to occur under natural conditions in Manawatū. This is because the soil and regolith are relatively permeable, especially when covered with forest vegetation. The vegetation protects the soil, and organic matter and microfauna create an open soil structure. As a result, Hortonian overland flow was, until recently, considered rare in New Zealand under natural conditions, making a significant contribution to runoff only in urban areas, where the surface has been paved or sealed through human activity.
106. The potential for Hortonian overland flow increases in response to vegetation changes or removal, or any activity which acts to compact or seal the ground surface. However, even then, in most situations the zone contributing Hortonian overland flow is only a very small portion of the catchment. The construction and presence of the Project will increase both the area and frequency of Hortonian overland flow, but these changes will be extremely small in terms of both area and frequency. This is because of the land use changes that have already occurred in the Project area. The effect of this on the runoff processes within the various sub-catchments will depend on the area affected, the distance downstream of the interfluvium, and the frequency and duration of intense rainstorms.

107. Therefore, overland flow, while it may be significant at smaller scales such as on the actual highway alignment, will be unimportant at larger scales e.g. at the individual catchment scale. Studies in forested areas have demonstrated that overland flow over mineral soil, in association with rapid subsurface flow, can be responsible for very rapid rises in streamflow during storms. Over larger areas, however, the dominant runoff processes change in response to reducing average rainfall intensities and increasing average infiltration rates (Figure D.13).

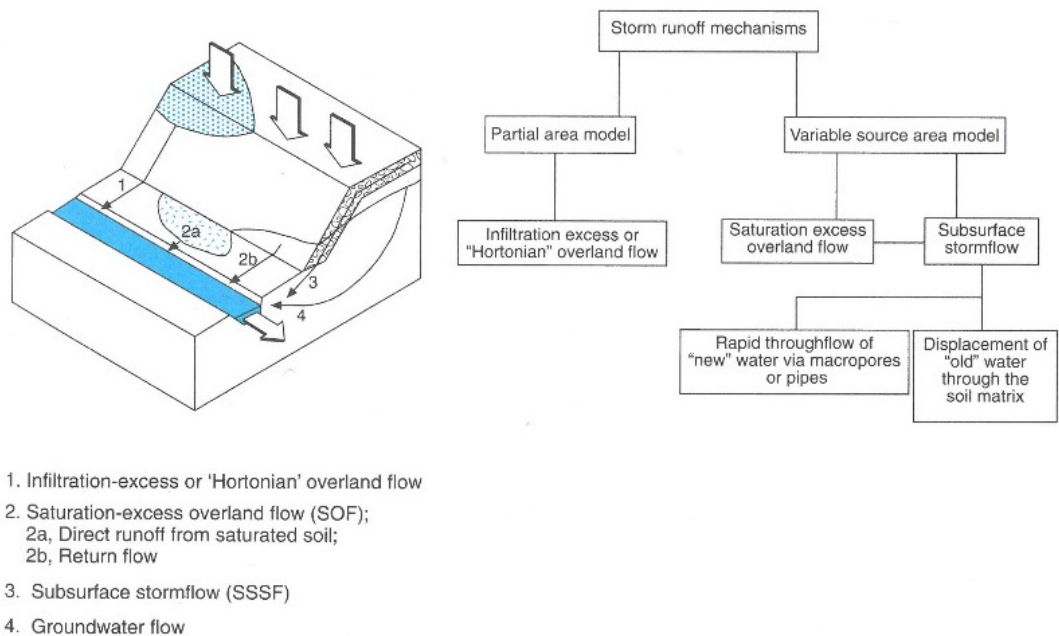


Figure D.13: Paths taken by precipitation to reach streams, and the mechanisms of streamflow generation.

108. Although gravity draws water downwards into the soil, the rate of moisture movement is reduced by viscosity, surface tension, and friction. Capillary forces within the soil can also cause the water to move upwards rather than downwards, particularly as the soil dries out. In relatively wet soils, however, it is the downward movement that predominates. Eventually the percolating moisture reaches a barrier to vertical movement. This barrier can be caused either because the saturated zone rises or because a layer of lower hydraulic conductivity (i.e. permeability) prevents the water percolating to greater depth. When percolating water meets this barrier it tends to flow parallel to the barrier in a downslope direction. Hydraulic gradients direct this flow towards the nearest topographic depression. As a result, the various flow paths converge, and movement slows, the water tends to 'pile up', and the level of saturation rises towards the ground surface. The entire regolith profile may even become saturated during high intensity or prolonged rainfall events. Because of

drainage from upslope, lower hydraulic gradients, and higher initial water tables, these zones of saturation usually occur in the valley bottoms or other topographic concavities. These areas are often described as 'springs' but they are actually only seepages of subsurface flow, generally on the bedrock interface, which intersect the ground surface. Rainfall landing on such areas cannot enter the ground, and either ponds in any depressions or flows downslope as saturated overland flow. Areas producing this type of runoff expand during storms and as total rainfall increases.

109. Much of the streamflow in those catchments likely to be affected by the Project, under natural conditions would have arrived as throughflow within the regolith mantling the slopes. This is water that infiltrates the soil surface and then moves laterally through the regolith to the stream channel. This movement can occur as either unsaturated flow (particularly through macropores such as root channels or cracks within the soil) or as a saturated layer. Variability in flow velocity and the amount of throughflow are a function of antecedent moisture conditions and the relative importance of the various flow paths at a given site. This in turn is a function of the characteristics of the soil, the macropore network, and the parent material at the base of the soil. At sites where the soil has an open structure and the parent material is shattered or permeable, the macropore network is a less important control on hydrological behaviour.
110. In other situations, saturated flow occurs within a shallow perched water table above the main groundwater zone. This type of flow is particularly common in the catchments likely to be affected by the Project, where shallow regolith overlies steep relatively impermeable bedrock. In such situations, the regolith rapidly saturates during prolonged or intense storms. The high lateral, relative to vertical, conductivity of the regolith promotes the horizontal movement of water in such situations, generally towards topographic hollows where it may intersect the ground surface.
111. Depending on the circumstances, water moving through the soil may encounter a saturated zone further down the slope. If this happens, the throughflow may be forced back to the surface (return flow) and become a component of the saturated overland flow. This emphasises the rather arbitrary nature of flow characterisation, particularly as the size of the study area increases.

112. Because of existing land use, many of the longer and slower flow paths no longer operate. Consequently, surface runoff processes are now more dominant than they were under natural conditions.

Runoff hydrograph

113. Streamflow at a point within a catchment fluctuates temporally, as a result of the processes discussed above, and can be plotted as a hydrograph (Figure D.14).

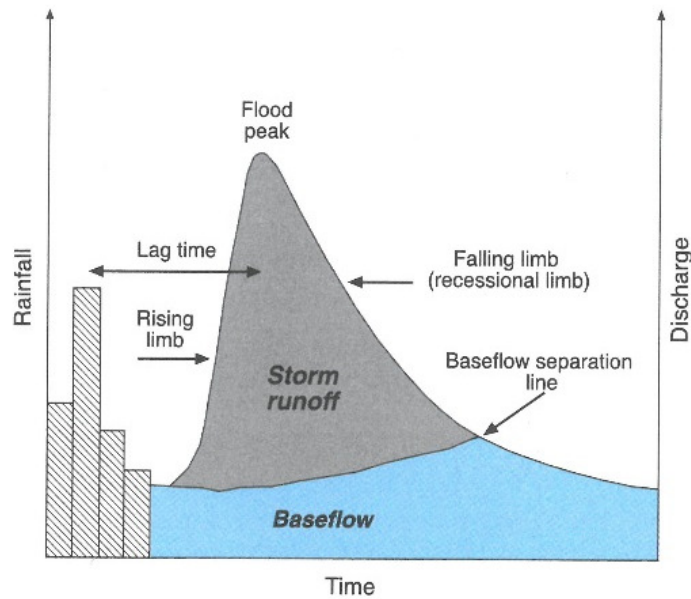


Figure D.14: Typical flood hydrograph showing the main elements and flow contributions.

114. The hydrograph reflects the integration of all the inputs, outputs, moisture stores, runoff generation, and streamflow processes operating higher in the catchment (Figure D.15).

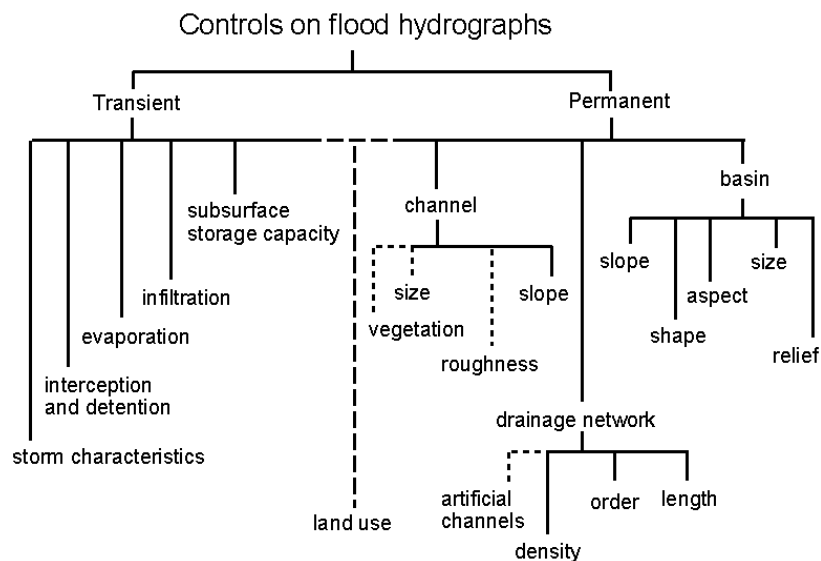


Figure D.15: Controls on the nature of storm runoff and therefore the flood hydrograph.

115. As mentioned earlier, water which arrives rapidly after the onset of precipitation is termed storm runoff (also known as direct runoff or quickflow). Water that takes longer or slower pathways is called baseflow (also known as dry weather flow or delayed flow). In practice, the separation of the stormflow from the baseflow within a flood hydrograph has often proved difficult in New Zealand, where catchment responses are quite different to those where the 'standard' methods were derived. For example, many New Zealand catchments are relatively small and steep, including those potentially affected by the Project, and therefore the flow separation line rises at least an order of magnitude faster than suggested by the international literature.
116. Flow separation is important because it affects estimates of catchment runoff coefficients, or the proportion of a rainstorm event that will appear as stormflow. While runoff coefficients are strongly influenced by antecedent conditions, a comparison can be made for extreme events when much of the catchment is saturated. Forested sub-catchments in the Manawatū have runoff coefficients of about 0.3, which increase to about 0.45 during a 1% AEP (i.e. 100-year ARI) event. Similar sub-catchments, but in pasture rather than forest, have runoff coefficients of about 0.44, which increase to about 0.65 for 100-year ARI events.
117. This separation of the components of flow is, however, rather arbitrary and changes at different points in the catchment. For example, storm runoff in the headwaters may be baseflow by the time it reaches the lower catchment.

Streamflow generation

118. The major control on streamflow in those catchments potentially affected by the Project is the location of the catchment and its headwaters with respect to the regional rainfall distribution. This effect is so strong that it tends to mask all others.
119. While the average flow regimes of rivers in the Manawatū are controlled largely by the orographic enhancement of precipitation (i.e. areas of higher elevation have higher rainfall and therefore higher streamflow), the specific discharge patterns are controlled by a range of other factors. This is because the steep slopes and shallow regolith have a very limited water storage capacity, so any precipitation tends to runoff very rapidly. The major controls on the flow regimes of specific rivers and streams are therefore: the location of the headwaters with respect to the precipitation pattern; and the shape, size, and slope of the catchment.

120. There is only very limited information regarding the flow regimes of the small streams potentially affected by the Project. There are a number of flow recorders on the Manawatū River and its various tributaries. However, the only flow recorder in the project area was installed by the Transport Agency during July 2019 in 'Stream 7'. While the flow series obtained to date is useful in defining the shape and character of runoff events, the period of data collection is too short to provide a reliable assessment of the flow regime of this catchment, and by inference the other small catchments.
121. However, it is likely that these small streams have highly variable discharges because of limited storage capacity within their catchments. Higher discharges are experienced following heavy rainfall, with a number of flood events occurring each year. These are separated by sustained periods of relatively low flows. As a result, the mean discharges for any river or stream can be quite misleading.
122. Flooding as a result of either intense or prolonged rainfall on steep slopes with thin soils is neither new, nor an anthropogenic phenomenon.
123. These small streams also exhibit a change in flow behaviour over their length. Flow within many of the drainage lines identified on the DTM, and discussed previously, is largely subsurface. Flow will only occur on the surface during and immediately following more extreme prolonged or intense rainfall. These drainage lines should not, in my opinion, be described as streams as there is no defined channel with observable bed and banks. In many instances it is actually these drainage lines, rather than streams, that will be potentially affected by the Project.
124. Further down the slope a defined channel can be observed. At this point, drainage from the upper catchment is sufficient, at least occasionally, to erode and transport sediment. However, while these may be described as streams, flow in the upper reaches is intermittent (i.e. they only flow during and immediately following rainfall events). From a hydrological perspective these channels may be streams when they contain water, but they are dry watercourses at other times. Consequently, the effect of the Project on the hydrology of these intermittent streams is also likely to be minor.
125. Once the upstream catchment is large enough to provide subsurface runoff during periods without rainfall (i.e. baseflow), flow becomes continuous. From this point the streams can be described as perennial, even though the volume of flow is still highly variable.

126. From a hydrological perspective therefore, the potential significance of the various streams and watercourse with a potential to interact with the Project increases from ephemeral, through intermittent to perennial; with perennial streams being of most importance.

METHODOLOGY

Background

127. The Transport Agency has separately given notice of its requirement for three designations for the Project ("**NoRs**"), and these NoRs are currently under appeal. I understand that the Transport Agency will ask the Environment Court, as part of those appeals, to modify the NoRs to provide for the Northern Alignment on which the Alliance's concept design is based.

128. I have familiarised myself with the technical assessments previously prepared by the Transport Agency in support of the NoRs in relation to hydrology and hydraulics, including:

- (a) Te Ahu a Turanga – Manawatū River Base Hydraulic Model. Report prepared by Bloxam Burnett & Olliver Ltd. (BBO). February 2019. (**Appendix D.2: Te Ahu a Turanga – Manawatū River Base Model**);
- (b) Te Ahu a Turanga: Manawatū Tararua Highway – Implementation. Contract No: NZTA 2018576. Appendix A3 – River and Bridge Hydraulics; and
- (c) Te Ahu a Turanga: Manawatū Tararua Highway – Implementation. Contract No: NZTA 2018576. Appendix A4 – Drainage.

129. I have also considered the following NoR documents in so far as they relate to the hydrology and hydraulics of the rivers, streams and other waterways which have the potential to interact with the Project:

- (a) Parts G and H of the AEE regarding bridge design and minimising effects on Parahaki Island. Part H also provides information regarding avoidance of natural hazards (including flooding);¹⁶
- (b) Appendix 4, which includes a bridge and retaining wall design philosophy statement;¹⁷ and

¹⁶ <https://www.nzta.govt.nz/assets/projects/sh3-Manawatū/NZTA-NOR-Volume-2.pdf>

¹⁷ In particular, sections 2.1.2.2, 2.1.4.1 and 2.1.5.2: <https://www.nzta.govt.nz/assets/projects/sh3-Manawatū/NZTA-NOR-Volume-2.4-Effects-on-Environment.pdf>

- (c) Technical Assessment 4 (Landscape, natural character and visual effects).¹⁸
130. My assessment has built on previous investigations by considering:
- (a) A comprehensive review of all rainfall data from the wider area;
 - (b) The latest guidance material relating to the potential impact of climate change on rainfall and flooding;
 - (c) The potential effects of climate change to 2120 rather than 2090 to allow for the life of the Project;
 - (d) Alternative bridge and pier configurations for both the Manawatū River and Mangamanaia Stream crossings on river processes and the flood hazard; and
 - (e) The effect of scour protection around the piers and abutments at both the Manawatū River and Mangamanaia Stream crossings on river processes and the flood hazard.
131. In particular, I have had regard to the Transport Agency's proposed conditions for the designations ("**Designation Conditions**"). This includes the following recommendations and conditions:
- (a) In the Panel recommendations at [277], the Panel approved of the Transport Agency's proposed measures to minimise effects of construction on Parahaki Island;¹⁹ and
 - (b) Designation condition PN1 provides for consultation with the Te Āpiti Ahu Whenua Trust in the preparation of an outline plan for works related to the bridging of the Manawatū River. Conditions 8 and 9 provide for compliance with condition PN1.²⁰
132. When I come to consider mitigation for the Project, I have sought to build on the mitigation proposed to date through the Designation Conditions. I explain this further below.

¹⁸ In particular, paragraphs 195-197, table 4.18, and appendix 4.A):
<https://www.nzta.govt.nz/assets/projects/sh3-Manawatū/NZTA-NOR-Volume-3.4-Landscape-character-visual.pdf>

¹⁹ <https://www.pncc.govt.nz/media/3131853/te-ahu-a-turanga-Manawatū-tararua-highway-recommendations-report-24519.pdf>

²⁰ <https://www.pncc.govt.nz/media/3131871/nzta-letter-to-councils-te-ahu-a-turanga-designation-decision-7-june-2019.pdf>

Design rainfalls

133. Rainfall is a key component of the hydrological system, and therefore a critical design parameter for a number of aspects of the Project. The intensity and distribution of rainfall can have a wide range of impacts on the environment; particularly those affecting runoff, erosion and sediment transport, and the location, magnitude, duration and impact of flooding. As the highway will interact with the existing environment, understanding the rainfall conditions, and therefore runoff regime in the area, is critical to ensuring appropriate, robust and resilient design.
134. Therefore, all data from rain-gauges in the wider vicinity of the Project was analysed as part of a hydrometric review. The review also included comparison of the empirical data with data derived from HIRDS v4 (High Intensity Rainfall Design developed by NIWA), and consideration of the spatial variability of rainfall and the most appropriate temporal rainfall distributions. This analysis ensures that the most representative rainfall data are used in the design of the Project.
135. In total, the records from 36 gauges were obtained, although none of these gauges are in close proximity to the Project. A rain gauge has been installed adjacent to the railway embankment and Stream 7, but at this stage it provides limited data for analysis.
136. The results of this comprehensive rainfall analysis are provided in a technical report prepared for the Project; *Design Rainfalls – Analysis and Recommendations*, which is attached as **Appendix D.1**.
137. The key conclusions of that analysis are:
 - (a) While there are at least 36 gauges in the wider area, there is no high-resolution long-term rainfall record from the actual Project area.
 - (b) There is some spatial variability in rainfall across the Project area. It is generally wetter to the east and drier in the west. In addition, orographic enhancement of rainfall by the Ruahine Range results in the highest rainfall at the highest elevations (i.e. in the middle of the Project area). These patterns are supported by both the empirical data and the mean annual rainfall.
 - (c) Data from five gauges was analysed in detail to provide a range of empirical design rainfalls from the wider area.

- (d) Comparison of the design rainfalls derived from the empirical data and those from HIRDS v4 demonstrated generally good agreement. It appears that the design rainfalls from HIRDS are slightly conservative (i.e. high) relative to the empirical rainfall records. In the absence of robust empirical data from close to the Project area, design rainfalls from HIRDS are considered appropriate to support the design and construction of the Project. Using design rainfalls from HIRDS is likely to lead to slightly conservative runoff estimates and therefore stormwater design.
- (e) The generally small size of the catchments intersected by the Project means that it is unnecessary to apply an Areal Reduction Factor (ARF) to rainfall. The effect of applying an ARF is likely to be within the uncertainty inherent in the design rainfalls, and certainly within the uncertainty associated with any subsequent stormwater modelling.
- (f) The Minimum Requirements provided by the Transport Agency (A4.2.2.1)²¹ necessitate at least two sets of design rainfall tables; one for each of the western and eastern extents of the Project area. However, rainfall variability across the Project area means that design rainfalls are also required for the middle of the Project area (i.e. the area of highest elevation). These design rainfalls are slightly higher than those at both the western and eastern extents.
- (g) Given the relatively small differences in the various design rainfall tables, that from the higher elevation, where the rainfall is highest, was used for the design and construction of all stormwater-related infrastructure. This ensures slightly conservative, but still realistic, design. Therefore, the design rainfalls in Table 13.1 of **Appendix D.1** were used for all infrastructure designed to perform under the current climate regime.
- (h) The Minimum Requirement of assuming a 2.1°C increase in temperature out to 2090 was based on MfE guidance from 2008.²² However, updated guidance has subsequently been provided by MfE in 2018²³ which refers to four RCP (Representative Concentration Pathways) scenarios. The

²¹ Te Ahu a Turanga: Manawatū Tararua Highway – Implementation. Contract No: NZTA 2018576. Appendix A3 – River and Bridge Hydraulics. 4p.

²² MfE 2008: *Climate Change Effects and Impact Assessment: A guide for local government in New Zealand*. Ministry for the Environment, May 2008.

²³ MfE 2018: *Climate Change Projections for New Zealand: Atmosphere projections based on simulations from the IPCC Fifth Assessment, 2nd Edition*. Wellington. Ministry for the Environment, September 2018.

RCP 6.0 scenario can be considered a “middle of the road” prediction of climate change and has been adopted by a number of territorial authorities and several major infrastructure projects. The adoption of RCP 6.0 for this Project has also been accepted in discussions with Horizons Regional Council. However, the RCP 6.0 scenario was not projected out to 2120 in the guidance provided by MfE. Since the change in temperature from 2030 to 2120 is non-linear for RCP 4.5 and RCP 8.5, a similar interpolated trend was applied to RCP 6.0. This provided a simple projection of the temperature change, assuming RCP 6.0, by 2120 of 2.3°C.

- (i) The design rainfalls over the 100-year life of the Project (i.e. in 2120, assuming RCP 6.0 and a 2.3°C rise in temperature) are provided in Table 13.2 of **Appendix D.1**. These design rainfalls are the most appropriate when designing resilient stormwater and associated infrastructure for the life of the Project. While rainfalls may increase to this level over the life of the Project, using those that may only likely to be experienced at the end of Project provides a level of conservatism to the design. Obviously, this conservatism will decrease over the life of the Project.
- (j) The majority of the sub-catchments intersected by the Project are small, with only two greater than 200ha. Consequently, the peak design flows were estimated using the internationally recognised and widely applied Rational Method. This method uses ‘lumped’ rainfall.
- (k) For catchments larger than about 100ha, some consideration is also required of the temporal distribution of the rainfall over the storm duration. The temporal distribution adopted can have a significant effect on the resulting peak flows.
- (l) The temporal distribution from the Auckland Council Guidelines for Stormwater Modelling in the Auckland Region²⁴ (TP108), stated in the Minimum Requirements, is not appropriate for the Project. The use of the TP108 distribution would result in unrealistically conservative peak discharges, and consequently significant over-design of stormwater infrastructure.

²⁴ Auckland Regional Council 1999: Guidelines for stormwater runoff modelling in the Auckland Region. TP108, April 1999. Report prepared for Auckland Regional Council by Beca Carter Hollings & Ferner Ltd. 19p.

- (m) Review of empirical data from the Pohangina at Alphabet Hut showed that the PMP temporal distribution²⁵ provides a more accurate model of longer storm hyetographs (i.e. the rainfall distribution throughout the storm). This temporal distribution was therefore adopted for the two larger sub-catchments.
- (n) For these larger sub-catchments in which culverts will be constructed, a sensitivity analysis of the effect of the temporal distribution was undertaken to confirm that the rainfall-runoff modelling was providing realistic peak flow estimates. Given the lack of available data, the assessment had to ultimately rely on professional judgement.
- (o) Using the assumed 1% AEP design rainfalls, adjusted for the potential effects of climate change over the life of the Project, the effect of the temporal distribution of rainfall on the peak discharges from the two largest sub-catchments was assessed (Table D.3).
- (p) Access Culvert (ACU-05), required for the Meridian Access Track, has a catchment area of 347.7ha, and Access Culvert (ACU-10) has a catchment area of 225.9ha.

Table D.3: Effect of the temporal rainfall distribution on the peak design flow in the two largest culvert sub-catchments.

Distribution	Peak flows (m ³ /s)					ToC (hr)
	TP108	PMP 1-hr	PMP 2-hr	HIRDS 1-hr	HIRDS 2-hr	
ACU-05	27.659	12.4	15.5	12.8	17.2	1.46
ACU-10	21.408	10.6	12	11.2	13.7	1.06

- (q) For the culvert sub-catchment ACU-10, which has a Time of Concentration (ToC) of about 1-hour, the difference between the PMP and HIRDS temporal distributions is small i.e. 0.6m³/s or 6%. Assuming the TP108 temporal distribution, however, results in a peak discharge about twice that of the other temporal distributions i.e. 21.4m³/s compared to about 11m³/s.
- (r) Similar results were obtained for the larger sub-catchment in which culverts will be constructed (ACU-05), which has a ToC of about 1.5-hours. Again, the differences between the PMP and HIRDS temporal distributions, for storm durations of either 1-hour or 2-hours, are small.

²⁵ Tomlinson, A.I and Thompson, C.S. (1992). Probable Maximum Precipitation in New Zealand - the development and application of generalised methods to provide nationwide estimates of PMP. Report prepared for the Electricity Corporation of New Zealand, New Zealand Meteorological Service, Wellington, New Zealand.

The difference for the 2-hour storm is greater at about 11%, although still within the likely uncertainty of the actual flow measurements. The discharge assuming a TP108 distribution, however, is significantly higher (i.e. 27.7m³/s compared to a maximum of 17.2m³/s). The TP108 temporal distribution therefore results in design flows over 60% higher than modelled using one of the other distributions. The assumption of a TP108 temporal distribution would therefore result in extremely conservative design flow estimates.

- (s) A single rainfall threshold can be used for monitoring the performance of erosion and sediment control structures. Every occasion when rainfall intensities exceeded 15mm/hr. was on a day when rainfall also exceeded 25mm/day. That is, the hourly rainfall intensity threshold would provide no additional information on the performance of the erosion and sediment control measures.
- (t) Adopting a rainfall threshold of 25mm/day at the Project area will lead to an average of five inspections each year (between 1 and 10). This is considered an appropriate number of visits each year to monitor the performance of the erosion and sediment control structures under 'near capacity' conditions.

Flow regimes

- 138. An understanding of the flow regimes, and particularly the frequency and magnitude of flooding, of both the Manawatū River and Mangamanaia Stream is required to:
 - (a) Inform the hydraulic design of the proposed bridges over the Manawatū River and Mangamanaia Stream;
 - (b) Support an assessment of the existing flood hazard in the vicinity of these proposed bridges; and
 - (c) Support an assessment of the potential effects of these bridges on the existing flood hazard.
- 139. There are three long-term flow monitoring sites in the wider vicinity of the Project (Figure D.16). All of these sites are maintained by Horizons (Manawatū Wanganui Regional Council).

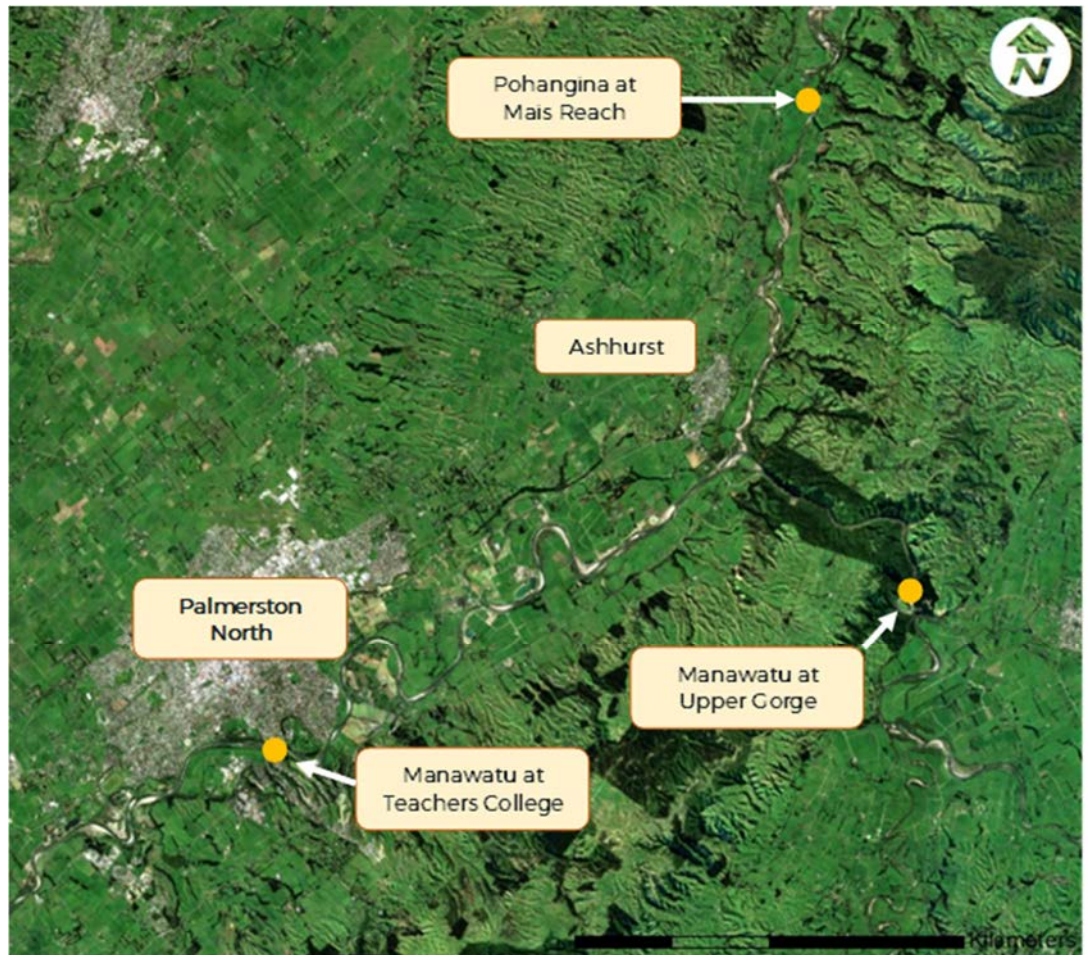


Figure D.16: Location of flow monitoring sites in the wider vicinity of the Project.
Manawatū - Upper Gorge

140. Flows in the Manawatū at Upper Gorge have been measured since 1976. Flows over this period have varied from as low as 5.9m³/s to a maximum of 2,698m³/s (Figure D.17). The mean flow is slightly higher than the median because of the effect of infrequent but large flood events. Summary flow statistics are in Table D.4 and the flow distribution is presented in Table D.5.

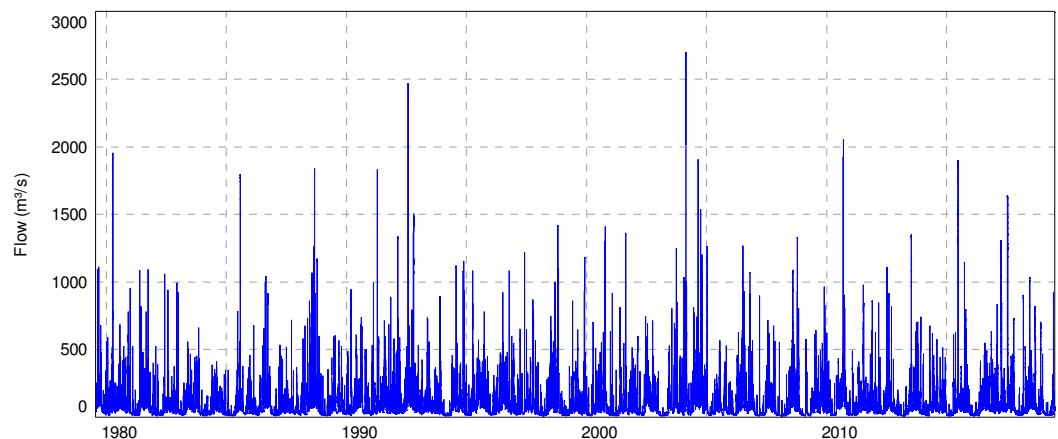


Figure D.17: Manawatū River at Upper Gorge flow series (1976-2019).

Table D.4: Summary flow statistics for the Manawatū River at Upper Gorge (1976-2019).

Minimum	Mean	Median	Maximum	U.Q.	L.Q.	Std. Dev.
5.9	86	52	2698	99	27	115

Table D.5: Distribution of flow recorded in the Manawatū at Upper Gorge (1976-2019).

	0	1	2	3	4	5	6	7	8	9
0	2698	540	401	338	296	265	242	223	208	194
10	183	173	164	156	149	142	136	131	126	121
20	117	113	109	106	102	99	96	94	91	88
30	86	84	82	80	77	75	74	72	70	68
40	67	65	63	62	60	59	57	56	55	53
50	52	51	50	49	48	46	45	44	43	42
60	41	40	39	38	37	36	35	34	33	32
70	32	31	30	29	28	27	26	25	24.4	23.5
80	22.7	21.8	21.0	20.2	19.4	18.7	18.0	17.2	16.6	15.9
90	15.2	14.5	13.9	13.3	12.8	12.1	11.3	10.6	9.8	8.9
100	5.9									

141. The flow regime of the Manawatū River is typical of a large river draining largely pastoral hill-country in New Zealand. The River has sustained periods of medium to low flow, interspersed by random flood events of varying magnitudes. In general, higher flows occur during winter and spring, and lower flows at the end of summer and into autumn. The flow regime over the last 43-years displays a cyclic pattern; typically, with larger flows occurring every 2-3 years. The largest recorded flood was in 2004.
142. Any potential effects of the Project on the Manawatū River, which will be extremely small given the footprint of the Project and the size of the various sub-catchments affected, will be further mitigated by flow from the Pohangina River; the confluence of which is approximately 600m downstream of the mouth of the Manawatū Gorge. The Pohangina River increases the size of the Manawatū catchment by about 550km²; with all the associated rainfall, runoff and land use effects. These effects are orders of magnitude larger than those likely to result from the Project.
143. The Manawatū at Upper Gorge flow series is the most suitable for assessing the design criteria for the proposed bridge over the Manawatū River, and the interaction of the bridge with the River. The increase in catchment area downstream of the flow recorder is only 15km², or <1% of the catchment upstream (3,200km²). There will be a small gain in flow through the Gorge, but this is likely to be within the measurement uncertainty at the flow recorder.
144. The flow record for the Manawatū River at Upper Gorge provides a record of all major flood events over the past 43 years; since 1976. Consequently, a frequency analysis was undertaken of the annual flood maxima series. Three

types of statistical distribution were assessed for how well they modelled the annual flood maxima series (i.e. Gumbel, Pearson 3 (PE3) and GEV). The distribution which provided the best fit to the annual maxima series was then used to estimate the peak flows for design events with a range of annual exceedance probabilities (AEPs) or average recurrence intervals (ARIs).

145. As is standard practice, the frequency analyses were performed on a 12-month partition. That is, only the largest flood in each complete year was plotted, and the most appropriate statistical distribution fitted to those annual values.
146. All statistical distributions fit the annual flood maxima series well out to a 5% AEP (i.e. 20-year ARI) event. After this, the GEV distribution starts to diverge from the other two statistical distributions. By the 1% AEP event, the Gumbel and PE3 distributions are still almost identical and fit the largest flood on record (16 Feb 2004) well (Figure D.18). The Gumbel distribution then starts to plot slightly higher than the PE3 distribution. The Gumbel distribution was adopted as it gives slightly conservative (i.e. high) design flows (Table D.6).

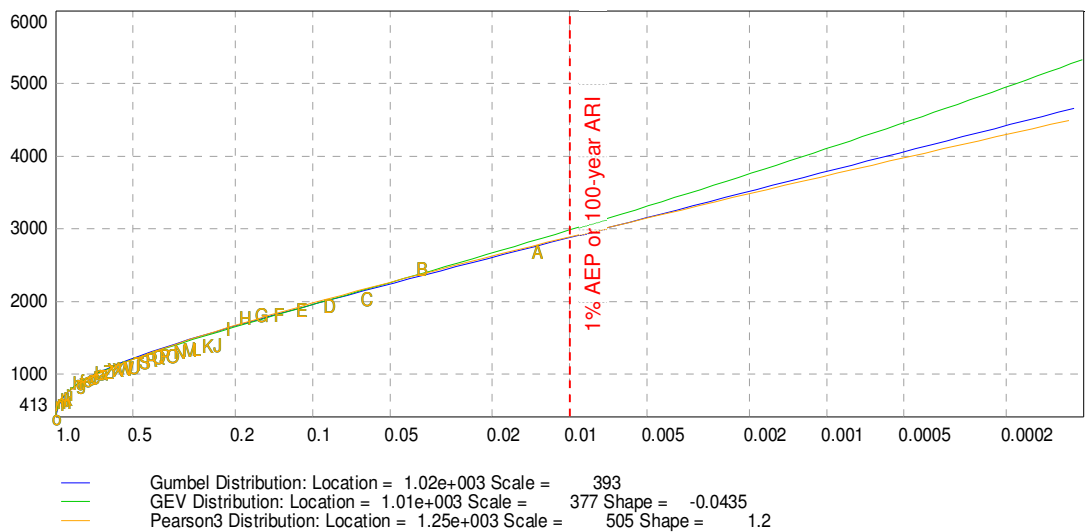


Figure D.18: Flood frequency analysis for the Manawatū at Upper Gorge annual flood maxima series.

Table D.6: Derived design flows for the Manawatū at Upper Gorge.

ARI (Years)	AEP (%)	Manawatū at Upper Gorge (m³/s)	Design flows from Minimum Requirements (m³/s)
2.33	43	1,246	1,169
5	20	1,609	
10	10	1,903	
20	5	2,186	
50	2	2,552	
100 (SLS)	1	2,827	2,994
1000	0.1	3,733	4,479
2500 (ULS)	0.04	4,094	4,759

147. The 2500-year design flood event, the Ultimate Limit State (ULS), was derived by extrapolation of the Y variate of the annual exceedance probability.
148. The design flows provided in the Minimum Requirements and used in some of the preliminary computational hydraulic models, are therefore slightly conservative. The design flow for the 1% AEP event is 6% higher, and for the Ultimate Limit State (ULS or 0.04% AEP) approximately 16% higher.

Design hydrograph

149. When modelling flood events through the Manawatū Gorge and assessing the potential effect of works associated with the Project, a design flood hydrograph is required. A type-hydrograph can be derived for the catchment by analysing the shape of various large floods in the flow record. These can also be compared to confirm the applicability of using a single type-hydrograph for the Manawatū Gorge.
150. To create a representative type-hydrograph for floods in the Manawatū Gorge, the ten largest events over the past 43-years were extracted from the flow record from the Manawatū at Upper Gorge (Figure D.19). The flood peaks were aligned and the average hydrograph of these ten events determined.

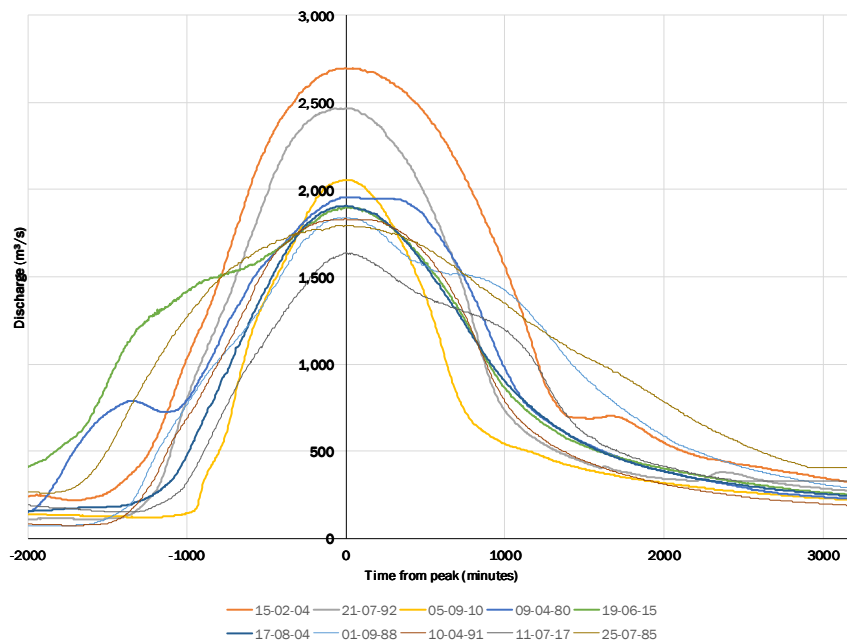


Figure D.19: The ten largest flood events recorded in the Manawatū Gorge.

151. The average type-hydrograph smooths out any irregularities or variability caused by a range of factors during each specific event but retains the representative shape and characteristics (Figure D.20). The resulting type-hydrograph can be scaled to the peak discharges during any design event in the Manawatū Gorge.

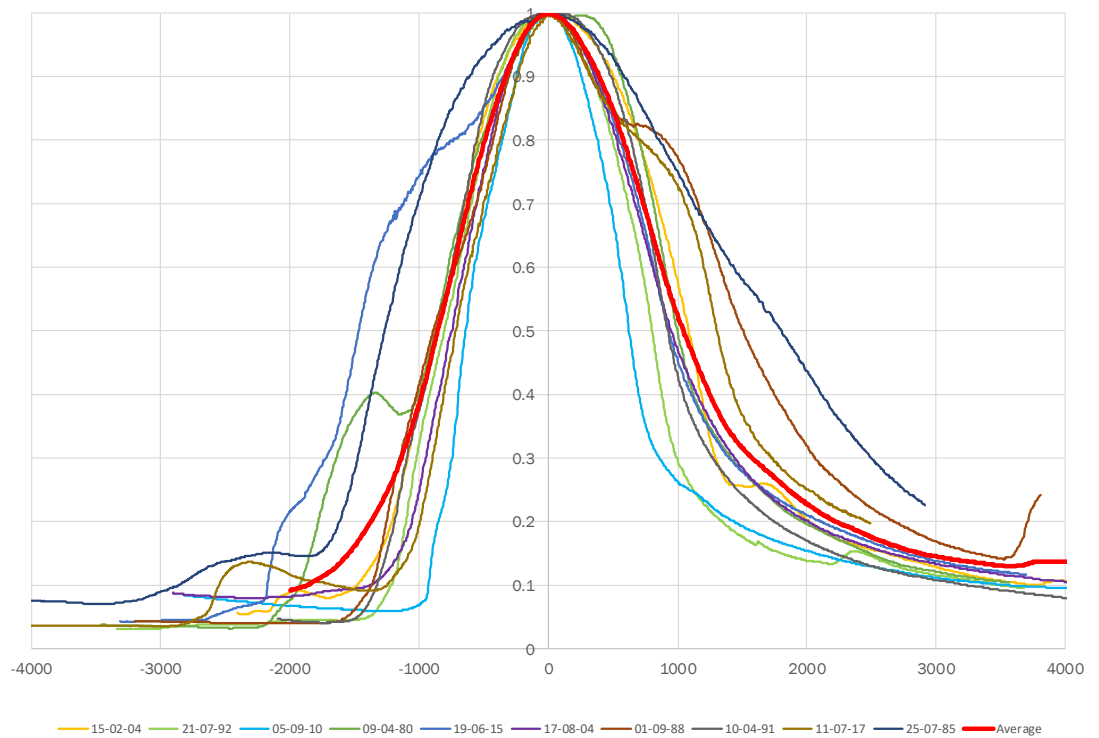


Figure D.20: Average design hydrograph derived from the ten largest flood events in the Manawatū at Upper Gorge.

Pohangina River

- 152. Flows have been recorded in the Pohangina River at Mais Reach since 1969, now providing approximately 50-years' information relating to the flow regime.
- 153. Flows in the Pohangina River reflect a similar pattern to the Manawatū, particularly with respect to higher flows, once the difference in catchment area is considered (Figure D.21). However, the low flows in the Pohangina are generally smaller than those in the Manawatū, even considering the difference in catchment area.

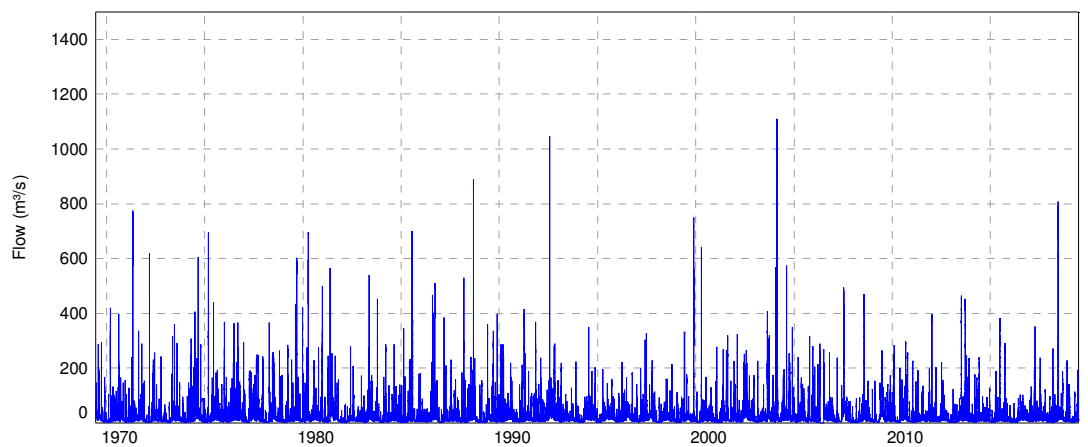


Figure D.21: Pohangina at Mais Reach flow series (1969-2019).

- 154. Summary flow statistics for the Pohangina River at Mais Reach are provided in Table D.7 and the flow distribution is in Table D.8.

Table D.7: Summary flow statistics (m³/s) for the Pohangina River at Mais Reach (1969-2019).

Minimum	Mean	Median	Maximum	U.Q.	L.Q.	Std. Dev.
0*	16.7	9.9	1109	18.2	5.5	275

* *Likely an erroneous measurement*

Table D.8: Distribution of flows (m³/s) recorded in the Pohangina River at Mais Reach (1969-2019).

	0	1	2	3	4	5	6	7	8	9
0	1109.1	121.6	81.3	64.6	54.9	48.6	43.9	40.2	37.4	34.9
10	32.8	31.1	29.5	28.1	26.9	25.8	24.8	23.8	22.9	22.1
20	21.4	20.7	20.0	19.4	18.8	18.2	17.7	17.2	16.7	16.3
30	15.8	15.4	15.0	14.6	14.3	13.9	13.6	13.3	13.0	12.7
40	12.4	12.1	11.8	11.5	11.3	11.0	10.8	10.6	10.3	10.1
50	9.9	9.7	9.5	9.3	9.1	8.9	8.7	8.5	8.3	8.1
60	7.9	7.7	7.6	7.4	7.2	7.1	6.9	6.7	6.6	6.4
70	6.3	6.1	6.0	5.8	5.7	5.5	5.4	5.2	5.1	5.0
80	4.8	4.7	4.6	4.4	4.3	4.1	4.0	3.9	3.8	3.6
90	3.5	3.4	3.3	3.1	3.0	2.9	2.7	2.6	2.4	2.0
100	0.0									

155. The flow record for the Pohangina River at Mais Reach provides a record of all major flood events over the past 50 years; since 1969. Consequently, a frequency analysis was undertaken of the annual flood maxima series. The same approach was adopted as for the Manawatū River at Upper Gorge flow record.

156. The Gumbel statistical distributions fits the annual flood maxima series best, including the largest flood so far recorded. The assumption of a Gumbel distribution persisting into the future was therefore adopted to derive design flows out to a 1% AEP event (Table D.9).

Table D.9: Design flows for the Pohangina at Mais Reach.

ARI (Years)	AEP (%)	Design flow (m ³ /s)
2.33	43	446
5	20	607
10	10	738
20	5	864
50	2	1027
100 (SLS)	1	1149

Manawatū River at Teachers' College

157. The longest recorded flow series in the area, and one of the longest in New Zealand, is from the Manawatū River at Teachers' College. Flow measurements commenced in 1926.

158. This flow site is approximately 21km downstream of the Pohangina confluence and therefore the Project area. Given the extremely small effects of the Project, even in the immediate vicinity of the proposed works, these would not be measurable in the flow record for Manawatū River at Teachers' College.

This flow site, however, is used to establish triggers relating to the abstraction of water from this reach of the Manawatū River.

159. As expected, flows in the Manawatū River downstream at the Teachers' College reflect a similar pattern to the Manawatū upstream of the Gorge (Figure D.22); although with significantly higher flows caused largely by the contribution from the Pohangina River.

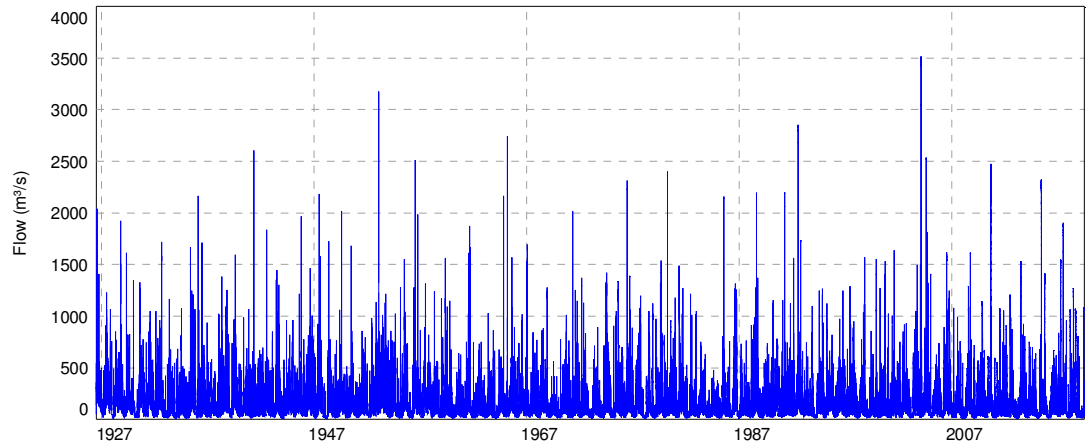


Figure D.22: Manawatū River at Teachers' College flow series (1926-2019).

160. Summary flow statistics for the Manawatū River at Teachers' College are provided in Table D.10 and the flow distribution is in Table D.11.

Table D.10: Summary flow statistics (m³/s) for the Manawatū River at Teachers' College flow series (1926-2019).

Minimum	Mean	Median	Maximum	U.Q.	L.Q.	Std. Dev.
8.4	113	71	3515	135	36	144

Table D.11: Distribution of flows (m³/s) recorded in the Manawatū River at Teachers' College flow series (1926-2019).

	0	1	2	3	4	5	6	7	8	9
0	3515.3	688.1	516.8	435.0	381.4	344.0	315.0	291.6	272.6	256.7
10	242.7	230.2	219.0	209.1	200.0	191.8	184.1	177.0	170.5	164.6
20	159.0	153.8	148.9	144.2	139.7	135.4	131.5	127.7	124.2	120.7
30	117.5	114.3	111.4	108.5	105.7	103.1	100.6	98.1	95.7	93.3
40	90.9	88.6	86.5	84.4	82.3	80.3	78.4	76.4	74.5	72.8
50	71.0	69.3	67.6	65.9	64.1	62.5	60.9	59.3	57.8	56.3
60	54.9	53.5	52.1	50.8	49.5	48.3	47.0	45.8	44.6	43.3
70	42.1	40.9	39.7	38.6	37.4	36.3	35.3	34.2	33.1	32.0
80	31.0	29.9	28.8	27.8	26.8	25.8	24.8	23.8	22.9	21.9
90	21.0	20.1	19.2	18.3	17.4	16.5	15.6	14.5	13.5	12.1
100	8.4									

161. While not used directly in the hydrological assessment and hydraulic design for the Project, this flow record provides confidence in the analysis undertaken. It also provides key information relating to the abstraction of water to support construction activities.

'Stream 7'

162. The hydrological processes and flow regime of Stream 7 are likely to be similar to those in the other small streams draining the slopes above the Manawatū Gorge (Figure D.23).



Figure D.23: Stream 7 is likely to be typical of the other small streams draining the slopes above the Manawatū Gorge.

163. As part of the monitoring associated with the Project, a water level recorder was installed at the upstream end of the culvert under the railway embankment; just upstream of the confluence of Stream 7 with the Manawatū River (Figure D.24).



Figure D.24: Water level and turbidity sensors at the upstream end of the culvert under the railway embankment on Stream 7.

164. At the present time there are very few data available for this stream, and that data available are largely stage (i.e. water level), rather than flow data (Figure D.25). This data is useful in defining the shape and characteristics of flood hydrographs of the streams draining the Project, although at their confluence with the Manawatū River rather than in the vicinity of the proposed works.

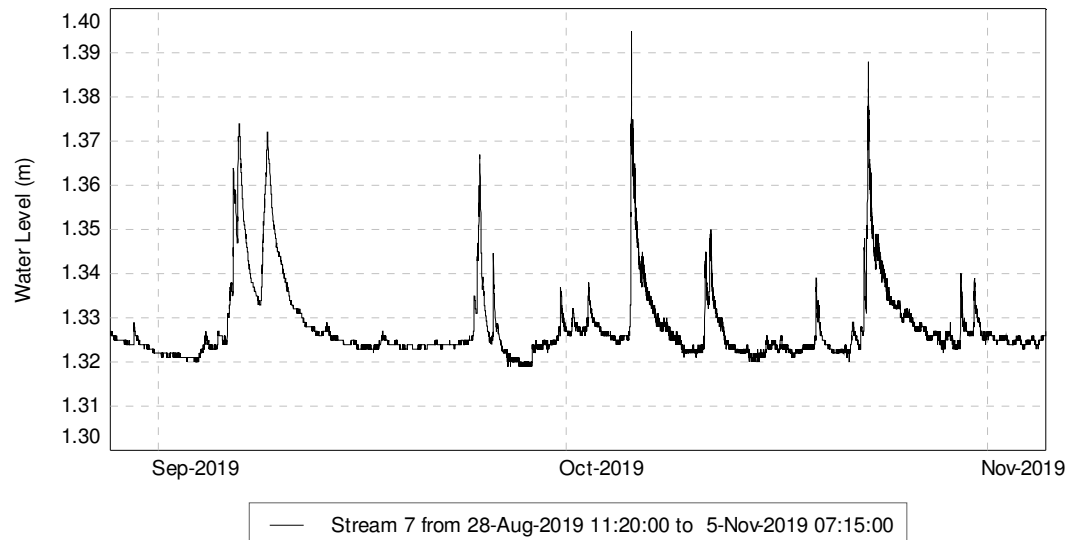


Figure D.25: Stage data from the water level recorder upstream of the culvert under the railway embankment in Stream 7.

165. There is also a rain gauge installed in this catchment adjacent to the railway embankment. This allows the response of the stream to rainfall in the catchment to be quantified. At this stage, however, only a number of relatively small rainfall and flow events have been recorded (Figure D.26).

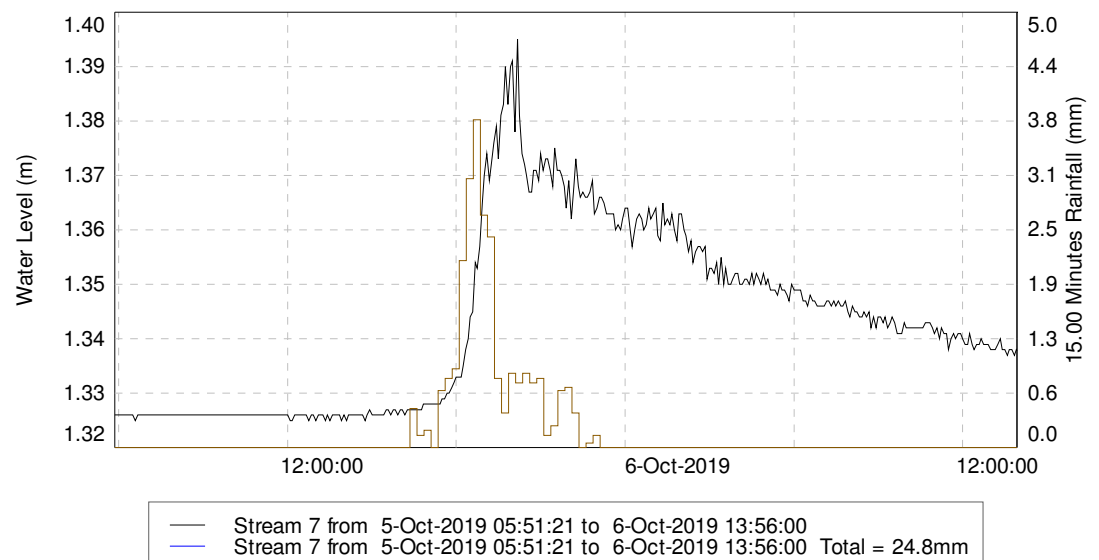


Figure D.26: Rainfall and water level at Stream 7 on 5 October 2019. The flow site has only been operating since mid-August 2019.

166. The lag time between the peak in rainfall and peak flow during this particular event was about 90-mins. However, this was a very small rainfall event

generating only an approximately 7cm rise in water level. It is likely that the lag time for larger events would be significantly shorter.

167. It should also be noted that this lag time was for an event in Stream 7 determined just upstream of its confluence with the Manawatū River. As discussed previously, the various sub-catchments draining the crest of the range above the Gorge generally have a flat profile in their upper reaches and a very steep profile down into the Gorge. Therefore, it is likely that the majority of the lag between the peak rainfall and peak flow will occur in the upper catchment and flow will be rapid down into the Gorge.

Mangamanaia Stream

168. The largest tributary with a potential to interact with the Project is on the eastern side of the Gorge; Mangamanaia Stream (Figure D.27). Given the size of this catchment, it was necessary to develop a computational hydraulic model to investigate the interaction of the Project with the Stream and vice versa.



Figure D.27: The Mangamanaia Stream upstream of the proposed bridge.

169. The Transport Agency provided Minimum Requirements that are to be complied with as part of the Project. This specifically includes describing abutment locations, pier locations and minimum design flows adjusted for climate change for Mangamanaia Stream. The bridge design must also be in

accordance with Appendix 3: River and Bridge Hydraulics of the Transport Agency State Highway Stormwater Specification.²⁶

170. Specific ‘Design Flows’ were provided (Table D.12) with a minimum requirement to model the hydraulics using a steady flow one-dimensional (1D) open-channel hydraulic model.

Table D.12: Minimum design flows provided by the Transport Agency for modelling and designing the bridge over the Mangamanaia Stream.

ARI (years)	AEP (%)	Flow (m ³ /s) adjusted for climate change (2090)
2.3	50	12
10	10	32
50	2	56
100 (SLS)	1	68
2500 (ULS)	0.04	93

171. Flow data available from the vicinity of the Mangamanaia catchment is shown in Figure D.28 and summarised in Table D.13. The only longer term monitoring site is on Mangapapa Stream.

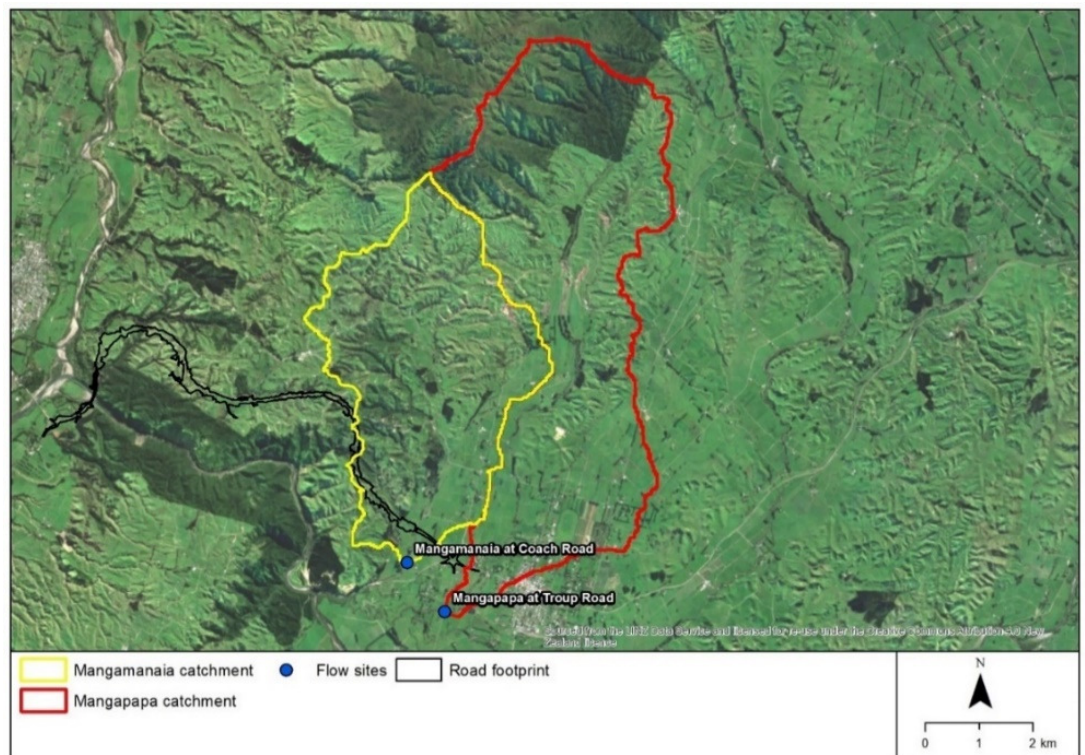


Figure D.28: Flow sites in the vicinity of Mangamanaia Stream.

²⁶ Te Ahu a Turanga: Manawatū Tararua Highway – Implementation. Contract No: NZTA 2018576. Appendix A3 – River and Bridge Hydraulics. 4p.

Table D.13: Summary of flow data from the vicinity of Mangamanaia Stream.

Site Name	Recording authority	Start date	End date	Length of record	Resolution	% Missing
Mangamanaia at Coach Road	NZTA	Jul-2019	Nov-2019	<4 months	5 minutes	0
Mangapapa at Troup Road	HRC	Mar-2006	Jun-2019*	~13 years	15 or 5minutes	<1

* Site is still active, but end of the data used in the analysis

172. A simple gap analysis was carried out on the data from Mangapapa Stream. It is assumed that the data has been quality assured and verified by the local recording authority (i.e. Horizons) and that each gap is genuine.

173. As part of the Project, a new hydrometric site was installed near the location of the proposed bridge over Mangamanaia Stream (Mangamanaia @ Coach Road). This site is operated and maintained by NIWA on behalf of the Transport Agency. At present, there is only a very short water level record available as there is insufficient data to convert these levels to corresponding flows. The current water level record is too short for detailed analysis, or to derive robust design flows (Figure D.29).

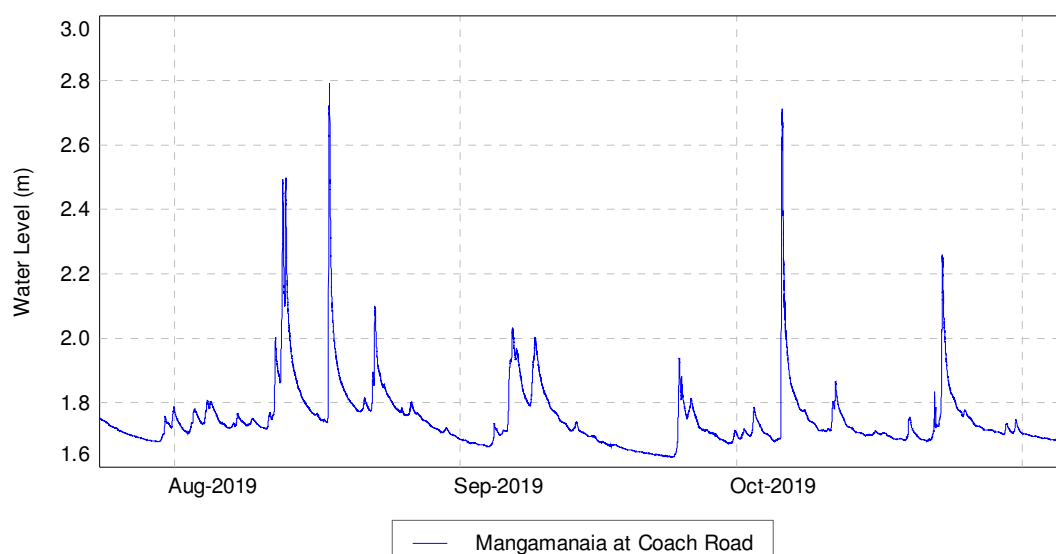


Figure D.29: Empirical water level data from Mangamanaia Stream near the location of the proposed bridge.

174. In the absence of comprehensive flow data for Mangamanaia Stream other methods of design flood estimation are required. Each has its strengths and weaknesses which need to be considered when determining which approach should be adopted.

175. Regional Flood Estimation and flow scaling procedures are developed using recorded flood data from a particular region. The regional flood estimation (RFE) method used in New Zealand is based on work carried out by

McKerchar & Pearson (1989)²⁷ that was updated in NIWA (2016).²⁸ An open-source database has been available since 2018 (NIWA, 2018).²⁹ The method is based on long-term flow records from throughout the country which are related in terms of their catchment area, and the relationship between catchment area and the mean annual flood. It is this relationship which is used to delineate hydrologically homogeneous areas. Growth factors then relate the magnitude of the mean annual flood to the magnitude of the 1% AEP (i.e. 1-in-100 year ARI) event; or any other design event.

176. This method is suitable for all rural catchments except those in which there is snow-melt, glaciers, lake storage, or significant ponding. This is because these features are known to affect the characteristics of a flood, including its magnitude. The RFE procedure should be used for rural catchments greater than approximately 10km².
177. It should be noted that the RFE procedure derives the magnitudes of design floods from the available long-term flow records from catchments with a similar rainfall-runoff relationship. It does not rely on any assumed relationship between rainfall, catchment parameters, and runoff. In this manner, the RFE method is less prone to individual errors relating to a number of variables, and the cumulative effect of these errors on the estimated peak discharge.
178. A simple flow scaling method differs from RFE in that it uses data from only one flow site; in close proximity and with similar catchment characteristics and rainfall-runoff behaviour. The site selected as a proxy for flow scaling needs to have similar topographic, rainfall, and catchment characteristics as the ungauged catchment for which design flows are required. This is because the flow record from the nearby site is scaled solely as a function of catchment area. This can only be done when catchments share the same rainfall-runoff characteristics. Ideally, the proxy site will have an annual flood maxima series of sufficient length to allow the robust estimation of the magnitudes of the required design floods.
179. In my opinion, this approach generally results in greater reliability of the estimates of design flows as it uses a flow record from close to the ungauged

²⁷ McKerchar and Pearson (1989). Flood frequency in New Zealand. Publication of the Hydrology Centre, NO. 20:87.

²⁸ NIWA (2016). Regional Flood Estimation Tool for New Zealand. Prepared for EnviroLink Tools (MBIE). August 2016.

²⁹ NIWA (2018). New Zealand River Flood Statistics. (Accessed 6 November 2019)

catchment. However, the method is prone to the ‘vagaries’ of a single flow record, which tend to be smoothed by the RFE method.

180. Both the RFE and flow scaling methods were adopted for estimating the design flows in Mangamanaia Stream in the vicinity of the proposed bridge.

Flow scaling by area

181. The nearest flow gauge to the Mangamanaia catchment is on Mangapapa Stream at Troup Road. This catchment is adjacent to the Mangamanaia and shares the same catchment characteristics e.g. topography, soils, geology, headwaters in the Ruahine Range, and lower reaches on a floodplain. Comparison of data from the period of overlapping record with the Mangamanaia suggests that the timing of each catchment’s response to rainfall is also similar (Figure D.30).
182. To derive design flows, a frequency analysis was undertaken on the annual flood maxima series derived from the 13-year flow record from Mangapapa at Troup Road. It should be noted that this record is relatively short when estimating the design flows during more extreme (rare) events.

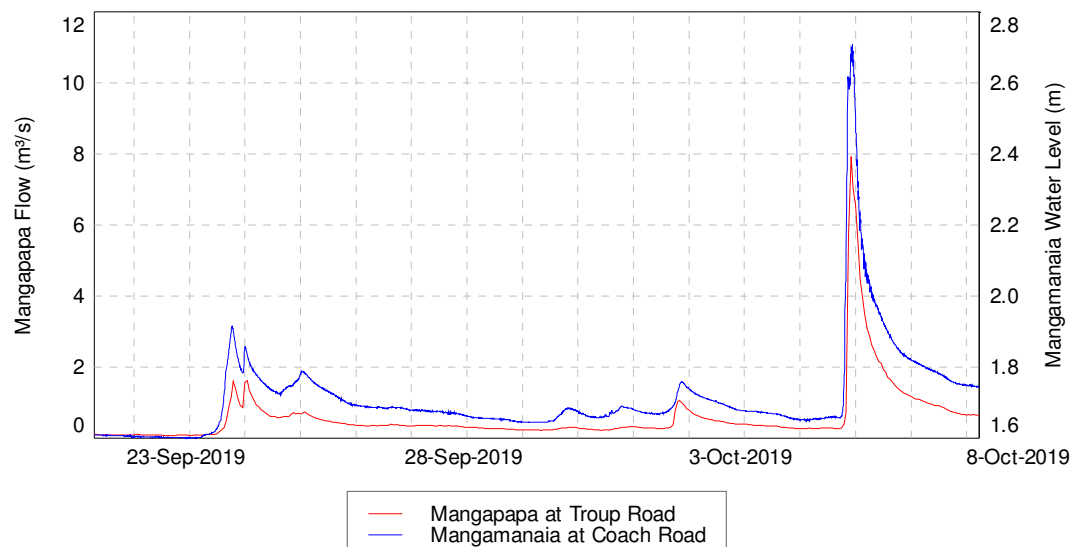


Figure D.30: Comparison of Mangapapa at Troup Road (flow data) with Mangamanaia at Coach Road (water level data).

183. No detailed quality assurance was undertaken on the flow data prior to the frequency analysis other than the gap analysis shown in Table D.13. It is assumed that the data has been collected using best practice, and no obvious erroneous data was observed. Discussions with Horizons, the local recording authority, stated the purpose of this gauge is low-flow monitoring (pers. comm. Brent Watson 21 October 2019). Therefore, there may be less confidence in

peak flows recorded at this site; although some high flows have been gauged, which reduces this uncertainty.

184. Three types of statistical distribution were again assessed for how well they modelled the annual flood maxima series (i.e. Gumbel, Pearson 3 (PE3) and GEV). The distribution which provided the best fit to the annual maxima series was then used to estimate the peak flows during a range of design events.
185. The annual flood maxima tend to approximate a PE3 distribution, although there is not much difference between this and the GEV (Figure D.31). The former, however, provides slightly more conservative flows for large magnitude events while still fitting the data well. The Gumbel statistical distribution provides a very poor fit to the annual maxima series.
186. The design flows for the Mangapapa at Troup Road were then scaled to the Mangamanaia using the ratio of catchment area to the power of 0.8. This is because it has been shown that floods in New Zealand, in adjacent catchments with the same rainfall-runoff relationship, vary as a function of area to the power of 0.8 and not simply area.³⁰

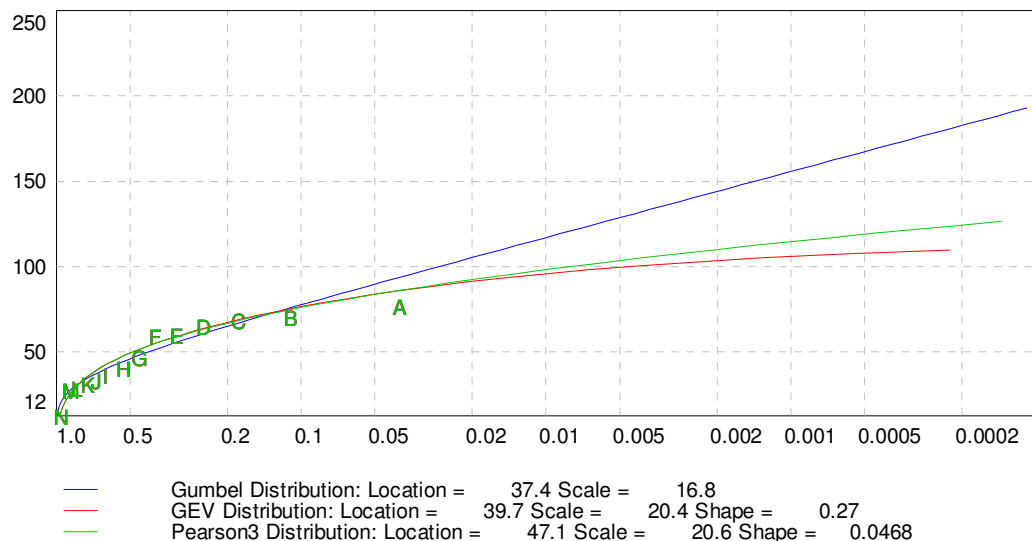


Figure D.31: Frequency distribution of annual flood maxima series from Mangapapa at Troup Road (2007-2018).

187. Assuming that future flood events continue to approximate a PE3 statistical distribution, it is possible to derive estimates of design flows of different magnitudes and frequencies (Table D.14).

³⁰ McKerchar and Pearson (1989). Flood frequency in New Zealand. Publication of the Hydrology Centre, NO. 20:87.

Table D.14: Design flows for the Mangapapa and Mangamanaia catchments. Values in italics were extrapolated.

ARI (years)	AEP (%)	Mangapapa at Troup Road (m ³ /s)	Mangamanaia at Coach Road (m ³ /s)
2.3	50	47.2	34.5
5	20	64.4	47.0
10	10	73.6	53.8
20	5	81.3	59.4
50	2	90.0	65.7
100	1	95.8	69.9
1000	0.1	112.2	81.9
2500	<i>0.04</i>	<i>126.0</i>	<i>92.0</i>

188. The 2500-year design flood event, the Ultimate Limit State (ULS), was derived by extrapolation of the Y variate of the AEP. It should be noted that there is significant uncertainty in this extrapolated value. As a general rule, design events should not be extrapolated beyond twice the length of the record. The extrapolation of these extreme events should therefore be treated with caution as the uncertainty of estimates increases rapidly with increasing magnitude.

Regional flood estimation

189. Design flood estimates derived from regional flood frequency analysis are one of the attributes in the New Zealand River Flood Statistics database.³¹ This database contains attributes for every reach in New Zealand's river network; including estimates of the mean annual flood and the magnitude of the 1% AEP design flood. The estimated design flows for Mangamanaia Stream are displayed in Table D.15.

Table D.15: Design flood estimates for Mangamanaia Stream derived from Reach No. 7039107 in the NZ River Flood Statistics database. Values in italics were extrapolated.

ARI (years)	AEP (%)	Mangamanaia (m ³ /s)
2.3	50	14.3
5	20	18.5
10	10	22.0
20	5	25.3
50	2	29.5
100	1	32.7
1000	0.1	43.3
2500	<i>0.04</i>	<i>48</i>

³¹ Booker, D.J., Whitehead, A.L. (2017). NZ River Maps: An interactive tool for mapping predicted freshwater variables across New Zealand. NIWA, Christchurch. <https://shiny.niwa.co.nz/nzrivermaps/>

190. As mentioned, there is increased uncertainty regarding the magnitude of more extreme events e.g. 1000-year and 2500-year ULS design floods.
191. The design flood estimates based on the RFE are significantly smaller than those obtained from 'at site scaling'. While there are uncertainties in both methods, it is considered that those obtained from 'at site scaling' are likely to be more reliable and provide the appropriate level of conservatism when used in the design of the bridge over Mangamanaia Stream.
192. Although various guidance and design manuals (e.g. the Transport Agency Bridge Manual) require the magnitudes of extreme events to be estimated, the actual relevance of this flood event in each river, and at each bridge crossing, needs to be carefully considered.
193. In many situations, such as the Mangamanaia, there are more critical aspects of the hydrology to consider than simply the size of an extreme runoff event in the local catchment. These considerations include:
- (a) Whether the design flood remains within the channel. In most situations, the extreme design event will include a significant component of overbank flow. It is critical that the relevance and significance of both the 'in-channel' and 'out of channel' components of flow are considered from design and bridge safety perspectives. In Mangamanaia Stream, for example, the majority of flow during larger events will be 'out of channel' and flowing over the adjacent floodplain;
 - (b) The size of the channel to be bridged. If the river is incised, then once the riverbanks have been overtopped the flood water will very likely spread across the floodplain; as is the case in the Mangamanaia. If the extreme design flow does not remain in the channel, any scour estimates based on the total flow are likely to be misleading;
 - (c) The nature of the topography upstream of the bridge. In many cases, much of the upstream catchment will be generally flat, and form part of an extensive floodplain. The lack of relative relief and tributaries, the existence of any stopbanks, and the presence of surface drains may indicate that a large proportion of the rainfall may never reach the main channel as storm runoff. This rainfall, while it may attenuate the flood event, will not contribute to the flood peak; and
 - (d) Backwater effects. In many situations the backwater effects formed by various stream confluences may actually be greater than the local flood

event in a tributary stream, and these effects are also likely to be more frequent.

194. Therefore, to model large events on the assumption that all storm rainfall and runoff reaches, and is contained within, the stream channel is misleading. Understanding the 'hydrological' context of the proposed bridge crossing, as well as the uncertainty inherent in any design flood estimation, are therefore critical considerations.
195. Rather than estimating the total design flow for a catchment, and then assuming this will all pass through/under the proposed bridge, it is necessary to determine the actual capacity of the channel, and the nature of the passage of flood-waters past the site. Scour protection can then be designed to mitigate the energy of these flows, rather than the total runoff from the entire upstream catchment, much of which will not pass under the bridge.

Design flood hydrograph

196. As discussed previously, robust hydraulic models require the input of a design flood hydrograph rather than just the peak discharge of the design event. Therefore, the same methodology applied to the ten largest floods in the Manawatū River to derive a type-hydrograph was also applied to Mangamanaia Stream.
197. The Mangamanaia flow record, however, is very short and there are currently only three flood peaks suitable for deriving a design hydrograph. Other flood hydrographs are unsuitable because either the peak is indistinct, or the flood hydrograph contained more than one peak (Figure D.32 & Figure D.33). Using only three flood hydrographs, particularly those of relatively small events, may bias the resulting design flood hydrograph. However, the shapes of all three hydrographs are remarkably consistent, particularly those for the two larger events (Figure D.33).

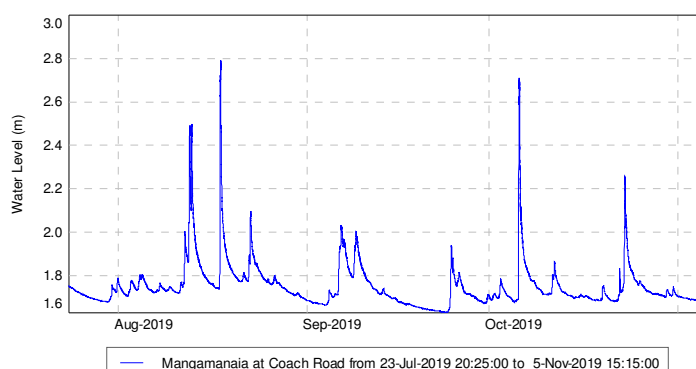


Figure D.32: Mangamanaia at Coach Road water level record.

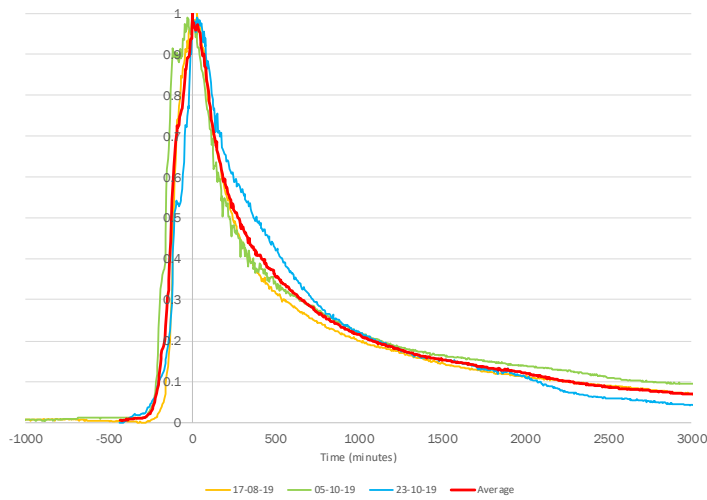


Figure D.33: Flood hydrographs used to derive the type-hydrograph for Mangamanaia Stream.

198. This type-hydrograph was compared with the design hydrograph derived in the same manner from the adjacent Mangapapa at Troup Road flow record. Ten large flood peaks across the 13-year record were selected; (Figure D.34).

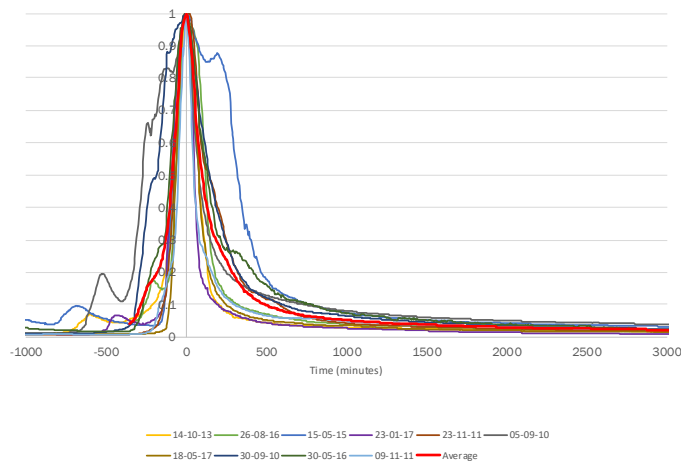


Figure D.34: Flood hydrographs used to derive the type-hydrograph for Mangapapa at Troup Road.

199. The comparison between the two type-hydrographs is displayed in Figure D.35.

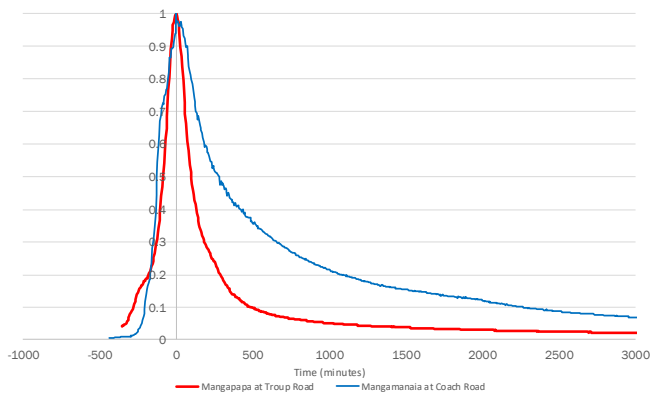


Figure D.35: Comparison of type-hydrographs from the Mangapapa at Troup Road and Mangamanaia at Coach Road.

200. Although the two sites are located in adjacent catchments with similar characteristics, there are differences in the shapes of the two type-hydrographs. The major difference is in their recessional limbs. The rising limbs are very similar. The longer and slower recession shown in the type-hydrograph for Mangamanaia Stream likely reflects the large area of flat floodplain with diffuse drainage in the lower catchment. Once this area gets inundated, it takes a long time for it to drain. This is reflected in the flatter and slower recessional limb on the type-hydrograph.
201. Therefore, while it is considered appropriate to use design flows scaled from the Mangapapa catchment, the type-hydrograph derived from the Mangamanaia record should be adopted. This is despite the fact that it was only derived from three flood events.
202. While the limited amount of empirical data does act as a constraint, it is considered that the design flows and type-hydrograph derived in the above manner are appropriate when analysing the interaction of the Project with Mangamanaia Stream and vice versa.

Design flows for 'small' catchments

203. For small catchments where there is no empirical flow data, various empirical formulae have been developed relating flood magnitude to catchment characteristics such as rainfall, area and slope. Almost all of these formulae are power laws, and they include catchment area as the only independent variable. The best known formula is the Rational Method, particularly for small urban catchments.
204. These formulae require the use of constants and coefficients that must be evaluated by judgment, albeit within guidelines.
205. The Rational Method is used universally and appeals because of its simplicity. It has, however, been the subject of much criticism because of its oversimplification of the rainfall-runoff process. Many of these criticisms are valid when the method is applied to larger catchments, and when it is used in a deterministic sense (i.e. to estimate the peak discharge of an observed storm).
206. The Rational Method is only applicable to small catchments because of its inability to account for the effects of catchment storage in attenuating the flood hydrograph. The recommended maximum size of the catchment to which the method should be applied is 25km² (2500ha) in urban catchments, and

between 3 and 10km² (300ha and 1000ha) for rural catchments; with uncertainty increasing with catchment size.

207. It is generally accepted that the Rational Method produces conservative design flood estimates i.e. higher than actually experienced. This is because users tend to adopt conservative (i.e. high) or 'worst case' runoff coefficients and rainfall parameters. Both of these parameters are harder to estimate accurately as catchment size and variability increase.
208. The small streams draining from the ridge crest into the Manawatū Gorge have catchment areas ranging from 96ha to 447ha (Table D.16). Design flows for Streams 3, 5, 6, and 7 were calculated using the Rational Method.

Table D.16: Catchment details for the streams draining to the Manawatū Gorge.

Stream	Area (ha)	Watercourse length (m)	Elevation (m)		Slope (m/km)	ToC (min)	Rainfall duration (min)	Runoff coefficient
			Min	Max				
3	118	2085	57	331	131	45	30	0.45
4*	447	4865	55	324	55	110	60	*
5	120	2216	53	390	152	47	30	0.45
6	96	2052	51	338	140	45	30	0.45
7	114	2029	50	307	127	45	30	0.45

* Modelled using HEC HMS.

209. A runoff coefficient of 0.45 was used for Streams 3, 5, 6, and 7. This was derived by weighting the proportion of the catchment in pasture and bush and using the runoff coefficients summarised in Table 6.2 of the Transport Agency Stormwater Treatment Standard for State Highway Infrastructure (2010). Catchment elevations were obtained from a 1m resolution digital terrain model (DTM) of the Project area and the height of the confluence of the particular stream with the Manawatū River (Table D.16).
210. Design rainfall intensities were taken from Table 13.1 (current climate) of **Appendix D.1**. The critical duration of the design storm was selected to be conservative (i.e. a slightly higher intensity was selected relative to the catchment ToC). The ToC is the time it takes rainfall from the furthest part of the catchment to reach the point of interest. This is used to determine the critical storm duration and therefore the maximum rainfall intensity.
211. Design flows for Stream 4 were modelled in HEC-HMS using the SCS curve number method outlined in TP108.³² An initial loss of 5mm was adopted

³² Auckland Regional Council 1999: Guidelines for stormwater runoff modelling in the Auckland Region. TP108, April 1999. Report prepared for Auckland Regional Council by Beca Carter Hollings & Ferner Ltd. 19p.

(TP108), and a SCS curve number of 74 (Table 3.3 of TP108 (Group C soils, in bush and pasture)).

212. One hour design rainfall hyetographs were generated using the North Island 1-6-hr. PMP temporal distribution, outlined in Tomlinson and Thompson (1992).³³ The appropriateness of this temporal distribution is discussed in **Appendix D.1**.

213. The resulting design flows for all five streams under the current climate are presented in Table D.17. The relatively small flows in Stream 4 during more frequent events is a result of the 5mm initial loss of rainfall assumed in the HEC-HMS model. This loss of rainfall is not considered within the Rational Method which assumes that all rainfall arrives as runoff (i.e. that there is no storage within the catchment).

Table D.17: Design flows for small streams draining to the Manawatū Gorge (current climate).

Stream	Area (ha)	Design event peak flow (m ³ /s)				
		2	10	20	50	100
3	118	3.5	5.6	6.8	8.2	9.4
4	447	1.3	4.3	5.9	9.1	14.5
5	120	3.6	5.7	6.9	8.4	9.6
6	96	2.9	4.6	5.5	6.7	7.7
7	114	3.4	5.4	6.6	8.0	9.1

Allowance for climate change

214. If predicted global climate change eventuates, it may cause more than just a rise in the world's temperature. Warmer temperatures mean that more water vapor will enter the atmosphere, while also increasing the air's ability to hold moisture.

215. How potential climate change has been incorporated into the design, and the assessment of actual and potential effects of the Project, are discussed in detail in **Appendix D.1**.

216. At the present time, the direct effect of global climate change on stream runoff, and particularly flooding, has not been quantified; however, it is often assumed that an increase in rainfall will result in an equal increase in runoff.

217. The design of stormwater-related infrastructure is based on rainfall and simple rainfall/runoff models (i.e. Rational Method) to estimate the peak discharge during a range of design events in each sub-catchment. The design rainfalls

³³ Tomlinson, A.I and Thompson, C.S. (1992). Probable Maximum Precipitation in New Zealand - the development and application of generalised methods to provide nationwide estimates of PMP. Report prepared for the Electricity Corporation of New Zealand, New Zealand Meteorological Service, Wellington, New Zealand.

adjusted for the effects of climate change to 2130 (given in Table 13.2 of **Appendix D.1**) were applied; either directly, or temporally distributed for the two larger catchments, for any particular design event.

218. The design of bridge crossings over larger streams and rivers followed a different approach to that used for the stormwater infrastructure. Flood estimates were obtained directly from flood frequency analysis of the annual flood maxima series as discussed previously. When analysing these instrumental flow records, climate stationarity was assumed (i.e. the flow record is not affected by climate change). This is considered reasonable given the relatively short length of most of these flow records.
219. To estimate the effects of future climate change on these flood estimates, it is necessary to relate the projected increases in temperature and rainfall (given in Table 8.6 & 8.7 of **Appendix D.1**) to the likely increases in flood peaks. This could be estimated potentially using a calibrated rainfall/runoff model for each catchment. However, because of the size and nature of the catchments concerned, the lack of rainfall and flow data, and the potential for strong orographic effects on rainfall, this is not practicable.
220. Various alternative methods are provided in MfE (2010).³⁴ However, the case studies provide mixed results in terms of the increase in flood magnitude relative to the projected increase in rainfall from the application of calibrated rainfall/runoff models. The assumption of a linear relationship between projected increases in rainfall and peak flood discharge, however, appears to be a reasonable assumption.
221. In considering the effects of future climate change to 2120 therefore, a simple factoring approach was adopted. This factoring approach assumes that the projected increases in flood magnitude approximate the projected increases in rainfall (i.e. the increase in temperature times the percentage increase in rainfall per degree of warming).

Small catchments

222. The potential effects of climate change over the 100-year life of the Project (i.e. to 2120) in the small streams draining from the Project area into the Manawatū Gorge were therefore accounted for by using Table 13.2 of **Appendix D.1**.

³⁴ Ministry for the Environment. (2010). Tools for estimating the effects of climate change on flood flows: a guide for local government in New Zealand. May 2010. Ministry for the Environment, Wellington.

The peak discharges during a range of design events are provided in Table D.18.

Table D.18: Design flows for small streams draining to the Manawatū Gorge (future climate (2120)).

Stream	Area (ha)	Peak flow (m ³ /s)				
		2	10	20	50	100
3	118	4.4	7.4	8.8	10.6	12.4
4	447	2.4	7.2	10.1	15.1	19.4
5	120	4.5	7.5	9.0	10.8	12.6
6	96	3.6	6.0	7.2	8.6	10.1
7	114	4.3	7.1	8.6	10.3	12.0

Manawatū River

223. For the Manawatū River at Upper Gorge, the 24-hour percentage increase in rainfall per degree of warming was adopted. This is based on the assumed ToC for the catchment being approximately 24-hours. Using a predicted average increase in temperature of 2.3°C by 2120, and an 8.6% increase in rainfall per degree of warming, the peak design flows can be adjusted (i.e. increased by 19.8%). This approach should provide some conservatism and resilience to the peak design flows over the life of the Project (Table D.19).

Table D.19: Current design flows and those following adjustment for climate change out to 2120s for the Manawatū River at Upper Gorge.

ARI (Years)	AEP (%)	Current climate (m ³ /s)	Adjusted for climate change to 2120 (m ³ /s)
2.3	43	1,246	1,490
5	20	1,609	1,930
10	10	1,903	2,280
20	5	2,186	2,620
50	2	2,552	3,060
100	1	2,827	3,390
1000	0.1	3,733	4,480
2500	0.04	4,094	4,910

Mangamanaia Stream

224. For Mangamanaia Stream, the 6-hour percentage increase per degree of warming was adopted. This is based on the assumption that the ToC of the catchment during large events is likely to be approximately 6-hours. A 2.3°C increase in temperature by 2120 was also adopted. The resulting design flows are presented in Table D.20.

Table D.20: Current design flows and those following adjustment for climate change out to 2120s for Mangamanaia Stream.

ARI (Years)	AEP (%)	Current climate (m ³ /s)	Adjusted for climate change to 2120 (m ³ /s)
2.3	43	34.5	42
5	20	47.0	58
10	10	53.8	67
20	5	59.4	75
50	2	65.7	83

100	1	69.9	88
1000	0.1	81.9	116
2500	0.04	92.0	127

Interaction of floods in the Manawatū and Pohangina Rivers

225. The proposed bridge across the Manawatū River is located approximately 600m upstream of the confluence with the Pohangina River. Since both of these large rivers have their headwaters in the Ruahine Range, they are likely to be affected by the same storm systems. Flows in the Pohangina River therefore have the potential to cause a backwater effect on flows in the vicinity of the proposed bridge
226. Backwater effects caused by the Pohangina River have the potential to elevate water levels and reduce flow velocities in the vicinity of the proposed bridge. The interaction of these two large rivers therefore needs to be understood and incorporated within the computational hydraulic model used to design and assess the potential effects of the proposed bridge.
227. The largest flood in each of these rivers occurred in February 2004 (Figure D.36). The flood peak in the Pohangina River occurred about 16-hours before that in the Manawatū.

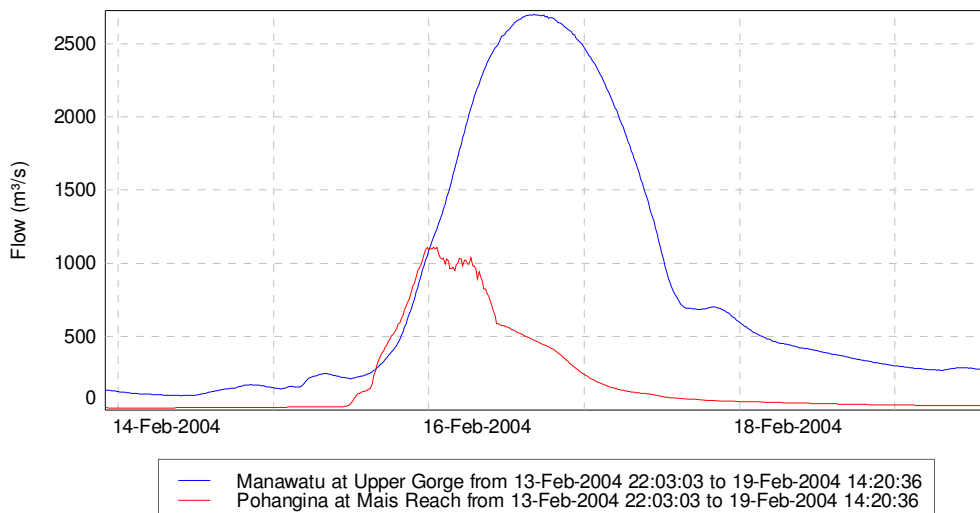


Figure D.36: The largest floods in both the Manawatū and Pohangina Rivers occurred in February 2004.

228. Analysis of the five largest floods recorded in the Manawatū River shows that the flood peaks in the Pohangina River occur on average about 13.6-hours before the corresponding flood peak in the Manawatū River. The shortest time difference between corresponding flood peaks was 10-hours. This suggests that the flood peaks are unlikely to coincide at the confluence of the two rivers; located about 600m downstream of the proposed Manawatū River bridge (BR02).

229. Since both flow recorders are located a significant distance upstream of the confluence, consideration was given to the time it would take the flood peaks to travel from the respective recorders to the confluence.
230. Using gauging data available from Horizons (who maintain both hydrometric sites) relationships were derived between discharge and mean velocity. In the Manawatū River at Upper Gorge, a mean velocity of 2m/s is attained at flows above about 1000m³/s. Higher flows do not result in higher velocities because of the 'throttling effect' of the relatively narrow entrance to the Gorge and the backwater effect this creates upstream.
231. In the Pohangina at Mais Reach, the mean velocity reaches about 3.1m/s at flows above about 800m³/s i.e. the 5% AEP or 20-year ARI event.
232. The mean velocity is the only data available but should provide a reasonable basis for assessing the velocity of the flood peak.
233. The difference in both distance and mean velocity between the two rivers means that it takes the flood peak approximately 10-mins longer to travel down the Manawatū River to the confluence than the flood peak in the Pohangina River.
234. Therefore, once adjusted for both distance and travel time, flood peaks in the Pohangina arrive approximately 13.5-hours before the corresponding flood peak in the Manawatū.
235. During the 2004 regional flood event, the peak discharges in both the Manawatū and Pohangina Rivers were almost equivalent to the 1% AEP design events (i.e. 2,700m³/s compared to 2,800m³/s and 1,109m³/s compared to 1,150m³/s respectively). By the time the flood peak arrived in the Manawatū River, flow in the Pohangina had already dropped so that it was equivalent to only about the mean annual flood (i.e. 477m³/s).
236. While every flood event is likely to be slightly different, a constant discharge equivalent to the 20% AEP event (i.e. 600m³/s) was applied to the upstream boundary of the Pohangina River in the hydraulic model. This simulates realistic conditions when modelling the various design events in the Manawatū River at the proposed bridge.

HYDRAULIC MODELLING

237. The construction of the Project will involve new bridges over the Manawatū River (BR02), at the downstream end of the Gorge, and Mangamanaia Stream (BR07). To inform the design and construction of these bridges, and to assess the interaction of these bridges with the existing fluvial processes and flood hazard, two computational hydraulic models were developed.
238. The roundabout at the eastern end of the Project is located on an extensive floodplain. How the roundabout will interact with the existing flood hazard therefore also needed to be assessed.
239. The computational hydraulic modelling of the two bridges was undertaken using “HEC-RAS version 5.0.7”. HEC-RAS, developed by the United States Army Corps of Engineers (USACE), is used worldwide for modelling open-channel flow and hydraulic structures. HEC-RAS is designed to perform one-dimensional (1D) and two-dimensional (2D) hydraulic calculations for a full network of natural and constructed channels; including overbank flow. In this case, a 2D flow approach was adopted because of the topography of the floodplain and irregular river channel.
240. Because of the lack of empirical data, modelling of the flood hazard in the vicinity of the eastern roundabout was undertaken using a 2D ‘rain-on-grid’ model in Tuflow™. Tuflow has particular strengths when modelling ‘random’ flow across floodplains.
241. Hydrodynamic modelling allows the user (with enough data) to estimate water levels, flows, and velocities at discrete locations and points in time over the duration of a flood.
242. In a 2D hydrodynamic model, flow, velocity and depth are calculated across a near-horizontal planar surface defined by a gridded mesh. Localised values of flow velocity (averaged over the depth) and depth are obtained across a grid network rather than over a channel cross-section as would be the case in a 1D model. This approach is especially useful when modelling flow across a floodplain where the horizontal flow direction is difficult to predict. A 2D model simulates energy losses as flow moves across the floodplain and when flow enters or exits the main channel.

Manawatū River Bridge (BR02)

243. At its western extent, the Project will start from the roundabout at the intersection with SH57. It will then cross the Manawatū River next to the culturally significant Parahaki Island (Figure D.37). Several bridge design options were assessed and the preferred option, based on a multi-criteria analysis, is a precast-concrete balanced-cantilever structure. The bridge will be supported by abutments at each end and three piers. Each pier will be 4m wide and 7.5m long and founded on four bored piles with a pier cap. The middle pier (Pier 2) will be located within the active channel of the Manawatū River upstream of Parahaki Island.



Figure D.37: The Manawatū River at the approximate location of the proposed bridge. Parahaki Island is in the left foreground. Existing erosion is visible on the true right bank.

244. The hydraulics of the bridge location are complex and influenced by rapid lateral expansion of flow at the outlet of the Gorge, braiding at lower flows, and flows from the Pohangina River.

245. Consequently, a 2D hydraulic model of the affected reach of the Manawatū River was developed to support assessments of:

- (a) The potential effects of the bridge on water levels and flow velocities during design events;
- (b) Freeboard during critical design events;
- (c) Bridge hydraulics and bridge design;
- (d) The risk and magnitude of scour, and the design of scour protection;
- (e) The potential effects of debris loading; and

- (f) The potential risk that the central pier might pose to Parahaki Island as a result of changes to the dynamics of flow during large flood events.

246. The development of this hydraulic model and its various assumptions are discussed in **Appendix D.2**.³⁵

247. The model extent, including the confluence with the Pohangina River is shown in Figure D.38.



Figure D.38: Extent and bathymetry of the 2D model of the Manawatū River.

248. The bathymetry used in the HEC-RAS model is a combination of LiDAR generated specifically for the Project, hydrographic survey of the channel bed, and topographic survey to link the various surveys.

249. The downstream limit of the hydrographic survey was approximately 3m upstream of the Ashhurst Bridge, because of shallow conditions under the bridge. To account for the potential hydraulic effect of the Ashhurst Bridge, the channel was extended downstream in the terrain model, using topographic survey and site photos. The Ashhurst Bridge piers and abutments were added to the model, based on as-built information, combined with the topographic survey and LiDAR information. The bridge piers were simulated by elevating mesh cells to the soffit level of the existing bridge. While the terrain model extends approximately 130m downstream of the Ashhurst Bridge, the

³⁵ Te Ahu a Turanga: Manawatū River Base Hydraulic Model. February 2019. Report prepared by Bloxam Burnett & Olliver Ltd (BBO), Hamilton. 9pgs + appendices.

downstream limit of the hydraulic model is approximately 185m upstream of the bridge centreline.

250. The upstream boundary conditions are the design flows for the Manawatū and Pohangina Rivers; the derivation of which was discussed earlier.
251. The initial computational hydraulic model, discussed in **Appendix D.2**, was updated and modified during the design phase of the Project. The various changes to the model, and the assumptions and design criteria adopted are discussed in detail in **Appendix D.3: Te Ahu a Turanga – Manawatū River Bridge 2D HEC-RAS Modelling and Design**.³⁶
252. The proposed Manawatū Bridge will be of Importance Level 4 in terms of the Transport Agency’s Bridge Manual.³⁷ Hence the hydraulic design must be consistent with the following criteria:
 - (a) Serviceability Limit State (SLS) event: 1% AEP flood;
 - (b) Ultimate Limit State (ULS) event: 0.04% AEP flood; and
 - (c) Allowance for climate change in accordance with Section 2.3.2c of the Transport Agency’s Bridge Manual.³⁸
253. The SLS is the state beyond which a structure (i.e. the proposed bridge) becomes unfit for its intended use and the ULS is the state beyond which the strength or ductile capacity of the structure is exceeded, or when it can no longer maintain its equilibrium and becomes unstable.
254. The design also has to satisfy the following Minimum Requirements:
 - (a) (A3.1.1.1) Abutment piles for the Manawatū River Bridge shall be placed outside the limits of the 2-year ARI flood extents. No more than one pier shall be placed in the Manawatū riverbed.
 - (b) (A3.1.1.5) The 100-year ARI design flow shall be used for scour calculations and the design of scour countermeasures. Scour induced by ULS conditions shall also be evaluated and reported, with bridge survival being the required performance standard.

³⁶ Te Ahu a Turanga: Manawatū River Bridge 2D HEC-RAS modelling and design.

³⁷ The Transport Agency (2018), “Bridge Manual”, 3rd edition, Amendment 3, a design manual produced by the New Zealand Transport Agency, Document Number SP/M/022, October 2018.

³⁸ The Transport Agency (2018), “Bridge Manual”, 3rd edition, Amendment 3, a design manual produced by the New Zealand Transport Agency, Document Number SP/M/022, October 2018.

- (c) (A3.1.1.7) The minimum freeboard for the new Manawatū River Bridge shall be 1.2m, measured from the water surface upstream of the bridge to the bottom of the bridge superstructure at the lowest point between the abutments, under 100-year ARI flood conditions.
- (d) (A3.1.1.8) The proposed Manawatū River Bridge must not cause an increase in water surface elevation, measured from downstream to upstream of the bridge, that exceeds 0.06m under exposure to 100-year ARI flood conditions.
- (e) (A3.1.1.12) Debris accumulation on piers shall be based on a rectangular raft, with the thickness determined in accordance with the Transport Agency Bridge Manual Section 2.3.5 and the width based on an estimated maximum tree height of 30m.³⁹

255. The original model included inflows only for the current climate. Therefore, to ensure that the bridge is suitable for use over its entire life, the inflows were adjusted for the potential effects of climate change to 2120 as discussed previously.

256. The original model also included a quasi, steady-state flood hydrograph with the peak discharge being sustained for a period of approximately 10-hours. As discussed above, such an assumption is very conservative (i.e. long). Therefore, the upstream boundary condition was modified to include the design hydrograph derived from detailed analysis of the ten largest floods recorded in the Manawatū River at the upstream end of the Gorge.

257. Since in steep rivers, such as the Manawatū, the flood extent is largely controlled by the peak discharge, and not its duration, this change should not have a significant effect on the extent and depth of flooding. However, it does allow the model to more accurately reflect the actual hydrologic processes operating.

258. The potential influence of the Pohangina River, and its effect on backwater levels, was investigated as discussed above. As a result of that analysis, flows in the Pohangina River during the design event were included as a fixed discharge equivalent to a 20% AEP event under the current climate (i.e. 600m³/s); except when modelling the mean annual flood in the Manawatū when a discharge of 300m³/s was adopted. It is recognised that higher flows

³⁹ Te Ahu a Turanga: Manawatū Tararua Highway – Implementation. Contract No: NZTA 2018576. Appendix A3 – River and Bridge Hydraulics. 4p.

in the Pohangina will generate a greater backwater effect with resulting higher water levels and lower velocities at the proposed bridge. These differences are likely to be within the resolution of the model and this was confirmed with a sensitivity analysis.

259. The final bridge design includes a 7.5m-long pier that is 4m-wide. This was inserted into the bathymetry by locally raising the riverbed to RL100m. The effect of the modelled bridge on the flow hydraulics is expected to be a good representation of the selected bridge design.
260. To allow for the potential effects of debris loading against the piers, the width of the central pier (Pier 2) was increased to 11.1m (i.e. increased by 7.1m) in the manner outlined in the NZ Transport Agency Bridge Manual.⁴⁰ However, a debris raft 3m thick and 30m wide, as opposed to the 15m recommended in the Bridge Manual, was assumed as dictated in the Minimum Requirements.⁴¹

Results

261. To recognise the uncertainty within the hydraulic model, and the fact that shallow flooding of short duration does not pose a hazard, all areas where the depth of flooding is less than 0.1m were removed. It should also be recognised that a depth of flooding of only 0.1m would not present a risk to either people or property. When comparing different scenarios, any change in depth less than ± 0.1 m or velocity less than ± 0.5 m/s was not considered significant.
262. A wide range of scenarios were modelled, and the results are presented in **Appendix D.3**.⁴² However, some key scenarios are discussed below.

Existing environment

263. The active channel of a river is generally defined as that area which is inundated during the mean annual flood i.e. an event with a 2.33-year ARI. The mean annual flood in the Manawatū River at this location has a peak flow of 1246m³/s. The extent of flooding during such an event, and assuming a flow of 300m³/s in the Pohangina River, is shown in Figure D.39. The abrupt lines at the rail bridge in the Pohangina River and upstream of the Ashhurst bridge are the extents of the hydraulic model.

⁴⁰ The Transport Agency (2018), "Bridge Manual", 3rd edition, Amendment 3, a design manual produced by the New Zealand Transport Agency, Document Number SP/M/022, October 2018.

⁴¹ Te Ahu a Turanga: Manawatū Tararua Highway – Implementation. Contract No: NZTA 2018576. Appendix A3 – River and Bridge Hydraulics. 4p.

⁴² Te Ahu a Turanga: Manawatū River Bridge 2D HEC-RAS modelling and design.



Figure D.39: Extent of inundation during a mean annual flood in the Manawatū River and hence the active channel under the existing environment.

264. While flow is confined within the Gorge, as would be expected, a significant portion of the upstream end of the bar forming what is known as Parahaki Island is inundated, as are some of the smaller vegetated bars in the lower Pohangina River.

265. The flood extent defines the minimum position of the two outside piers, relative to the active channel, for the proposed bridge over the Manawatū River.

266. The extent and depth of flooding during the SLS event (i.e. the 1% AEP flood increased to allow for climate change to 2120) is shown in Figure D.40. As discussed previously, a flow of 600m³/s was assumed in the Pohangina River.

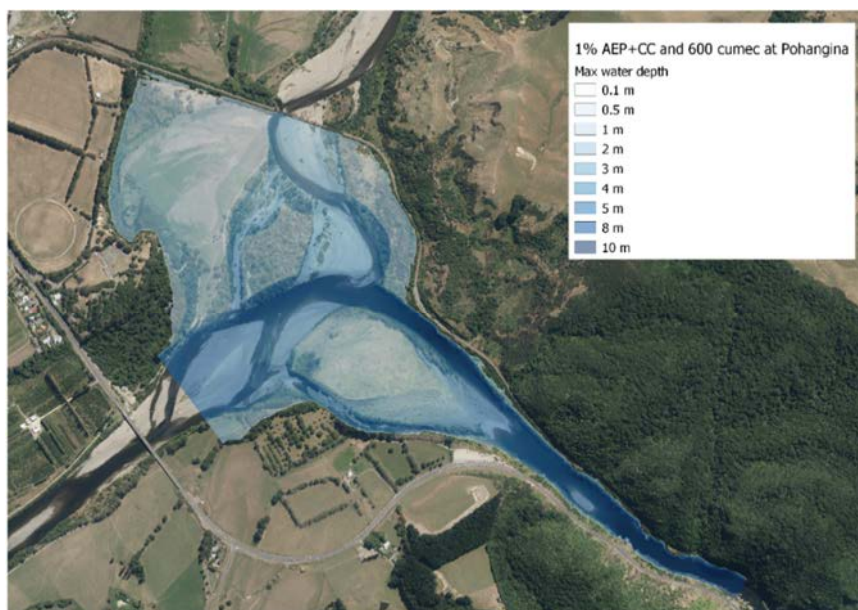


Figure D.40: Extent and depth of inundation during the SLS event (1% AEP + CC) in the Manawatū River without the proposed bridge (BR02).

267. During the SLS, the entire floodplains of both the Manawatū and Pohangina Rivers are inundated. It should also be noted that Parahaki Island is inundated by at least 0.5m, and up to 3m at the upstream end of the gravel bar.
268. The velocity of floodwater during the SLS is shown in Figure D.41. The fastest velocities are in the main channel and thalweg as expected because this is where the greatest depths (i.e. least friction) are also found.

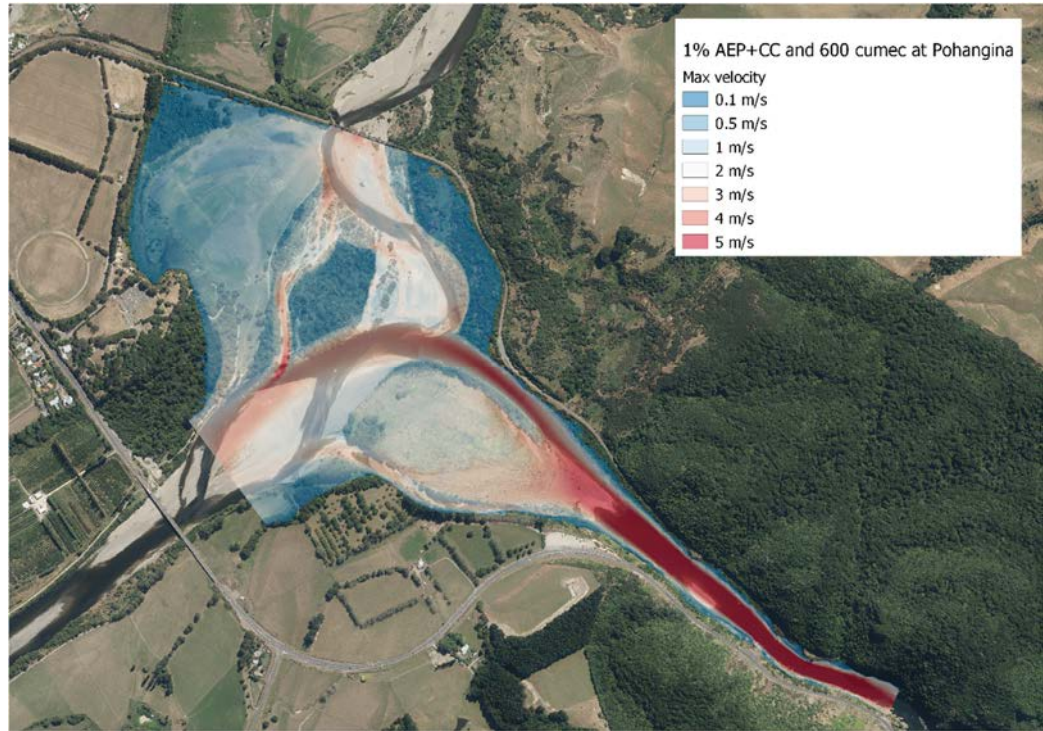


Figure D.41: Velocity of floodwater during the SLS event (1% AEP + CC) in the Manawatū River without the proposed bridge (BR02).

269. Outside of the main channel of the rivers, the velocities are relatively slow i.e. $<0.5\text{m/s}$ as would be expected for shallow water flowing across vegetated terrain. The velocities at the upstream end of the bar forming Parahaki Island are up to 3m/s , and therefore have the potential to erode material with a diameter of approximately 100mm .⁴³
270. Therefore, during a SLS event and under the current channel environment erosion of both the upstream and downstream extents of Parahaki Island might be expected.
271. As discussed, considerable investigation was undertaken into the coincidence of large floods in the Manawatū and Pohangina Rivers. Despite the results of this investigation, there remains uncertainty as to the flows in the respective rivers during the design event. Therefore, the SLS design event in the

⁴³ Sundborg, A. 1956: The River Klarälven, a study of fluvial processes. *Geografiska Annaler* 38: 127-316.

Manawatū River was modelled with both a 600m³/s and 300m³/s flow in the Pohangina River. The differences in water depth and velocity between the two scenarios are shown in Figure D.42 & Figure D.43.

272. Most of the changes in water level are in the immediate vicinity of the Manawatū – Pohangina confluence. However, even in this area water levels only increase by a maximum of 0.35m when the assumed peak discharge doubles (Figure D.42).
273. Any change in water level in the vicinity of the proposed bridge is within the resolution of the hydraulic model $\pm 0.1\text{m}$ (Figure D.42). The assumption regarding discharge in the Pohangina therefore has no significant effect on water level at the proposed bridge; at least over the range of flows modelled.

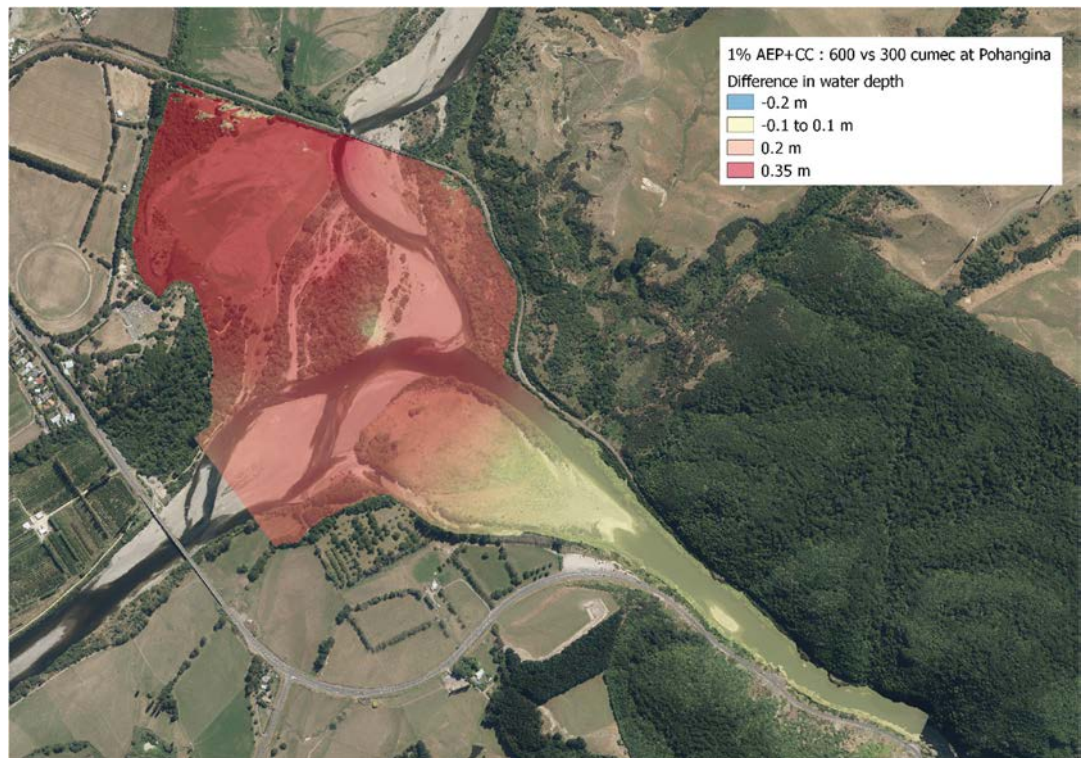


Figure D.42: Difference in water depth during the SLS event (1% AEP + CC) in the Manawatū River, assuming either 300m³/s or 600m³/s in the Pohangina River, without the proposed bridge (BR02).

274. The greater discharge in the Pohangina River results in a greater backwater effect in the Manawatū River. This results in slightly lower velocities, but any change is negligible (i.e. $<0.08\text{m/s}$). The very small change in velocity is a result of the extremely large design flow in the Manawatū River i.e. 3,390m³/s.
275. Likewise, the assumed discharge in the Pohangina River has only a very small effect on the velocity of flow during the SLS design event. Velocities increase slightly within the Pohangina River, as would be expected because of the

increase in discharge. However, the maximum increase is only 0.3m/s (Figure D.43).

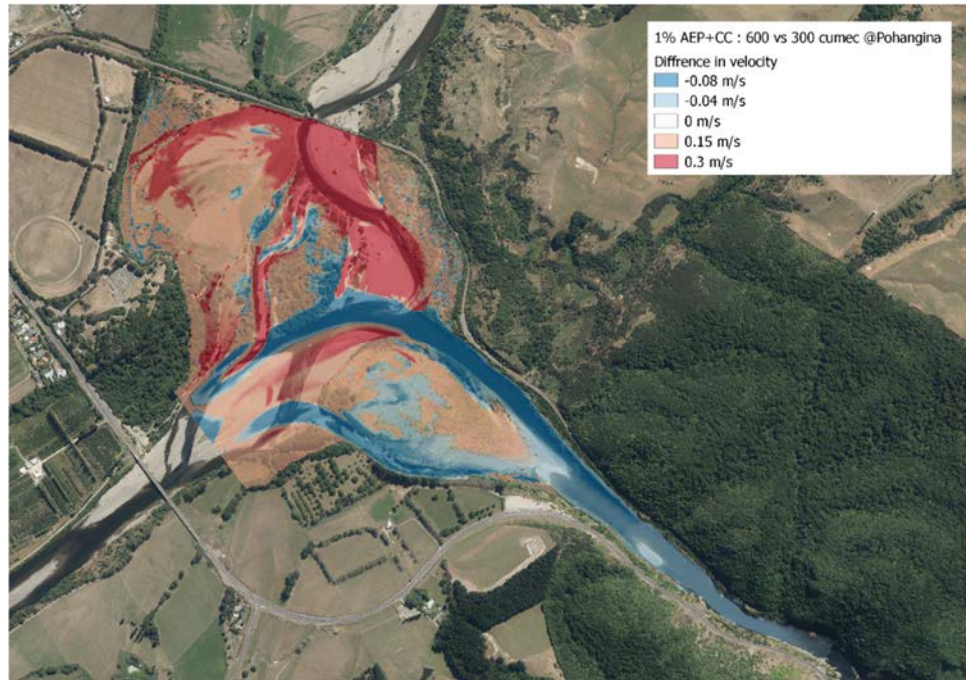


Figure D.43 : Difference in velocity during the SLS event (1% AEP + CC) in the Manawatū River, assuming either 300m³/s or 600m³/s in the Pohangina River, without the proposed bridge (BR02).

With the Project

276. Following modelling of the existing situation, the bathymetry of the model was changed to include the proposed pier and scour protection. The model was then run with the altered configuration (Figure D.44 & Figure D.45).

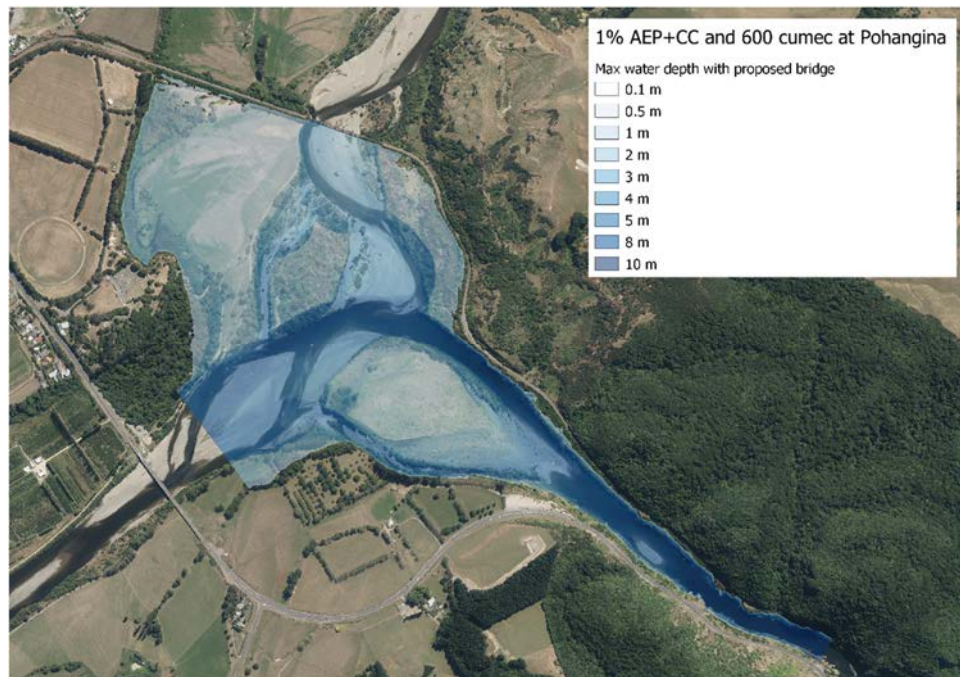


Figure D.44: Extent and depth of inundation during the SLS event (1% AEP + CC) in the Manawatū River following construction of the bridge (BR02).

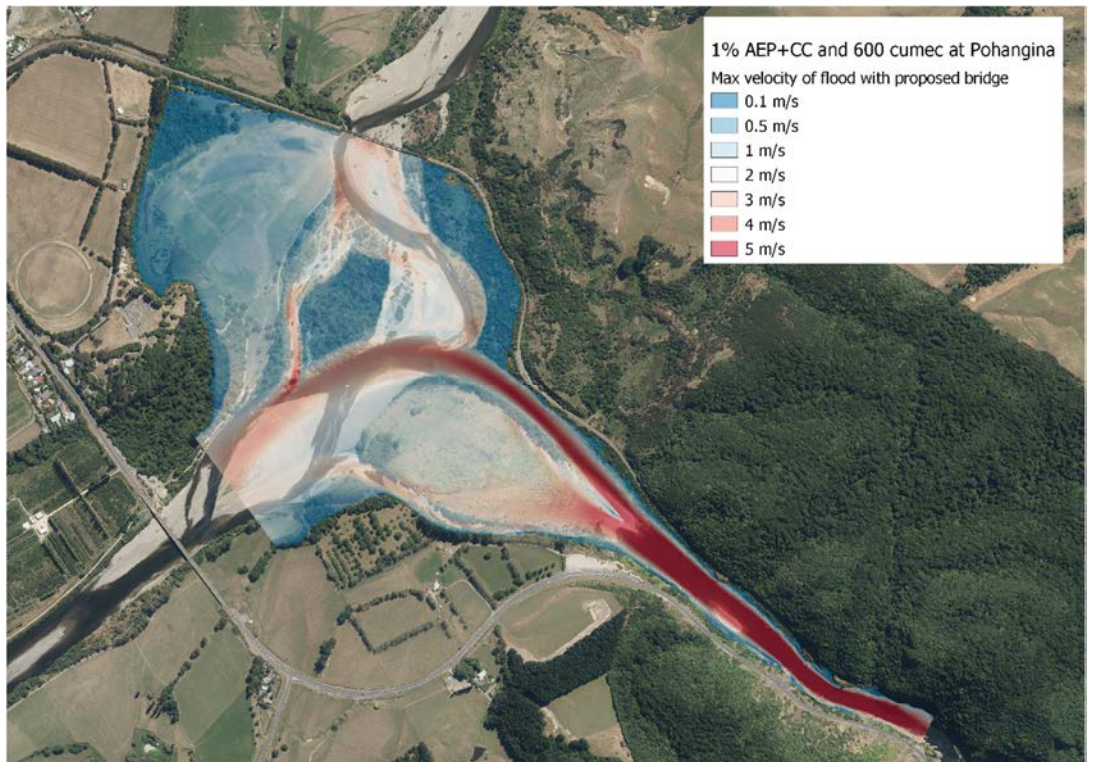


Figure D.45: Velocity of floodwaters during the SLS event (1% AEP + CC) in the Manawatū River following construction of the bridge (BR02).

277. To highlight the potential effect of the pier associated with the proposed bridge, the differences between the two scenarios (with and without the pier) were determined (Figure D.46 & Figure D.47).

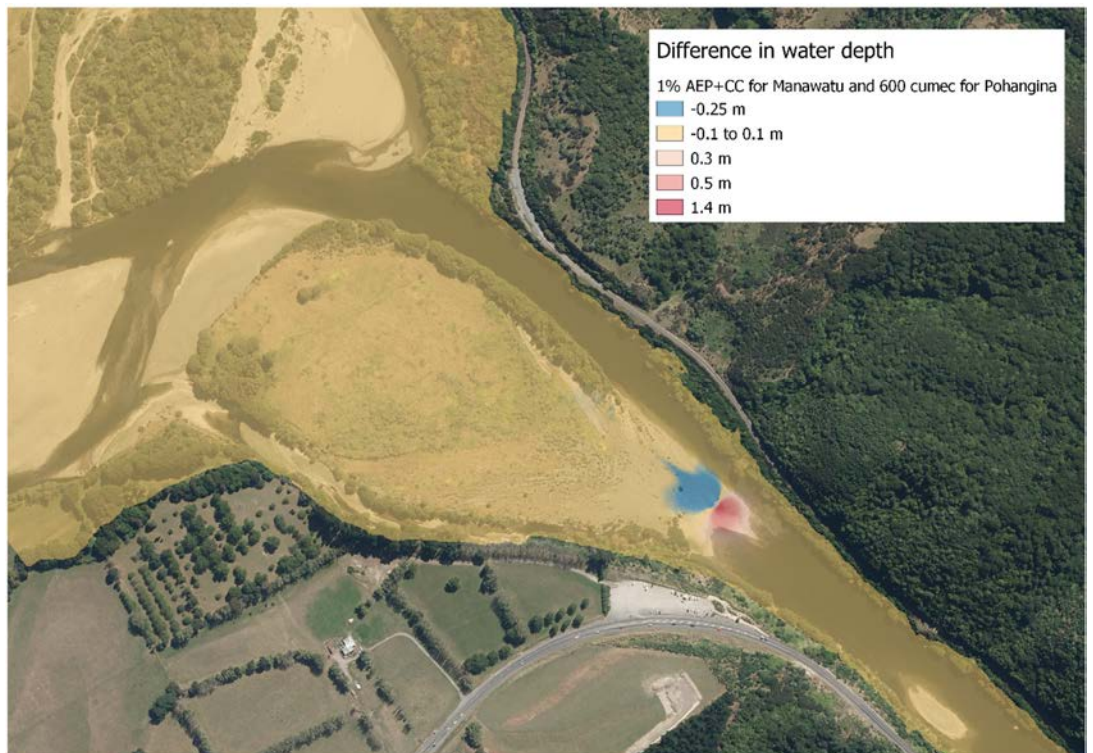


Figure D.46: Differences in water depth during the SLS event (1% AEP + CC) in the Manawatū River following construction of the bridge (BR02) and provision of scour protection.

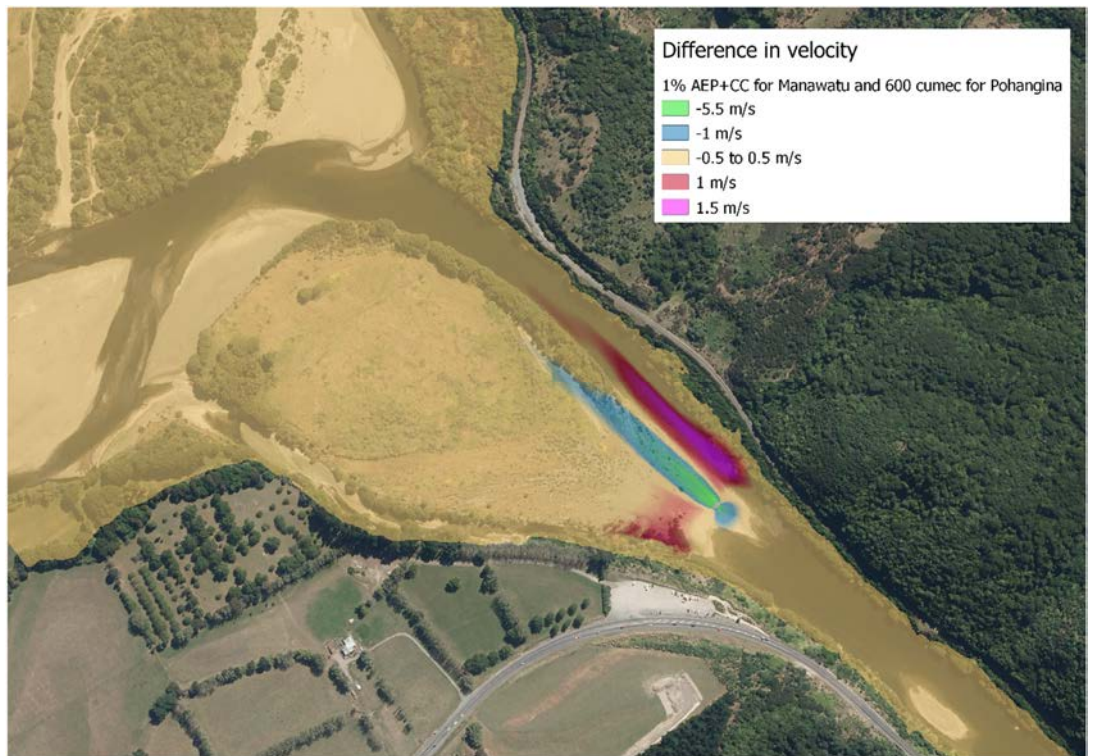


Figure D.47: Differences in velocity during the SLS event (1% AEP + CC) in the Manawatū River following construction of the bridge (BR02) and provision of scour protection.

278. As expected, the effects of the pier during the SLS design event are both very small and extremely localised (Figure D.46). The ‘bow-wave’ upstream of the pier results in a local water level increase of up to 1.4m. This effect, however, dissipates rapidly upstream.
279. Downstream, and in the lee of the pier, there is a slight reduction in water level; up to 0.25m but this will have no significant effect.
280. With respect to Parahaki Island, there is a slight reduction in water level, up to 0.25m, but this is generally restricted to the upstream gravel bar and the left bank of the main channel of the Manawatū River.
281. A similar pattern is shown with respect to velocity. Any significant change (i.e. change greater than $>\pm 0.5\text{m/s}$) is restricted to three locations. The greatest change in velocity, an increase of up to 1.5m/s, is within the centre of the active channel. On the true right of the gravel bar upstream of Parahaki Island the velocity decreases by 1.2m/s. There is also a small increase in velocity (i.e. 0.4m/s) at the entrance to the ‘bypass channel’ on the true left of the Manawatū River (Figure D.47). This increase in velocity could result in slightly more water being ‘deflected’ into this bypass channel and there could be a slight increase in the risk of erosion at the upstream end of this channel. The velocity on the true right of this bypass channel also increase by about 1m/s.

282. There is generally no change to the flow velocity across Parahaki Island. This is expected because of the relatively shallow depth of flooding and good vegetation cover. There is, however, a decrease in velocity along the edge of the gravel bar at the upstream end of Parahaki Island (Figure D.47). This could potentially lead to the deposition of sediment and accretion of this zone of the gravel bar.
283. To illustrate the scale of the differences in water level and velocity caused by the construction of the pier associated with the proposed bridge, a long section was extracted parallel to the flow and passing through the centre of the pier.
284. Water levels in the vicinity of the pier start to increase approximately 70m upstream. They increase very slowly initially and only exceed 0.3m closer than 20m upstream of the pier. While water levels are 'depressed' slightly in the lee of the pier, this is only by about 0.15m (Figure D.48).

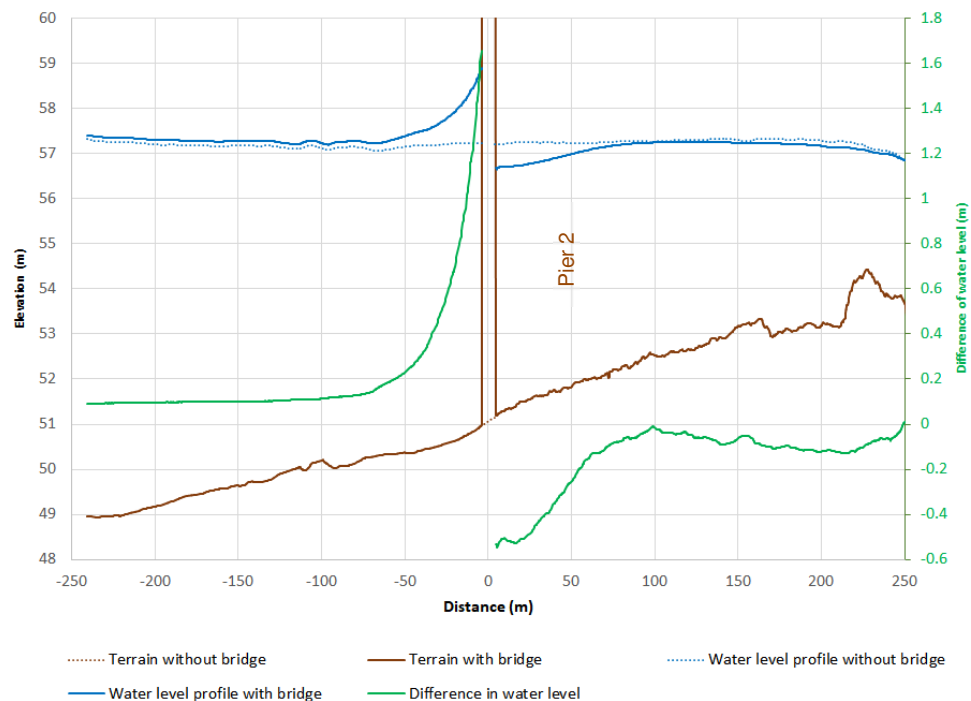


Figure D.48: Changes in water level as a result of construction of Pier 2 of the Manawatū River Bridge (BR02).

285. The effect of the pier on the flow velocity is also very localised. There is a decrease in velocity immediately upstream of the pier which is acting as a 'barrier'. While velocities start to decrease about 50m upstream of the pier, they only reduce by more than 0.5m/s about 30m upstream. At the pier velocities decrease by about 4.5m/s (Figure D.49).
286. The effect of the pier dissipates more slowly in a downstream direction with velocities increasing at a slower rate than they decreased upstream (Figure D.49). After approximately 250m they are still about 0.5m/s slower than they

would be without the pier. Note that this reduced velocity is in the vicinity of the gravel bar upstream of Parahaki Island and it could lead to the deposition of any slightly coarser material.

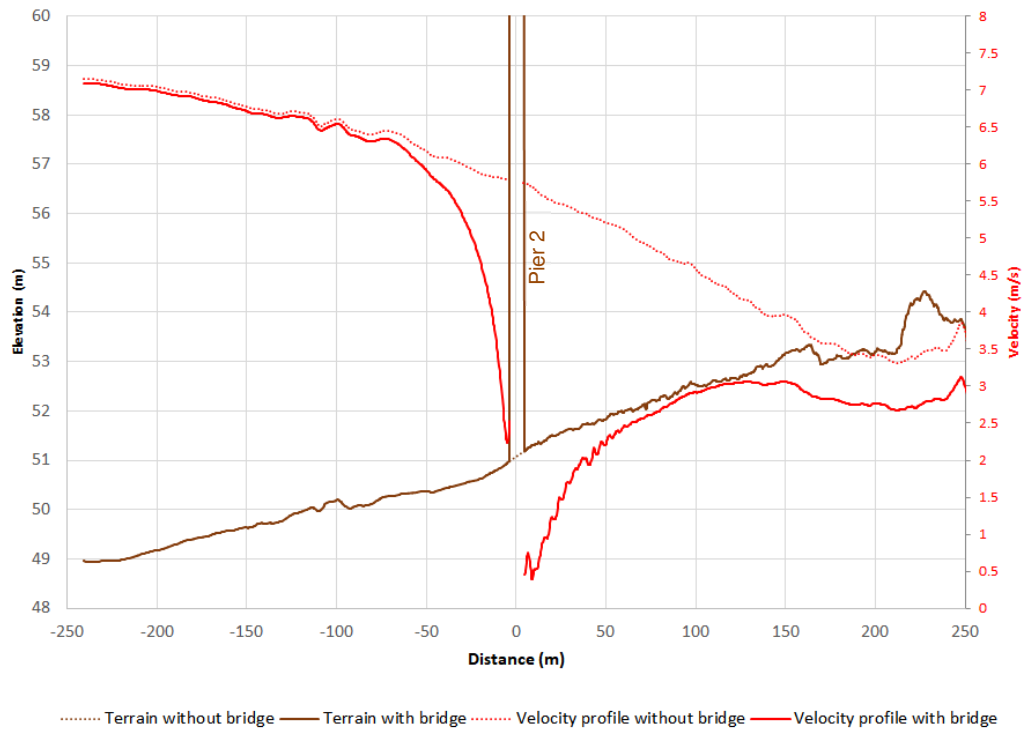


Figure D.49: Changes in velocity as a result of construction of Pier 2 of the Manawatū River Bridge(BR02).

287. The relationship between the change in water level and velocity with distance from the pier is shown in Figure D.50.



Figure D.50: Changes in water level and velocity as a result of construction of Pier 2 and the Manawatū River Bridge (BR02).

Scour

288. The location of a pier for the bridge in the active channel of the Manawatū River has the potential to generate scour (Figure D.51). The potential for scour was assessed using the water depths and velocities from the 2D HEC-RAS model during the design events, and the methodology outlined in the Minimum Requirements⁴⁴ and Melville & Coleman (2000).⁴⁵

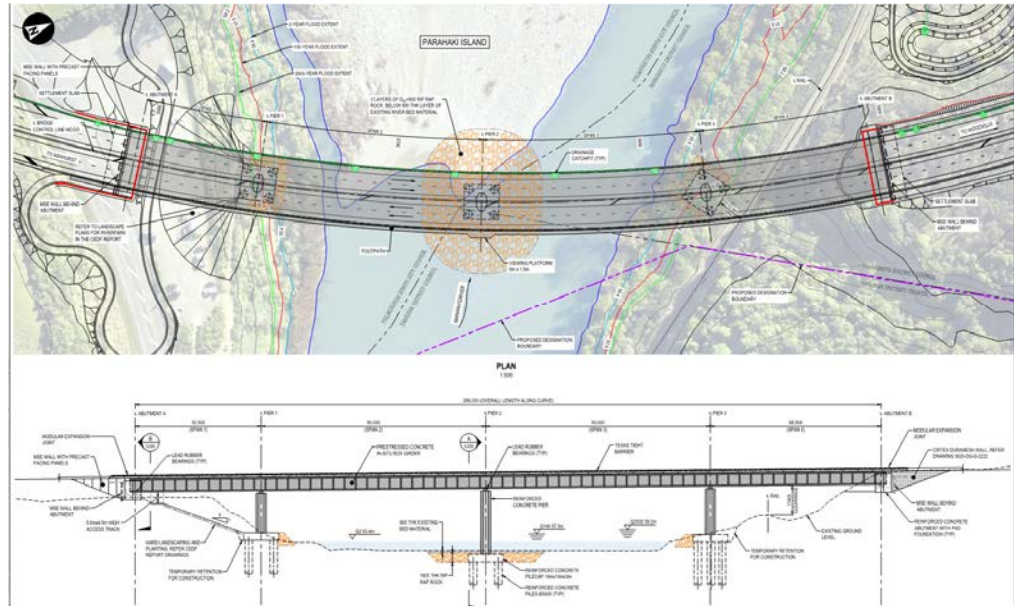


Figure D.51: Preliminary configuration of the proposed bridge over the Manawatū River.

289. At this stage, there is limited detailed geologic information (cross-sections, borehole logs, particle size analysis, etc) available (Figure D.52). Hence the preliminary scour analysis and design are based on the following conservative assumptions:

- (a) All bed and bank material to the bottom of the piles is of a sandy-gravel material with a median particle size of 150mm (based on site information);
- (b) Scour is not limited by the presence of bed rock; and
- (c) The thalweg of the river will not shift significantly north (i.e. towards the true right bank and away from Pier 2) from its present position.

290. The scour analysis, reported in **Appendix D.3**, shows that in general the bed level will scour down to a maximum of RL 49.3m and RL 48.4m respectively

⁴⁴ Te Ahu a Turanga: Manawatū Tararua Highway – Implementation. Contract No: NZTA 2018576. Appendix A3 – River and Bridge Hydraulics. 4p.

⁴⁵ Melville B W and Coleman S E (2000), “Bridge Scour”, Water Resources Publications, 2000.

during the SLS and ULS events. The thalweg during these two design events will scour down to a maximum of RL 47.1m and RL 45.5m respectively.

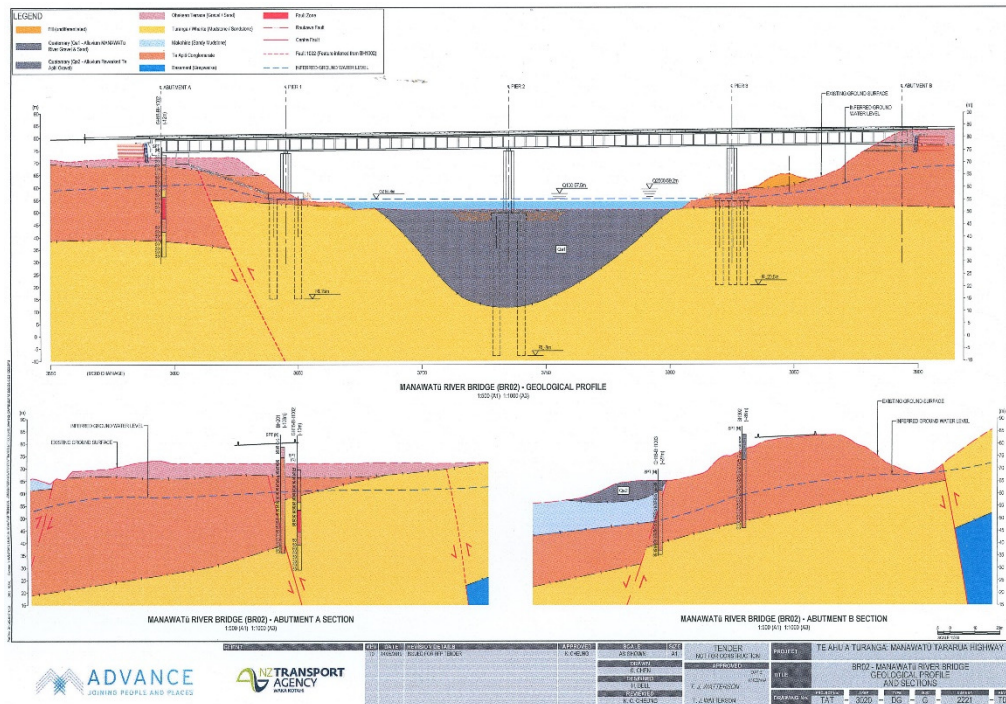


Figure D.52: Geological profile and sections at the location of the proposed bridge.

291. It is unlikely that the thalweg will migrate to coincide with the centre pier as the Manawatū River at this location is generally migrating towards the true right bank. This is because the thalweg, the line of maximum depth and therefore velocity, is towards this bank. This explains the current erosion of the right bank downstream of the proposed bridge location.

292. The lowest local bed levels near the centre pier are expected to be RL 37.9m and RL 34.2m for the SLS and ULS events respectively. This assumes a 30m wide, 3m thick debris raft on the pier (i.e. an extreme scenario).

293. Estimates of the maximum scour at the three piers during various design events are shown in Table D.21. These estimates allow for general scour, local scour, and the effects of a debris raft. It should be noted that these estimated scour depths are likely to be extremely conservative (i.e. high) because of the assumption of an ‘infinite’ depth to bedrock. In reality, scour will be limited by the actual depth to bedrock.

Table D.21: Estimates of the maximum scour at the piers based on conservative assumptions.

Design event	Flood level	Velocity (m/s)	Pier 1	Pier 2	Scour depth below Pier 2 pile cap	Pier 3
100-year (SLS)	RL 57.5	5.2	51.6m	RL 34.1	12.5m	N/A
2500-year (ULS)	RL 59.2	7.0	50.6	RL 27.3	19.3m	N/A

294. The potential for scour will be refined following comprehensive exploratory drilling and bed material characterisation.
295. Note that there is no potential for scour at Pier 3 because it is outside of the active flow path, even during the most extreme design event.
296. Rocks with a median size (i.e. D_{50}) of 0.9m may be required to minimise the potential effect of scour on Parahaki Island during the SLS event (i.e. the 1% AEP flood increased to allow for the potential effects of climate change to 2120). It has been assumed that 2350m² (4230m³) of scour protection will be required and this has been included in the hydraulic model discussed above. This is the scenario adopted when assessing the potential effect of construction of the pier and bridge on the river hydraulics.

Conclusions on Manawatū River Bridge (BR02)

297. The hydraulic computational model allows the potential effects of the proposed bridge across the Manawatū River to be quantified. These effects are both very small and extremely localised. The 'bow-wave' upstream of Pier 2 results in a local water level increase of up to 1.4m, however, this effect dissipates rapidly upstream. Downstream, and in the lee of the Pier 2, there is a slight reduction in water level; up to 0.25m.
298. Any significant change in velocity is restricted to three locations. The greatest change is an increase in velocity, up to 1.5m/s, within the centre of the active channel. There is also a small increase in velocity at the entrance to the 'Parahaki bypass channel' on the true left of the Manawatū River. The other change is a reduction in velocity in the lee of Pier 2.
299. The construction of the bridge and piers will have no adverse effects on Parahaki Island. There will be a slight reduction in water level, up to 0.25m, but this is generally restricted to the upstream gravel bar and the left bank of the active channel of the Manawatū River. There is no change to the flow velocity across Parahaki Island because of the relatively shallow depth of flooding and good vegetation cover. There is, however, a decrease in velocity along the edge of the gravel bar at the upstream end of Parahaki Island. This could potentially lead to the deposition of sediment and accretion of this zone of the gravel bar.
300. Scour protection will mitigate any potential adverse effects to Parahaki Island.

301. In my professional opinion, the effects of constructing the proposed bridge over the Manawatū River are likely to be extremely small and localised to the immediate vicinity of the centre pier (Pier 2). Any changes to the existing flood hazard will in my professional opinion be no more than minor.

Mangamanaia Bridge (BR07)

302. Towards its eastern end, the Project will cross Mangamanaia Stream (Figure D.53). A 2-D computational hydraulic model was developed to assess:

- (a) The potential interaction of the proposed bridge with the Stream;
- (b) The effect of the proposed bridge on the existing flood hazard; and
- (c) To provide a range of design parameters for the bridge.



Figure D.53: Mangamanaia Stream in the approximate location of the proposed bridge.

303. The development of the model, its assumptions, and a range of results are discussed in detail in **Appendix D.4: Te Ahu a Turanga - Manawatū Tararua Highway: Mangamanaia Bridge 2D Hydraulic Analysis**.⁴⁶ The extent of the hydraulic model is shown in Figure D.54 and extends approximately 350m upstream and downstream of the proposed bridge.

304. The derivation of the design flows and the design hydrograph for Mangamanaia Stream have been outlined previously. These include design flows under both the existing climate and that which may exist by 2120.

⁴⁶ Te Ahu a Turanga - Manawatū Tararua Highway: Mangamanaia Bridge hydraulic analysis.

305. Flow at the upstream boundary of the model was the design hydrograph with a peak discharge appropriate for the specific design event. Flow at the downstream limit of the model, at the start of each model run, was the water depth under normal conditions. This was calculated from the average channel slope (i.e. 0.7%).

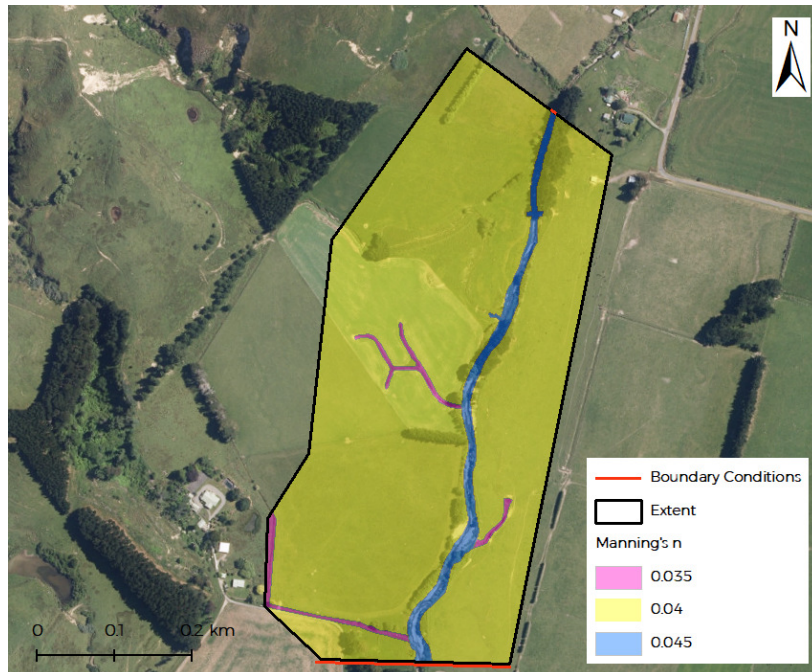


Figure D.54: Extent of the hydraulic model of Mangamanaia Stream, the location of the boundary conditions, and the distribution of Manning's roughness.

306. The banks of Mangamanaia Stream are covered in long grass and weeds with occasional trees and have collapsed into the stream at various locations (Figure D.55). The riverbed is composed mainly of gravel and sand (Figure D.56). This information, together with the size and slope of the channel, was used to estimate an appropriate range of friction values for the channel (Manning's n).



Figure D.55: Mangamanaia Stream showing typical bank collapse and the material comprising the bed and banks.



Figure D.56: A short reach of Mangamanaia Stream showing typical channel form and the characteristics of the bed and banks.

307. A wide range of scenarios were modelled to inform the design of the bridge and associated scour protection. These included the 10% AEP, 1% AEP and 0.04% AEP events under the current climate, and the 1% AEP event adjusted for the potential effects of climate change over the life of the Project.
308. A sensitivity analysis showed that over the ranges tested, the roughness of the channel and friction slope used for the downstream boundary condition have no significant effect on the depth and velocity of the flood waters.
309. Therefore, although the hydraulic model of Mangamanaia Stream is largely uncalibrated, it is considered to provide a realistic indication of both the existing flood hazard and the potential effects of the proposed bridge. While there may be some uncertainty regarding the precise numbers (i.e. the exact depths and velocities), the relative changes between the different scenarios are likely to be representative.
310. It must be recognised that this reach of Mangamanaia Stream flows across an extensive floodplain. Consequently, the extent of overbank flooding is significant even during the current 10% AEP (i.e. 10-year ARI) event (Figure D.57).
311. To recognise the uncertainty within the hydraulic model, and the fact that shallow flooding of short duration does not pose a hazard, all areas where the depth of flooding is less than 0.1m have been removed.
312. During a 10% AEP flood there is considerable flooding of the true right bank and the filling of drainage depressions and flow paths across the floodplain. Apart from the various paleochannels and larger drainage depressions, where the depth flooding can be up to 0.8m, flooding is generally shallow i.e. <0.3m.

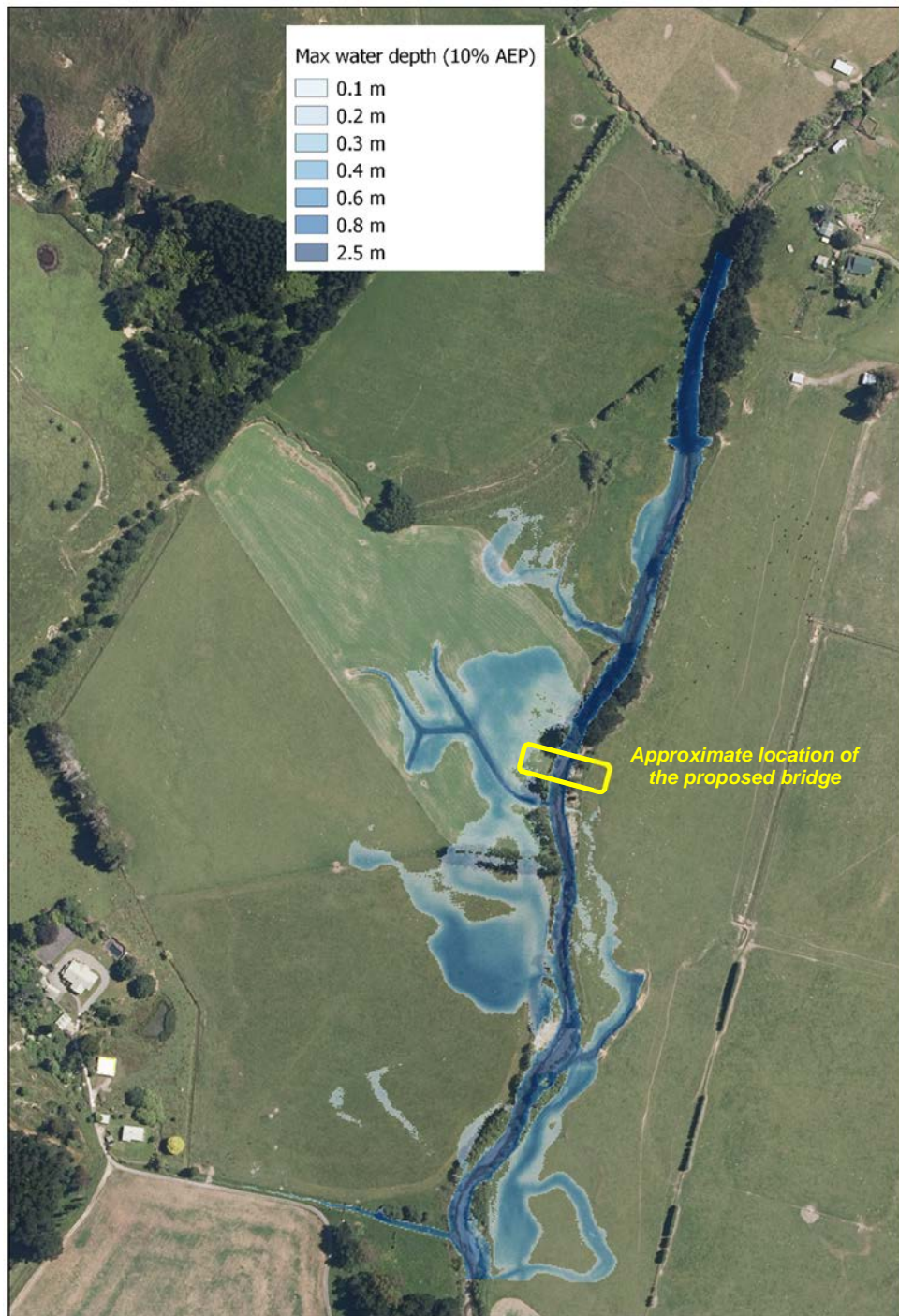


Figure D.57: Depth of the flooding during a 10% AEP event under the current climate.

313. Given the nature of rainfall over the Mangamanaia catchment during the design event, there will also be flooding of the various stream and tributaries that flow across the floodplain. The extent of this type of flooding is not shown in Figure D.57 but will be largely consistent under all scenarios.

314. Given the limited empirical flow information available for the Mangamanaia catchment, there is some uncertainty regarding the magnitude of the various design flood peaks. The peak discharges used in this analysis are significantly higher than those provided in the Minimum Requirements (and therefore more

conservative). It is worth noting, however, that the 10% AEP design flow provided in the Minimum Requirements largely remains within the channel, with limited overbank flooding. This is considered unrealistic as bankfull discharge, when the channel reaches capacity and overbank flow occurs, is generally about a 2.33-year ARI event. This suggests that the design flows in the Minimum Requirements are too low. The flows used in this analysis are considered more realistic, although possibly a little high (i.e. conservative).

315. The effect of the peak discharge on the extent and depth of flooding, however, is not as great as might be imagined. This is because of the relatively extensive floodplain, and the fact that a large change in peak discharge can be accommodated by a relatively small change in the depth and extent of flooding.
316. The area of flooding shown in Figure D.57 is approximately 41,087m². Increasing the water depth by only 0.1m would increase the volume of water 'stored' over this area by approximately 4,100m³. Given the short duration of floods in Mangamanaia Stream, this is equivalent to a significant difference in the peak discharge.
317. The relatively small effect of changing the peak discharge can also be seen in Figure D.58. Increasing the magnitude of the design event from 10% AEP under the current climate (54m³/s) to 1% AEP adjusted for climate change to 2120 (88m³/s) results in a relatively small increase in the area which is inundated; 75,000m² compared to 41,000m², or only an 83% increase for a much more severe event. The increased volume of water is accommodated by a relatively small increase in the depth of flooding rather than a large increase in the area inundated. Again, the area flooded is dominated by paleochannels across the surface of the floodplain, with a slight expansion of the area inundated and the 'connection' of adjacent areas which are flooded.
318. Since the SLS for the bridge, as defined in the Transport Agency Bridge Manual, is the 1% AEP event (including consideration of the potential effect of climate change over the life of the Project) this scenario was modelled both with and without the proposed bridge.

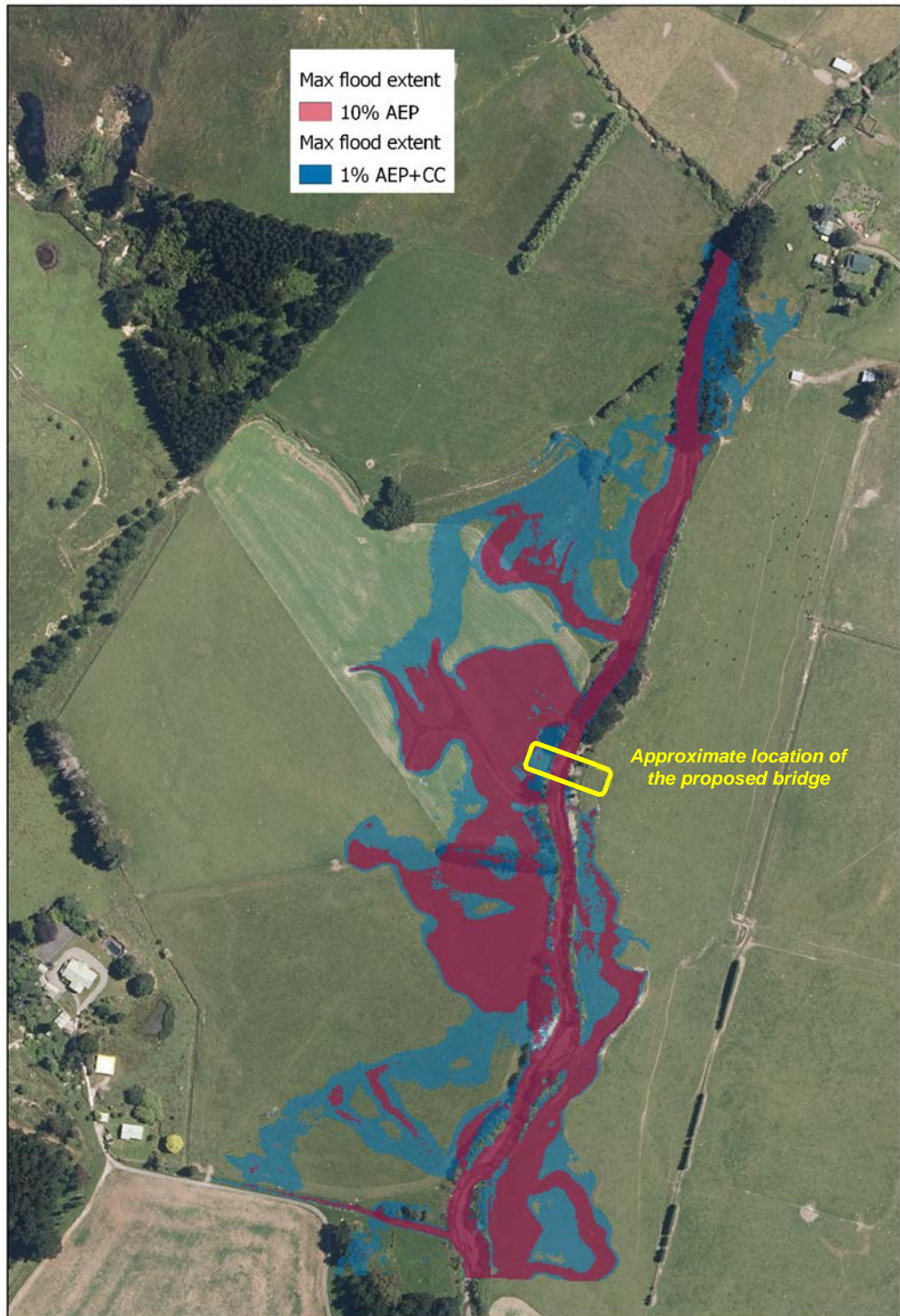


Figure D.58: Extent of flooding during a 10% AEP event under the current climate and a 1% AEP event adjusted for climate change to 2120.

Results

Existing environment

319. The depth and velocity of overbank flooding during the 1% AEP event, including the effects of climate change to 2120, are shown in Figure D.59 & Figure D.60.

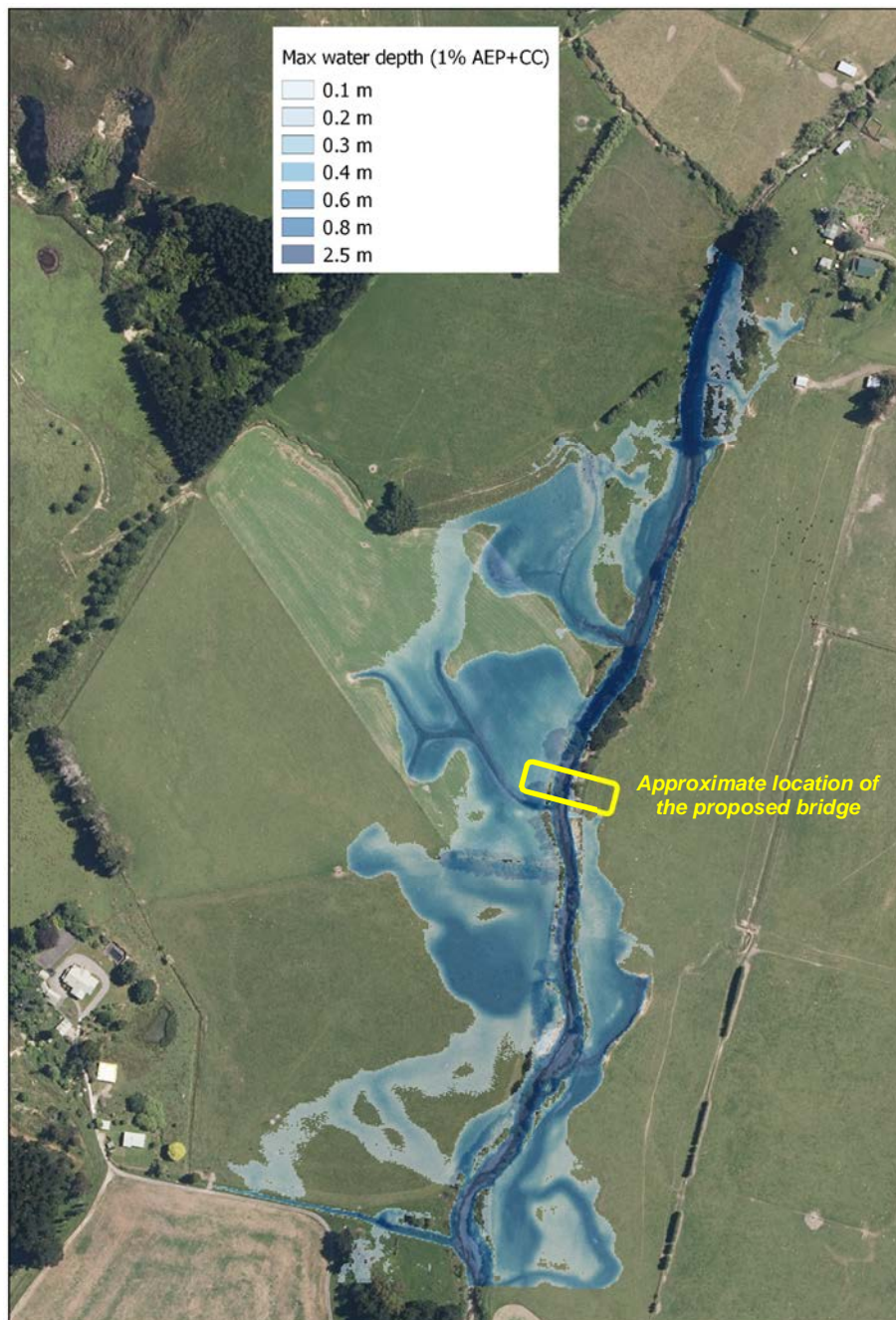


Figure D.59: Maximum depth of flooding during a 1% AEP event adjusted for climate change to 2120.

320. As for the smaller design event, the bulk of the flooding occurs on the true right bank, with only limited 'spill' occurring onto the left bank. The majority of the flooding is less than 0.6m, and that outside of obvious paleochannels is generally less than 0.3m (Figure D.59).

321. It is also apparent that most of the flood water is essentially inundation of lower lying areas with 'standing water' rather than flowing water with a significant velocity component. While velocities within the main channel can be up to 2.5m/s, flow within the paleochannels is generally less than 0.8m/s, and that across the floodplain less than 0.5m/s (Figure D.60).

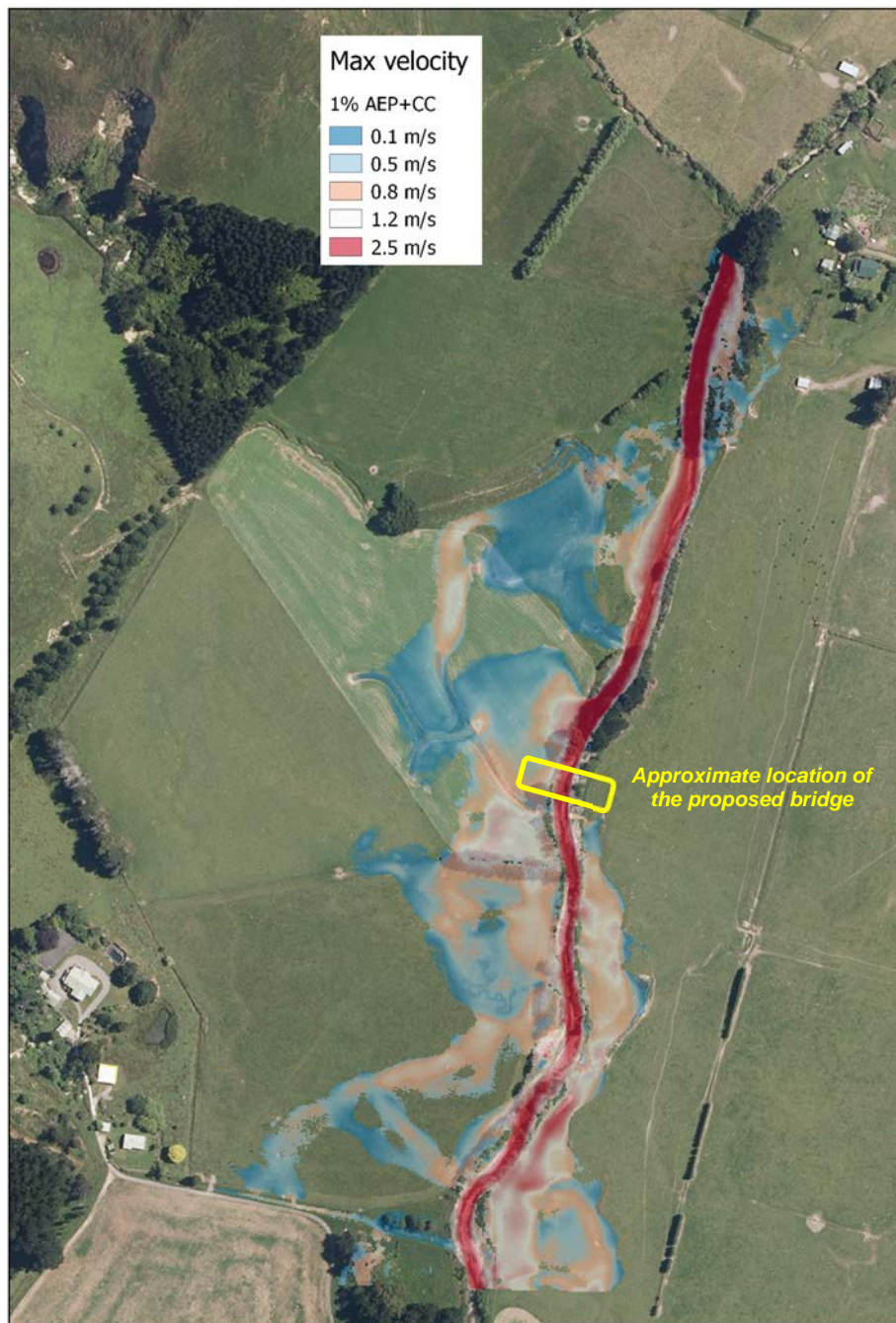


Figure D.60: Maximum velocity of flood waters during a 1% AEP event adjusted for climate change to 2120.

322. These velocities are so low that they are unlikely to pose a hazard, or cause erosion of the vegetated ground and the mobilisation of any sediment.

323. Flooding during even this extreme event, outside of the main stem of Mangamanaia Stream, is generally of shallow depth and slow velocity.

With the Project

324. The preliminary design of the proposed bridge over Mangamanaia Stream is shown in Figure D.61. The proposed bridge and abutments were included in the hydraulic model by modifying the underlying terrain to reflect that likely after

construction of the bridge. It should be noted that the proposed bridge is supported by abutments on either bank. There is no pier within the channel which could interfere with the ‘natural’ hydraulic behaviour of the Stream. It should also be noted that the preliminary design includes a constructed wetland adjacent to the upstream side of the bridge on the true right bank. This was included in the model on the assumptions that: its extent is as shown on the plans; it would not be bunded; it would be formed in the existing terrain; and it would have a depth of approximately 1.5m. The relatively small volume of this wetland relative to floods in the Mangamanaia catchment mean that its effect on flooding, while positive, is small.

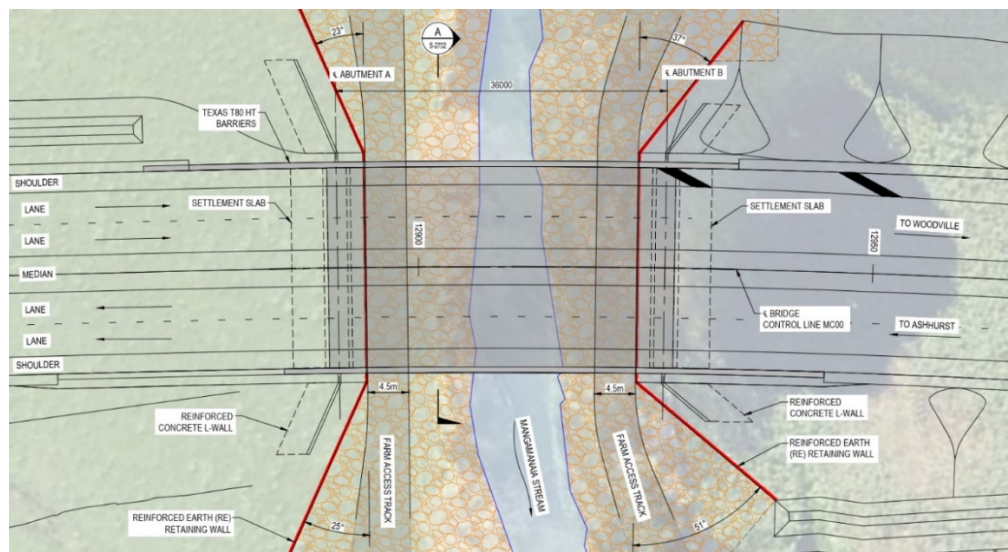


Figure D.61: Concept design of the proposed bridge over Mangamanaia Stream (BR07).

325. All of the effects of the construction of the proposed bridge over Mangamanaia Stream are restricted to the immediate vicinity of the bridge (Figure D.62 & Figure D.63). Most of these effects are actually a result of the highway constructed across the floodplain rather than the actual bridge. The raising of the highway relative to the existing terrain will displace some floodwater. This leads to less flooding in some areas but slightly deeper flooding in others. Much of the displaced floodwater will be accommodated within the wetland constructed on the upstream side of the bridge.
326. It is also apparent that changes in the velocity of the floodwater as a result of the bridge reflect the changes in depth (Figure D.63). Those areas where the depth of flooding has reduced are also those where the velocity of flow has reduced. Likewise, those areas where the depth of flooding has increased also experience a small increase in the velocity of flow.

327. In general, the changes in both the depth and velocity of flooding modelled as a result of constructing the proposed bridge (BR07) are small, even during a very large design event. The effects during smaller floods in the Mangamanaia catchment will be even smaller (i.e. negligible).

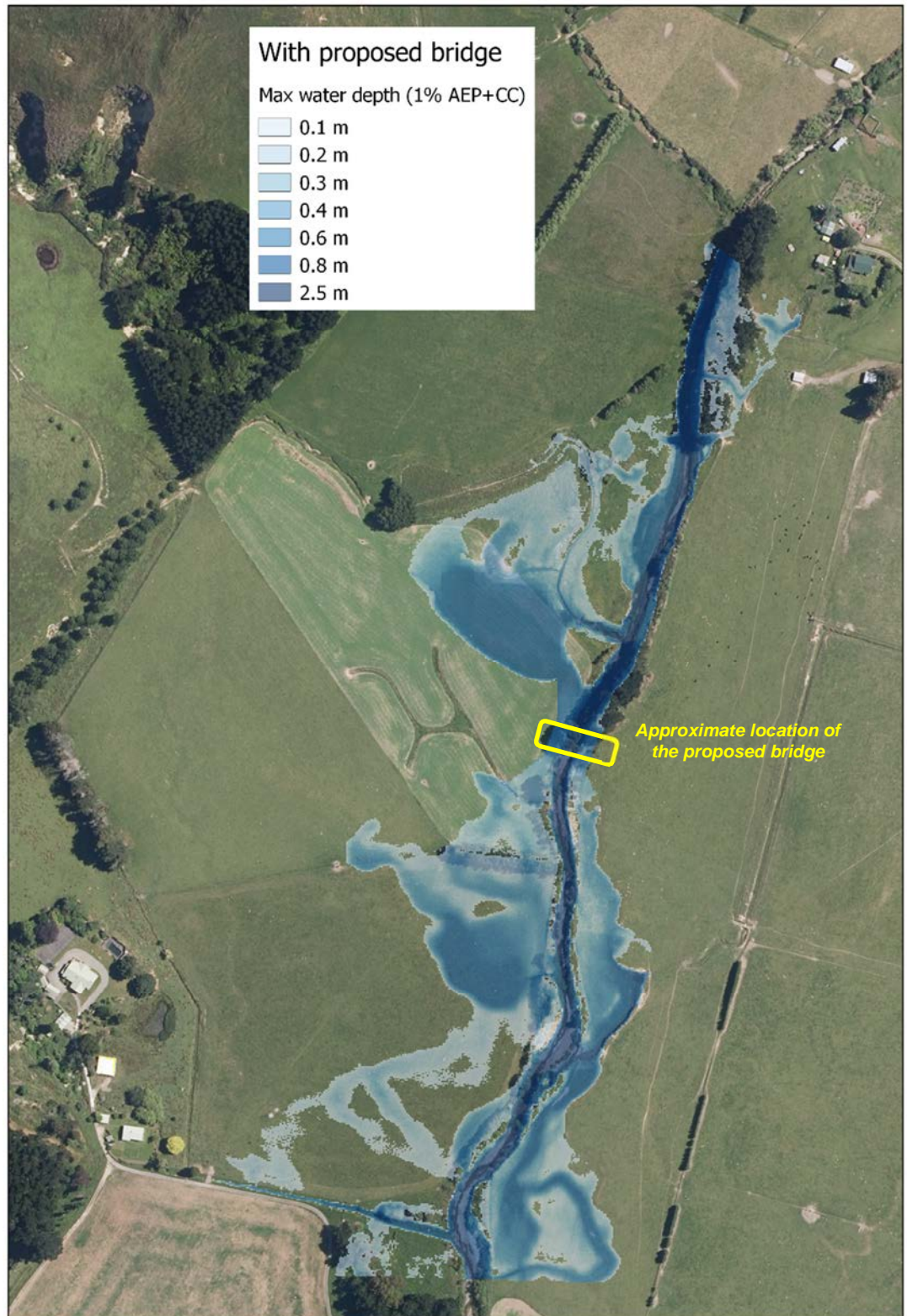


Figure D.62: Maximum depth of flooding during a 1% AEP event adjusted for climate change to 2120 following construction of the proposed bridge.

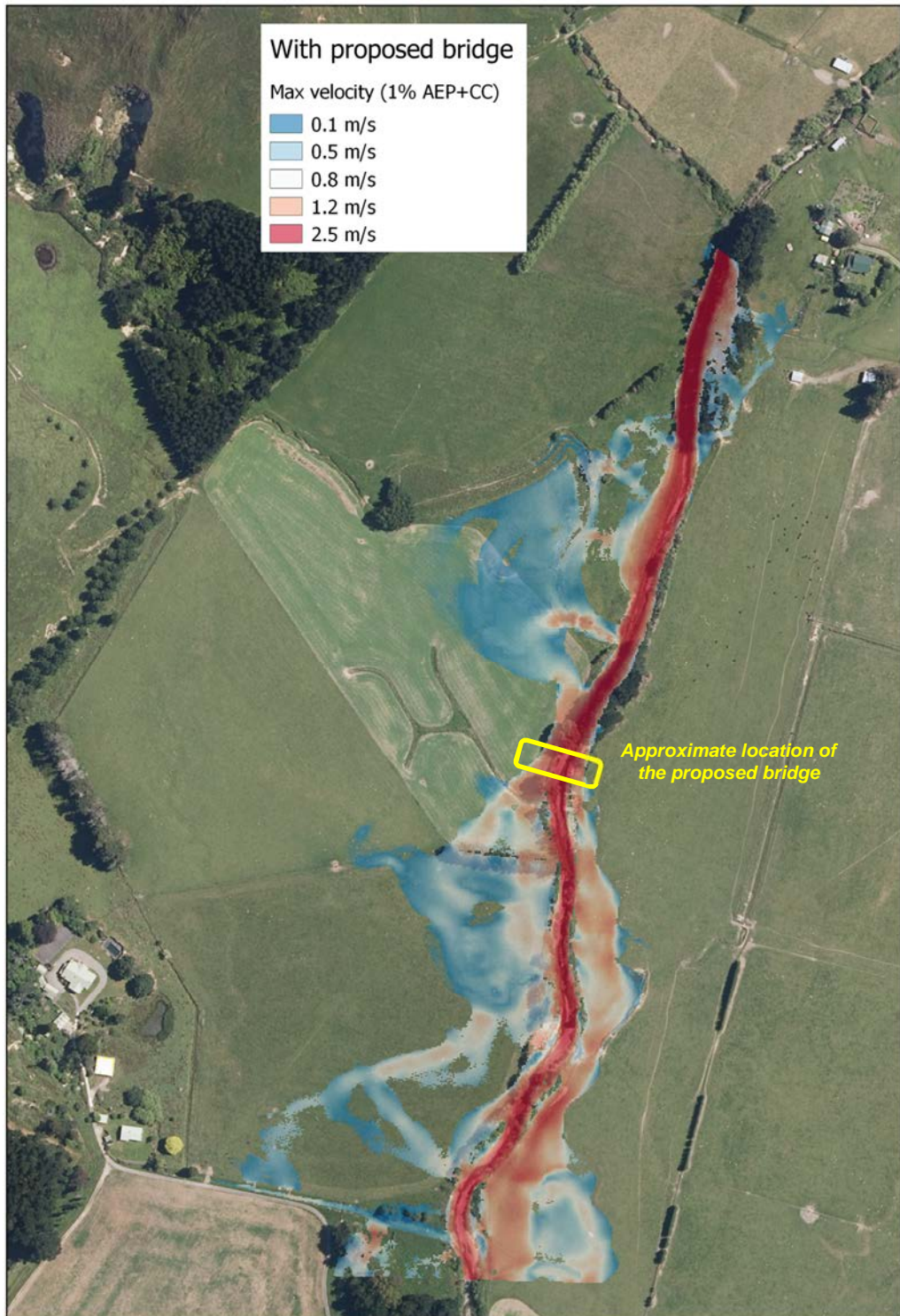


Figure D.63: Maximum velocity of flooding during a 1% AEP event adjusted for climate change to 2120 following construction of the proposed bridge.

328. To highlight the potential effects of the proposed Mangamanaia bridge during the 1% AEP design event, including the effects of climate change to 2120, the water depths and velocities from the two hydraulic models (i.e. that with and that without the proposed bridge) were compared.

329. Following construction of the bridge there is a small increase in water depth immediately upstream of the Project (Figure D.64). Approximately half of the

increase in depths greater than 0.5m is within the wetland which will be constructed in association with the Project. This wetland will be approximately 1.5m deep, hence the area of increased water levels.

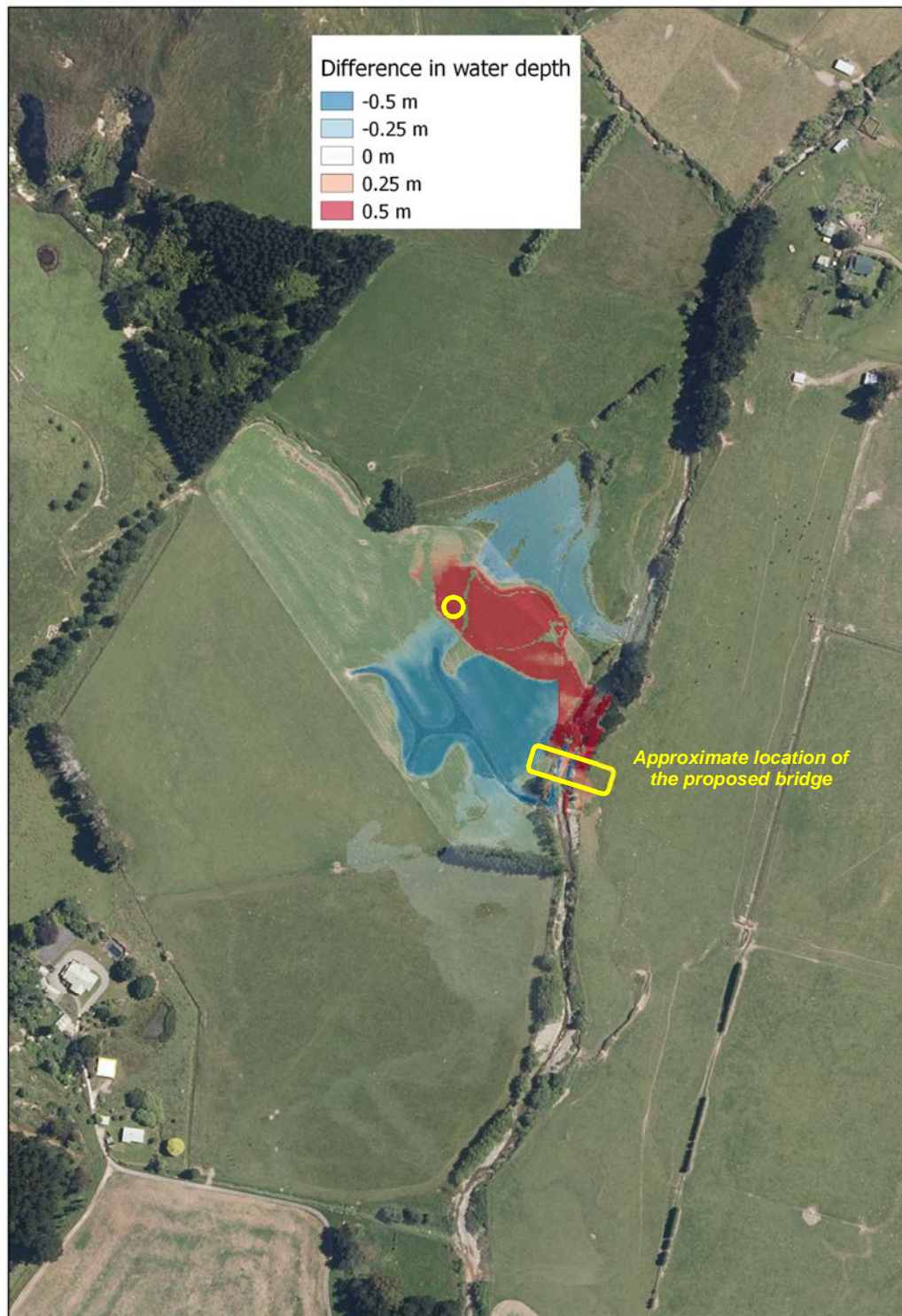


Figure D.64: Difference in water depth during a 1% AEP event, including the effects of climate change to 2120, following construction of the proposed bridge. The yellow circle shows the location used for analysis of flood duration.

330. There will also be a significant area, upstream and on the true right bank, where water depths will reduce by up to 0.5m as a result of construction of the bridge.
331. Downstream of the bridge, and adjacent to the highway, there is also a significant area where the depth of flooding will decrease by more than 0.5m.
332. Overall, the construction of the Project will cause water levels to increase by up to 0.5m over approximately 4600m² (or 0.46ha) and decrease by up to 0.5m over 5700m² (or 0.57ha). The net effect therefore is that water levels during the design event will decrease by up to 0.5m over approximately 0.11ha. This is a relatively small but positive change, and all these changes are within the existing floodplain of Mangamanaia Stream (Table D.22).

Table D.22: Difference in water depth (±0.5m) and velocity (±0.6m/s) following construction of the proposed bridge.

Criteria	Area (m ²)	Area (ha)
Area where increase in water depth up to 0.5m	4584	0.46
Area where decrease in water depth up to 0.5m	5728	0.57
<i>Nett change in area of lower water depths</i>	<i>1144</i>	<i>0.11</i>
Area where increase in velocity up to 0.6m/s	1935	0.19
Area where decrease in velocity up to 0.6m/s	5369	0.54
<i>Nett change in area of lower velocity</i>	<i>3434</i>	<i>0.34</i>

333. There will also be small changes in the velocity of floodwaters (Figure D.65). Again, the effects of the construction of the bridge are relatively small and limited to the immediate vicinity of the bridge. There is a slight increase, by up to 0.6m/s, through the bridge and in the overflow channel immediately upstream back into the main channel. There is also a slight increase in velocity immediately downstream of the bridge as a result of the improved hydraulic efficiency of the channel. The majority of the overbank flooding will experience a reduction in velocity; by up to 0.6m/s.
334. Overall, the construction of the bridge will cause velocities to increase by up to 0.6m/s over approximately 1900m² (or 0.19ha) and decrease by up to 0.6m/s over 5400m² (or 0.54ha). The net effect therefore is that the velocity of floodwaters will decrease by up to 0.6m/s over approximately 0.34ha (Table D.22).
335. The construction of the bridge over Mangamanaia Stream will result in relatively minor changes to flooding and the flood hazard during the 1% AEP design event. All these changes will be in close proximity to the bridge. While the depth of inundation will increase by up to 0.5m over approximately 0.46ha, much of this will be within a constructed wetland. Furthermore, while the depth of flooding will increase over a relatively small area, the velocity of the

floodwater will decrease by up to 0.6m/s over a slightly larger area. Overall, the construction of the Mangamanaia Bridge is likely to result in a slight reduction in the existing flood hazard.

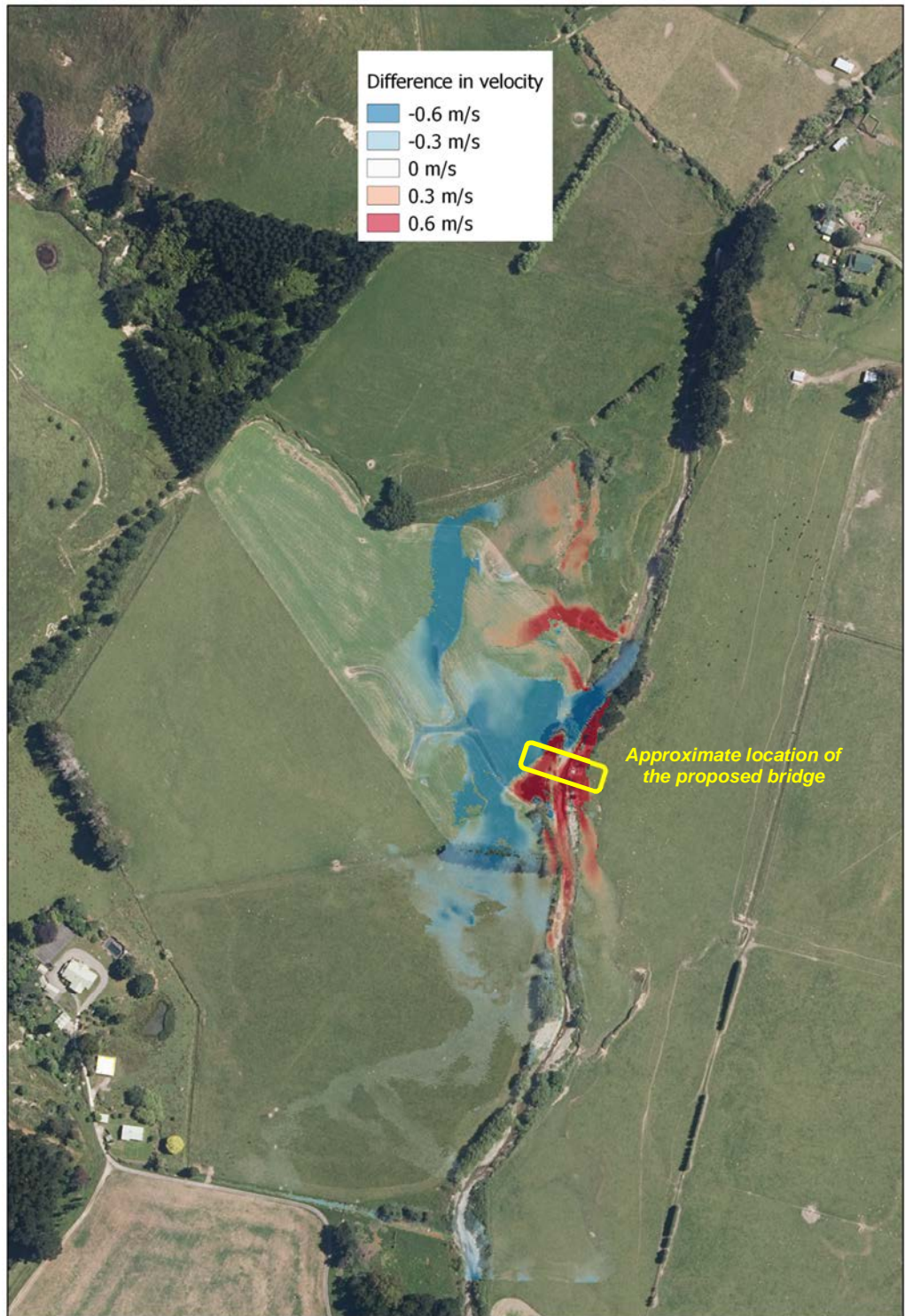


Figure D.65: Difference in velocity during a 1% AEP event, including the effects of climate change to 2120, following construction of the proposed bridge.

336. As well as changes to the depth and velocity of flood waters, a key consideration is the duration of any inundation. A flood hydrograph was therefore extracted from the hydraulic model for the area that experiences an

increase in inundation of up to 0.5m during the 1% AEP design event, increased to allow for the potential effects of climate change (Figure D.64 & Figure D.66).

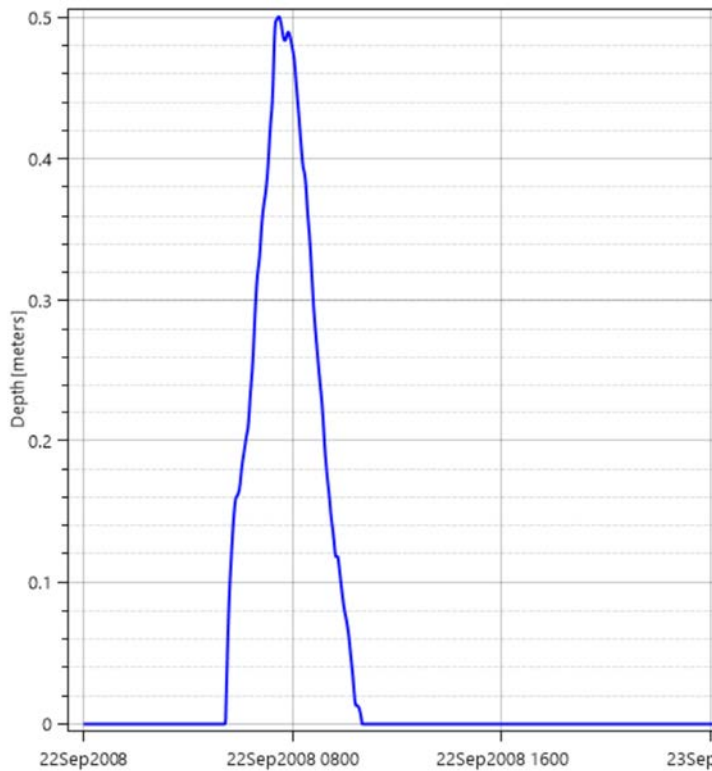


Figure D.66: Flood hydrograph for a region of the Mangamanaia floodplain in the vicinity of the proposed bridge.

337. Figure D.66 can be summarised in terms of the time the depth of flooding exceeds particular levels (Table D.23).

Table D.23: Duration of inundation of various depths during the 1% AEP design event, including the effects of climate change to 2120.

Depth (m)	Duration (mins)	Duration (hrs)
>0.0 (Any flooding)	306	5.1
>0.1	257	4.3
>0.2	180	3.0
>0.3	132	2.2
>0.4	83	1.4
>0.5	14	0.2

338. Inundation of the floodplain of the Mangamanaia Stream during the 1% AEP design event, increased to allow for the potential effects of climate change to 2120, following construction of the bridge lasts for a total of about 5-hours. However, flooding exceeds 0.3m at this location for only 2.2-hours.

339. Since this area already floods during the design event, the effect of the bridge in this area where any effects are likely to be greatest would be to increase the duration of inundation by a maximum of 2-hours. The effect during smaller events will be significantly less.

Conclusions on the Mangamanaia Stream Bridge (BR07)

340. In my professional opinion, the effects of constructing the proposed bridge over Mangamanaia Stream are likely to be positive, although it is difficult to weigh changes in depth against changes in velocity. Any changes to the existing flood hazard will, however, in my professional opinion be less than minor.

Eastern Roundabout

341. The Project involves the construction of a roundabout on the extensive floodplain to the west of Woodville.
342. As the Project will raise the ground surface and modify the topography in this area, there is the potential to disrupt existing overland flow paths on the floodplain. Disrupting overland flow paths has the potential to increase the flood hazard and therefore an assessment was undertaken to quantify the extent and magnitude of any impact.
343. Overland flow is generated when rainfall exceeds the storage capacity within the catchment, including surface ponding and soil storage, and surface runoff occurs. Surface runoff will flow towards any streams or artificial drainage channels, and when the capacity of these is exceeded overbank flooding will occur.
344. To quantify overland flow and the existing flood hazard, a 2-dimensional hydraulic model was constructed in Tuflow™ (**Appendix D.5: *Te Ahu a Turanga - Manawatū Tararua Highway: Flood Risk Analysis – Eastern Roundabout***). The model was initially of the existing situation including land use, topography, catchment extent, and temporally varying rainfall during the design event.
345. The rainfall hyetograph for the 1% AEP design event (with allowance for climate change to 2120) developed as described earlier was applied to a gridded representation of the terrain. An areal reduction factor of 95% was applied to the design rainfall to account for the size of the catchment (approximately 32km²). Rainfall was then also reduced by 40% to allow for losses and storage within the catchment. A temporally varying rainfall profile (i.e. hyetograph) was developed for a 6-hour duration storm which is considered to be the critical storm duration for this catchment i.e. the storm that generates the greatest runoff. The resulting overland flow was then routed through the catchment.

Results

346. Flow is essentially from north to south across the area. It should be noted that only four existing culverts were included in the model which is based almost solely on the existing terrain captured in the LiDAR information. This is the reason for the overland flow and flooding immediately upstream of the existing State Highway (Figure D.67). It is likely therefore that the depth of flooding shown is greater than that which would actually occur.



Figure D.67: Overland flow paths and flooding during a 1% AEP 6-hr design rainstorm (increased to allow for the potential effects of climate change to 2120) with the existing terrain. The location of the proposed roundabout following construction is shown by the dotted outline.

347. Since there are no flow data from this catchment, the Tuflow™ model is uncalibrated. However, at a qualitative level the model seems to provide a realistic interpretation of potential overland flow paths and flooding during the design event.

348. To recognise the inherent uncertainty of hydraulic models, particularly uncalibrated models, all areas of flooding with a depth less than 0.1m were removed from the results. It should also be recognised that a depth of flooding of only 0.1m would not present a risk to either people or property.

349. In general, the depth of flooding is shallow as might be expected over the extensive floodplain i.e. less than 0.5m. Slightly deeper flooding occurs immediately upstream of the existing highway i.e. up to 1m. The only areas of

flooding deeper than 1m are within the main channels and a few topographic hollows across the floodplain (Figure D.67).

350. The proposed roundabout is located in an area that currently floods, although to a depth of less than 1m. Consequently, the raising of the ground with the construction of the roundabout will displace some flood water to other locations. Given the relatively small area from which floodwaters will be displaced, any increase in flooding of other areas already inundated will be extremely small i.e. millimetres.
351. The Tuflow™ model was adapted to represent the catchment following construction of the Project and proposed roundabout. This included changes to land use, topography and any proposed culverts. No changes were made to the design rainfall or its characteristics.
352. Overland flow and the nature of any flooding following construction of the proposed roundabout is shown in Figure D.68. As expected, any changes are small and localised to the immediate vicinity of the proposed roundabout. Again, areas of flooding with a depth less than 0.1m are not shown as they have a negligible effect and are within the resolution of the model.



Figure D.68: Overland flow paths and flooding during a 1% AEP 6-hr design rainstorm (increased to allow for the potential effects of climate change to 2120) following construction of the roundabout which is shown.

353. To highlight the potential effects of the construction of the roundabout, the water depths in each scenario (with and without the bridge) were compared

(Figure D.69). The emphasis of the scale is on differences in the depth of flooding greater than $\pm 0.1\text{m}$ for the reasons discussed earlier.



Figure D.69: Differences in the depth of flooding during a 1% AEP 6-hr design rainstorm (increased to allow for the potential effects of climate change to 2120) following construction of the roundabout, which is shown. The black circle shows the location used for determining the duration of inundation.

354. All the potential adverse effects of the proposed roundabout on the existing flood hazard are extremely localised (i.e. mostly within 10-20 metres of the roundabout) and are limited to areas of pasture. The vast majority of any increase in the depth of flooding is less than 0.5m. The only area where flooding increases by up to 1m is immediately up-gradient of the eastern limb of the roundabout; located in pasture and a significant distance from any buildings.
355. The construction of the Project, by raising the elevation of the ground surface, reduces the depth of flooding both along the alignment and downgradient to the southwest. However, the water that is displaced by the Project increases the depth of flooding immediately up-gradient of the proposed highway and roundabout. The area with the greatest increase in depth of inundation, to the northeast of the roundabout, is the result of construction of a stormwater treatment wetland.
356. The proposed construction of Culvert 19 (CU-19), with increased capacity, allows greater flow past the existing highway and consequently an increased

depth of flooding downstream of the culvert i.e. to the south (Figure D.69). This additional floodwater flows towards Mangapapa Stream approximately 600m to the south. This flooding is a natural phenomenon and would occur currently if the existing culverts were constructed to convey the design flows.

357. Since the flood hazard is a function of the duration as well as the depth of flooding, a flood hydrograph was derived for the area likely to experience the greatest increase in flooding (Figure D.70). This hydrograph was used to determine the duration of inundation of various depths (Table D.24).

358. Flooding to a depth of over 0.3m persists, even during the very large design event modelled, for less than approximately 4-hours. This duration is slightly longer than might be expected on a riparian floodplain because of the topography and generally poor drainage of the area. It should be noted that flooding in this area occurs at present, although potentially for a slightly shorter time than once the roundabout is constructed. However, the improved hydraulic efficiency and conveyance of culverts following construction of the roundabout may actually result in a shorter duration of flooding (i.e. the area will drain more efficiently and therefore inundation will persist for less time).

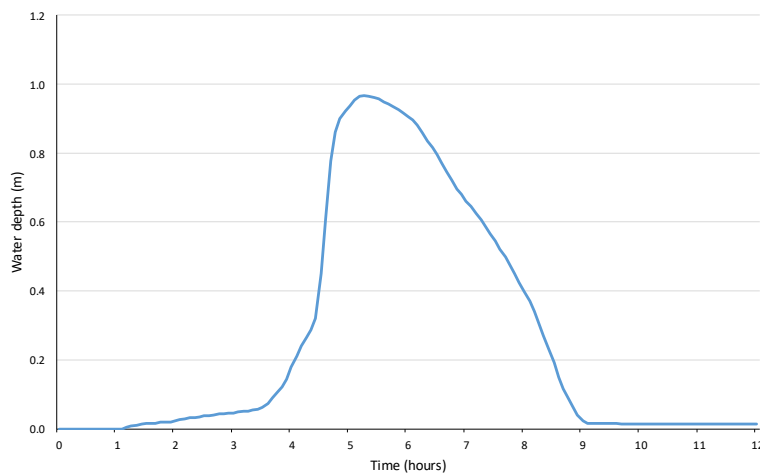


Figure D.70: Hydrograph for the area undergoing the greatest change in the depth of flooding as a result of construction of the roundabout.

Table D.24: Duration of inundation of various depths during the 1% AEP design event, including the effects of climate change to 2120, following construction of the roundabout.

Depth (m)	Duration (hrs)
>0.0 (Any flooding)	8.0
>0.1	4.96
>0.2	4.48
>0.3	4.40
>0.4	3.57
>0.5	3.23
>0.6	2.76
>0.7	2.23
>0.8	1.86
>0.9	1.33

Conclusions on Eastern Roundabout

359. The area on which the eastern roundabout will be constructed is a floodplain. The raising of the ground will displace some floodwater but any effects of the roundabout are extremely localised (i.e. mostly within 10-20 metres from the roundabout) and are limited to areas of pasture.
360. A greater area will be affected by shallower flooding after construction of the roundabout than will experience deeper flooding. Increases in the depth of inundation are generally less than 0.5m, except within constructed wetlands associated with the Project. Even during the very large design event modelled (i.e. the 1% AEP rainfall increased for the potential effects of climate change) flooding exceeding 0.3m will persist for less than approximately 4-hours. This is likely to be very similar to, although potentially of shorter duration, than under the current environment because of improved drainage as a result of the Project.
361. The effects of the proposed roundabout will therefore be generally positive. Any adverse effects will be extremely localised and of short duration.

Existing backwater flooding

362. It should be noted that there is an existing flood hazard to SH2 west of Woodville. During any event larger than the mean annual flood (2.33-year ARI) in the upper Manawatū catchment, backwater flooding occurs upstream of the Gorge (Jeff Watson, pers. comm. Horizons, 23/01/2020). This is because the narrow entrance to the Manawatū Gorge constricts and restricts flow.
363. Flooding caused by the backwater effect of the Gorge, is both a relatively frequent and persistent problem that can affect roads in the area. It sometimes caused the closure of SH3 through the Manawatū Gorge when it was operational (Figure D.71 & Figure D.72).
364. To quantify the magnitude of the flood hazard caused by backwater flooding, Horizons developed a Mike 21 computational hydraulic model. The model was used to determine both the extent and depth of flooding during 1% AEP and 0.5% AEP design events (Figure D.73). The design flows used in the hydraulic model were those derived assuming the existing climate. If predicted climate change and its effect on rainfall and runoff eventuates, then both the extent and depth of flooding will increase, as will its frequency.



Figure D.71: Backwater flooding upstream of the Gorge during the 5 May 1941 event.



Figure D.72: Backwater flooding upstream of the Gorge during the 16 February 2004 event.

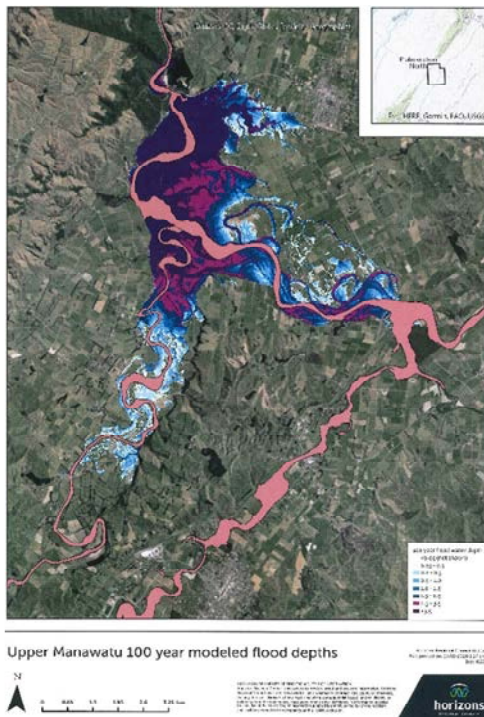


Figure D.73: Extent of backwater flooding during a 1% AEP flood.

365. The proposed alignment of SH2 and the eastern roundabout will avoid this existing flood hazard area (Figure D. 74).

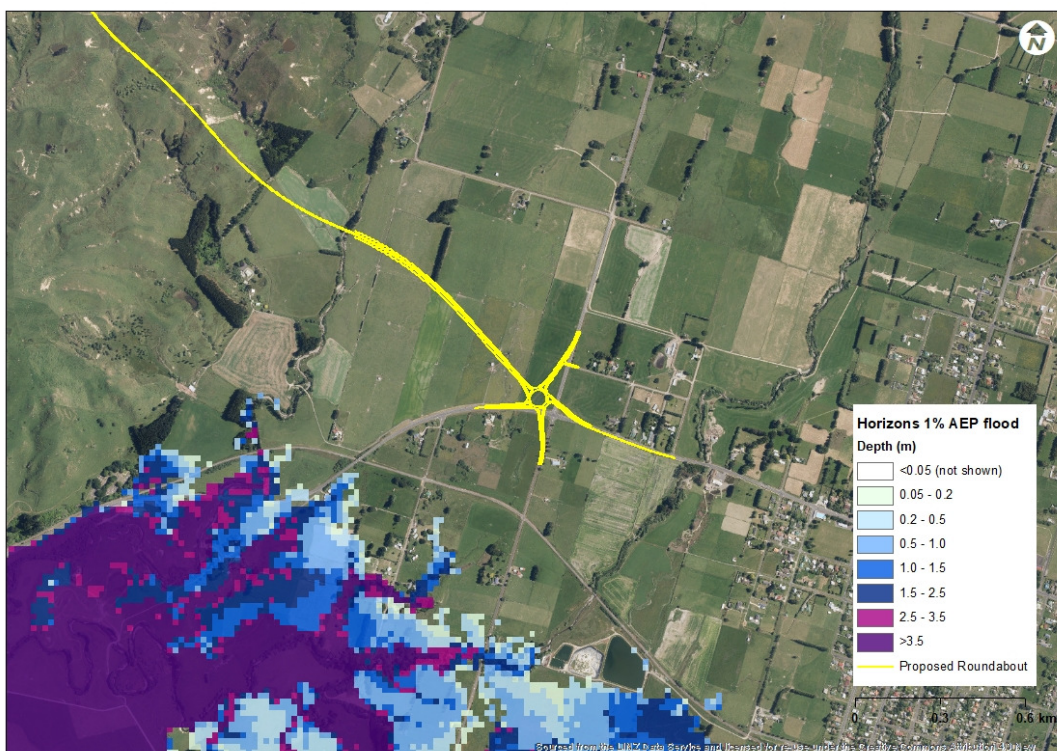


Figure D. 74: The proposed alignment of SH2 and the location of the eastern roundabout will avoid the existing hazard caused directly by backwater flooding upstream of the Manawatū Gorge during a 1% AEP event.

366. While the proposed alignment and roundabout will avoid the direct effects of backwater flooding, there will still be indirect effects which propagate up the various rivers and streams that drain to the Manawatū River e.g. Mangamanaia and Mangapapa Streams. These effects, however, are impossible to quantify because of the lack of available flow data and uncertainty regarding the contemporaneous nature of flooding in the Manawatū River and its various tributaries.

367. The Project, however, will significantly reduce the pre-existing flood hazard to travellers along SH3 through the Manawatū Gorge that was caused by backwater flooding. It will also avoid the existing flood hazard from backwater flooding of the floodplain upstream of the Gorge.

ASSESSMENT OF POTENTIAL EFFECTS

368. Despite the relatively large scale of the Project, its actual and potential effects on the hydrology of the area are small. There are a number of reasons for this:

- (a) The magnitude of any potential effects is small relative to the size and existing dynamics of the receiving environment. For example, the entire

area potentially impacted by the Project (not just the footprint) represents less than 0.3% of the Manawatū catchment (if the Upper Mangamanaia catchment is excluded).

- (b) The area has already been subject to significant land cover and land use change. Any changes as a result of the Project will be extremely small relative to those that have occurred in the past.
- (c) Any actual and potential effects of the Project will be strictly avoided, managed and mitigated through the proposed stormwater and erosion and sediment control measures. This is different to many of the permitted land use activities which currently occur throughout the area.

Manawatū River Bridge (BR02)

- 369. The crossing of the Manawatū River will involve placing one pier within the active channel (Pier 2) and a pier on each bank (Pier 1 & Pier 3). A computational hydraulic model allowed the potential effects of the proposed Manawatū River Bridge to be quantified during a range of design events, including the SLS and ULS.
- 370. The model shows that any effects of Pier 2 are both very small and extremely localised. The 'bow-wave' upstream of Pier 2 results in a local water level increase of up to 1.4m, however, this effect dissipates rapidly upstream. Downstream, and in the lee of Pier 2, there is a slight reduction in water level; up to 0.25m.
- 371. Any significant change in velocity is restricted to three locations. The greatest change is an increase in velocity, up to 1.5m/s, within the centre of the active channel. There is also a small increase in velocity at the entrance to the 'Parahaki bypass channel' on the true left of the Manawatū River. The other change is a reduction in velocity in the lee of Pier 2.
- 372. The construction of the bridge and piers will have no adverse effects on Parahaki Island. There will be a slight reduction in water level, up to 0.25m, but this is generally restricted to the upstream gravel bar and the left bank of the Manawatū River. There is no change to the flow velocity across Parahaki Island because of the relatively shallow depth of flooding and good vegetation cover. There is, however, a decrease in velocity along the edge of the gravel bar at the upstream end of Parahaki Island. This could potentially lead to the deposition of sediment and accretion of this zone of the gravel bar.

373. The proposed scour protection will mitigate any potential adverse effects to Parahaki Island.

Central alignment

374. The majority of the highway over the Ruahine Range will cross only ephemeral streams and the upper reaches of small perennial streams. These catchments are already highly modified by vegetation clearance and current land use activities. Consequently, the natural runoff processes are already highly modified.

375. This area is characterised by thin regolith, generally rolling slopes, and presence of loess (i.e. silty) soils. This means that the existing infiltration and percolation rates are low and slow, and the moisture holding potential of the regolith is low. The regolith therefore has only a limited potential to moderate and attenuate the effect of rainfall on the slopes.

376. The removal of the natural forest cover from most of these slopes has further limited the natural ability of the regolith to moderate and attenuate the effect of rainfall.

377. As a result, runoff is generally diffuse, and the flow regimes of these small drainage lines is intimately connected to rainfall. There is only a very limited capacity for moisture in the regolith to sustain streamflow for any significant period once rainfall ceases. This is why the small perennial streams tend to terminate at a distance downstream of the interfluvium i.e. there is insufficient moisture storage to sustain baseflow once rainfall ceases.

378. It is likely that the regolith can only moderate and attenuate the effects of relatively small rainstorm events i.e. events smaller than 10% AEP. During larger and longer rainstorms, the regolith behaves as though it is sealed and saturated i.e. it behaves as though it is a paved surface.

379. The construction of the Project will affect only a small proportion of the various catchments intersected by the highway. Any effects will consequently also be very small relative to the catchment runoff processes. Any effects will also be extremely localised.

380. In addition, for the reasons discussed above, any potential effects of the Project will only occur during relatively small rainstorms when the regolith properties provide some limited moisture storage capacity. For events larger than 10% AEP, there will be no difference in the rainfall-runoff behaviour of the

regolith under existing conditions and the ground following completion of the Project.

381. These small effects during small rainstorms will be minimised, mitigated, moderated and attenuated by the proposed stormwater treatment design and management. The stormwater treatment devices will intercept and treat runoff from the Project during all rainstorms up to the 10% AEP event. During larger rainstorms, any runoff from the Project will behave in the same manner as the existing slopes. Furthermore, runoff from the Project will be a small proportion of the total runoff and hence any potential effects will be so small that they could not be identified and quantified.
382. In my opinion therefore, any effects of the Project along the 'central alignment' will be extremely small. It is unlikely that they could be measured. Furthermore, runoff from the Project will be treated, attenuated and moderated which does not happen under the current land use management regime.

Mangamanaia Stream Bridge (BR07)

383. Following construction of the bridge, there is a small increase in water depth immediately upstream and against the foundation on which the Project will be constructed during the design event modelled (i.e. the 1% AEP event increased to allow for the potential effects of climate change to 2120). Much of the area where the depth of flooding will increase by more than 0.5m is within a constructed wetland. There will also be a significant area, upstream and on the true right bank, where water depths will reduce by up to 0.5m as a result of the construction of the bridge.
384. Downstream of the bridge, and adjacent to the highway, there is also a significant area where the depth of flooding will decrease by more than 0.5m.
385. Overall, the construction of the bridge will cause water levels to increase by more than 0.5m over approximately 4600m² (or 0.46ha) and decrease by more than 0.5m over 5700m² (or 0.57ha). Therefore, the net effect is that water levels during the design event will decrease by more than 0.5m over approximately 0.11ha. This is a relatively small change, and all these changes are within the existing floodplain of the Mangamanaia Stream.
386. There will also be small changes in the velocity of floodwaters (Figure D.65). Again, the effects of the construction of the bridge are relatively small and limited to the immediate vicinity of the bridge. There is a slight increase, by up to 0.6m/s, through the bridge and in the overflow channel immediately

upstream back into the main channel. There is also a slight increase in velocity immediately downstream of the bridge as a result of the improved hydraulic efficiency of the channel. The majority of the overbank flooding actually experiences a reduction in velocity; by up to 0.6m/s.

387. Overall, the construction of the bridge will cause velocities to increase by up to 0.6m/s over approximately 1900m² (or 0.19ha) and decrease by up to 0.6m/s over 5400m² (or 0.54ha). The net effect therefore is that the velocity of floodwaters will decrease by up to 0.6m/s over approximately 0.35ha.
388. The construction of the bridge over Mangamanaia Stream will therefore result in relatively minor changes to flooding and the flood hazard during the 1% AEP design event (increased to allow for the potential effects of climate change to 2120). All these changes will be in close proximity to the bridge. Overall, the construction of the Mangamanaia Stream Bridge is likely to result in a slight reduction in the flood hazard.
389. Inundation of the floodplain of the Mangamanaia Stream during the 1% AEP design event following construction of the bridge lasts for a total of about 5-hours. However, flooding exceeds 0.3m in this location for only 2.2-hours.
390. Since this area already floods during the design event, the effect of the bridge, in the area where any effects are likely to be greatest, would be to increase the duration of inundation by a maximum of 2-hours. Obviously, the effect during small events will be significantly less.
391. In my professional opinion, the effects of constructing the proposed bridge over Mangamanaia Stream will be extremely small, and overall are likely to be positive; although it is difficult to weigh changes in depth against changes in velocity.

Eastern Roundabout

392. The Eastern Roundabout will be constructed on an active floodplain. The raising of the ground for the Project will displace some floodwater, but any effects of the roundabout are extremely localised (i.e. within 10-20 metres from the roundabout).
393. A greater area will have reduced flooding after construction of the Project than will experience deeper flooding. Increases in the depth of inundation are generally less than 0.5m, except within constructed wetlands associated with the Project. Even during the very large design event modelled, flooding

exceeding 0.3m will persist for less than 4-hours. This is likely to be very similar to, and potentially of shorter duration, than in the current environment because of improved drainage as a result of the Project.

394. SH2 west of Woodville is currently affected by infrequent but persistent flooding caused by the backwater effect upstream of the Manawatū Gorge. The new road alignment and roundabout will avoid this existing flood hazard.
395. The effects of the proposed Roundabout will therefore generally be positive. Any adverse effects will be extremely localised and of short duration.

SUMMARY

396. The Project will certainly have an effect on the hydrology of the area; in terms of adverse effects, in my professional opinion they will almost certainly be no more than minor. In addition, the Project will result in a number of environmental benefits; particularly relating to the continuity of streamflow generation and flood hazard mitigation.

John (Jack) McConchie

APPENDICES

- D.1:** *Design Rainfalls – Analysis and Recommendations.* Report prepared by Dr. J.A. McConchie for Te Ahu a Turanga. TAT-00DR-02000-CO-RP-0001. 20 December 2019. 36p.
- D.2:** *Te Ahu a Turanga – Manawatū River Base Hydraulic Model.* Report prepared by Bloxam Burnett & Olliver Ltd. (BBO). February 2019. 9p + appendices.
- D.3:** *Te Ahu a Turanga: Manawatū River Bridge 2D HEC-RAS modelling and design.* Report prepared by Franciscus Maas for Te Ahu a Turanga. 21 February 2020. 20p + appendices.
- D.4:** *Te Ahu a Turanga - Manawatū Tararua Highway: Mangamanaia Bridge 2D hydraulic analysis.* Report prepared by Courtenay Giles for Te Ahu a Turanga. November 2019. 35p.
- D.5:** *Te Ahu a Turanga - Manawatū Tararua Highway: Flood risk analysis – Eastern Roundabout.* Memorandum prepared by Louise Algeo and Kirsty Duff. 29 November 2019. 10p.

Appendix D.1: *Design Rainfalls – Analysis and Recommendations.*

Design Rainfalls

Analysis and Recommendations


TeAaT Manawatū Tararua Highway

Document Number	TAT-0-DR-02000-CO-RP-0001
Revision	Revision B - Final
Date	20/12/2019



Document Control

Document History and Status

Revision	Date Issued	Author	Reviewed By	Approved By	Status
Draft	7/11/2019	Jack McConchie	David Hughes	Julia Lovelock	Issued
Final	18/12/2019	Jack McConchie	David Hughes	Julia Lovelock	Issued
	Role	Hydrology & Hydraulics Lead	Civil Design Lead	Planner	
	Signatures:				

Revision Details

Revision	Details
A	Draft issued to Waka Kotahi NZ Transport Agency and Horizons Regional Council for information.
B	Final

Table of Contents

1	Introduction.....	1
2	Minimum Requirements	1
3	Hydrometric Data.....	2
4	Data Quality.....	4
5	Rainfall Analysis	6
	5.1 Suitability of gauges.....	8
6	Rainfall IFD Analysis.....	10
	6.1 Depth, duration and intensity analysis	10
	6.2 HIRDS v4	14
	6.3 Applicability.....	17
7	Recommended Design Rainfalls	18
8	Climate Change.....	20
	8.1 Minimum requirements.....	20
	8.2 Climate change 2120	23
	8.3 Changes to stormwater flows	24
	8.4 Changes to channel flow.....	25
9	Critical Rainfall Duration	25
10	Areal Reduction Factor (ARF).....	26
11	Temporal Distribution.....	27
12	Erosion and sediment control thresholds.....	30
	12.1 Rainfall analysis.....	30
	12.2 AEPs of depth and intensity thresholds	30
	12.3 Frequency of threshold exceedances	30
	12.4 Sensitivity to threshold	32
	12.5 Scaled rainfall	33
13	Conclusions.....	34
14	References.....	35

1 Introduction

The Te Ahu a Turanga Highway will replace SH3 through the Manawatū Gorge in the southern foothills of the Ruahine Range. The highway will intersect a number of waterways, all of which are tributaries of the Manawatū River. The new highway will also discharge stormwater runoff, via a treatment and detention system, into these tributaries.

Rainfall is a key component of the hydrological system and therefore a critical design parameter for a number of aspects of the Te Ahu a Turanga Highway. The intensity and distribution of rainfall can have a wide range of impacts on the environment; particularly those affecting runoff, erosion and sediment transport, and the location, magnitude, duration and impact of flooding. As the highway will interact with the natural environment, understanding the rainfall conditions and therefore runoff regime in the area is critical to ensuring appropriate, robust and resilient design.

Therefore, all data from rain-gauges in the wider vicinity of the Te Ahu a Turanga Highway was analysed as part of a hydrometric review. The review also included comparison of the empirical data with that from HIRDS v4, and consideration of the most appropriate spatial and temporal rainfall distributions. This analysis ensures that the most representative rainfall data are used in the design process for the new highway.

2 Minimum Requirements

Waka Kōtahi NZ Transport Agency (NZTA) provided minimum requirements (MRs) that are to be complied with as part of the Te Ahu a Turanga: Manawatū Tararua Highway Implementation. These specifically include describing how the drainage design will be in accordance with the NZTA P46 State Highway Stormwater Specification and comply with Horizons Regional Council Regional Plan (the One Plan), as well as specifying acceptable methodologies for hydrological calculations.

The 'Design Rainfall' section (MR A4.2.2) describes the minimum requirements in relation to rainfall that shall be used as part of the design process. This includes the following:

- Using HIRDS Version 4 for design rainfall depths;
- Using the TP108 24-hour temporal pattern;
- Applying a 2.1°C climate change adjustment to derived rainfall; and
- Applying HIRDS design rainfalls in two distinct zones:
 - From the western extent of the project to Chainage 6000, with the measurement taken near the proposed roundabout between SH57 and SH3; and
 - From Chainage 6000 to the eastern extent of the Project, with the measurement taken at the proposed roundabout between SH3 and Woodlands Road.

In some cases, these requirements are not practical or representative of the overall project area.

This is particularly apparent with respect to the design rainfall depths. As shown in Figure 2.1, the highway traverses the Ruahine Range adjacent to the Manawatū Gorge. The minimum requirements, however, state that design rainfalls for the western and eastern extents of the project should be used (Figure 2.1). However, these points are located at elevations of approximately 60masl; while the highest point of the new highway will be at approximately 300masl. As a result of orographic enhancement i.e. the increase in rainfall with altitude, significantly more rainfall would be expected in the middle of the project area than at either the

western or eastern extents. The design rainfalls for this higher elevation terrain are therefore likely to be of greater relevance to both the design and construction of the highway than those in the areas set out in the MRs. It is noted, however, that the NZTA recommendations were ‘minimum requirements’ and therefore these can be augmented by additional information and design rainfalls.

This report therefore includes an assessment of the minimum requirements against available empirical data to determine the most suitable methodology and design rainfalls for the project and challenging the minimum requirements where a more representative or robust option is available. This will ensure the best inputs for the design of infrastructure are used, increasing the certainty that the network will be resilient to various rainfall-runoff events.

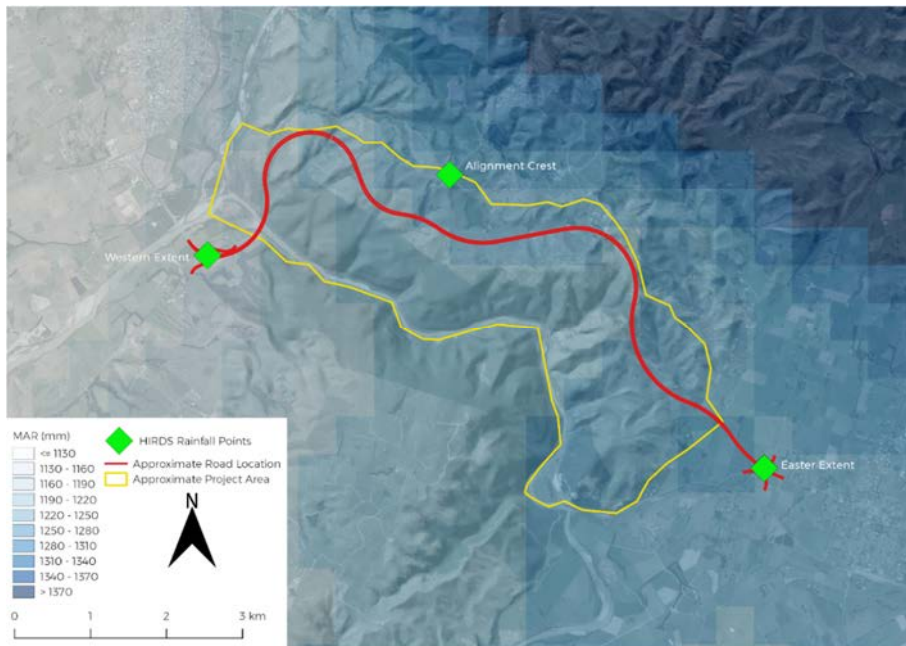


Figure 2.1: Project area for the Te Ahu a Turanga; Manawatū Tararua Highway, including the approximate road alignment and suggested and proposed design rainfall locations.

3 Hydrometric Data

An extensive review was undertaken of available rain gauges in the wider vicinity of the Te Ahu a Turanga; Manawatū Tararua Highway. In total, the records from 36 gauges were obtained, although none are in close proximity to Te Ahu a Turanga. These gauges are summarised in Table 3.1 and their locations shown on Figure 3.1.

Table 3.1: Rainfall records from gauges in the wider vicinity of the highway alignment. Sites highlighted in bold were investigated in detail.

Site Name	Elevation (m)	Recording authority	Start	End	Length of record	Resolution	Percent missing
Ashhurst, Herb Farm	118	NIWA	1999-04-02	2003-09-01	<5	Daily	11
Ballantrae2 Edr	171	NIWA	1969-12-11	1985-04-01	15	Daily	0.3
Kiritaki	216	NIWA	1971-02-02	2019-05-01	48	Daily	0
Te Rehunga	305	NIWA	1954-05-02	2019-08-01	65	Daily	1
Waipuna Woodville	85	NIWA	1924-11-02	2019-08-01	95	Daily	0.2

Woodville, Ballantrae1	347	NIWA	1970-01-02	1983-06-01	13	Daily	0
Te Apiti at Ngarangi	317	NIWA	2019-07-31	2019-10-04	<1	10 min	0
Woodville, Saddle Rd	183	NIWA	1937-06-02	1942-03-01	<5	Daily	10
Palmerston North Ews	21	NIWA	2001-03-30	2019-08-04	18	10 min	1
Palmerston North Aws	40	NIWA	2000-01-01	2019-08-19	20	Daily	0
Palmerston N Aero	45	NIWA	1959-05-02	1988-10-01	29	Daily	0
Palmerston N Haydon St	41	NIWA	1963-05-02	1989-06-01	26	Daily	1
Pahiatua Ews	110	NIWA	03-06-10	30-09-19	9	10 min	0
Massey University	75	NIWA	02-01-67	01-02-83	16	Daily	1
Aokautere	34	NIWA	02-01-71	01-09-06	36	Daily	24
Atawhai	34	NIWA	02-10-21	01-06-75	54	Daily	0
Aokautere - Hort Research	37	HRC	1971-01-05	1982-01-01	11	Daily	24
Komako - Mr B Besley	289	HRC	1941-01-01	2001-12-01	61	Daily	0
Kumeti	711	HRC	1965-05-15	1981-03-25	16	Storage	0
Kumeti at Rua Roa	263	HRC	1975-12-17	2019-08-07	6	6 min-30 min	15
Maharahara	953	HRC	1965-01-26	1981-01-03	16	Storage	0
Mangahao at South Range Road	365	HRC	1978-06-20	1988-04-07	10	6 min-30 min	0
Mangaone at Milson Line	36	HRC	2001-05-18	2019-05-06	18	6 min	<0
Mangaone at Valley Road	142	HRC	1987-03-03	2019-08-29	33	6 min-15 min	<0
Mangatainoka at Pahiatua, Mangamutu	125	HRC	1927-10-10	1986-01-01	58	Daily	0
Ngahere Park Climate Station	75.8	HRC	2009-12-11	2019-08-27	10	6 min	0
Pohangina at Alphabet Hut	416	HRC	1977-07-10	2019-09-04	42	6 min	23
Pohangina at Mais Reach	100	HRC	2006-03-15	2016-08-17	10	6 min - hourly	0
Pohangina at Range View Farm	408	HRC	2008-07-01	2019-08-09	11	6 min	0
Pohangina Valley - A S Crosland	161	HRC	1967-01-01	1992-12-01	26	Daily	2

Te Rehunga - M L Caswill	334	HRC	1954-05-02	1986-01-01	32	Daily	<0
Tiraumea at Ohehua Repeater	241	HRC	1989-10-19	2018-01-31	28	6 min - 15 min	<0
Wharite Peak	887	HRC	1967-01-02	1986-08-20	20	Daily	2

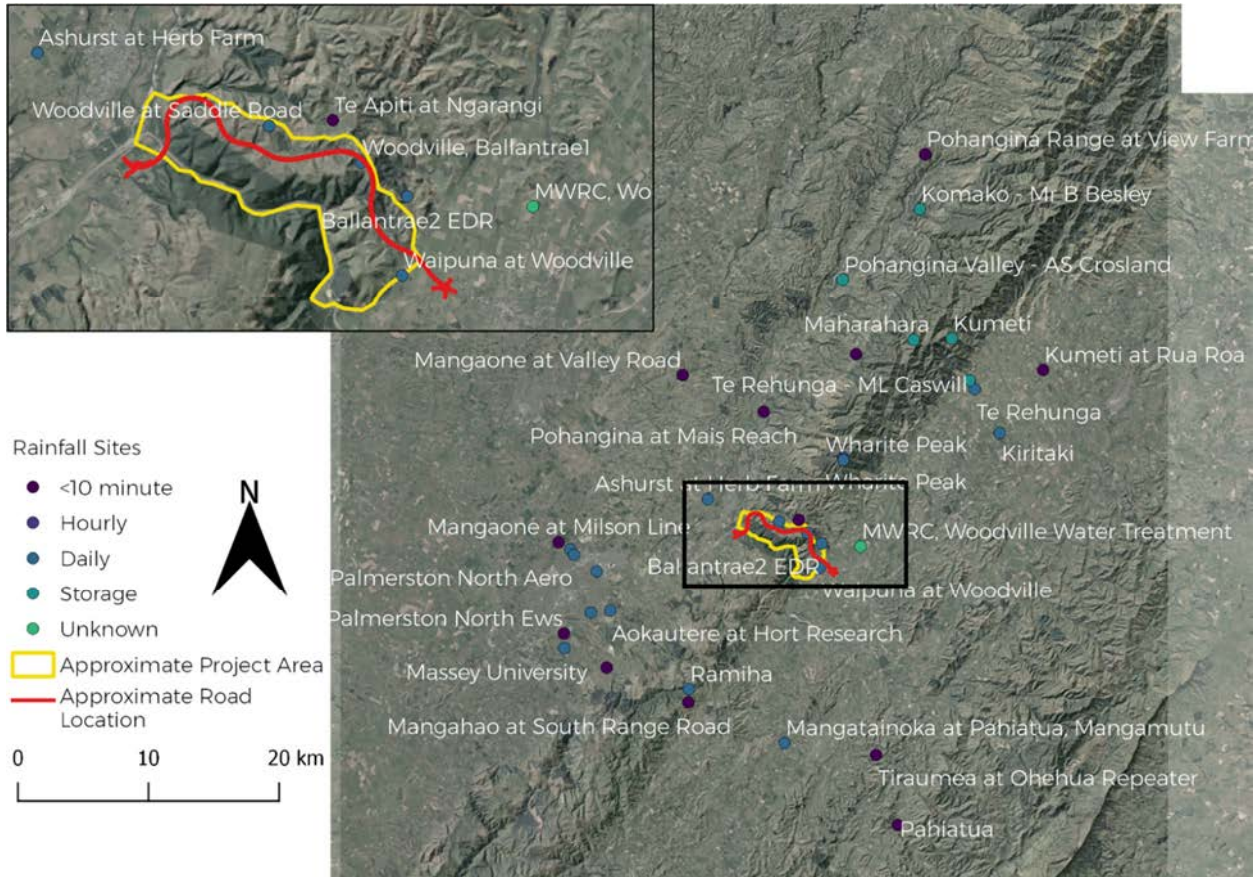


Figure 3.1: Rain gauges in the wider vicinity of Te Ahu a Turanga, including the temporal resolution of the data.

4 Data Quality

As identified in Table 3.1, some of the rainfall records contain periods of missing data i.e. gaps. These are summarised in Table 4.1, which includes both the number and duration of periods of missing data. It is assumed that the data have been verified by the local recording authority and that each gap is genuine. It is important to note that gaps in the record may impact on the reliability and robustness of the results of any analysis, particularly the magnitude and frequency of design events if large rainstorms occurred during any period of missing data. Understanding the nature and characteristics of the gaps helps to determine their potential impact on the quality of the record and any limitations for detailed analysis. For example, one large gap of several years in a 100-year record may be less problematic than numerous shorter gaps throughout the record that could potentially affect a range of rainfall statistics.

In general, the majority of the records have few, if any, gaps. Of the records where there is significant missing data, these tend to be in the longer records and are caused by the site being inoperative for a period of time e.g. Kumeti and Pohangina at Alphabet Hut. These records, however, are still of sufficient length for robust analysis.

Therefore, reasonable confidence can be placed in the data from the rain gauges throughout the wider area. Despite the lack of rainfall data specific to the project area, the rainfall data from other locations can be used to indicate rainfall depths, intensities and distributions likely to affect the highway.

Table 4.1: Number of gaps and duration of missing data in the various rainfall records.

Site Name	No. of gaps	% of missing data
Ashhurst, Herb Farm	22	11
Ballantrae2 Edr	7	0.3
Kiritaki	0	0
Te Rehunga	1	1
Waipuna Woodville	1	0.2
Woodville, Ballantrae1	1	0
Te Apiti at Ngarangi	0	0
Woodville, Saddle Rd	4	10
Palmerston North Ews	23	1
Palmerston North Aws	0	0
Palmerston N Aero	0	0
Palmerston N Haydon St	4	1
Pahiatua Ews	2	0
Massey University	0	1
Aokautere	3	24
Atawhai	0	0
Aokautere - Hort Research	3	24
Komako - Mr B Besley	2	0
Kumeti	0	0
Kumeti at Rua Roa	1	15
Maharahara	0	0
Mangahao at South Range Road	0	0
Mangaone at Milson Line	10	<0
Mangaone at Valley Road	2	<0
Mangatainoka at Pahiatua, Mangamutu	2	0
Ngahere Park Climate Station	0	0
Pohangina at Alphabet Hut	6	23
Pohangina at Mais Reach	0	0
Pohangina at Range View Farm	0	0
Pohangina Valley - A S Crosland	2	2
Te Rehunga - M L Caswill	1	<0
Tiraumea at Ohehua Repeater	2	<0
Wharite Peak	13	2

5 Rainfall Analysis

A key consideration when deriving design rainfalls for Te Ahu a Turanga is the spatial distribution of rainfall across the project area. Te Ahu a Turanga intersects the Ruahine Range, from the west to the east, with elevations ranging from 50m to over 400m. Given the prevailing westerly winds, there is significant spatial variability in rainfall across the project area. This variability is exacerbated by orographic enhancement of rainfall i.e. higher elevations receive more rainfall than lower-lying areas.

As discussed, there is limited rainfall information directly within the project area. This acts as a significant constraint on the confidence that can be placed in any design rainfalls. However, this limitation can be mitigated by taking a conservative approach; first to the adoption of design rainfall parameters, and then to design.

To quantify the spatial variability in rainfall across the project area, the annual summary statistics are provided in Table 5.1 for all sites listed in Table 3.1 that have at least 5 years' of data with a daily or higher temporal resolution. Sites which only have storage gauges were excluded as it is impossible to be sure that they are checked annually.

The mean annual rainfall at each site was compared with that from the national Mean Annual Rainfall (MAR) layer, along with the percentage difference (Table 5.2). The MAR layer (NIWA, 2018) provides a nationally consistent estimate of the mean annual rainfall across New Zealand. The estimate of the MAR was derived from a thin-plate smoothing spline model of available mean annual rainfall data held in national and regional hydrometric archives throughout the country (Tait *et al.*, 2006). These estimates are particularly useful where there are no, or only limited, empirical measurements such as in the current situation.

Table 5.1: Summary statistics for rain gauges in the vicinity of Te Ahu a Turanga.

Site name	Mean annual (mm)	Median annual (mm)	Maximum annual (mm)
Aokautere	943	913	1201
Aokautere - Hort Research	850	863	1091
Atawhai	1016	1026	1264
Ballantrae2 Edr	1192	1184	1580
Kiritaki	1285	1275	1642
Komako - Mr B Besley	1277	1272	1642
Kumeti at Rua Roa	1385	1381	1791
Mangahao at South Range Road	1554	1594	1794
Mangaone at Milson Line	949	917	1313
Mangaone at Valley Road	938	963	1246
Mangatainoka at Pahiatua, Mangamutu	1288	1294	1842
Massey University	955	938	1234
Ngahere Park Climate Station	1176	1148	1361
Pahiatua Ews	1057	1088	1440
Palmerston N Aero	953	946	1274
Palmerston N Haydon St	966	978	1151
Palmerston North Ews	963	1030	1193
Pohangina at Alphabet Hut	1343	1359	1912

Pohangina at Mais Reach	967	1026	1244
Pohangina at Range View Farm	1187	1232	1371
Te Rehunga	1710	1700	2560
Tiraumea at Ohehua Repeater	840	837	1132
Waipuna Woodville	1294	1305	1750
Wharite Peak	2081	2073	2554
Woodville, Ballantrae1	1157	1136	1390

Table 5.2: Comparison of site-specific mean annual rainfalls with those from the national MAR surface.

Site name	Mean annual (mm)	Mean annual rainfall from MAR layer (mm)	Difference (%)
Aokautere	943	889	-6%
Aokautere - Hort Research	850	890	4%
Atawhai	1016	889	-14%
Ballantrae2 Edr	1192	1355	12%
Kiritaki	1285	1523	16%
Kumeti at Rua Roa	1385	1596	13%
Mangahao at South Range Road	1554	1204	-29%
Mangaone at Milson Line	949	874	-9%
Mangaone at Valley Road	938	913	-3%
Mangatainoka at Pahiatua, Mangamutu	1288	1273	-1%
Massey University	955	938	-2%
Ngahere Park Climate Station	1176	938	-25%
Pahiatua Ews	1057	938	-13%
Palmerston N Aero	953	882	-8%
Palmerston N Haydon St	966	889	-9%
Palmerston North Ews	963	938	-3%
Pohangina at Alphabet Hut	1343	1416	5%
Pohangina at Mais Reach	967	1313	26%
Pohangina at Range View Farm	1187	1402	15%
Te Rehunga	1710	1697	-1%
Tiraumea at Ohehua Repeater	840	1242	32%
Waipuna Woodville	1294	1271	-2%
Wharite Peak	2081	1558	-34%
Woodville, Ballantrae1	1157	1346	14%

Figure 5.1 shows the MARs from both the empirical rainfall data and that from the national MAR relative to elevation. Overall, there appears to be a moderate relationship between the mean annual rainfall and elevation. This is to be expected given the orographic enhancement of precipitation. The relationship is actually stronger using the empirical data i.e. r^2 of 0.66, than using the interpolated MAR surface i.e. r^2 of 0.49. However, site specific factors, and both the duration and period of record, can have a significant effect on the rainfall statistics for a particular site. This is particularly an issue with short rainfall records which is why these were excluded from analysis. In addition to the relationship between rainfall and elevation being not as strong using data from the MAR surface, the relationship is also ‘flatter’, i.e. rainfall does not increase with elevation at the same rate as shown in the empirical data.

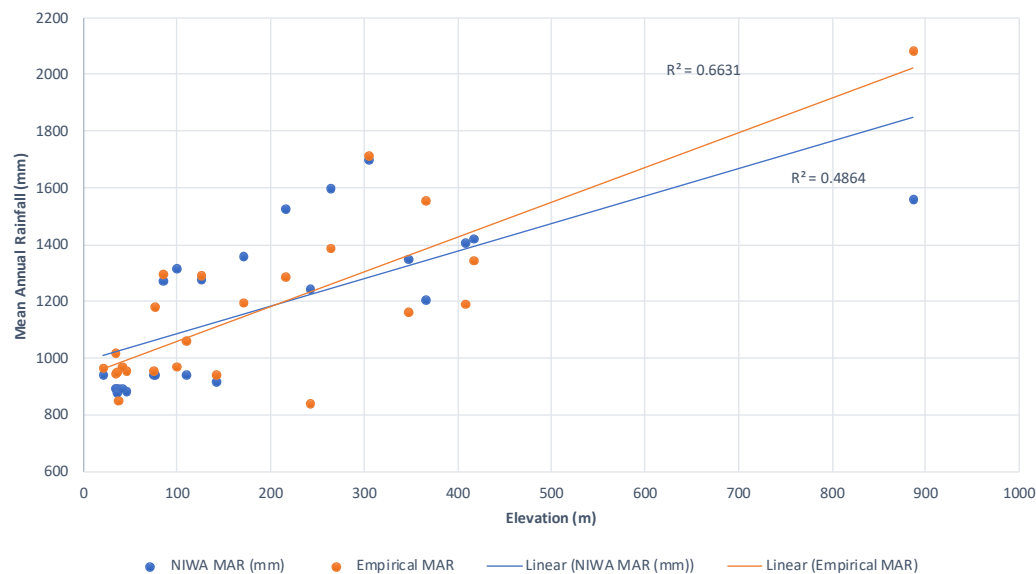


Figure 5.1: Mean annual rainfall relative to the elevation of each rain gauge.

The use of rainfall data from the generalised MAR layer would therefore result in slightly lower design parameters, although the MAR layer does demonstrate significant rainfall variability across the project area. There is a significant difference in rainfall from west to east and also with increasing elevation.

5.1 Suitability of gauges

Of the rainfall data available, none are from within the project area. However, those located outside of the area can still be used for characterizing the expected rainfall regime. For the empirical data to be of use in characterizing rainfall in the project area, it needs to meet the following requirements:

- Situated in the same catchment or in an area with similar characteristics (e.g. elevation, topography, soils, geology, rainfall-runoff relationship etc.);
- Be of sufficient length to identify any longer-term trends (i.e. >10 years);
- Be recorded at a high enough resolution to derive temporal patterns (i.e. < hourly); and
- Have few gaps or periods of missing record.

Using the above criteria, the majority of the rainfall records can be used to determine the spatial variability of rainfall across the project area. For detailed rainfall analysis, such as deriving design rainfalls and temporal storm patterns, those sites in Table 3.1 that are in bold were investigated further. The records from these five gauges are shown in Figure 5.2 through Figure 5.6.

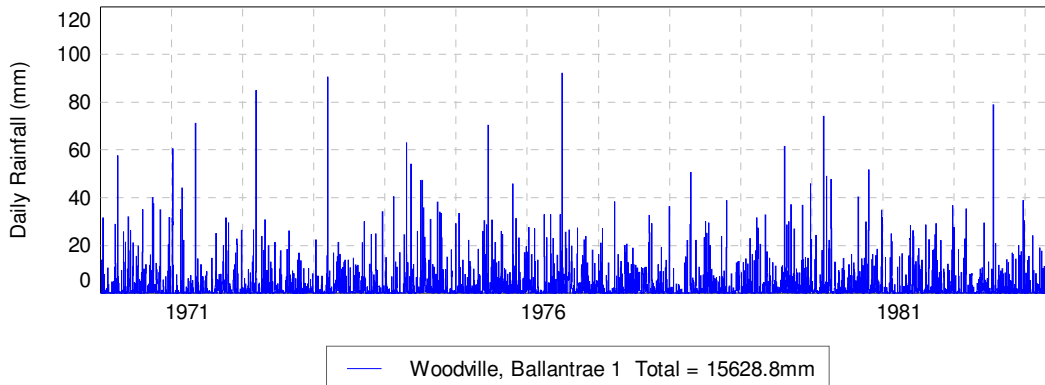


Figure 5.2: Rainfall record for Woodville, Ballantrae 1.

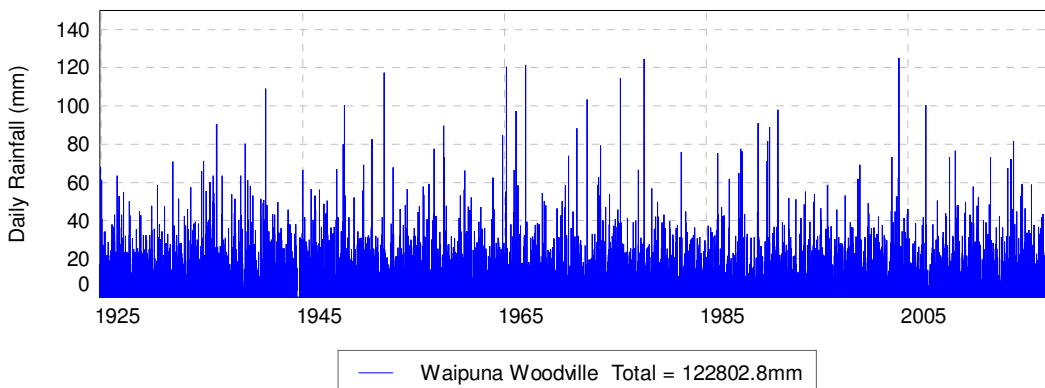


Figure 5.3: Rainfall record for Waipuna at Woodville.

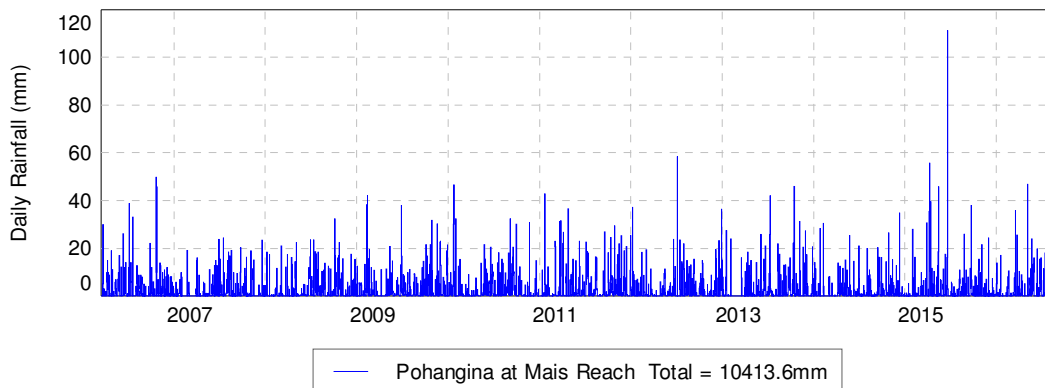


Figure 5.4: Rainfall record for Pohangina at Mais Reach.

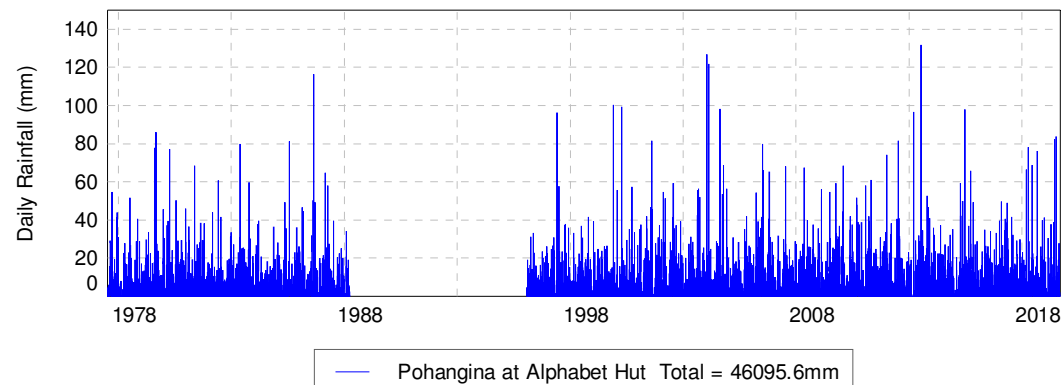


Figure 5.5: Rainfall record for Pohangina at Alphabet Hut.

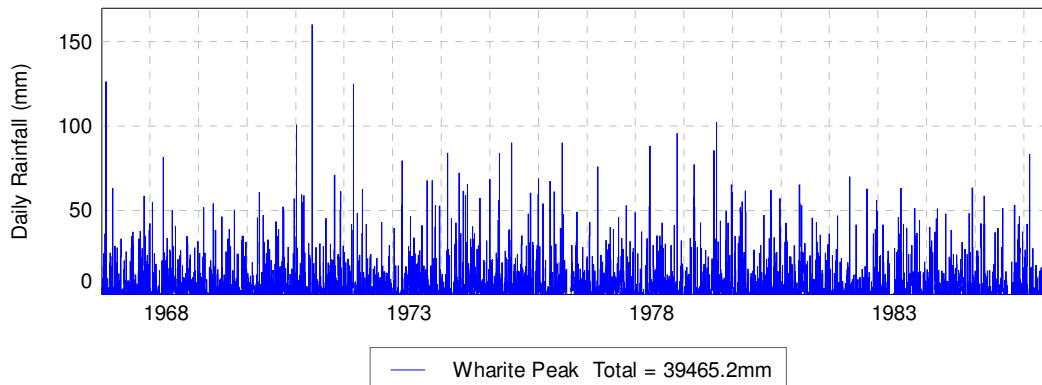


Figure 5.6: Rainfall record for Wharite Peak.

Woodville, Ballantrae 1 is the closest, long-term rain gauge to the project area, although it is no longer operating and only recorded daily rainfall. Waipuna at Woodville provides one of the longest rainfall records which is reasonably close to the project area on the eastern side of the Ruahine Ranges. Pohangina at Alphabet Hut provides a high-resolution rainfall record at higher altitude which can be used to assess the orographic effect across the site. Pohangina at Mais Reach is a high-resolution site close to the project area on the western side of the Ruahine Ranges; although it only provides 10-years of data. Wharite Peak is the closest high-elevation gauge to the project area. When combined with data from Alphabet Hut, these data are useful for determining design rainfalls at higher elevations.

Although a new rain gauge has been installed in the middle of the project area, Te Apiti at Ngarangi, it has only been operational for a few months. Therefore, there is insufficient data from this site to be useful at the present. If a significant rainfall event occurs over the duration of the project, this site may provide useful temporal data.

6 Rainfall IFD Analysis

6.1 Depth, duration and intensity analysis

To derive design rainfall depths, frequency analyses were undertaken on the annual rainfall maxima, over different durations, derived from the entire length of the records from the five gauges. Note that the daily gauges could not be used to derive design rainfalls for events with durations shorter than 1-day.

No detailed quality assurance was undertaken on the rainfall data prior to the frequency analyses other than the gap analysis shown in Table 4.1. It is assumed that the data has been collected using best practice, and no obvious erroneous data was observed.

Three types of statistical distribution were assessed for how well they modelled the actual annual rainfall maxima series (i.e. Gumbel, Pearson 3 (PE3) and GEV). The distribution which provided the best fit to the annual maxima series was then used to estimate the annual exceedance probabilities (i.e. AEPs), or average recurrence intervals (i.e. ARIs), of each design rainfall event. The criteria adopted in this study were:

- The distribution that provided the best-fit through all the data points;
- The distribution with the most realistic shape; and
- The distribution that provides the closest approximation to the extreme values.

While this process may appear subjective, in most cases the choice of a specific statistical distribution for the annual maxima series results in relatively minor differences in the estimated duration-intensity-frequency table; at least for the relatively more frequent events i.e. with AEPs greater than 2%.

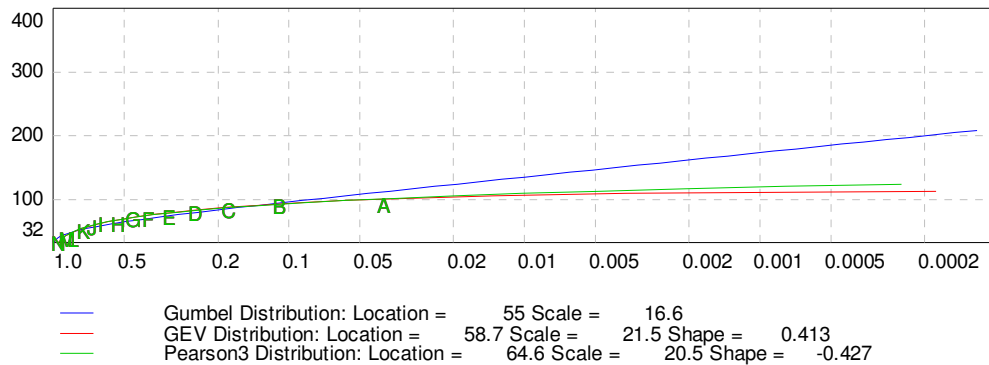


Figure 6.1: Frequency distribution for Woodville, Ballantrae 1 – 24-hour.

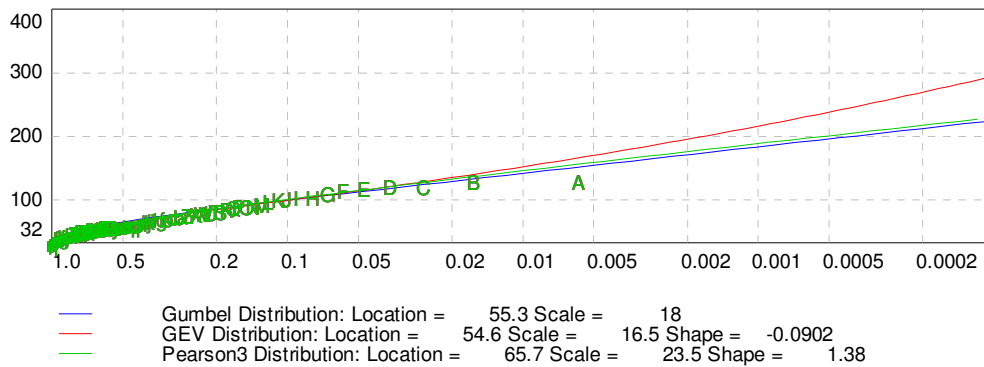


Figure 6.2: Frequency distribution for Waipuna – 24-hour.

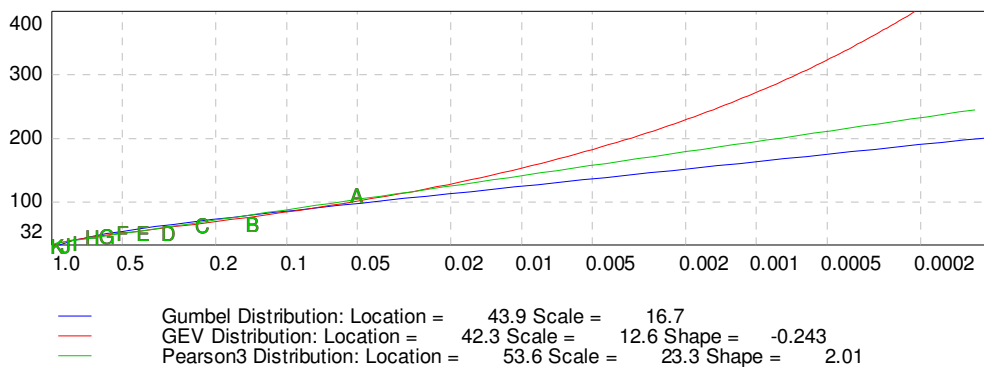


Figure 6.3: Frequency distribution for Pohangina at Mais Reach – 24-hour.

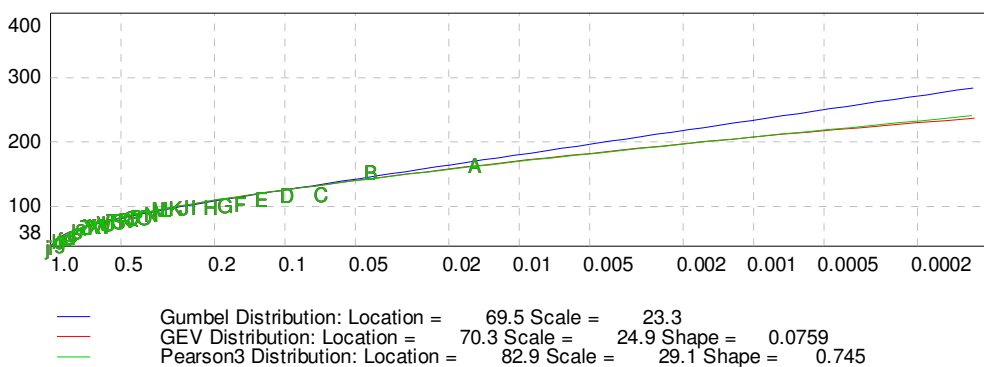


Figure 6.4: Frequency distribution of Pohangina at Alphabet Hut – 24-hour.

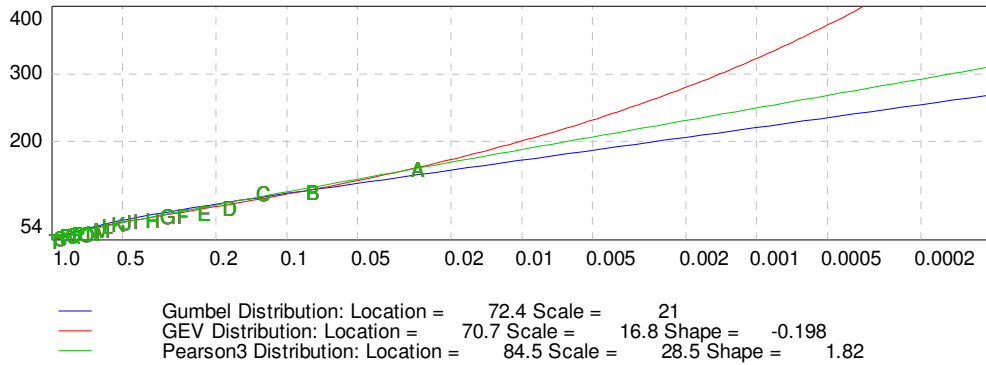


Figure 6.5: Frequency distribution for Wharite Peak – 24-hour.

The annual rainfall maxima tend to approximate a PE3 statistical distribution at all sites; except Waipuna at Woodville where the most extreme events aligned well with Gumbel (Figure 6.1 through Figure 6.5). For the two high-resolution sites; Pohangina at Mais Reach and Pohangina at Alphabet Hut, the PE3 distribution was also appropriate for the shorter durations, as demonstrated for the 1-hour event shown in Figure 6.6 & Figure 6.7.

Assuming that future rainfall events continue to approximate a PE3 statistical distribution for all sites, apart from Waipuna where Gumbel is more suitable, it is possible to derive good estimates of design rainfalls of different magnitudes, frequencies and durations. These are displayed in Table 6.1 through Table 6.5.

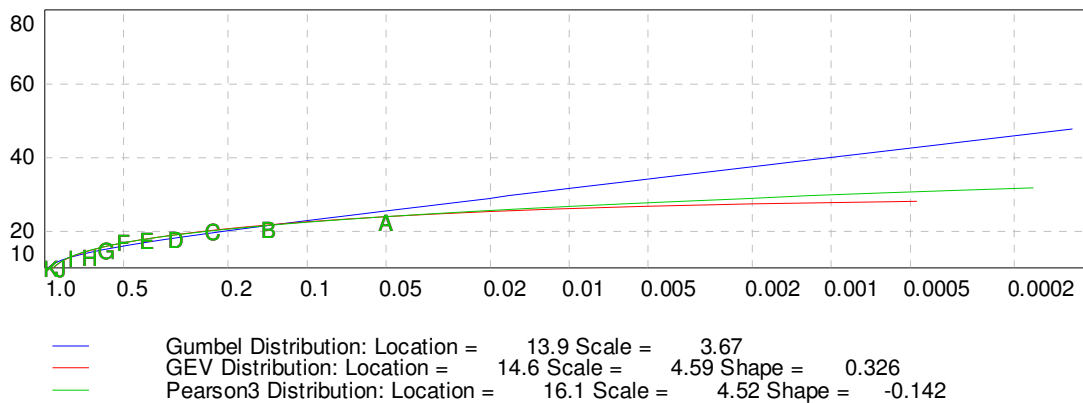


Figure 6.6: Frequency distribution for Pohangina at Mais Reach – 1-hour.

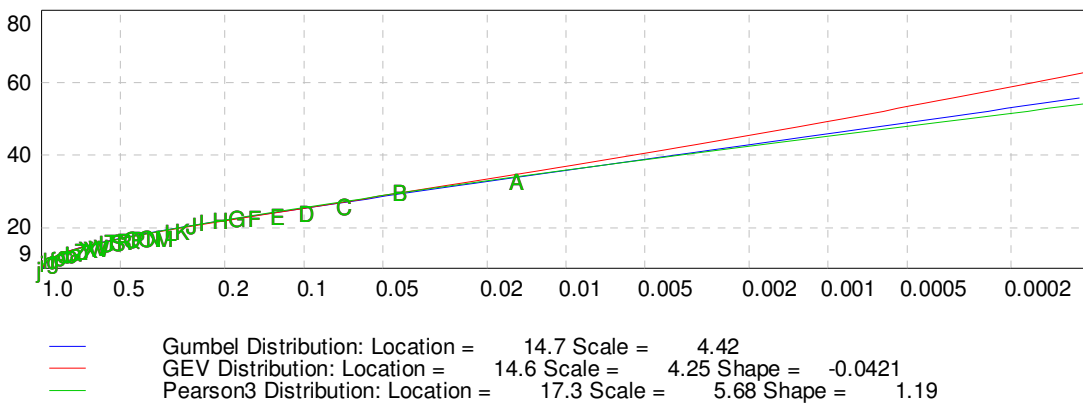


Figure 6.7: Frequency distribution for Pohangina at Alphabet Hut – 1-hour.

Table 6.1: Design rainfalls at Ballantrae 1.

AEP (%)	ARI (yrs.)	Duration										
		10-min	20-min	30-min	1-hr	2-hr	6-hr	12-hr	1-day	2-days	3-days	
50	2									70	78	87
20	5									82	95	104
10	10									90	107	117
5	20									96	119	129
2	50									102	132	143
1	100									106	142	154

Table 6.2: Design rainfalls at Waipuna.

AEP (%)	ARI (yrs.)	Duration										
		10-min	20-min	30-min	1-hr	2-hr	6-hr	12-hr	1-day	2-days	3-days	
50	2									66	85	94
20	5									82	105	116
10	10									96	121	133
5	20									109	137	150
2	50									126	157	171
1	100									138	172	187

Table 6.3: Design rainfalls at Pohangina at Mais Reach.

AEP (%)	ARI (yrs.)	Duration									
		10-min	20-min	30-min	1-hr	2-hr	6-hr	12-hr	1-day	2-days	3-days
50	2	8	12	14	17	20	32	42	50	61	71
20	5	10	14	16	20	24	39	51	68	81	95
10	10	10	15	18	22	28	44	58	84	99	114
5	20	11	16	19	23	32	49	65	100	117	132
2	50	12	17	20	25	37	55	72	121	140	155
1	100	12	17	20	26	41	59	78	138	157	171

Table 6.4: Design rainfalls at Pohangina at Alphabet Hut.

AEP (%)	ARI (yrs.)	Duration									
		10-min	20-min	30-min	1-hr	2-hr	6-hr	12-hr	1-day	2-days	3-days
50	2	7	10	13	17	24	42	60	85	106	116
20	5	9	14	17	21	29	52	76	106	133	145
10	10	11	17	20	25	31	60	87	122	154	168
5	20	13	20	24	28	34	67	98	136	173	188
2	50	16	24	28	32	37	76	111	154	196	213
1	100	18	27	32	35	39	83	120	166	213	230

Table 6.5: Design rainfalls at Wharite.

AEP (%)	ARI (yrs.)	Duration										
		10-min	20-min	30-min	1-hr	2-hr	6-hr	12-hr	1-day	2-days	3-days	
50	2									81	119	139
20	5									103	149	175
10	10									122	174	205
5	20									141	199	233
2	50									166	231	269
1	100									185	255	296

6.2 HIRDS v4

HIRDS is an acronym for High Intensity Rainfall Design System. It is a generalised procedure to obtain spatially and temporally consistent depth-duration-frequency design rainfalls for New Zealand. HIRDS Version 1 was a computer-based program, developed in 1992, to allow a quick and consistent determination of high intensity design rainfall depths (and associated standard errors) over mainland New Zealand, by simply supplying geographical coordinates. Apart from incorporating additional data from archives held by NIWA and local territorial authorities, the various revisions of HIRDS use more robust estimation techniques associated with regional frequency analysis.

In the absence of site-specific data, HIRDS (version 4) can be used to provide estimates of design rainfall depths and intensities, including the potential effects of climate change. While HIRDS provides national coverage using a consistent methodology, it does not replace the use of site-specific data when they are available. Consequently, it is worth validating those data from HIRDS against empirical rainfall records where possible to ensure that they are appropriate for a specific location.

The HIRDS design rainfall at each of the five rain gauge locations are displayed in Table 6.6 through Table 6.10.

Table 6.6: HIRDS v4 design rainfalls for Woodville, Ballantrae 1.

AEP (%)	ARI (yrs.)	Duration									
		10-min	20-min	30-min	1-hr	2-hr	6-hr	12-hr	1-day	2-days	3-days
50	2	7	9	11	15	21	35	47	62	78	88
20	5	10	13	15	21	28	46	61	80	100	112
10	10	12	16	19	25	34	54	72	93	116	129
5	20	15	19	22	29	40	63	83	107	132	147
2	50	18	23	27	36	48	75	99	126	154	171
1	100	21	27	31	41	54	85	111	140	171	189

Table 6.7: HIRDS v4 design rainfalls for Waipuna.

AEP (%)	ARI (yrs.)	Duration									
		10-min	20-min	30-min	1-hr	2-hr	6-hr	12-hr	1-day	2-days	3-days
50	2	7	9	11	15	21	36	49	65	83	93
20	5	9	12	14	20	28	47	64	85	107	119
10	10	11	15	17	24	33	55	75	99	124	138
5	20	13	17	20	28	38	64	87	114	142	158
2	50	16	21	25	33	46	76	103	134	167	184
1	100	18	24	28	38	52	86	115	149	185	205

Table 6.8: HIRDS v4 design rainfalls for Pohangina at Mais Reach.

AEP (%)	ARI (yrs.)	Duration									
		10-min	20-min	30-min	1-hr	2-hr	6-hr	12-hr	1-day	2-days	3-days
50	2	7	9	11	14	19	30	39	51	65	75
20	5	9	13	15	20	26	40	51	66	84	95
10	10	12	15	18	23	31	47	61	77	97	110
5	20	14	18	21	28	36	55	70	89	111	126
2	50	17	22	26	34	44	66	83	105	130	147
1	100	20	26	30	39	50	74	94	118	145	163

Table 6.9: HIRDS v4 design rainfalls for Pohangina at Alphabet Hut.

AEP (%)	ARI (yrs.)	Duration									
		10-min	20-min	30-min	1-hr	2-hr	6-hr	12-hr	1-day	2-days	3-days
50	2	7	10	12	16	23	41	58	79	103	118
20	5	10	13	16	22	31	54	75	101	131	149
10	10	12	16	19	26	37	63	88	118	152	171
5	20	15	19	23	31	43	74	101	135	172	194
2	50	18	24	28	38	52	88	119	158	200	225
1	100	21	27	32	43	60	99	134	176	222	248

Table 6.10: HIRDS v4 design rainfalls for Wharite.

AEP (%)	ARI (yrs.)	Duration									
		10-min	20-min	30-min	1-hr	2-hr	6-hr	12-hr	1-day	2-days	3-days
50	2	10	13	16	21	29	47	64	88	122	147
20	5	13	18	21	28	38	61	83	112	153	184
10	10	16	22	25	34	45	72	96	130	176	211
5	20	20	26	30	40	53	83	110	148	200	238
2	50	24	32	37	48	63	98	130	173	231	274
1	100	28	36	42	55	72	110	145	192	254	300

To test the validity of the design rainfalls from HIRDS, the various empirical design rainfalls from each of the five gauges were compared (Table 6.11 through Table 6.15). Positive values (green cells) indicate that the HIRDS design rainfall depths are higher; negative values (red cells) show that the empirically-derived design rainfall depths are greater than those interpolated from HIRDS.

Table 6.11: Percentage difference between design rainfalls from empirical data and HIRDS v4 – Woodville, Ballantrae 1.

AEP (%)	ARI (yrs.)	Duration									
		10-min	20-min	30-min	1-hr	2-hr	6-hr	12-hr	1-day	2-days	3-days
50	2								-13	0	1
20	5								-3	5	7
10	10								3	8	9
5	20								11	10	12
2	50								19	14	16
1	100								24	17	19

Table 6.12: Percentage difference between design rainfalls from empirical data and HIRDS v4 – Waipuna.

AEP (%)	ARI (yrs.)	Duration									
		10-min	20-min	30-min	1-hr	2-hr	6-hr	12-hr	1-day	2-days	3-days
50	2								-1	-3	-2
20	5								3	2	3
10	10								3	2	4
5	20								4	4	5
2	50								6	6	7
1	100								7	7	9

Table 6.13: Percentage difference between design rainfalls from empirical data and HIRDS v4 – Pohangina at Mais Reach.

AEP (%)	ARI (yrs.)	Duration									
		10-min	20-min	30-min	1-hr	2-hr	6-hr	12-hr	1-day	2-days	3-days
50	2	-18	-26	-29	-18	-4	-6	-7	2	7	4
20	5	-1	-9	-11	-2	5	3	0	-3	3	0
10	10	10	2	1	7	8	7	4	-9	-2	-4
5	20	21	13	11	16	11	11	8	-13	-5	-5
2	50	33	25	24	26	16	17	13	-16	-7	-5
1	100	41	34	32	33	19	21	17	-17	-8	-5

Table 6.14: Percentage difference between design rainfalls from empirical data and HIRDS v4 – Pohangina at Alphabet Hut.

AEP (%)	ARI (yrs.)	Duration									
		10-min	20-min	30-min	1-hr	2-hr	6-hr	12-hr	1-day	2-days	3-days
50	2	3	-8	-10	-6	-5	-2	-5	-7	-3	2
20	5	8	-5	-7	2	8	4	-1	-5	-2	2
10	10	8	-6	-7	5	15	6	1	-3	-1	2
5	20	11	-4	-5	9	22	9	3	-1	0	3
2	50	14	0	-1	15	29	13	7	3	2	6
1	100	18	3	2	19	34	16	10	6	4	7

Table 6.15: Percentage difference between design rainfalls from empirical data and HIRDS v4 – Wharite.

AEP (%)	ARI (yrs.)	Duration									
		10-min	20-min	30-min	1-hr	2-hr	6-hr	12-hr	1-day	2-days	3-days
50	2								8	2	5
20	5								8	3	5
10	10								6	1	3
5	20								5	1	2
2	50								4	0	2
1	100								4	0	1

The comparison shows that generally there is good agreement between the design rainfalls from HIRDS and the empirical data; although HIRDS generally provides slightly higher rainfall depths. There are slight differences at the various sites.

The design rainfalls for Ballantrae1 using the empirical data are less than those from HIRDS; except for the 1-day 50% and 20% AEP magnitude events. The differences for the larger events are up to 24% for the 1-day, 24-hour event. This suggests that HIRDS over-estimates the design rainfalls for more extreme events. This site is no longer operating but was used in HIRDS v4. It was the only gauge located on the alignment of Te Ahu a Turanga. The differences are likely because of the length and timing of the record (13-years, from 1970-1983). This period does not contain many of the large rainfall events recorded at other gauges outside of this period. The HIRDS v4 results are likely to be a reasonable indication, albeit slightly conservative, of the design rainfalls at this location.

Waipuna HIRDS v4 values are greater for all events except the 50% AEP, where the empirical data is slightly greater. The biggest differences are for the more frequent events; however, this is still less than 10%. This

long-term site was used in developing HIRDS v4, as was Ballantrae2. As one of the longest sites available, the very small differences indicate the wider applicability of using design rainfalls from HIRDS v4.

Pohangina at Mais Reach has some of the greatest differences, particularly for the short duration, high magnitude events. Design rainfalls from HIRDS are generally higher except for the longer duration events i.e. greater than 1 day. This site was operated by HRC but is no longer maintained. It was also a 'backup' rainfall site, meaning only an intensity gauge was present and there was no check gauge. However, the record has no missing data and the rainfall data are consistent with other sites in the area. The difference observed for the longer duration events is probably the result of the large rainfall event that occurred on 20 June 2015 (Figure 5.4). This was the largest event in the 10-year record. It was a 'real' event and flooding occurred, particularly in the Whanganui catchment. This rainfall event was also recorded at other nearby gauges e.g. Pohangina at Alphabet Hut (Figure 5.5). That gauge, however, was not used in developing HIRDS v4, suggesting that design rainfall from HIRDS may be conservative.

Design rainfalls from Pohangina at Alphabet Hut, which provides high-resolution data from the highest elevation, have generally small to moderate differences when compared to those from HIRDS v4, except for the 1% AEP events; particularly the 2-hour event where HIRDS values are nearly double those from the empirical data. This suggests HIRDS would likely over-estimate design rainfalls for events of 2-hour duration. This could lead to the slight over-design of infrastructure. This has potential implications when using HIRDS design rainfalls for modelling runoff from the higher elevation areas of the highway alignment i.e. the design rainfalls will be conservative for much of this area. This gauge was used in developing HIRDS v4 but considered data only up until the end of 2015. The empirical record analysed in this report contains data up to September 2019. Over the past four years there have been several heavy rainfall events. This contrasts with the relatively benign years from 2004-2010 (Figure 5.5). This may be contributing to the differences in the two sets of design rainfalls.

The design rainfalls for Wharite derived from the two sources are also in general agreement. Overall, the design rainfalls from HIRDS are higher than those from the empirical data, but only by up to 8%. Data from this gauge was included in developing HIRDS v4, and this is likely to contribute to the good agreement between the two datasets. This rain gauge is at the highest elevation in the wider project area, suggesting that HIRDS accurately interpolates across the terrain and provides robust consideration of the effects of orographic enhancement across the project area.

6.3 Applicability

The results of the above analysis suggest that design rainfalls from HIRDS v4 are in generally good agreement with those obtained using the latest empirical data. This is particularly the case where specific gauges were used in developing HIRDS v4. Design rainfalls from HIRDS v4 are generally slightly conservative when compared to those obtained using the empirical records. The use of data from HIRDS v4 is therefore likely to lead to slightly conservative design. The only exceptions tend to be for longer-duration and greater magnitude events. The relatively small catchments potentially affected by the highway, however, mean that this increased uncertainty will have no effect on the design parameters adopted.

The reliability of estimates of design rainfall depths is a function of the length of rainfall record used in the analysis and the appropriateness of the rainfall record for a particular purpose. As a general rule of thumb, AEPs should not be extrapolated beyond twice the length of the record (Davie, 2008). NIWA, however, suggest reliability persists up to five times the length of record. The rainfall records analysed above were longer than those used in developing HIRDS v4; those records ended in either 2015 or 2016. Therefore, design rainfalls using the empirical records from gauges which are still operating are likely to be more accurate; particularly for less frequent, higher magnitude rainfall events.

However, as the design rainfalls from HIRDS v4 are generally higher than those derived using the empirical data, they provide a level of conservatism while still being realistic. Generally, design rainfalls from HIRDS v4 are 5-10% higher than those from the empirical data. The exceptions are at Pohangina at Mais Reach and Ballantrae 1. This may be the result of the shorter records at these sites (10 and 13 years respectively).

The use of design rainfalls from HIRDS should therefore provide a slightly conservative approach for stormwater modelling and the design of infrastructure to treat, convey and discharge runoff. This has the additional environmental benefit of further mitigating any inherent risk of extreme or over-design events. In the absence of empirical rainfall data from the project area, it is considered good practice to use the design rainfalls from HIRDS v4 to guide the design and construction of Te Ahu a Turanga.

7 Recommended Design Rainfalls

Waka Kōtahi NZ Transport Agency (NZTA) provided minimum requirements (MRs) that are to be complied with as part of the Te Ahu a Turanga: Manawatū Tararua Highway Implementation. These specifically include describing how the drainage design will be in accordance with the NZTA P46 State Highway Stormwater Specification and comply with Horizons Regional Council Regional Plan (the One Plan), as well as specifying acceptable methodologies for hydrological calculations.

The above analysis suggests that the use of design rainfalls from HIRDS v4 are likely to be appropriate in the absence of long-term empirical data from the project area. However, the minimum requirements indicate that design rainfalls from HIRDS v4 shall be taken and applied in two distinct zones; effectively the western and eastern extents of the project area.

However, as described earlier, the spatial distribution of mean annual rainfall (Figure 2.1) shows significant orographic enhancement across the project area. The west-east spatial variation is also highlighted by the design rainfalls from HIRDS v4 for each of the two locations (Table 7.1 & Table 7.2). These locations are at the lowest elevations at the western and eastern extents of the project. Low elevation areas typically have lower rainfall than on the Ruahine Range, which will be traversed by Te Ahu a Turanga.

As demonstrated, rainfall is generally greatest at higher elevations i.e. at the mid-point of the project area. Therefore, it is more appropriate and practical, as well as providing some conservatism to rainfall and runoff estimation, to use the design rainfalls from HIRDS v4 at this higher elevation for the entire project area. This ensures that the highest design rainfalls are used and avoids the need to decide which portion of the alignment should be designed using which design rainfall i.e. either that from the west or east.

The design rainfalls for the western and eastern extents of the project are shown in Table 7.1 and Table 7.2. The design rainfalls for the highest elevation on the alignment of Te Ahu a Turanga (marked as 'Alignment Crest' in Figure 2.1) are displayed in Table 7.3. While the design rainfalls at the eastern extent are slightly greater for less frequent, long durations events, the difference is very small and within the margin of error of HIRDS v4. This means that the design rainfalls from HIRDS v4 for the higher elevation area are still likely to provide conservative rainfall depths across the entire project area.

Table 7.1: HIRDS for design rainfalls on western side. Latitude -40.3093 Longitude 175.7624

AEP (%)	ARI (yrs.)	Duration									
		10-min	20-min	30-min	1-hr	2-hr	6-hr	12-hr	1-day	2-days	3-days
50	2	7	9	11	14	20	31	41	53	67	77
20	5	9	12	15	19	26	41	53	68	86	97
10	10	11	15	18	23	31	48	62	80	100	113
5	20	13	18	21	28	36	56	72	92	114	128
2	50	17	22	26	34	44	67	86	108	133	149
1	100	19	25	29	39	50	76	96	121	148	166

Table 7.2: HIRDS for design rainfalls on eastern side. Latitude -40.3324 Longitude 175.8503

AEP (%)	ARI (yrs.)	Duration									
		10-min	20-min	30-min	1-hr	2-hr	6-hr	12-hr	1-day	2-days	3-days
50	2	7	9	10	14	19	32	44	59	76	87
20	5	9	12	14	19	26	42	58	77	99	112
10	10	11	14	17	22	31	50	68	90	115	130
5	20	14	17	20	27	36	58	79	103	131	148
2	50	17	21	25	32	44	70	94	122	154	173
1	100	20	24	28	37	50	79	105	137	171	192

Table 7.3: HIRDS for design rainfalls for the central, high elevation, area. Latitude -40.2984 Longitude 175.797. This is the recommended design rainfall table to be used for further analysis.

AEP (%)	ARI (yrs.)	Duration									
		10-min	20-min	30-min	1-hr	2-hr	6-hr	12-hr	1-day	2-days	3-days
50	2	7	10	12	16	22	35	46	60	78	89
20	5	10	13	16	21	29	45	60	78	99	113
10	10	12	16	19	26	34	54	70	90	115	130
5	20	15	19	23	30	40	62	81	104	131	148
2	50	18	24	28	37	48	74	96	122	153	172
1	100	21	27	32	42	55	84	108	136	169	191

When the various design rainfalls for the different locations are compared, the expected general relationship of greater rainfall at higher elevations is apparent (Table 7.4 & Table 7.5). Where the numbers are green, the design rainfalls from the higher elevation are greater. This is the case in almost every storm scenario. When the lower elevation areas have higher design rainfalls these are generally only 1% different i.e. within the uncertainty of the data.

This suggests that using the one HIRDS design rainfall table will ensure conservative rainfall and runoff depths. In the most extreme situation, the design rainfalls might be up to 14% too high; although since there are no empirical rainfall data from the project area this cannot be confirmed.

Table 7.4: Percentage difference between the design rainfalls from HIRDS v4 in high elevation areas and those from the western extent of the project area.

AEP (%)	ARI (yrs.)	Duration									
		10-min	20-min	30-min	1-hr	2-hr	6-hr	12-hr	1-day	2-days	3-days
50	2	9	9	9	9	9	10	11	12	13	14
20	5	9	8	8	9	9	10	11	12	13	14
10	10	9	8	8	9	9	10	11	12	13	13
5	20	8	8	9	9	9	10	11	12	13	14
2	50	9	8	8	9	9	10	11	11	13	13
1	100	9	8	8	9	9	10	11	11	12	13

Table 7.5: Percentage difference between the design rainfalls from HIRDS v4 in high elevation areas and those from the eastern extent of the project area.

AEP (%)	ARI (yrs.)	Duration									
		10-min	20-min	30-min	1-hr	2-hr	6-hr	12-hr	1-day	2-days	3-days
50	2	8	12	14	13	12	7	4	2	2	2
20	5	8	11	13	13	11	7	4	1	0	1
10	10	8	11	12	13	11	6	3	1	0	0
5	20	7	11	12	12	10	6	3	1	0	0
2	50	7	11	12	12	10	6	2	0	-1	-1
1	100	8	11	12	12	10	5	3	-1	-1	-1

8 Climate Change

If predicted global climate change eventuates, it may cause more than just a rise in the world’s temperature. Warmer temperatures mean that more water vapor will enter the atmosphere, while also increasing the air’s ability to hold moisture. Furthermore, sensitivity analysis has indicated that changes in rainfall are often amplified in runoff.

8.1 Minimum requirements

As part of the minimum design requirements stated by NZTA in Appendix A4 – Drainage: “A 2.1°C adjustment shall be applied for climate change.”

This was in line with previous climate change guidelines recommended by the Ministry for the Environment (MfE) and summarized in Table 5.2 of MfE (2008). This table included different percentage increases in rainfall per degree of warming, depending on the duration and magnitude of the event.

The assumption of a temperature increase of 2.1°C was to provide a conservative allowance for the estimated increase in rainfall out to 2090.

However, MfE have subsequently released newer climate change predictions for New Zealand based on the IPCC 5th Assessment (MfE, 2016). For the IPCC 5th Assessment, a set of four forcing scenarios was developed, known as representative concentration pathways (RCPs). These pathways are identified by their approximate total (accumulated) radiative forcing by 2100, relative to 1750.

These RCPs include; one mitigation pathway (RCP2.6) which requires removal of some of the CO₂ presently in the atmosphere, two stabilisation pathways (RCP4.5 and RCP6.0), and one pathway (essentially ‘business as usual’) with very high greenhouse gas concentrations by 2100 and beyond (RCP8.5).

In 2018, MfE released new climate change guidance (MfE, 2018). This revision incorporates the results relating to very extreme rainfall; the “HIRDS” report (NIWA, 2018). That report updated “augmentation factors” for deriving extreme rainfall depths from future increases in temperature. These augmentation factors differ to those presented in earlier reports.

The HIRDS study adopted six of the Global Climate Models (GCMs) used for the IPCC future predictions of the four RCPs, for further downscaling to higher resolution Regional Climate Models (RCMs) for New Zealand. Results from these RCMs were used to determine the rainfall augmentation factors (Table 8.1), and future New Zealand temperatures increases (Table 8.2), for 1-hour through 24-hour storm durations. It is important that the two tables are used together to determine the percentage increase in rainfall for each degree increase in temperature. These tables are effectively an update of Table 5.2 of MfE (2008).

Table 8.1: Percentage increase in rainfall per degree increase in temperature. Most likely change shown on top line with the range provided in brackets. Values based on RCM results across New Zealand (from Table 13 of MfE, 2018).

Duration	1% AEP
1-hour	13.6 (10.7-19.4)
2-hour	13.1 (10.1 – 19.6)
6-hour	11.5 (8.5 - 17.4)
12-hour	10.11 (7.3-15.4)
24-hour	8.6 (5.2-12.8)

Table 8.2: Projected increases in mean annual temperature by 2040 and 2090 for New Zealand (from Table 14 of MfE, 2018).

Scenario	2031-2050 i.e. 2040 (°C)	2051-2100 i.e. 2090 (°C)
RCP2.6	0.59	0.59
RCP4.5	0.74	1.21
RCP6.0	0.68	1.63
RCP8.5	0.85	2.58

Note: The data in the columns are from Table 14 in Ministry for the Environment (2018). The MfE table covers the projected mean temperature change between 1986-2005 and the periods 2031-2050 (2040), 2081-2100 (2090). They are the average of the six RCM model simulations (driven by different GCM).

At the present time, the direct effect of global climate change on stream runoff, and particularly flooding, has not been quantified; however, it is often assumed that an increase in rainfall will result in an equal increase in runoff.

NZTA have set as a minimum requirement, a 2.1°C warming of temperature leading to increased rainfall and runoff. However, this minimum requirement may not now produce the desired resilience to climate change i.e. the different RCP pathways may produce greater increases in rainfall than the assumed 2.1°C of warming.

To assess how the different climate change methodologies might affect the design rainfalls, the design rainfalls from HIRDS displayed in Table 7.3 were adjusted, assuming both a 2.1°C increase in temperature and the four RCP pathways in MfE (2018). The percentage change factors applied to the design rainfall depths for the 2.1°C increase used the values from MfE (2018), which were originally presented in NIWA (2018).

The results showed that for all durations and frequencies of events, the design rainfalls adjusted for a 2.1°C increase in temperature produced higher rainfalls than the RCP 2.6, RCP 4.5 and RCP 6.0 pathways over both future periods i.e. 2040 and 2090 (Table 8.3). This was also true for the RCP 8.5 pathway out to 2040 (Table 8.4). However, for the RCP 8.5 pathway out to 2090, the 2.1°C adjusted rainfalls were slightly less; although only by 3-5% (Table 8.5).

Table 8.3: Design rainfalls at high elevation from HIRDS adjusted for climate change by assuming a 2.1°C warming, using percentage increases as per Table 13 in MfE (2018) out to 2090.

AEP (%)	ARI (yrs.)	Duration									
		10-min	20-min	30-min	1-hr	2-hr	6-hr	12-hr	1-day	2-days	3-days
50	2	9	12	15	20	27	42	54	69	88	99
20	5	13	17	20	27	36	55	71	90	113	128
10	10	16	21	24	33	43	66	84	106	132	148
5	20	19	25	29	39	51	76	97	122	151	169
2	50	23	30	36	47	62	92	116	144	177	197
1	100	27	35	41	54	70	104	131	161	196	219

Table 8.4: Design rainfalls at high elevation from HIRDS adjusted for climate change by assuming an RCP 8.5 pathway adjustments as per MfE (2018) out to 2090.

AEP (%)	ARI (yrs.)	Duration									
		10-min	20-min	30-min	1-hr	2-hr	6-hr	12-hr	1-day	2-days	3-days
50	2	10	13	15	21	28	43	56	71	90	102
20	5	13	18	21	28	38	58	74	93	116	131
10	10	16	22	26	34	45	68	87	109	135	152
5	20	20	26	30	40	53	80	101	126	155	173
2	50	24	32	38	50	65	96	120	148	182	202
1	100	28	37	43	57	74	109	136	167	202	225

Table 8.5: Differences in the design rainfalls adjusted for projected climate change using the two methodologies (mm). Positive numbers indicate RCP 8.5 pathway values are greater than 2.1°C warming values.

AEP (%)	ARI (yrs.)	Duration									
		10-min	20-min	30-min	1-hr	2-hr	6-hr	12-hr	1-day	2-days	3-days
50	2	5	4	4	5	5	4	4	3	3	3
20	5	5	5	5	5	5	4	4	3	3	3
10	10	5	5	5	5	5	4	4	3	2	3
5	20	5	5	5	5	5	4	4	3	3	3
2	50	5	5	5	5	5	4	4	3	3	3
1	100	5	5	5	5	5	5	4	4	3	3

This indicates that the assumption of a 2.1°C adjustment of the design rainfalls for the project area is quite conservative. Only the most extreme RCP 8.5 pathway out to 2090 exceeds these projections.

The RCP 8.5 pathway assumes that current global emissions will continue to rise i.e. this is the worst-case scenario. The adoption of this RCP is justified by an awareness that current emissions are tracking this pathway, and a desire to design infrastructure to be resilient. However, this emission pathway assumes no reduction in emissions over the coming century, and abundant fossil fuel use in future production. It has been suggested that fossil fuel use at this rate will result in the depletion of all known coal and oil resources by 2070 (Wang *et al.*, 2017). Based on current policies and pledges made by countries around the world (including New Zealand), this emission’s pathway (driven by anthropogenic emissions) may not eventuate.

Therefore, the minimum requirement to use 2.1°C warming for future climate change is likely to produce conservative results; although not to the extent predicted by the RCP 8.5 pathway. However, it allows a reasonably high level of conservatism in design and ensures a resilient design offering a potentially higher level of service. The use the design rainfalls in Table 8.3 is therefore recommended to support the design and construction of Te Ahu a Turanga out to 2090.

8.2 Climate change 2120

As indicated above, the ‘Minimum Requirements’ only discuss the potential impact of climate change out to 2090. However, consideration of the potential impact of 100-years climate change analysis is now standard practice for hydrological advice for major infrastructure projects. Since Te Ahu a Turanga will be completed in approximately 2024, a 100-year timeframe would extend to approximately 2120 rather than 2090. Therefore, the potential impact of predicted climate change on the design rainfalls out to 2120 was also considered.

As discussed above, MfE (2016) provides climate change predictions for the different regions of the New Zealand. The change in mean temperature was estimated assuming four different representative concentration pathways (RCPs). However, because of time and cost constraints only three of the four RCP scenarios were projected out to 2120 (Figure 8.1).

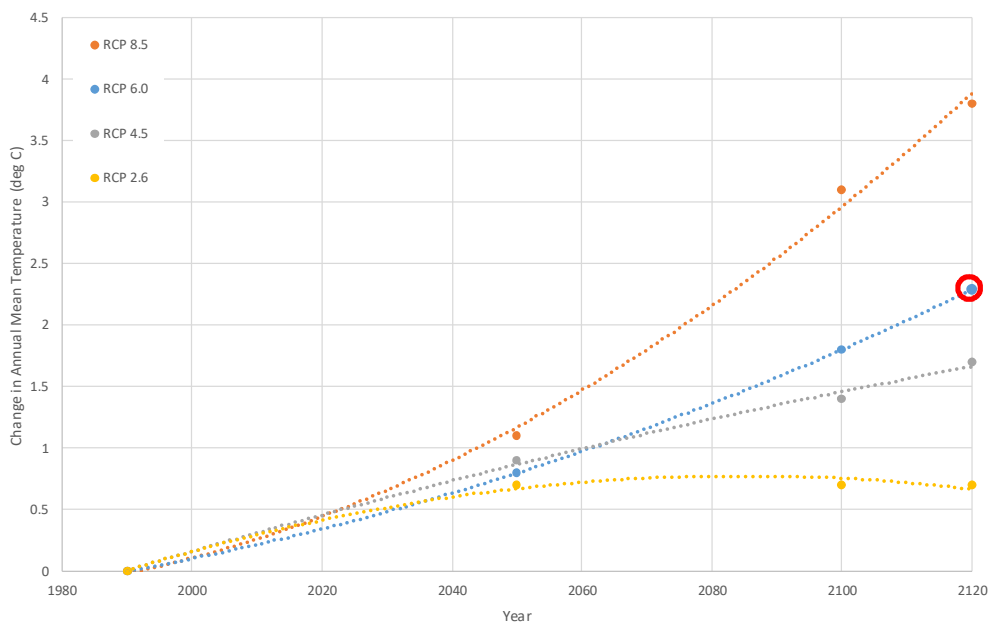


Figure 8.1: Temperature projections assuming various RCPs. Since RCP 6.0 was not modelled, it has been extrapolated. The projected 2120 temperature increase under RCP 6.0 is highlighted in red.

The RCP 6.0 scenario can be considered a “middle of the road” prediction of climate change and has been adopted by a number of TLAs and several major infrastructure projects. However, this scenario was not projected out to 2120. Since the change in temperature from 2030 to 2120 is non-linear for RCP 4.5 and RCP 8.5, a similar interpolated trend was applied to RCP 6.0. This provided a simple projection of the temperature change in 2120 (Figure 8.1). Using the longer-term trend in temperature increase, the projected increase over various timeframes can be determined (Table 8.6).

Table 8.6: Projected temperature increase over different time periods for Manawātū.

Climate change scenario	Temperature increase (°C) 2031-2050	Temperature increase (°C) 2081-2100	Temperature increase (°C) 2101-2120
RCP 8.5	1.1	3.1	3.8
RCP 6.0	0.8	1.8	2.3
RCP 4.5	0.9	1.4	1.7
RCP 2.6	0.7	0.7	0.7

These increases in temperature can then be used, with the modelled increase in rainfall described previously and listed in Table 8.7, to adjust the design rainfalls for Te Ahu a Turanga.

Table 8.7: Percentage increase in rainfall per degree increase in temperature.

ARI (yrs.)	Duration							
	10-min	20-min	30-min	1-hr	2-hr	6-hr	12-hr	24-hrs
2	12.2	12.2	12.2	12.2	11.7	9.8	8.5	7.2
5	12.8	12.8	12.8	12.8	12.3	10.5	9.2	7.8
10	13.1	13.1	13.1	13.1	12.6	10.8	9.5	8.1
20	13.3	13.3	13.3	13.3	12.8	11.1	9.7	8.2
30	13.4	13.4	13.4	13.4	12.9	11.2	9.8	8.3
40	13.4	13.4	13.4	13.4	12.9	11.3	9.9	8.4
50	13.5	13.5	13.5	13.5	13.0	11.3	9.9	8.4
60	13.5	13.5	13.5	13.5	13	11.4	10.0	8.5
80	13.6	13.6	13.6	13.6	13.1	11.4	10.0	8.5
100	13.6	13.6	13.6	13.6	13.1	11.5	10.1	8.6

The design rainfalls in 2120, assuming the RCP 6.0 and RCP 8.5 scenarios, are provided in Table 8.8 and Table 8.9 respectively.

Table 8.8: Design rainfalls at high elevation from HIRDS adjusted for climate change by assuming 2.3°C warming (i.e. RCP 6.0) and the percentage increases (Table 8.7) out to 2120.

AEP (%)	ARI (yrs.)	Duration									
		10-min	20-min	30-min	1-hr	2-hr	6-hr	12-hr	1-day	2-days	3-days
50	2	9	12	15	20	27	42	55	70	88	100
20	5	13	17	20	28	37	56	72	91	114	129
10	10	16	21	25	33	44	67	85	107	133	149
5	20	19	25	30	39	52	78	99	124	153	170
2	50	24	31	36	48	63	93	118	145	179	199
1	100	28	36	42	55	72	106	133	163	198	221

Table 8.9: Design rainfalls at high elevation from HIRDS adjusted for climate change by assuming 3.8°C warming (i.e. RCP 8.5),) and the percentage increases (Table 8.7) out to 2120.

AEP (%)	ARI (yrs.)	Duration									
		10-min	20-min	30-min	1-hr	2-hr	6-hr	12-hr	1-day	2-days	3-days
50	2	11	14	17	23	31	47	61	77	96	108
20	5	15	20	23	32	42	63	81	101	124	140
10	10	18	24	29	38	50	75	95	118	146	162
5	20	22	29	34	45	59	88	111	136	167	185
2	50	27	36	42	56	72	106	132	161	196	216
1	100	32	42	49	64	83	120	149	180	217	241

8.3 Changes to stormwater flows

The design of stormwater-related infrastructure is based on rainfall inputs using simple lumped rainfall/runoff models to estimate runoff from each sub-catchment. The design rainfalls adjusted for the effects of climate change to 2130, given in Table 8.8 (or Table 8.9), can therefore be applied directly as the rainfall hyetographs for any particular design event. Given the results of the analysis above, it is suggested that the design rainfalls in Table 8.8 are the more appropriate and allow for a reasonable level of conservatism.

8.4 Changes to channel flow

The design of bridge crossings over larger streams and rivers on Te Ahu a Turanga follow a different approach to that for the stormwater infrastructure. Flood estimates have been obtained directly from flood frequency analysis of the annual maxima series from hydrological gauging station records. This assumes climate stationarity over the period of each historic flow record which is reasonable given their relatively short length.

To estimate the effects of future climate change on these flood estimates (based on current climate conditions), it is necessary to relate the projected increases in rainfall given in Table 8.8 (or Table 8.9) to the likely increases in the flood estimates. Normally this could be estimated using a calibrated rainfall/runoff model for each catchment. However, because of the size and nature of the catchments concerned, the lack of rainfall and flow data, and the potential for strong orographic effects on rainfall from the catchment topography, this is not possible.

The case studies given in MfE (2010a) also provided mixed results in terms of the increase in flood magnitude relative to the projected increase in rainfall from the application of calibrated rainfall/runoff models. However, the assumption of a linear relationship between increases in flood discharge and projected increases in rainfall is in the right order.

In considering the effects of future climate change to 2120 therefore, a simple factoring approach was adopted for the base estimates of flood magnitude. This factoring approach assumes that the projected increases in flood magnitude approximate the projected increases in rainfall i.e. the increase in temperature times the percentage increase in rainfall per degree of warming.

9 Critical Rainfall Duration

A key characteristic of rainstorms is that the greatest intensities are experienced over short durations and limited areas. As the storm duration increases the average intensity will decrease, even though the total depth of rainfall increases. Consequently, the total volume of storm runoff might increase but the specific flood peak will decrease.

The Time of Concentration (T_c) is therefore critical. The T_c defines the minimum storm duration necessary for the entire catchment to contribute water to the point of interest. As such, it also defines the maximum intensity that can be sustained over the catchment to give the peak discharge. While shorter duration storms may have greater intensities, unless the entire catchment is contributing runoff the flood peak will be reduced. Longer duration events also have lower average intensities, therefore also reducing the flood peak.

Analysis of total rainfall depths and average intensities is relatively straightforward when only the peak discharge is required e.g. when using the Rational Method. However, it is more complicated when these data are required for input to quantitative models e.g. HEC-RAS™ or MIKE™. In these situations, it is necessary to distribute the total rainfall depth over the storm duration. The greater the resolution (shorter time-step) the greater the potential problem.

It should be noted that the distribution of storm rainfall varies as a function of storm duration, even though the total rainfall depth may be the same. One-hour duration events may have a different rainfall distribution to 6-hour events, which may be different again from 24-hour duration events. As described above, the temporal distribution of rainfall within a specific storm is often reduced to a simplified hyetograph; such as that provided by the 'Chicago Storm' and used within the Auckland Council standard design guide TP108.

However, it must be remembered that the distributed total storm rainfall depth over the storm duration may produce significantly lower intensities than would be sustained for similar time periods determined from

shorter duration storms. Again, this is because higher intensities cannot be sustained over longer durations. If higher intensities occur then, in general, the total storm duration will be short.

The critical storm duration is that which is long enough for all parts of the catchment to be just providing runoff to the point of interest. Any shorter and runoff from some parts of the catchment will not have arrived. Any longer and the intensity of the rainfall will start to decrease. Defining runoff for a particular design storm event requires an understanding of:

- The area which will contribute runoff;
- The critical duration of the storm;
- The total depth of rainfall; and
- The temporal distribution of rainfall throughout the storm event.

Critical storm durations in the project area, apart from the Manawatū and Mangamanaia catchments, are likely to be from 1-6 hours, and even shorter for most sub-catchments. This is because of the relatively small catchments, steep terrain, shallow soils and generally limited forest cover. The lack of storage and channel conveyance capacity will also prevent attenuation of the runoff.

10 Areal Reduction Factor (ARF)

In hydrological design and planning, it is usually necessary to assign a design rainfall consisting of a set of rainfall depths or intensities varying in space (i.e. areal variation) and time. The characteristics of the design storm should reflect conditions that can realistically be expected to occur within the catchment.

Gauge rainfall data are point-based, and the measured rainfall is likely to be accurate only for a relatively small area immediately around the gauge. Since rainfall varies as a function of the size of the storm, these point estimates of rainfall must be converted to average rainfall depths over a specific area i.e. areal depth. This involves the adoption of an Areal Reduction Factor (ARF). This is particularly important for larger catchments, as rainfall is unlikely to fall across the catchment in a uniform manner. The application of an 'unscaled' design rainfall across the entire area results in extremely high, and unrealistic, runoff volumes.

NIWA (2018) conducted a review of areal reduction calculations and derived an empirical equation for deriving ARFs for various sized-catchments (Figure 10.1). The analysis looked at ARF for areas from 10km² to 500km² and storm durations from 1-hour to 100-hours. In general, the ARF decreased for shorter events and larger catchments; smaller catchments i.e. 10km² had the least variability of ARF.

The various sub-catchments intersected by Te Ahu a Turanga are generally small, apart from the Manawatū and Mangamanaia catchments i.e. generally <1km². The ARF analysis provided in NIWA (2018) did not consider catchments smaller than 10km². Figure 10.1 suggests the ARF that could be applied would range from 0.96 to 0.9775. Therefore, not applying an ARF will have little effect on the design rainfalls and the resulting runoff, apart from the fact that they will be slightly conservative i.e. high. Any difference from not applying an ARF will be within the level of uncertainty of both the design rainfalls and any subsequent modelling. Therefore, the application of an ARF to the design rainfalls is not recommended except in the case of the Mangamanaia catchment, for which there is no robust flow record.

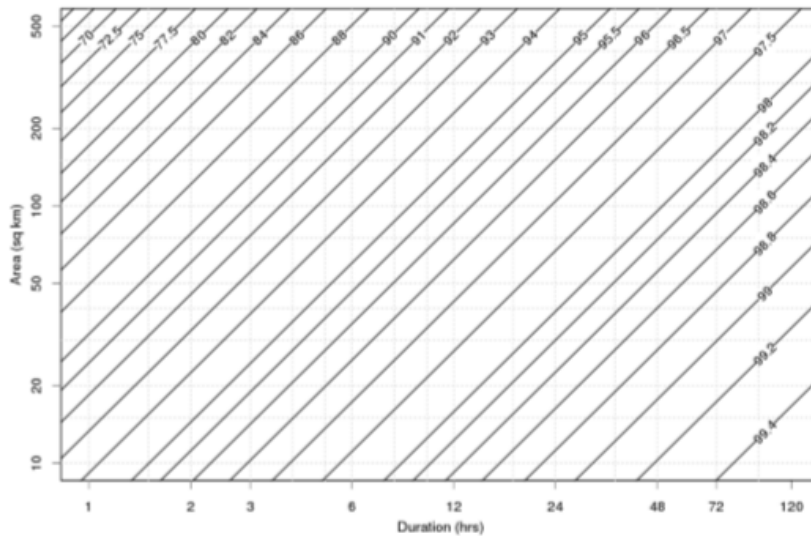


Figure 10.1: Area reduction factors (in %) derived from the empirical model fitted to all three regions in New Zealand (NIWA, 2018).

11 Temporal Distribution

The distribution of rainfall throughout a storm event can have a significant effect on the results of rainfall-runoff computations and stormwater models. While the total storm runoff volume is not affected by the temporal distribution of rainfall, both the peak discharge and its associated lag time can be affected dramatically. This is more apparent in larger catchments with longer storm durations (i.e. greater than 1-hour). Generalised models that distribute the storm rainfall evenly throughout the storm event produce a lower peak discharge than a model that 'lumps' the bulk of the rain over only one part of the storm event. Furthermore, the actual temporal distribution of a storm at a specific site may be distinctly different from the generalised distributions that are used around New Zealand. The temporal variability needs to be accommodated within any rainfall-runoff calculation if it is to produce realistic estimates of peak discharge.

Therefore, the temporal distributions of the design rainfalls used in the design and construction of Te Ahu a Turanga need to be determined so that the most appropriate storm hyetographs can be used for stormwater modelling in those sub-catchments greater than 200ha. For smaller sub-catchments, where the Rational Method was used, a lumped total storm rainfall approach was adopted.

The most common generalised temporal rainfall distributions applied in New Zealand are TP108, Probable Maximum Precipitation (PMP), and the HIRDS nested storm.

TP108 uses a nested hyetograph where, for any specified duration, from 10-minutes through to 24-hours, the maximum intensity of rainfall for each duration has the same Annual Exceedance Probability (AEP). This 'type-hyetograph', however, does not represent any measured historical rainstorm. When combined with the correct time of concentration this allows the catchment runoff analysis to operate on the relevant duration embedded within the nested storm. TP108, however, has only been validated for catchments up to 12km² in Auckland. The project area for Te Ahu a Turanga is unlikely to share the same rainfall patterns as Auckland, meaning the temporal distribution will also differ.

The use of the TP108 distribution tends to produce a much higher peak discharge when compared to either actual storm hyetographs, or the Probable Maximum Precipitation (PMP). Consequently, the use of the TP108 rainfall distribution can lead to conservative design and greater expenditure than required to provide the desired level of service.

The Probable Maximum Precipitation (PMP) temporal distribution, in contrast to TP108, was derived from autographic rainfall charts from North Island storms, using a temporal pattern of average variability, as proposed by Pilgrim *et al.* (1969 & 1975). This method is aimed at producing, from the recorded intense bursts of a given duration, a temporal pattern with an average variation in intensities, together with a most likely sequence of these varying intensities. The temporal sequences were then 'smoothed' to reduce any inconsistencies within the temporal pattern. The PMP provides temporal distributions for various storm durations; from 1-hour up to 96-hours (Tomlinson & Thompson, 1992). As this method was derived using empirical data, it may be more representative for Te Ahu a Turanga. However, the method did not consider any recent storm data from the project area, where the majority of the empirical data records only begin in the mid-1980s.

A temporal design storm methodology was developed as part of the recent review of HIRDS. A reconnaissance study was undertaken of storm hyetographs using a conventional analysis of suitably long records from clusters of rain gauges throughout New Zealand. This involved about 70 rain gauges measuring at 15-minute intervals or less and having a long common record length of at least 30 years. These gauges were subsequently split into six regions across the country. It was found that an asymmetric hyperbolic tangent function provided a simple and robust model for cumulative hyetographs when using the empirical data. Although there was little regional difference between the cumulative hyetographs for short durations, variability increased with storm duration. There is no apparent influence of return period or storm magnitude on the results. For most cases when a duration of 24-hours or less is used, the generic New Zealand-wide hyetograph varies little from those of the six regions. This is not the case for longer storm durations (NIWA, 2018).

The HIRDS approach uses actual temporal rainfall records similar to the PMP but includes more recent data and a greater range across the country. However, it requires further investigation for storm durations less than 1-hour, and more gauges with sufficient length of record to make substantive progress in empirical calculations of design hyetographs (NIWA, 2018).

To determine the most appropriate temporal distribution to apply to sub-catchments over 200ha intersected by Te Ahu a Turanga, the average temporal pattern of the five largest rainfall events recorded at the closest high-resolution gauge were used; Pohangina at Alphabet Hut. This site was selected over Pohangina at Mais Reach as it has a longer record and is at an altitude similar to the maximum elevation traversed by Te Ahu a Turanga. These events were compared to the PMP, TP108 and HIRDS nested distributions over various storm durations (Figure 11.1 through Figure 11.3). The HIRDS distribution does not have a 'set' 2-hour pattern, so the 1-hour distribution was used for comparison.

The analysis shows that the empirical storm rainfall hyetograph generally follows the PMP distribution for the 1-hour and 2-hour durations. For 6-hour storms, the HIRDS temporal distribution provides a better fit; although there was still some variation from the empirical data, particularly over the later part of the storm.

This analysis clearly shows that the temporal distribution assumed in TP108 is not appropriate for the design and construction of Te Ahu a Turanga. The use of the TP108 distribution would result in excessive peak discharges and consequently significant over-design of stormwater infrastructure.

Therefore, in the smaller sub-catchments where the Rational Method was adopted for assessing peak discharge, a lumped total storm rainfall approach was used. In those cases when a temporal rainfall distribution was required i.e. the larger sub-catchments, the PMP temporal distribution is recommended for storms of up to 2-hours duration. In any larger sub-catchment, where the T_c approaches 6-hours, the storm hyetograph should be developed using the HIRDS temporal distribution.

For these larger sub-catchments, a sensitivity analysis of the effect of the temporal distribution was undertaken to confirm that the rainfall-runoff modelling was providing realistic peak flow estimates.

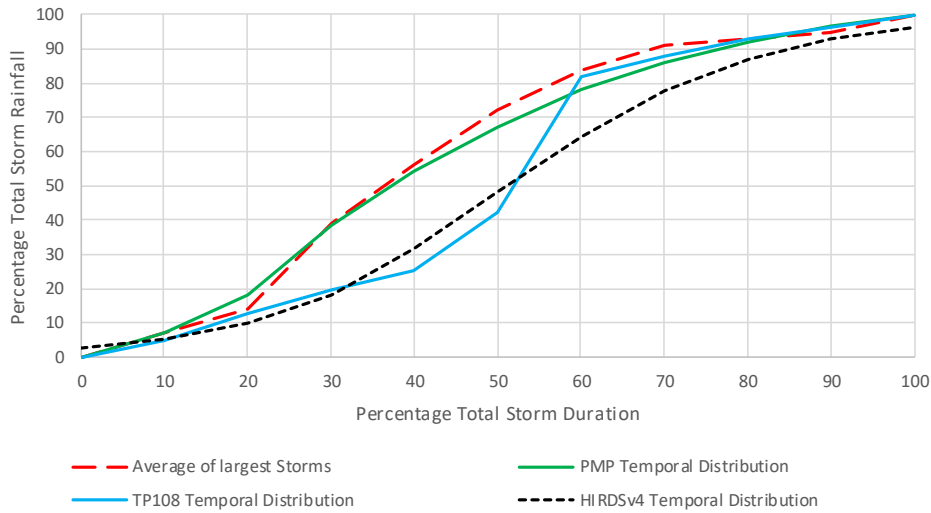


Figure 11.1: 1-hour temporal distribution, Pohangina at Alphabet Hut.

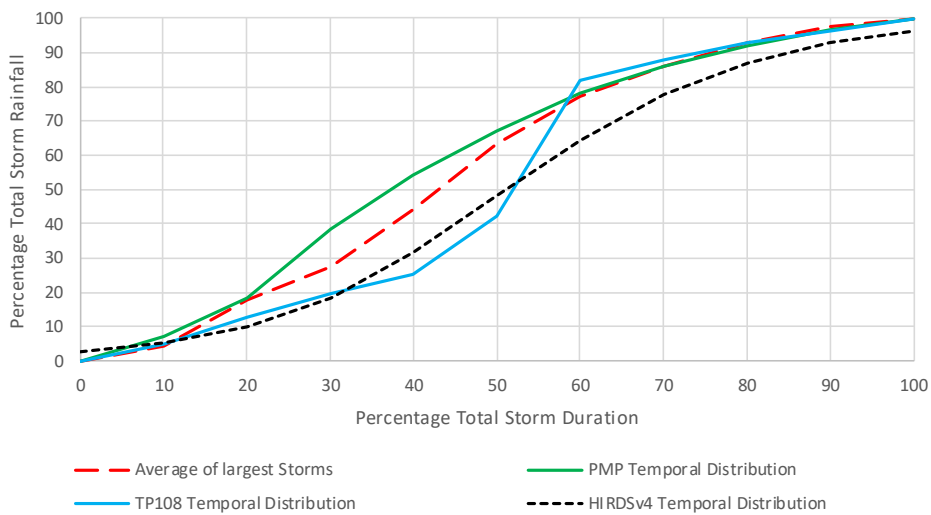


Figure 11.2: 2-hour temporal distribution, Pohangina at Alphabet Hut.

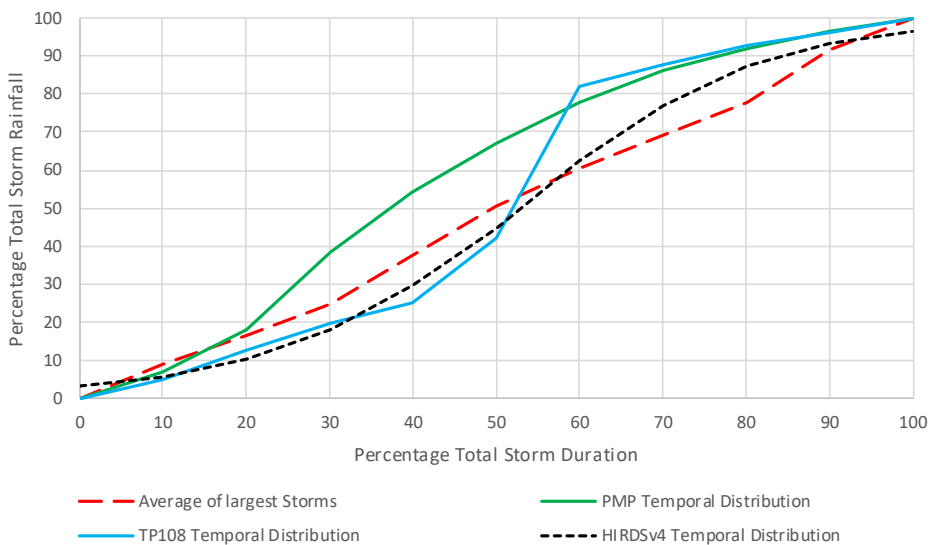


Figure 11.3: 6-hour temporal distribution, Pohangina at Alphabet Hut.

12 Erosion and sediment control thresholds

Erosion and sediment control structures are an integral component of the design of the Te Ahu a Turanga Highway. These structures will capture material mobilised during storm events and mitigate any potential adverse environmental effects. These structures need to be maintained and inspected regularly to ensure that they are operating effectively.

In addition to routine inspections and maintenance, it is common practice to inspect the erosion and sediment control structures following significant rainfall events when the devices are likely to be stressed or nearing capacity. However, defining a significant rainfall event can be problematic, particularly in areas with limited rainfall information.

Erosion and sediment control structures are normally designed to treat either 200m³/ha (2%) or 300m³/ha (3%) of runoff from the catchment. These runoff volumes equate to 20mm or 30mm of rainfall, assuming 100% runoff.

In previous large-scale infrastructure projects, two design rainfalls have been used to define when inspections of erosion and sediment control infrastructure should be undertaken; >15mm/hr or >25mm over 24-hours. However, whether these thresholds are appropriate for the Project needs to be confirmed.

12.1 Rainfall analysis

As discussed, there are no empirical rainfall data of suitable length that can be used to characterise the rainfall regime of the project area. Previous analysis has shown that HIRDS v4 can be used to derive representative design rainfalls. HIRDS, however, does not provide a time series that can be used to quantify the frequency at which these thresholds might be exceeded. The most representative, high-resolution rain gauge in the vicinity of the project area is Pohangina at Alphabet Hut. The record from this site was therefore used to determine the likely frequency of site inspections based on the two thresholds.

12.2 AEPs of depth and intensity thresholds

The AEPs for design rainfalls of both >15mm/hr or >25mm over 24-hours, derived using the empirical data from Pohangina at Alphabet Hut and the HIRDS, are displayed in Table 12.1. The AEPs were derived by interpolation of the design rainfalls for the respective durations i.e. 1-hr and 24-hrs.

Table 12.1 : AEPs of the two thresholds based on both the empirical data and HIRDS.

	>15mm/hr.	>25mm in 24hrs
Pohangina at Alphabet Hut	60.75%	100%
HIRDS project site	44.56%	100%

A rainfall event of more than 25mm over a 24-hr period could be expected to occur at least once a year, and generally significantly more often. While the likelihood of rainfall exceeding 15mm/hr is slightly less, it still has a high probability of occurring in any given year. It should be noted that the frequency of higher rainfall events is greater at Alphabet Hut than in the project area; as a result of orographic enhancement of rainfall over the Ruahine Range.

12.3 Frequency of threshold exceedances

Using the Pohangina at Alphabet rainfall record, the frequency that the two thresholds are exceeded was assessed (Table 12.2 & Figure 12.1).

Table 12.2: The total number of times the two rainfall thresholds have been exceeded at Pohangina at Alphabet Hut and the frequency each year.

	Total	Minimum	Mean	Median	Maximum
15mm/hr	21	0	1	<1	4
25mm/day	327	1	9	9	18

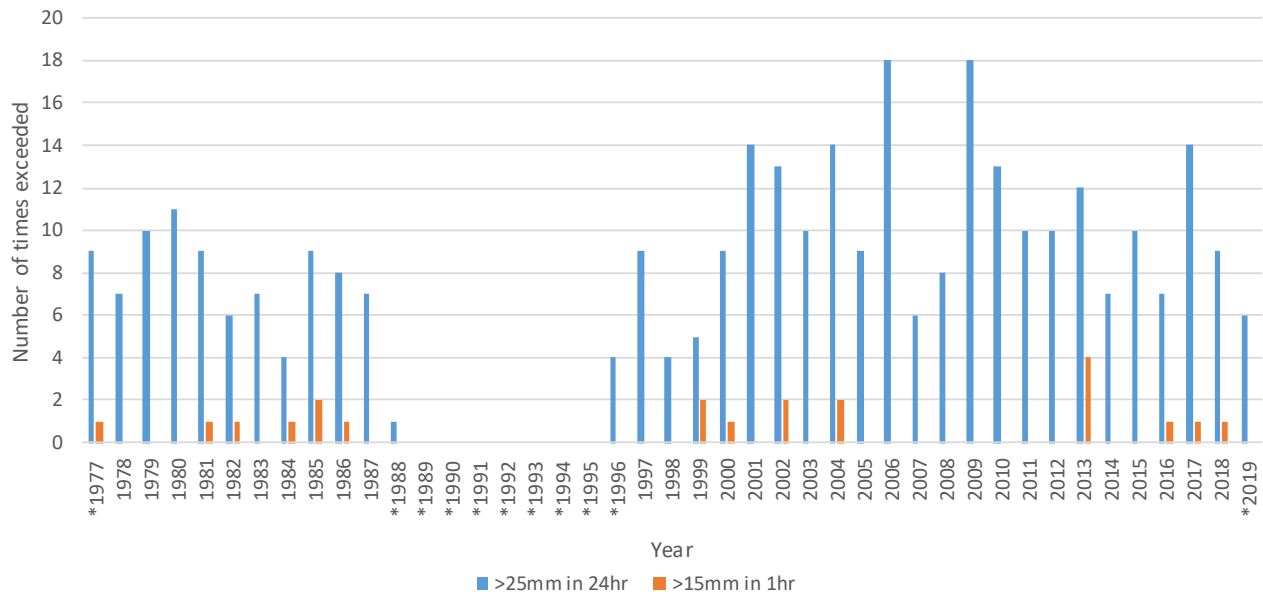


Figure 12.1: Comparison of number of times the two thresholds were exceeded at Pohangina at Alphabet Hut. Asterisk indicates missing or partially missing years.

On average, there have been 9 times each year when at least 25mm of rainfall was recorded at Pohangina at Alphabet Hut over 24-hours. In contrast, the higher but shorter intensity of 15mm/hr only occurs once a year on average. There have been only 21 instances of rainfall at this intensity being recorded over the entire record.

Having two distinct thresholds to monitor the erosion and sediment control structures may not be an efficient use of resources if the thresholds are not mutually exclusive; i.e. if the 15mm/hr occurs within the 24-hour period when more than 25mm of rainfall is recorded. Analysis was therefore carried out to compare the number of times when both thresholds were triggered contemporaneously.

Figure 12.2 & Table 12.3 show that when there is at least 15mm of rainfall recorded over an hour, there is always at least 25mm of rainfall over the same day. There have been no instances of the 15mm/hr. threshold being exceeded when the 25mm/day threshold was not. There has been one occasion when over 15mm/hr. of rainfall was recorded four times on the same day (18 March 2013) and four other occasions when two bursts of rainfall at this intensity occurred on the same day.

This result suggests that only having one threshold e.g. 25mm over 24-hours, is necessary for this project. The inclusion of the other threshold adds nothing to the frequency of site visits and quality control of the sediment and erosion control devices. Furthermore, because of site access and the very short response time of the catchments upstream of the majority of the control devices, it would be impossible to check for performance or damage after any 15mm/hr. rainfall event in a proactive manner.

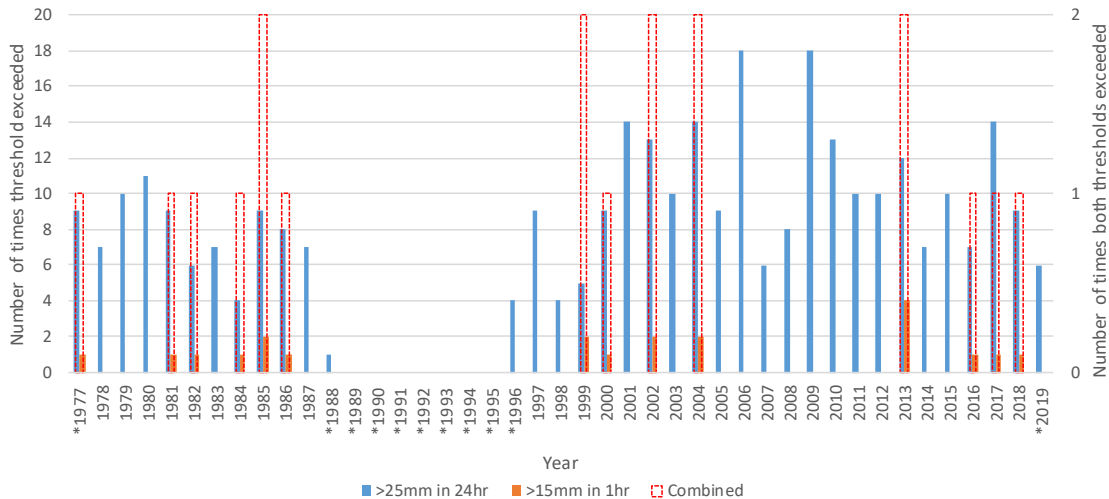


Figure 12.2: Comparison of number of times the two thresholds were exceeded at Pohangina at Alphabet Hut, as well as when the two thresholds occurred contemporaneously. Asterisk indicate missing or partially missing years.

Table 12.3: Total number of occasions when the two thresholds occurred contemporaneously, and the number of times each year.

	Total	Minimum	Mean	Median	Maximum
15mm/hr and 25mm/day	19	0	1	0	2
15mm/hr only	0	0	0	0	0
25mm/day only	308	1	9	9	16

12.4 Sensitivity to threshold

The two thresholds used in the above analysis were chosen because they have been used in previous large scale infrastructure projects. However, it has not been possible to find a robust justification for the use of these thresholds, except that a rainfall of approximately 25mm/day has the potential to fill the treatment device to capacity.

Since with respect to this Project the hourly rainfall threshold added no greater information, it was not considered further. The potential effect of adopting a range of different daily rainfall thresholds was therefore reviewed (Table 12.4). For the 24-hour event, using rainfall data from the Pohangina at Alphabet Hut, a threshold of 25mm/day would be exceeded on 9 times a year on average, but up to 18 times. Increasing the threshold to 30mm/day reduces the number of occurrences by a third i.e. an average of 6/yr. Decreasing the threshold to 20mm/day increased the number of occurrences by 60% i.e. an average of 14/yr.

The use of a threshold of approximately 30mm/day based on the Pohangina at Alphabet Hut gauge, therefore appears to provide a reasonable frequency of site visits to confirm the performance and operation of the erosion and sediment control structures under 'near capacity' conditions.

Table 12.4: Comparison of the effect of different thresholds using rainfall data from the Pohangina at Alphabet Hut.

	Total	Minimum	Mean	Median	Maximum
20mm/day	518	2	14	14	28
25mm/day	327	1	9	9	18
30mm/day	219	1	6	6	12

This threshold (30mm/day measured at the Pohangina at Alphabet Hut gauge) would result in an average of six visits per year, although there could be up to 12. A rainfall of 30mm/day at the Pohangina at Alphabet Hut gauge is equivalent to about 23mm/day at the crest of the project area as discussed below.

12.5 Scaled rainfall

The above analysis used the empirical data from Pohangina at Alphabet Hut. Previous analysis has shown that rainfall at the Pohangina at Alphabet Hut gauge is higher than in the project area because of orographic enhancement. Therefore, the analysis is likely to indicate a greater number of occasions when the thresholds are exceeded than in the project area.

Consequently, the empirical rainfall data measured at Pohangina at Alphabet Hut was scaled as a simple function of the difference in the design rainfalls from HIRDS at both locations. A scaling factor of 0.77 was used to 'correct' the empirical record from the Pohangina at Alphabet Hut to provide rainfall more indicative of the project area.

Using the scaled rainfall record for the project area, the number of days when >25mm of rainfall occurred over a 24-hour period was determined (Table 12.5 & Figure 12.3).

As expected, there are fewer days that exceed this threshold in the project area than at the Pohangina at Alphabet Hut site. This is because of the lower elevation and consequently lower expected rainfall.

Table 12.5: Comparison of total number of days exceeding the threshold and the number of days each year.

	Total	Minimum	Mean	Median	Maximum
>25mm/day for Pohangina at Alphabet Hut	327	1	9	9	18
>25mm/day for project area	182	1	5	5	10

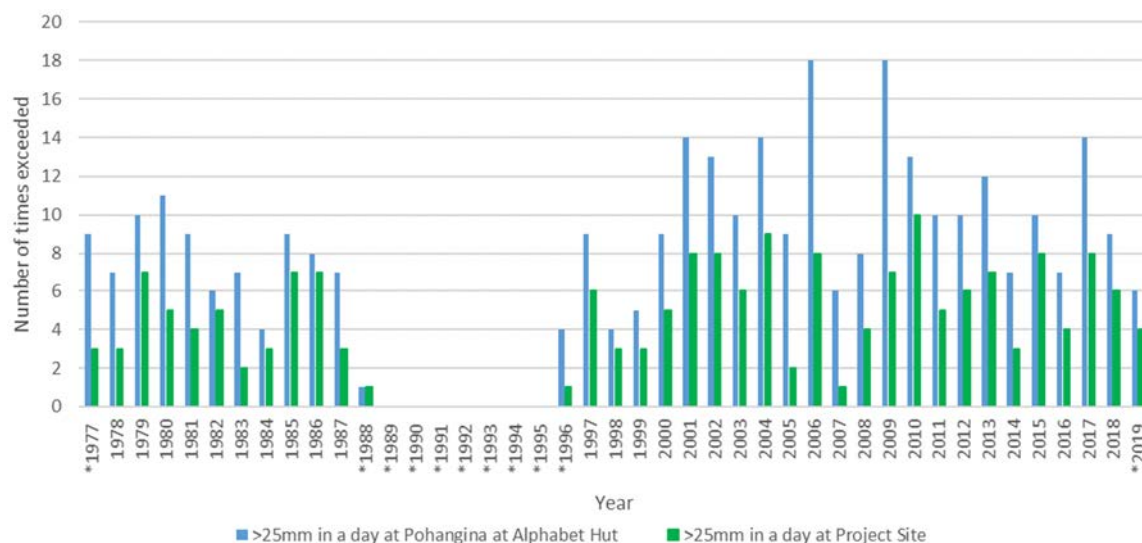


Figure 12.3: Comparison of number of times >25mm over 24-hours was recorded at Pohangina at Alphabet Hut compared to the scaled rainfall record at the project site. Asterisk indicated missing or partially missing years.

The sensitivity of the number of times the threshold was exceeded to the magnitude of the threshold was also assessed. A threshold of 25mm/day in the project area is exceeded on average about five times a year; although it can be up to ten times (Table 12.6).

Table 12.6: Comparison of the number of times the different thresholds have been exceeded at the project area based on scaling empirical data.

	Total	Minimum	Mean	Median	Maximum
20mm/day	300	1	8	8	17
25mm/day	182	1	5	5	10
30mm/day	120	0	3	3	9

A rainfall threshold of 25mm/day would therefore appear an appropriate trigger for additional inspections of the erosion and sediment control devices when they are likely to be under ‘near capacity’ conditions.

13 Conclusions

This rainfall analysis has shown that:

- While there are at least 36 gauges in the wider area, there is no high-resolution long-term rainfall record from the actual project area.
- There is some spatial variability in rainfall across the project area. It is generally wetter to the east and drier in the west. In addition, orographic enhancement of rainfall by the Ruahine Range results in the highest rainfall at the highest elevations i.e. in the middle of the project area. These patterns are supported by both the empirical data and the mean annual rainfall (MAR).
- Data from five gauges was analysed in detail to provide a range of empirical design rainfalls from the wider area.
- Comparison of the design rainfalls derived from the empirical data and HIRDS v4 demonstrated generally good agreement. It appears that the design rainfalls from HIRDS are slightly conservative i.e. high relative to the empirical rainfall records. In the absence of robust empirical data from close to the alignment, design rainfalls from HIRDS are considered appropriate to support the design and construction of Te Ahu a Turanga. Using design rainfalls from HIRDS is likely to lead to slightly conservative runoff estimates and stormwater design;
- The generally small size of the catchments intersected by Te Ahu a Turanga means that it is unnecessary to apply an Areal Reduction Factor (ARF). The effect of applying an ARF is likely to be within uncertainty inherent in the design rainfalls, and certainly within the uncertainty associated with any stormwater modelling;
- The minimum requirements provided by NZTA necessitate at least two sets of design rainfall tables; one for each of the western and eastern extents of the project area. However, rainfall variability across the project area means that design rainfalls are also required for the middle of the project area i.e. the area of highest elevation. These design rainfalls are slightly higher than those at both the western and eastern extents. Given the relatively small differences in the various design rainfall tables, that from the higher elevation could be used for the design and construction of all stormwater-related infrastructure. This would ensure slightly conservative, but still realistic, design. Therefore, the design rainfalls in Table 13.1 are recommended for infrastructure designed to perform under the current climate regime.

Table 13.1: HIRDS for design rainfalls in central project, high elevation area. Latitude -40.2984 Longitude 175.797. This is the recommended design rainfall table to be used for further analysis.

AEP (%)	ARI (yrs.)	Duration									
		10-min	20-min	30-min	1-hr	2-hr	6-hr	12-hr	1-day	2-days	3-days
50	2	7	10	12	16	22	35	46	60	78	89
20	5	10	13	16	21	29	45	60	78	99	113
10	10	12	16	19	26	34	54	70	90	115	130
5	20	15	19	23	30	40	62	81	104	131	148
2	50	18	24	28	37	48	74	96	122	153	172
1	100	21	27	32	42	55	84	108	136	169	191

- The minimum requirement of assuming a 2.1°C increase in temperature out to 2090 was based on MfE (2008). However, updated guidance has subsequently been provided in MfE (2018) which refers to four RCPs scenarios. The RCP 6.0 scenario can be considered a “middle of the road” prediction of climate change and has been adopted by a number of TLAs and several major infrastructure projects. However, this scenario was not projected out to 2120. Since the change in temperature from 2030 to 2120 is non-linear for RCP 4.5 and RCP 8.5, a similar interpolated trend was applied to RCP 6.0. This provided a simple projection of the temperature change in 2120.
- The design rainfalls over the 100-year life of the project i.e. in 2120, assuming the RCP 6.0 (2.3°C) scenario are provided in Table 13.2. It is suggested that these design rainfalls are the most appropriate when designing resilient stormwater and associated infrastructure for the life of the project.

Table 13.2: Design rainfalls at high elevation from HIRDS adjusted for climate change by assuming 2.3°C warming (i.e. RCP 6.0) and the percentage increases (Table 8.7) out to 2120.

AEP (%)	ARI (yrs.)	Duration									
		10-min	20-min	30-min	1-hr	2-hr	6-hr	12-hr	1-day	2-days	3-days
50	2	9	12	15	20	27	42	55	70	88	100
20	5	13	17	20	28	37	56	72	91	114	129
10	10	16	21	25	33	44	67	85	107	133	149
5	20	19	25	30	39	52	78	99	124	153	170
2	50	24	31	36	48	63	93	118	145	179	199
1	100	28	36	42	55	72	106	133	163	198	221

- Detailed analysis of the temporal distribution of storm rainfall using high-resolution data from a gauge at high elevation i.e. Pohangina at Alphabet Hut, indicates that for storms up to 2-hours duration the PMP distribution is appropriate. For longer duration storms e.g. 6-hour events, the HIRDS temporal distribution is more appropriate.
- The temporal distribution from TP108, stated in the minimum requirements, is not appropriate Te Ahu a Turanga. The use of the TP108 distribution would result in excessive peak discharges and consequently significant over-design of stormwater infrastructure.
- A single rainfall threshold can be used for monitoring the performance of erosion and sediment control structures. Every occasion when rainfall intensities exceeded 15mm/hr. was on a day when rainfall also exceeded 25mm/day i.e. the hourly rainfall intensity threshold would provide no additional information on the performance of the erosion and sediment control measures.
- Analysis shows that adopting a rainfall threshold of 25mm/day at the project site will lead to an average of five inspections each year (between 1 and 10). This is considered an appropriate number of visits each year to monitor the performance of the erosion and sediment control structures under ‘near capacity’ conditions.

14 References

- Ministry for the Environment. (2008). *Climate change effects and impacts assessment: A guidance manual for local government in New Zealand*. (2nd Ed). Mullan, B., Wratt, D., Dean, S., Hollis, M., Allan, S., Williams, T., Kenny, G. and MfE. Ministry for the Environment, Wellington.
- Ministry for the Environment. (2010a). *Preparing for future flooding: a guide for local government in New Zealand*. May 2010. Ministry for the Environment, Wellington.

- Ministry for the Environment. (2010b). Tools for estimating the effects of climate change on flood flows: a guide for local government in New Zealand. May 2010. Ministry for the Environment, Wellington.
- Ministry for the Environment. (2016). Climate change projections for New Zealand: Atmospheric projections based on simulations undertaken for the IPC fifth assessment.
- Ministry for the Environment. (2018). Climate change projections for New Zealand: Atmospheric projections based on simulations undertaken for the IPC fifth assessment; 2nd Edition.
- NIWA, (2018). High Intensity Rainfall Design System, Version 4. Prepared for Envirolink by National Institute of Water & Atmospheric Research Ltd. Report no. 2018022CH. August 2018.
- Pilgrim, D.H., Cordery, I. (1975). Rainfall temporal patterns for flood designs, Proc. Amer. Soc. Civ. Engrs., J Hydraulics Div., 100, No HY1, 81-95.
- Pilgrim, D.H., Cordery, I., French, R. (1969). Temporal patterns of design rainfall for Sydney. Civ. Engg. Trans., I.E. Aust., Vol. CE11, pp 9-14
- Tait A, Henderson R, Turner R, Zheng, XG. (2006). Thin plate smoothing spline interpolation of daily rainfall for New Zealand using a climatological rainfall surface. International Journal of Climatology, 26 (14): 2097–2115
- Tomlinson, A.I.; Thompson, C.S. 1992: Probable Maximum Precipitation in New Zealand - the development and application of generalised methods to provide nationwide estimates of PMP. Report prepared for the Electricity Corporation of New Zealand, New Zealand Meteorological Service, Wellington, New Zealand.

Appendix D.2: *Te Ahu a Turanga – Manawatū River Base Hydraulic Model.*

Te Ahu A Turanga

Manawatu River Base Hydraulic Model
February 2019

Job Number: 145850

Report Prepared by:  8/2/2019
Eugene Vodjansky Date

S.S. Joshi.
Suyash Joshi 08/02/2019
Date

Checked by:  08/02/2019
Constantinos Fokianos Date

Approved for issue by:  8/2/2019
Scott Bready Date

Document History and Status

Issue	Ver.	Issued To	Qty	Date	Prepared	Reviewed	Approved

Printed:
File Path: K:\145850 Te Ahu a Turanga\Stormwater\Report\Te Ahu A Turanga - hydraulic modelling report.docx
Project Manager:
Name of Organisation:
Name of Project:
Name of Document:
Document Version:
Project Number: 145850

Bloxam Burnett & Olliver Ltd
Level 4, 18 London St
PO Box 9041
HAMILTON

Phone: (07) 838 0144
email: consultants@bbo.co.nz

Contents

1.0	Introduction	1
1.1	Project Description.....	1
1.2	Scope and Purpose.....	1
2.0	Modelling Methodology	3
2.1	HEC-RAS Software	3
2.2	Input data.....	3
2.2.1	Terrain data and hydrographic survey	3
2.2.2	Upstream and Downstream Hydraulic Model Boundary Conditions	4
2.2.3	Hydraulic Model 2D Mesh.....	6
2.2.4	Channel Roughness.....	6
3.0	Conclusion.....	8

References

Appendix A – Flow Estimates

Appendix B – Roughness Coefients

1.0 Introduction

1.1 Project Description

The Te Ahu a Turanga: Manawatū Tararua Highway (TATP) is a designated new 2-lane road with 2 additional full-length crawler lanes that is to replace the existing Manawatu Gorge on SH3. It extends 11.4km across the Manawatū Saddle from Ashhurst in the west to Woodville in the east.

Figure 1.1 provides a general project location and shows the realignment of SH3 compared to the existing alignment.

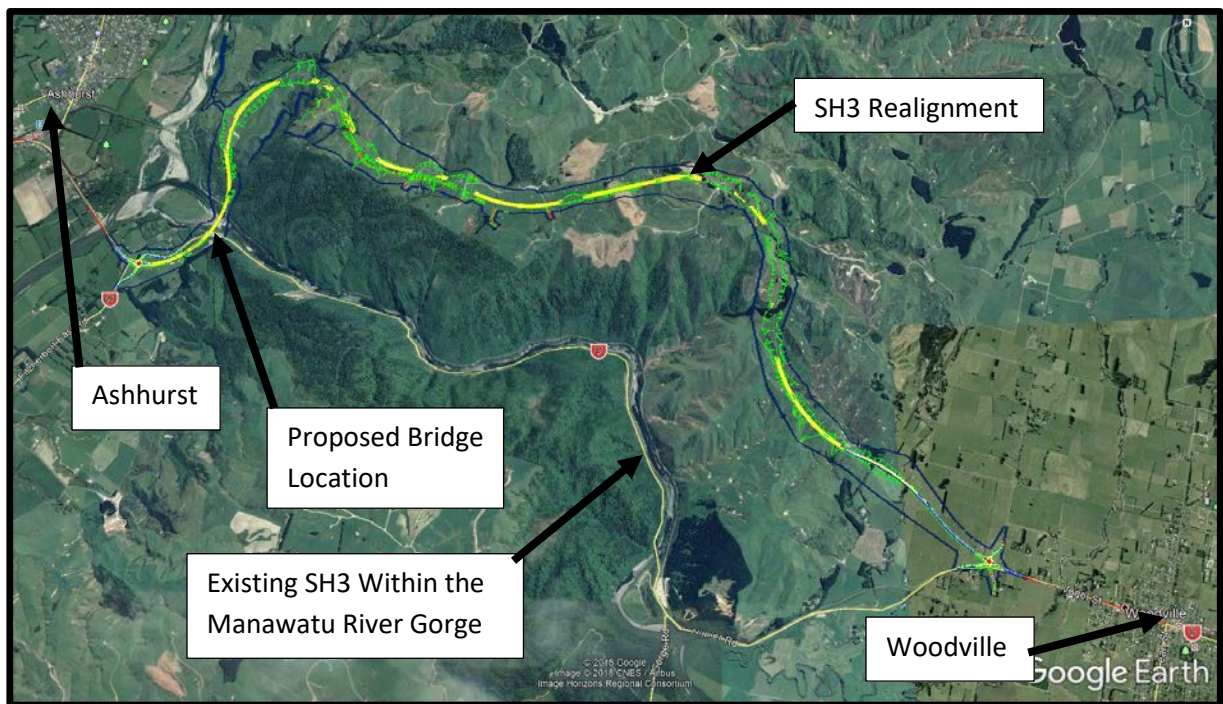


Figure 1-1.1 - Project Location and SH3 Realignment

1.2 Scope and Purpose

The Te Ahu A Turanga project requires a bridge across the Manawatu River at the downstream end of the Manawatu River Gorge. The hydraulics of the bridge location are complex and influenced by rapid flow expansion, braiding/anabranching, a confluence with the Pohangina River, and the Ashhurst Bridge. Due to this hydraulic complexity and project program constraints, a 2D hydraulic model of the affected reach of the Manawatu River has been developed for bridge hydraulics, assessment of scour, design of scour countermeasures, estimation of debris loading, and freeboard of the bridge over the design flood. If the bridge design proposed by the Tenderer is intended to completely span the Manawatu River, without pier, then this model will provide the design water levels for freeboard and abutment placement.

This report provides a general description of the hydraulic model, the inputs used to generate it, and the current limitations of the hydraulic model. Figure 1.2 shows the confluence of the Manawatu River with the Pohangina River and the general extents of the hydraulic modelling.

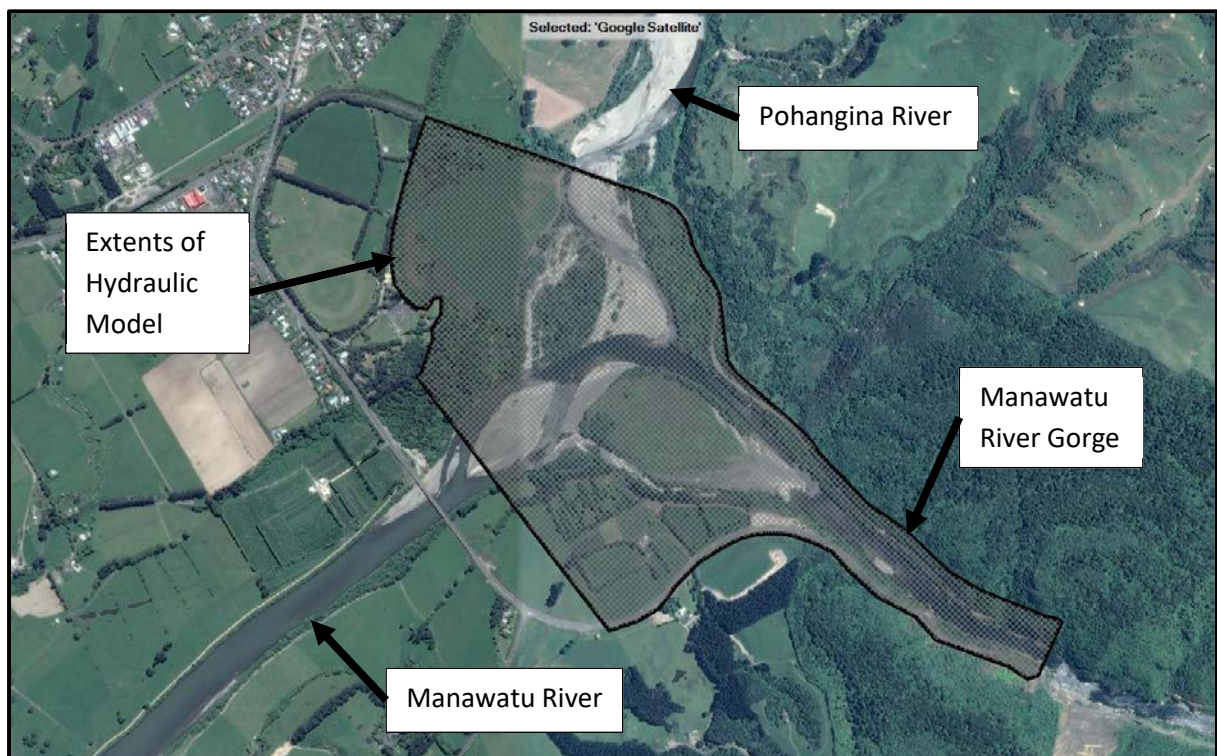


Figure 1-2 - Affected Reach and Extents of 2D HEC-RAS Model

2.0 Modelling Methodology

2.1 HEC-RAS Software

The affected reach of the Manawatu River, including its confluence with the Pohangina River, have been modelled using HEC-RAS version 5.0.6. HEC-RAS is a river analysis software developed by U.S. Army Corps of Engineers. HEC-RAS is designed to perform one-dimensional and two-dimensional hydraulic calculations for a full network of natural and constructed channels, overbank/floodplain areas, levee protected areas, etc.

Due to the highly variable main channel characteristics, including pool-riffle lengths, anabranching, and braiding, all combined with the confluence and the Ashhurst Bridge at the downstream limit of the model, a fully 2D model was necessary. The provided HEC-RAS 2D model solves for the 2D Saint Venant equations, with full momentum for turbulence and Coriolis effects. The computational mesh is unstructured. The HEC-RAS mesh does not have a flat bottom and cell faces/edges do not have to be a straight line or be limited to a single elevation. Each cell and cell face is based on the underlying terrain details, meaning the mesh lays on the terrain and the detail of the model is limited by the terrain model, not the size of the computational mesh.

HEC-RAS also allows variable time steps, eliminating unnecessary calculation iterations and shortening model run times. The variable time step option was used in the existing condition model.

2.2 Input data

2.2.1 Terrain data and hydrographic survey

The terrain model used in the HEC-RAS model is a combination of LiDAR generated specifically for the project, hydrographic survey of the channel bed, and topographic survey to tie the LiDAR and hydrographic survey together. The LiDAR was generated with an airborne laser scanner, generating 7.5 points per square metre. The hydrographic survey was generated using a survey grade single beam echo sounder towed behind a Jet Ski. Depth data was used to develop a 1m grid. Topographic survey was completed around the water's edge and other accessible locations where additional detail was needed. Figure 2.1 provides an overall view of the terrain model within the HEC-RAS model.

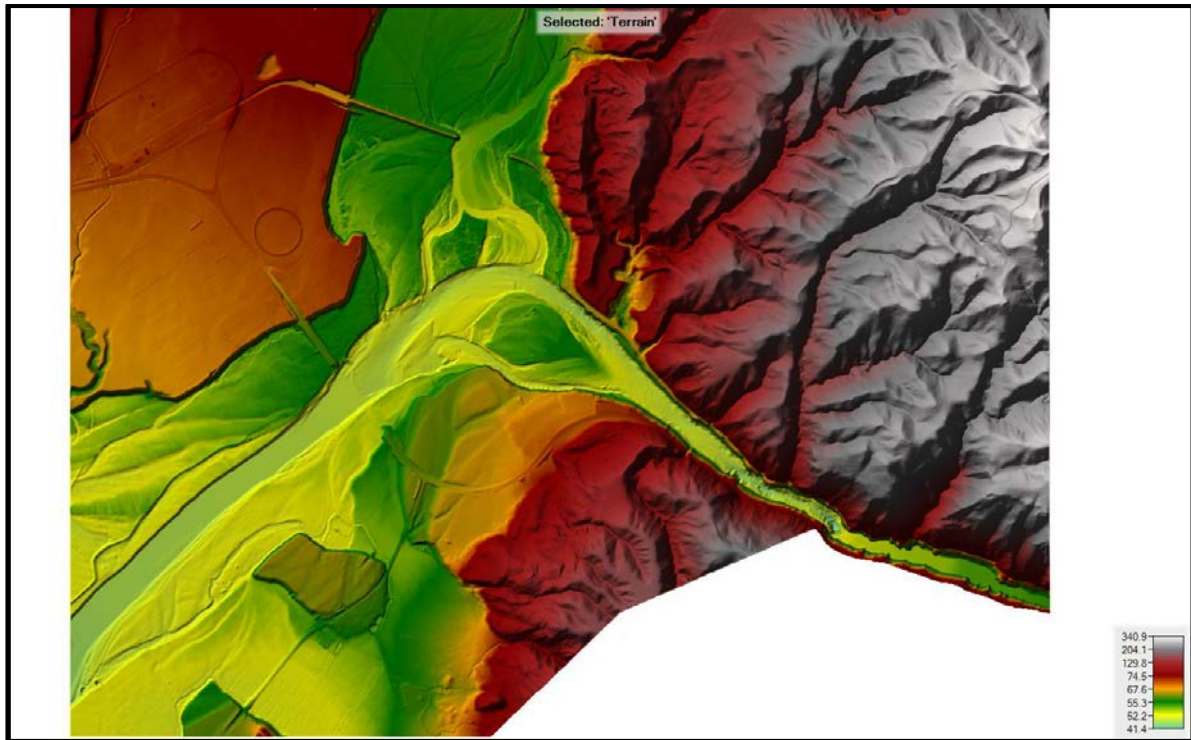


Figure 2-1, snapshot of processed terrain data (with hillshade effect) used for the purpose of HEC-RAS modelling

The downstream limit of the hydrographic survey was approximately 3m upstream of the Ashhurst Bridge, due to shallow conditions under the bridge. In order to account for the hydraulic effect of the Ashhurst Bridge, the channel was extended downstream in the terrain model, using topographic survey and site photos. Additional topographic survey will be acquired during the summer low flow period, allowing verification of the bed levels. The Ashhurst Bridge piers and abutments were then added to the model, based on as-built information, combined with the topographic survey and LiDAR information. The bridge piers have been simulated by elevating mesh cells to the soffit level of the existing bridge. While the terrain model extends approximately 130m downstream of the Ashhurst Bridge, the downstream limit of the hydraulic model is approximately 185m upstream of the bridge centerline.

2.2.2 Upstream and Downstream Hydraulic Model Boundary Conditions

Upstream boundary conditions are the estimated design flows for the Manawatu and Pohangina Rivers. The design flows are based on gauge data that has been statistically processed by Horizons Regional Council (HRC) to determine standard design flows for return periods, based on different statistical distribution methods. Values obtained by Gumbel Extreme Value (GEV) distribution were used in the model. The spreadsheet printouts from HRC have been included in Appendix A. The flow data was provided for the Manawatu River gauge at the Upper Gorge and the Pohangina River gauge at Mais Reach. The river gauge locations are as shown in Figure 2.3.

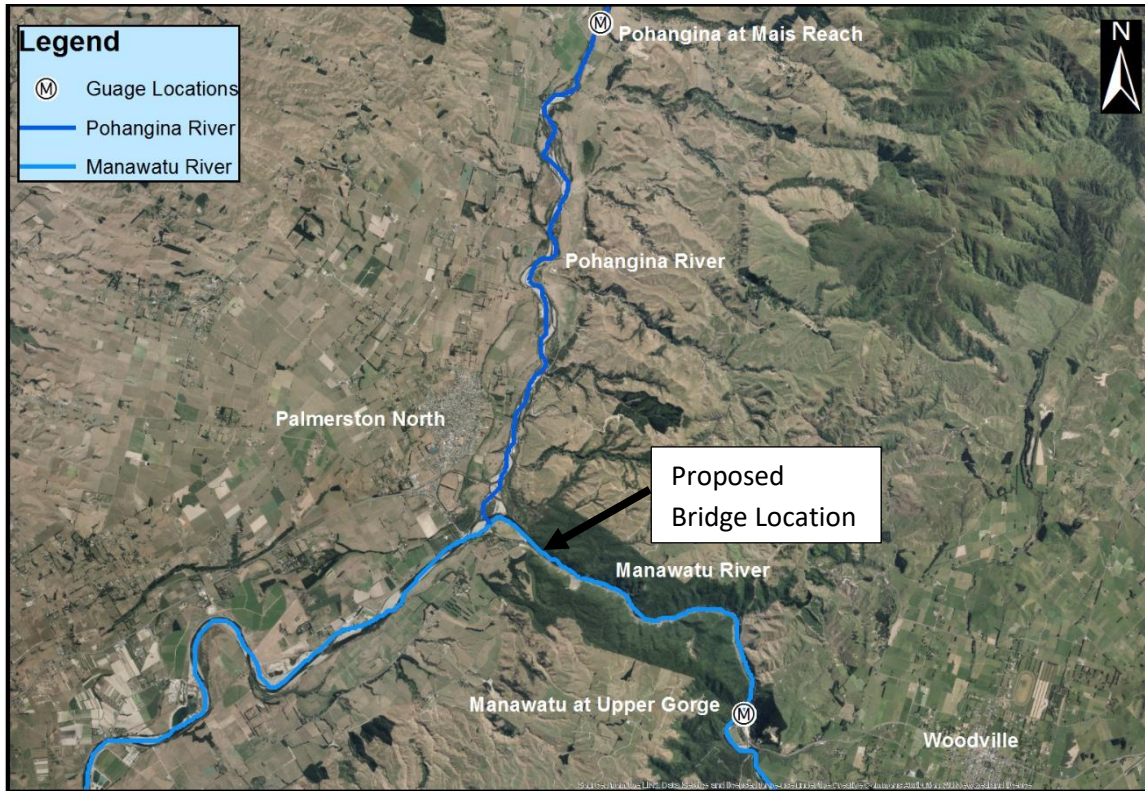


Figure 2-2 River gauge locations relative to bridge location

The design return periods are based on the NZTA Bridge Manual requirements for a bridge with an Importance Level of 4. This indicates that the return period for the serviceability limit state (SLS) is 100 years and the return period for for the ultimate limit state is 2,500 years. The 2-year return period storm (or ARI) has also been included in the model.

In order to determine the 2,500 year flow, the Gumbel Extreme Value (GEV) distribution equation was applied. As the flow measurements were not available in the immediate vicinity of the model limit, it was necessary to adjust the flows for location. This adjustment was accomplished using the methodology described in the Bridge Manual and *Flood frequency in New Zealand*, Section 3.

$$Q_1/Q_2 = (A_1/A_2)^{0.8}$$

Where:

Q is flood discharge
A is catchment area

Table 2.1 shows the location adjusted design flows for the selected return periods used in the model.

River	Location Adjusted Design Flows for Required Return Period		
	2 year	100 year	2,500 year
Manawatu	1169 m ³ /s	2994 m ³ /s	4759 m ³ /s
Pohangina	456 m ³ /s	1453 m ³ /s	2699 m ³ /s

Finally, unsteady flow must be applied in 2D HEC-RAS models. Standard bridge hydraulics, scour assessments, and scour countermeasure design methods are based on steady flow calculations. In

order to accommodate the unsteady flow requirement and provide the equivalent of steady flow output, flow hydrographs were entered into the model that provide quasi steady flow conditions for a 10-hour time period.

The downstream boundary condition is essentially the tailwater level of the modelled system. Tailwater levels for the various design flows were determined by running them through detailed hydraulic models of the Ashhurst Bridge. For the SLS (100-year) and smaller flows, an extended 2D model was created, with the piers and abutments built into the terrain. The ULS (2,500-year) resulted in the flood level reaching the superstructure of the bridge, therefore a 1D model was developed to determine the flood level that was used as the tailwater for the provided hydraulic model. Table 2.2 provides the tailwater levels assigned as downstream boundary conditions in the hydraulic model, provided.

Table 2.2 Flood levels used for the downstream boundary condition

Downstream Stage Level (Downstream Boundary Condition)		
2-year ARI	100-year ARI	2,500-year ARI
RL 52.87m	RL 55.96m	RL 57.85m

2.2.3 Hydraulic Model 2D Mesh

As mentioned earlier, the computational mesh is unstructured, with variations in shape and a “soft bottom” to the individual cells. The sides of the cells do not have to be straight lines, nor do they have to be confined to a single level. Terrain model variation within the cells of the mesh is taken into account.

Multiple computational mesh sizes were tested, along with multiple time steps. The mesh size selected was 3.0m. Again, this computational mesh size does not superced the 1.0m terrain model grid. To achieve model stability with this mesh size, combined with variable time steps, variation in the Courant number had to be allowed between the limits of 0.5 and 3.0. This is consistent with the HEC-RAS 2D Modelling Users Manual and *Applied Hydrology* by Chow, Maidment, and Mays (1988), for full momentum applications, using the Saint Venant Equations.

2.2.4 Channel Roughness

Roughness of the riverbeds, banks, and floodplains are entered into the model using Manning’s Roughness Coefficients or N values. The Manning’s N values were determined based on available aerial images, site photos, and field observations. A spatially varied Manning’s N value land cover layer was created to assign roughness coefficients within various locations. Manning’s N applied in the model varies from 0.035 for the channel of the river to a higher value of 0.12 in the areas with dense vegetation/tree cover. Figure 2.2.3 shows the spatial variation of Manning’s N across the model.

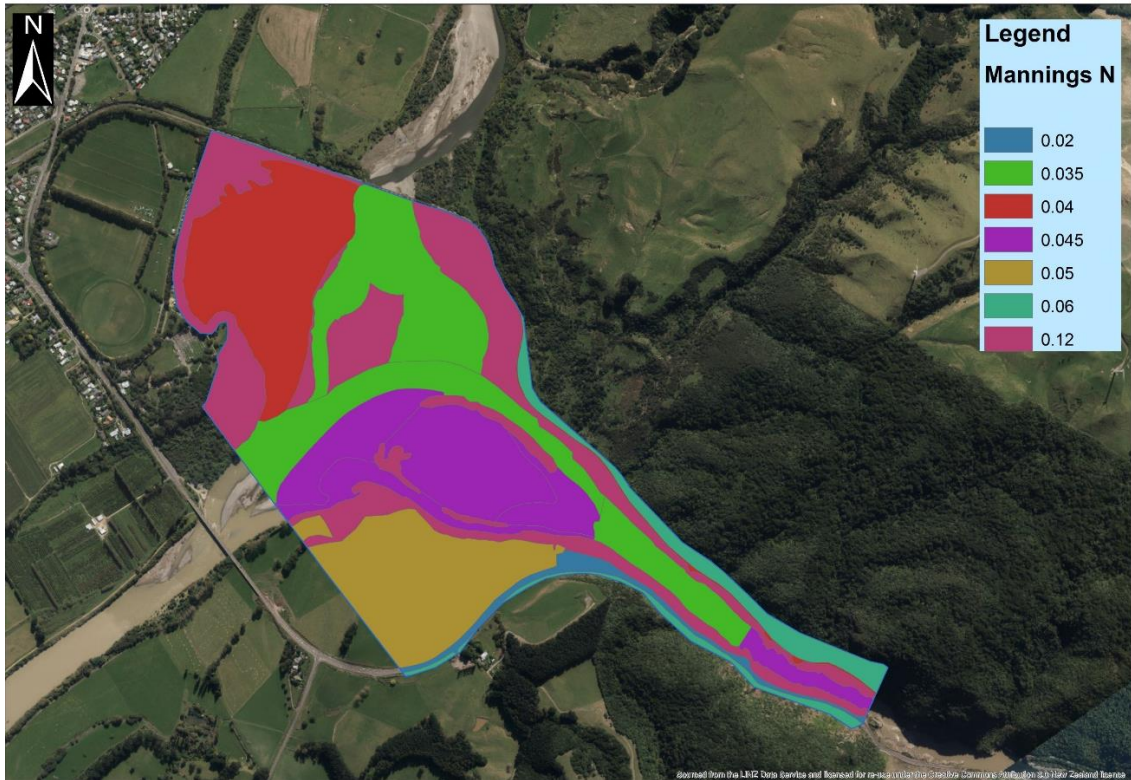


Figure 2-3 Spatial variation of the assigned Manning's Roughness Coefficients (N values)

3.0 Conclusion

The base hydraulic model is intended to be used by Tenderers for bridge hydraulics analysis and bridge scour assessments. Design flows were developed from river gauge information provided by HRC. Existing condition model results were checked against available aerial images and correlated well with HRC modelled flood levels at the Pohangina River confluence with the Manawatu River. The bed and banks of the Manawatu and Pohangina Rivers within the modelled area are very dynamic, therefore the model terrain represents a snapshot from the time of the survey. This snapshot is the accepted basis for bridge hydraulics, bridge scour assessment, and debris loads/impacts.

References

US Army Corps of Engineers Hydrologic Engineering Center, *HEC-RAS 2D Modelling User's Manual*, Version 5.0, February 2016

US Army Corps of Engineers Hydrologic Engineering Center, *HEC-RAS Release Notes*, Version 5.0.6, November 2018

Ven Te Chow, *Open Channel Hydraulics*, International Edition, 1973

Hicks and Mason, *Roughness Characteristics of New Zealand Rivers*, NIWA, September 1998

Chow, *Maidment and Mays, Applied Hydrology*, 1988

Appendix A

Flow Estimates

L Moments

For Site: For Site: Manawatu at Upper Gorge (1979 to 2013)

n= 35

Formula from Hosking 1990

Mean	Std. Dev.	Skew	Kurtosis
L1	L2	T3	T4
1264.9	269.3	0.2118	0.2355

For EV1

$$\alpha = \frac{l_2}{\ln 2} = 388.520$$

$$\xi = l_1 - 0.5772 \alpha = 1040.695$$

$$y_T = -\ln(-\ln(1 - \frac{1}{T}))$$

$$Q_{T1} = \xi + \alpha y_T$$

For GEV

$$z = 2/(3 + l_3) - \log 2 / \log 3 = -0.00823203$$

$$k = 7.8590z + 2.9554z^2 = -0.06449525$$

$$\alpha = l_2 k / \{ (1 - 2^{-k}) \Gamma(1+k) \} = 364.726636$$

$$\xi = l_1 + \alpha \{ \Gamma(1+k) - 1 \} / k = 1029.67758$$

$$y_T = -\ln(-\ln(1 - \frac{1}{T}))$$

$$Q_{T2} = \xi + \frac{\alpha}{k} (1 - e^{-ky_T})$$

For Log Pearson 3

Mean of ln Q: $\ln \bar{Q} = 7.070$

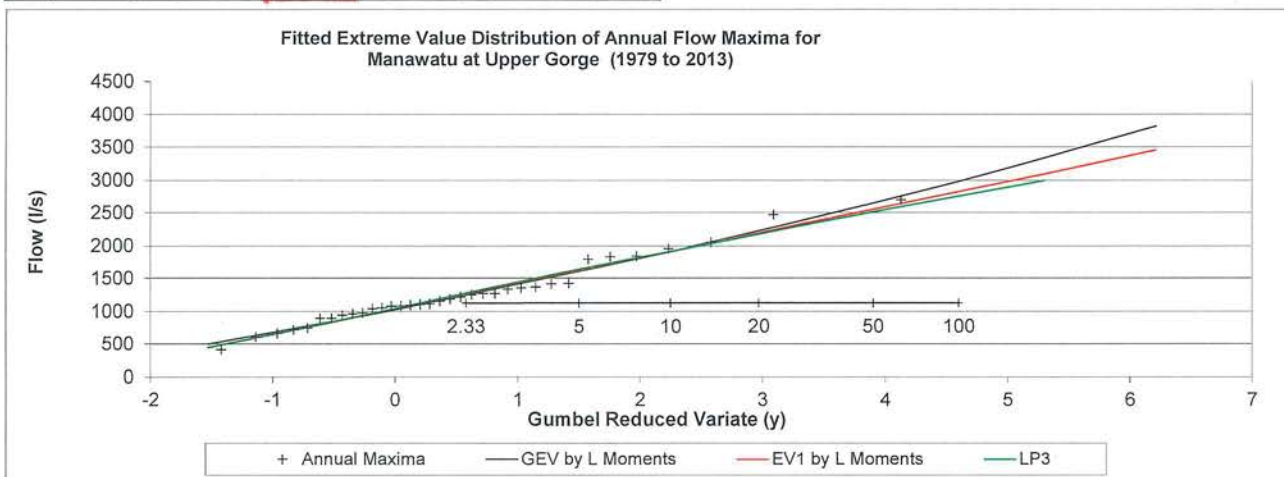
Standard deviation of ln Q: $\sigma_{\ln Q} = 0.3895$

Skewness of ln Q: $C_s = -0.1867$

$$Q_{T3} = \exp(\ln \bar{Q} + K \sigma_{\ln Q})$$

i	Sample Values (Q _i)	F(Q _i)	y(Q _i)	ln Q _i
1	413.46	0.016	-1.420	6.025
2	604.67	0.044	-1.136	6.405
3	663.36	0.073	-0.963	6.497
4	718.25	0.101	-0.828	6.577
5	747.24	0.130	-0.714	6.616
6	895.75	0.158	-0.611	6.798
7	896.72	0.187	-0.517	6.799
8	945.78	0.215	-0.429	6.852
9	965.77	0.244	-0.345	6.873
10	980.60	0.272	-0.263	6.888
11	1041.96	0.301	-0.184	6.949
12	1058.68	0.329	-0.105	6.965
13	1082.60	0.358	-0.028	6.987
14	1083.53	0.386	0.050	6.988
15	1092.43	0.415	0.127	6.996
16	1105.48	0.443	0.206	7.008
17	1114.44	0.472	0.285	7.016
18	1155.04	0.500	0.367	7.052
19	1185.13	0.528	0.450	7.078
20	1216.07	0.557	0.536	7.103
21	1249.23	0.585	0.625	7.130
22	1265.89	0.614	0.718	7.144
23	1270.12	0.642	0.815	7.147
24	1332.33	0.671	0.918	7.195
25	1348.39	0.699	1.028	7.207
26	1364.68	0.728	1.147	7.219
27	1411.26	0.756	1.275	7.252
28	1418.35	0.785	1.417	7.257
29	1794.25	0.813	1.576	7.492
30	1831.13	0.842	1.758	7.513
31	1840.03	0.870	1.973	7.518
32	1956.97	0.899	2.236	7.579
33	2056.78	0.927	2.581	7.629
34	2469.34	0.956	3.091	7.812
35	2697.50	0.984	4.131	7.900

Return Period	EV1	GEV	LogPearson3
T	Y _T	Q _{T1}	Q _{T2}
1.01	-1.5293	447	499
1.1	-0.8746	701	720
1.5	-0.0940	1004	995
2	0.3665	1183	1165
2.33	0.5786	1265	1245
5	1.4999	1623	1604
10	2.2504	1915	1913
20	2.9702	2195	2224
25	3.1985	2283	2325
50	3.9019	2557	2648
100	4.6001	2828	2983
200	5.2958	3098	3332
500	6.2136	3455	3817



CLIENT: NZTA

PROJECT: TE AHU A TURANGA

SUBJECT: MANAWATU

UPPER GORGE 2500 YR FLOWS

GUMBEL EXTREME VALUE

$$Q_{T2} = \xi + \frac{\alpha}{k} (1 - e^{(-k\gamma T)})$$

For $T = 2500$

$$Q = 4741 \text{ m}^3/\text{s}$$

CLIENT: NZTA

PROJECT: TE AHU A TURANGA

SUBJECT: MANAWATU

DESIGN FLOWS AT BRIDGE
LOCATION

$$\frac{Q_1}{Q_2} = \left(\frac{A_1}{A_2}\right)^{0.8}$$

$$Q_1 = Q_2 \text{ AT UPPER MANAWATU} = 1165 \text{ m}^3/\text{s}$$

$$A_1 = 3185 \text{ Km}^2$$

$$Q_2 = Q_2 \text{ AT BRIDGE LOCATION}$$

$$A_2 = 3200 \text{ Km}^2$$

$$Q_2 = \frac{1165}{\left(\frac{3185}{3200}\right)^{0.8}} = 1169 \text{ m}^3/\text{s}$$

CLIENT: NZTA

PROJECT: TE AHU A TURANGA

SUBJECT: MANAWATU

DESIGN FLOWS AT BRIDGE
LOCATION

$$\frac{Q_1}{Q_2} = \left(\frac{A_1}{A_2} \right)^{0.8}$$

SLS CONDITION

$$Q_1 = Q_{100} \text{ AT UPPER MANAWATU} = 2983 \text{ m}^3/\text{s}$$

$$A_1 = 3185 \text{ km}^2$$

$$Q_2 = Q_{100} \text{ AT BRIDGE LOCATION}$$

$$A_2 = 3200 \text{ km}^2$$

$$Q_2 = \frac{2983}{\left(\frac{3185}{3200} \right)^{0.8}} = 2994 \text{ m}^3/\text{s}$$

ULS CONDITION

$$Q_{2500}^2 = \frac{4741}{\left(\frac{3185}{3200} \right)^{0.8}} = 4759 \text{ m}^3/\text{s}$$

L Moments

For Site: 32576 Pohangina at Mais Reach

n= 43

Formula from Hosking 1990

Mean	Std. Dev.	Skew	Kurtosis
L1	L2	T3	T4
466.4	120.2	0.2590	0.1275

For EV1

$$\alpha = \frac{l_2}{\ln 2} = 173.346$$

$$\xi = l_1 - 0.5772 \alpha = 366.304$$

$$y_T = -\ln(-\ln(1 - \frac{1}{T}))$$

$$Q_{T1} = \xi + \alpha y_T$$

For GEV

$$z = 2/(3 + t_3) - \log 2 / \log 3 = -0.01725$$

$$k = 7.8590z + 2.9554z^2 = -0.13466$$

$$\alpha = l_2 k / \{(1 - 2^{-k})\Gamma(1+k)\} = 150.587$$

$$\xi = l_1 + \alpha \{\Gamma(1+k) - 1\} / k = 356.4874$$

$$y_T = -\ln(-\ln(1 - \frac{1}{T}))$$

$$Q_{T2} = \xi + \frac{\alpha}{k} (1 - e^{(-ky_T)})$$

For Log Pearson 3

Mean of ln Q: $\ln \bar{Q} = 6.046$

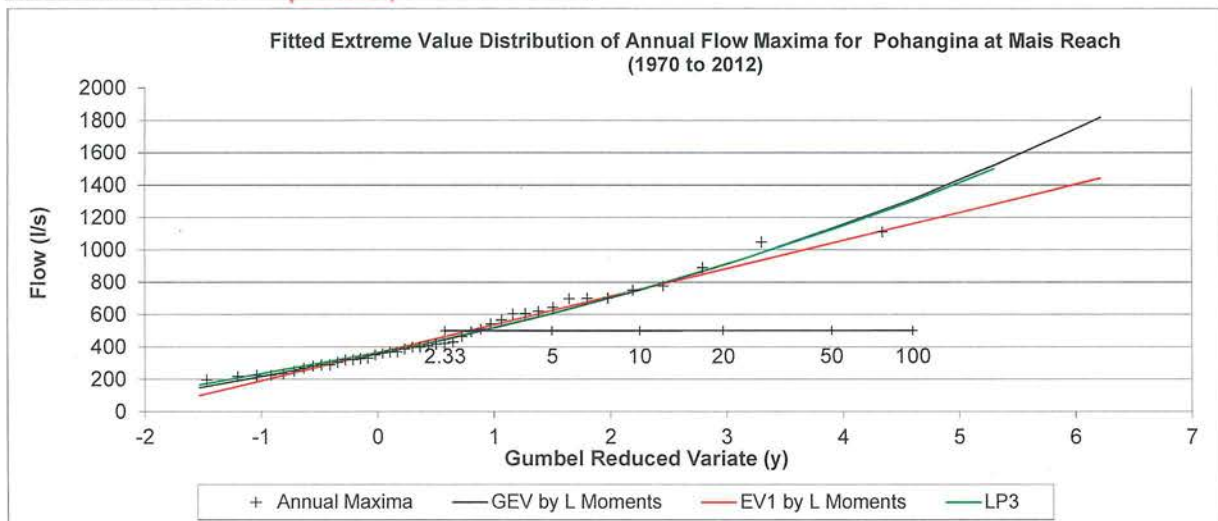
Standard deviation of ln Q: $\sigma_{\ln Q} = 0.4431$

Skewness of ln Q: $C_s = 0.3033$

$$Q_{T3} = \exp(\ln \bar{Q} + K \sigma_{\ln Q})$$

i	Sample Values (Q _i)	F(Q _i)	y(Q _i)	ln Q _i
1	195.6	0.013	-1.469	5.276
2	215.2	0.036	-1.200	5.372
3	221.8	0.059	-1.038	5.402
4	223.8	0.083	-0.914	5.411
5	232.3	0.106	-0.809	5.448
6	249.3	0.129	-0.717	5.519
7	266.9	0.152	-0.633	5.587
8	280.5	0.175	-0.555	5.637
9	287.7	0.199	-0.481	5.662
10	287.8	0.222	-0.410	5.662
11	303.2	0.245	-0.341	5.714
12	317.2	0.268	-0.275	5.760
13	319.3	0.291	-0.210	5.766
14	325.2	0.314	-0.146	5.784
15	327.7	0.338	-0.082	5.792
16	349.3	0.361	-0.019	5.856
17	359.8	0.384	0.044	5.886
18	366.6	0.407	0.107	5.904
19	367.7	0.430	0.171	5.907
20	386.5	0.454	0.235	5.957
21	397.3	0.477	0.300	5.985
22	399.3	0.500	0.367	5.990
23	406.1	0.523	0.434	6.007
24	416.4	0.546	0.503	6.032
25	420.6	0.570	0.575	6.042
26	428.6	0.593	0.648	6.060
27	463.1	0.616	0.724	6.138
28	493.2	0.639	0.804	6.201
29	508.8	0.662	0.887	6.232
30	540.2	0.686	0.974	6.292
31	565.5	0.709	1.066	6.338
32	602.0	0.732	1.164	6.400
33	605.0	0.755	1.270	6.405
34	618.1	0.778	1.384	6.427
35	643.0	0.801	1.508	6.466
36	695.6	0.825	1.646	6.545
37	697.0	0.848	1.802	6.547
38	699.7	0.871	1.980	6.551
39	749.7	0.894	2.191	6.620
40	776.0	0.917	2.451	6.654
41	889.2	0.941	2.794	6.790
42	1046.3	0.964	3.301	6.953
43	1109.1	0.987	4.337	7.011

Return Period	EV1	GEV	LogPearson3		
T	Y _T	Q _{T1}	Q _{T2}	K	Q _{T3}
1.01	-1.5293	101	148	-2.102	167
1.1	-0.8746	215	232	-	-
1.5	-0.0940	350	342	-	-
2	0.3665	430	413	-0.051	413
2.33	0.5786	467	447	-	-
5	1.4999	626	607	0.824	609
10	2.2504	756	752	1.309	755
20	2.9702	881	906	-	-
25	3.1985	921	959	1.850	959
50	3.9019	1043	1129	2.213	1126
100	4.6001	1164	1316	2.546	1306
200	5.2958	1284	1520	2.859	1500
500	6.2136	1443	1820	-	-



CLIENT: NZTA

PROJECT: TE AHU A TURANGA

SUBJECT: POHANGINA

MAIS REACH 2500 YR FLOWS

GUMBEL EXTREME VALUE

$$q_{T2} = \xi + \frac{\alpha}{K} (1 - e^{(-k\gamma_T)})$$

For $T = 2500$

$$q = 2445 \text{ m}^3/\text{s}$$

CLIENT: NZTA

PROJECT: TE AHU A TURANGA

SUBJECT: POHANGINA DESIGN
FLOWS

$$\frac{Q_1}{Q_2} = \left(\frac{A_1}{A_2}\right)^{0.8}$$

$$Q_1 = Q_2 \text{ AT MAIS REACH} = 413 \text{ m}^3/\text{s}$$

$$A_1 = 487 \text{ km}^2$$

$$Q_2 = Q_2 \text{ AT CONFLUENCE}$$

$$A_2 = 551 \text{ km}^2$$

$$Q_2 = \frac{413}{\left(\frac{487}{551}\right)^{0.8}} = 456 \text{ m}^3/\text{s}$$

CLIENT: NZTA
PROJECT: TE AHU A TURANGA

SUBJECT: POHANGINA DESIGN
FLOWS AT CONFLUENCE

$$\frac{Q_1}{Q_2} = \left(\frac{A_1}{A_2}\right)^{0.8}$$

SLS CONDITION

$$Q_1 = Q_{100} \text{ AT MAIS REACH} = 1316 \text{ m}^3/\text{s}$$

$$A_1 = 487 \text{ km}^2$$

$$Q_2 = Q_{100} \text{ AT CONFLUENCE}$$

$$A_2 = 551 \text{ km}^2$$

$$Q_2 = \frac{1316}{\left(\frac{487}{551}\right)^{0.8}} = 1453 \text{ m}^3/\text{s}$$

ULS CONDITION

$$Q_{2500}^2 = \frac{2445}{\left(\frac{487}{551}\right)^{0.8}} = 2699 \text{ m}^3/\text{s}$$

Appendix B

Roughness Coefficients

ottonwood trees 8 to 10 years old, inter-rush, none of the vegetation in foliage, eater than 2 ft, and (c) growing season—ntergrown with some weeds in full foliage vegetation along channel bottom, where 2 ft.

comparable to the following: (a) turf n of flow is less than one-half the height n—bushy willows about 1 year old, inter-ge along side slopes, or dense growth of with any value of hydraulic radius up to n—trees intergrown with weeds and brush, e of hydraulic radius up to 10 or 15 ft.

the degree of meandering depends on the the straight length of the channel reach. minor for ratios of 1.0 to 1.2, appreciable re for ratios of 1.5 and greater.

od for determining the n value, several method does not consider the effect of values given in Table 5-5 were developed 0 cases of small and moderate channels. tionable when applied to large channels say, 15 ft. The method applies only to ways, and drainage channels and shows a n value of such channels. The minimum may be as low as 0.012 in lined channels tory flumes.

s Roughness Coefficient. Table 5-6 gives various kinds.¹ For each kind of channel ximum values of n are shown. The nor-s given in the table are recommended only enance. The boldface figures are values ign. For the case in which poor mainte-e, values should be increased according to : 5-6 will be found very useful as a guide to value to be used in a given problem. A prepared by Horton [34] from an examina-ments at his time.² Table 5-6 is compiled

was observed in the Hydraulic Engineering Labora-3]. Such a low n value may perhaps be obtained t no observations have yet been reported. her elements from 269 observations made on many iven by King [35].

TABLE 5-5. VALUES FOR THE COMPUTATION OF THE ROUGHNESS COEFFICIENT BY EQ. (5-12)

Channel conditions		Values	
Material involved	Earth	n_0	0.020
	Rock cut		0.025
	Fine gravel		0.024
	Coarse gravel		0.028
Degree of irregularity	Smooth	n_1	0.000
	Minor		0.005
	Moderate		0.010
	Severe		0.020
Variations of channel cross section	Gradual	n_2	0.000
	Alternating occasionally		0.005
	Alternating frequently		0.010-0.015
Relative effect of obstructions	Negligible	n_3	0.000
	Minor		0.010-0.015
	Appreciable		0.020-0.030
	Severe		0.040-0.060
Vegetation	Low	n_4	0.005-0.010
	Medium		0.010-0.025
	High		0.025-0.050
	Very high		0.050-0.100
Degree of meandering	Minor	m_5	1.000
	Appreciable		1.150
	Severe		1.300

0.011

0.020

0.010

SINUOSITY = 1.06

$\mu = 0.089$



**Roughness
Characteristics of
New Zealand Rivers**

NIWA

Taikaro Nukurangi

Roughness Characteristics of New Zealand Rivers

by D M Hicks and P D Mason

*A handbook for assigning
hydraulic roughness
coefficients to river reaches
by the "visual comparison"
approach*

National Institute of Water and Atmospheric Research Ltd
September 1998

Water Resources Publications, LLC

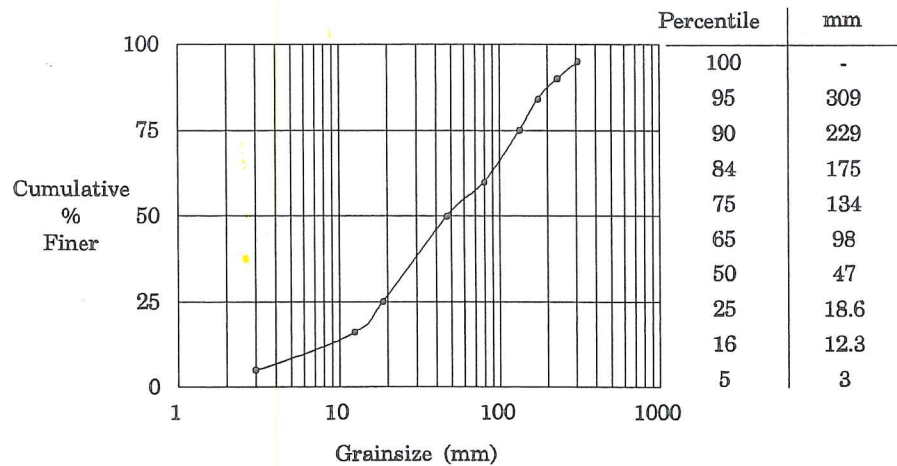
$n = 0.088$

58902: Pelorus at Bryants.

Map reference:- O27:573891 (Metric); S021:891251 (Yard).
 Catchment area:- 375 km².
 Period of record:- October 1977 - January 1990.
 Mean annual flood:- 957 m³/s.
 Mean flow:- 20.8 m³/s.

Surveyed reach:-
 Cross-sections:- 5 along a 472 m reach.
 Manning's n range:- 0.021-0.17
 Channel description:- Bed consists predominantly of large cobbles with some small cobbles and gravel. Bedrock crops out on both banks, which are lined with native bush towards the upstream end of the reach. Left bank is grassed along lower section of reach.

Bed Surface Material



$n = 0.088$



View upstream towards top cross-section.



View downstream towards bottom cross-section.

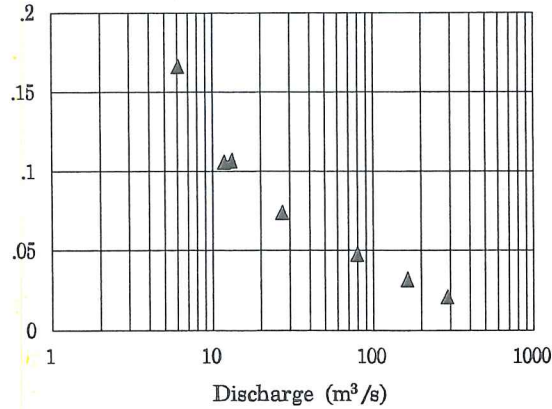
$n = 0.088$

Hydraulic Properties of Reach

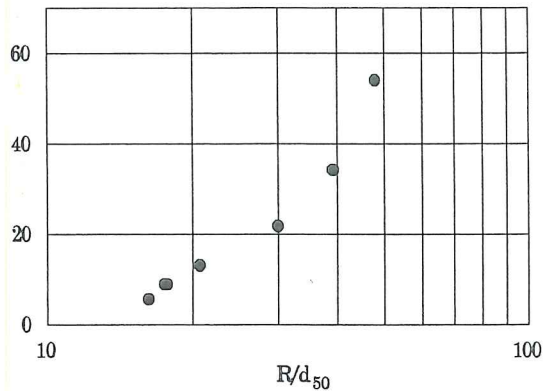
Discharge (m ³ /s)	Water Surface Slope	Friction Slope	Area (m ²)	Expansion (%)	Hydraulic Radius (m)	Mean Velocity (m/s)	Manning n	Chezy C	Error (%)
6.13*	0.00366	0.00364	26.9	-51	0.76	0.27	0.17	5.6	8
11.8*	0.00356	0.00352	31.7	-50	0.83	0.44	0.11	8.9	8
13.1*	0.00381	0.00375	33.2	-56	0.82	0.47	0.11	8.9	8
27.3*	0.00415	0.00390	42.7	-66	0.97	0.78	0.074	13.1	8
79.7*	0.00337	0.00273	66.3	-60	1.41	1.38	0.048	21.9	8
164*	0.00326	0.00183	92.3	-62	1.84	2.04	0.032	34.2	11
290*	0.00333	0.00102	124	-65	2.25	2.65	0.021	54.0	22

* Estimated from rating based on gaugings

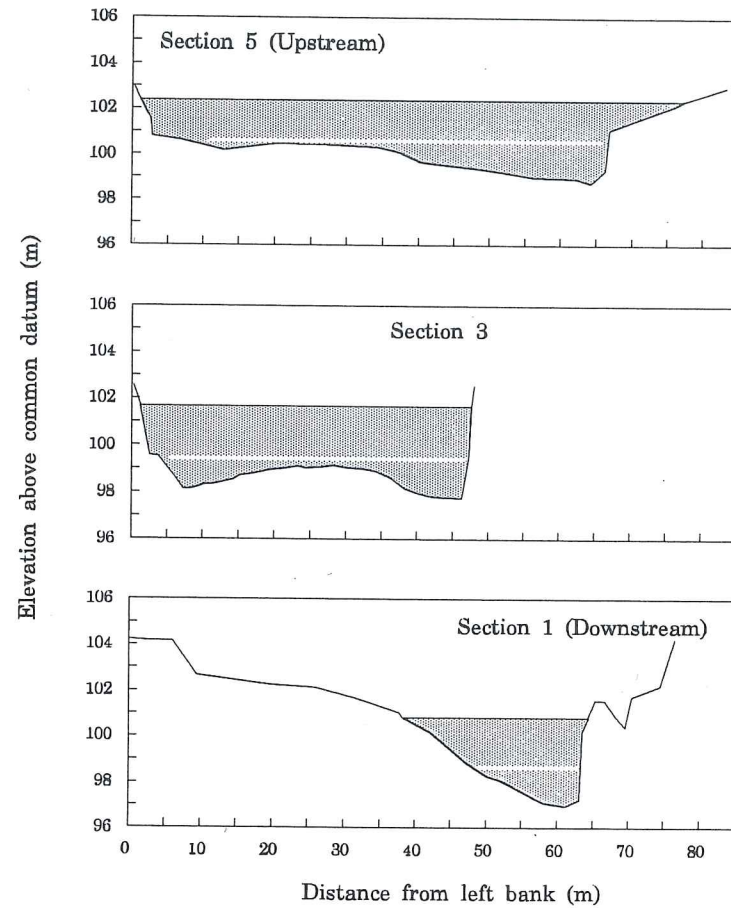
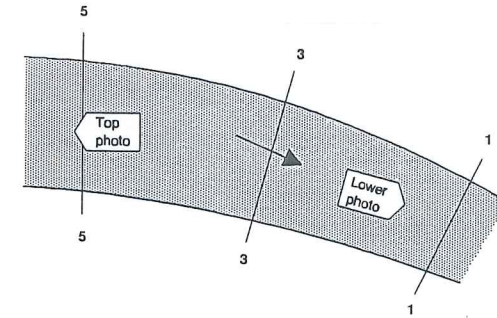
Manning
n



Chezy
C



$n = 0.088$



Plan (not to scale) and cross sections, Pelorus at Bryants.

93901: Ngakawau at Lineslip.

- Map reference:-* L28:177548 (Metric); S024:358903 (Yard).
- Catchment area:-* 186 km².
- Period of record:-* June 1974 - Present.
- Mean annual flood:-* 676 m³/s.
- Mean flow:-* 25.6 m³/s.

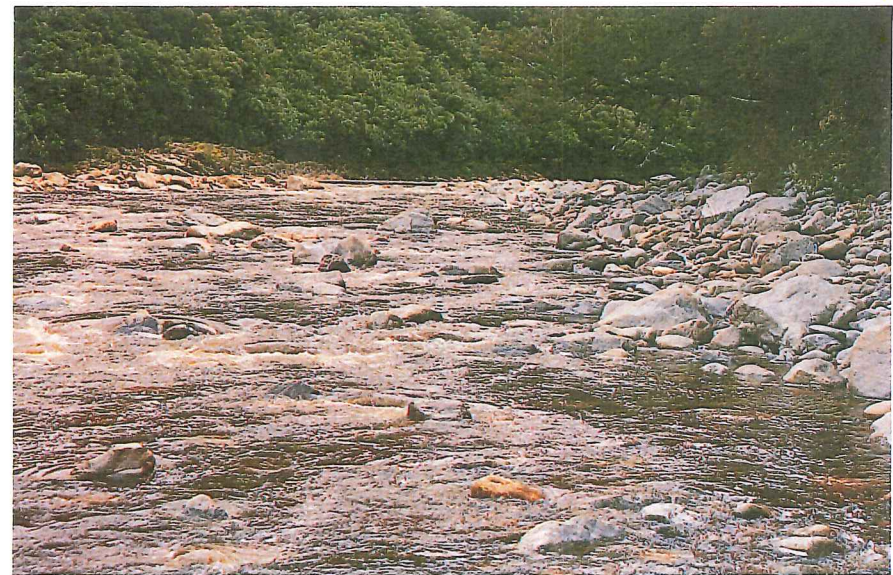
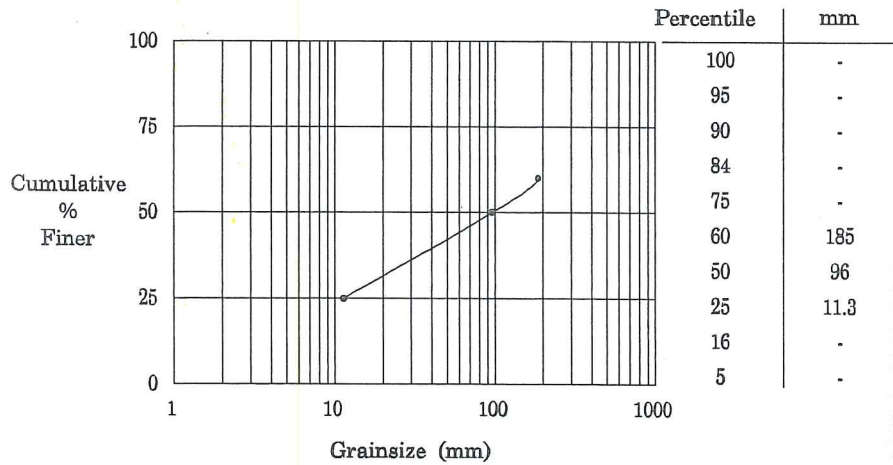
- Surveyed reach:-*

 - Cross-sections:-* 5 along a 462 m reach.
 - Manning's n range:-* 0.057-0.25
 - Channel description:-* Bed material comprises 50% boulders and 50% sand and cobbles. Banks are formed of sand and boulders and are bush covered.



View downstream from middle of reach.

Bed Surface Material



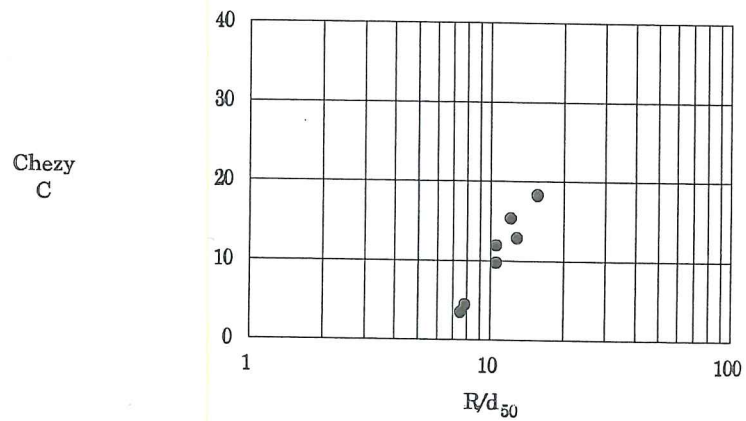
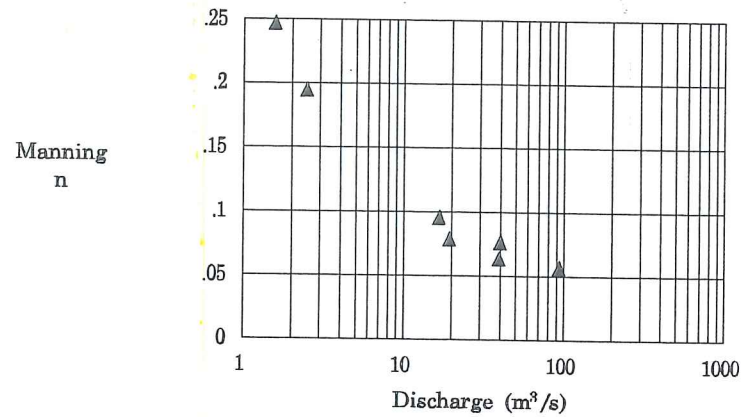
View upstream from bottom of reach.

$$n = 0.088$$

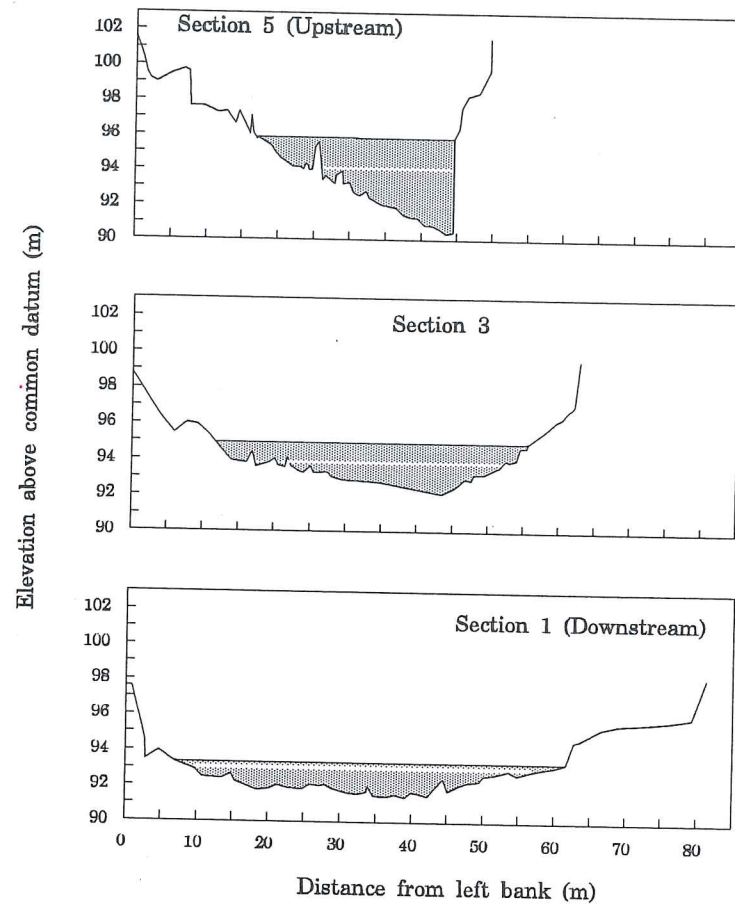
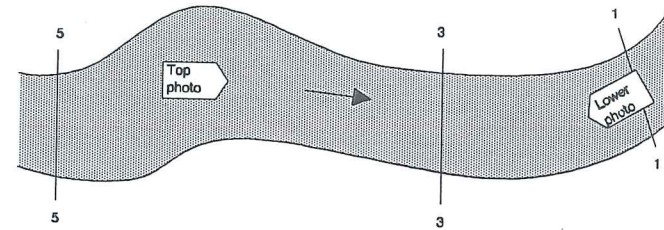
Hydraulic Properties of Reach

Discharge (m ³ /s)	Water Surface Slope	Friction Slope	Area (m ²)	Expansion (%)	Hydraulic Radius (m)	Mean Velocity (m/s)	Manning n	Chezy C	Error (%)
1.64	0.00330	0.00329	18.6	-63	0.72	0.12	0.25	3.5	8
2.50	0.00334	0.00333	20.0	-60	0.75	0.16	0.19	4.5	8
16.7*	0.00372	0.00369	35.5	-35	1.01	0.51	0.096	9.8	8
19.5*	0.00363	0.00358	35.5	-32	1.01	0.60	0.079	12.0	8
39.5*	0.00399	0.00392	45.1	-26	1.16	0.91	0.064	15.4	8
40.3*	0.00416	0.00411	49.6	-25	1.23	0.83	0.077	12.9	8
94.1*	0.00460	0.00446	66.1	-18	1.50	1.44	0.057	18.3	8

* Estimated from rating based on gaugings



$$n = 0.088$$



Plan (not to scale) and cross sections, Ngakawau at Lineslip.

Appendix D.3: *Te Ahu a Turanga: Manawatū River Bridge 2D HEC-RAS modelling and design.*



Te Ahu a Turanga

Manawatū River Bridge 2D HEC-RAS Modelling and Design



Contact Details

Name: Franciscus Maas

L9, Majestic Centre, 100 Willis St
PO Box 12 003, Thorndon, Wellington 6144
New Zealand

Telephone: +64 4 471 7000

Mobile: +64 21 221 7829

Document Details:

Date: February 2020

Reference: 5-C3567.00

Status: FINAL

Prepared By



Franciscus Maas

Reviewed By

Jack MConchie

Approved for Release By

David Hughes

Contents

Disclaimers and Limitations.....	5
1 Introduction	1
1.1 Background	1
1.2 Design Standards.....	1
1.3 Purpose.....	1
2 Hydraulic Model.....	2
2.1 Introduction.....	2
2.2 Levels and Projection.....	3
2.3 Changes to Model	3
3 Results.....	5
3.1 Introduction.....	5
3.2 Water Levels & Extent.....	5
3.3 Flow Velocity.....	6
3.4 Adopted Design Parameters	7
4 Scour Analysis.....	8
4.1 Introduction.....	8
4.2 Assumptions.....	8
4.3 Bed Scour.....	12
4.4 Local Scour at Piers	13
4.5 Summary.....	14
5 Scour Protection.....	14
5.1 Introduction.....	14
5.2 Pier 2	15
5.3 Pier 1	15
6 Summary	17
7 Glossary.....	18
8 References.....	18
Appendix A - Figures.....	21
Appendix B - Calculations.....	31

List of Figures

Figure 2-1 Approximate outline of 2D HEC-RAS model.....	3
---	---

Figure 2-2	Hydrographs of design events adjusted for climate change.	4
Figure 2-3	Representation of piers columns in the terrain without (left) and with debris (right).	5
Figure 3-1	ULS (0.04% AEP adjusted for the potential effects of climate change to 2090) design event flow velocities (with 1m/s contours) near Pier 1.	7
Figure 4-1	Plan and elevation of proposed bridge (Advance, 2019).	8
Figure 4-2	Details of pier including foundations.	9
Figure 4-3	Manawatū River looking upstream from the confluence with the Pohangina River and Parahaki Island in the foreground to the Manawatū Gorge.	10
Figure 4-4	Cross-section from the 2D HEC-RAS model bathymetry used for the scour calculations.	11
Figure 4-5	Manawatū River bed material near the proposed location of Pier 2.	12
Figure 4-6	Manawatū River bed material at the upstream end of Parahaki Island.	12
Figure 5-1	Manawatū River channel looking upstream from Parahaki Island with existing vegetation near proposed Pier 1 on the true right bank.	16
Figure 5-2	Details of the proposed ground modifications between the south abutment and Pier 1 (Advance, 2019).	17

List of Tables

Table 2-1	Peak design flows for the Manawatū River.	4
Table 3-1	Summary of cross-sectional averaged peak water levels.	6
Table 3-2	Summary of cross-sectional averaged peak water levels.	6
Table 3-3	Pier 1 hydraulic scour analysis and protection design parameters for the design events considered.	7
Table 3-4	Key hydraulic design parameters for the proposed bridge.	7
Table 4-1	Pier geometry data.	9
Table 4-2	Effect of the components of bed scour on the bed level.	13
Table 4-3	Effect of local pier scour at a pier outside the thalweg and without a debris raft.	13
Table 4-4	Effect of local pier scour at a pier outside the thalweg with a debris raft.	13
Table 4-5	Effect of local pier scour at Pier 2 coinciding with the thalweg and without a debris raft.	14
Table 4-6	Effect of local pier scour at a pier coinciding with thalweg with a debris raft.	14
Table 4-7	Summary of bed levels under the various combinations of scour effects considered.	14
Table 5-1	Recommended maximum velocities for bare and vegetated channels (source: Queensland, 2004).	16
Table 6-1	Summary of final scoured local bed levels for the design events considered.	18
Table 6-2	Details of selected scour protection.	18

Document History and Status

Revision	Date	Author	Reviewed by	Approved by	Status
1	24/04/2019	F Maas			
2	10/12/2019	F Maas			
3	07/02/2020	F Maas			

Revision Details

Revision	Details
2	Corrected typos
3	Updated with latest detailed design info

Disclaimers and Limitations

This report ('**Report**') has been prepared by WSP exclusively for the New Zealand Transport Agency ('**Client**') in relation to hydraulic analysis and design of the Manawatu River Bridge ('**Purpose**') and in accordance with the Contract with the Client. The findings in this Report are based on and are subject to the assumptions specified in the Report. WSP accepts no liability whatsoever for any reliance on or use of this Report, in whole or in part, for any use or purpose other than the Purpose or any use or reliance on the Report by any third party.

In preparing the Report, WSP has relied upon data, surveys, analyses, designs, plans and other information ('**Client Data**') provided by or on behalf of the Client. Except as otherwise stated in the Report, WSP has not verified the accuracy or completeness of the Client Data. To the extent that the statements, opinions, facts, information, conclusions and/or recommendations in this Report are based in whole or part on the Client Data, those conclusions are contingent upon the accuracy and completeness of the Client Data. WSP will not be liable in relation to incorrect conclusions or findings in the Report should any Client Data be incorrect or have been concealed, withheld, misrepresented or otherwise not fully disclosed to WSP.

1 Introduction

1.1 Background

The section of SH3 that passes through the Manawatū Gorge was closed indefinitely to traffic in July 2017. A new road is to replace this closed section of SH3 as the Saddle Road is not suitable replacement of the previous alignment. NZTA has engaged two Alliances to design a replacement road.

The Te Ahu a Turanga Highway starts from the west at the roundabout intersection with SH57 and crosses the Manawatu River next to the culturally significant Parahaki Island. Several bridge design options have been assessed and the Advance team has selected the precast concrete balanced cantilever structure for the Manawatu River Bridge based on the multi-criteria assessment. The proposed bridge is supported by bridge abutments at each end and three piers, with each pier consisting of 4 bored piles and a pier cap to provide support for the BRO2 Manawatu River Bridge. The middle pier is located within the Manawatu River Bed.

1.2 Design Standards

The proposed Manawatū Bridge will be an Importance Level 3 Bridge in terms of NZTA's Bridge Manual (NZTA, 2018). Hence the hydraulic design is with respect to the following criteria:

- Serviceability Limit State (SLS) event: 1% Annual Exceedance Probability (AEP)
- Ultimate Limit State (ULS) event: 0.04% AEP
- Allow for climate change in accordance with Section 2.3.2c of NZTA (2018).

In the above the SLS is the state beyond which a structure (i.e. the proposed bridge) becomes unfit for its intended use and the ULS is the state beyond which the strength or ductile capacity of the structure is exceeded, or when it cannot maintain its equilibrium and becomes unstable.

The design will also have to satisfy the following Minimum Requirements (MR):

- (A3.1.1.1) Abutment piles for the Manawatū River Bridge abutments shall be placed outside the limits of the 2-year ARI flood extents. No more than one pier shall be placed in the Manawatū riverbed.
- (A3.1.1.5) The 100-year ARI design flow shall be used for scour calculations and the design of scour countermeasures. Scour induced by ULS conditions shall also be evaluated and reported, with bridge survival being the required performance standard.
- (A3.1.1.7) The minimum freeboard for the new Manawatū River Bridge shall be 1.2m, measured from the water surface upstream of the bridge to the bottom of the bridge superstructure, at the lowest point between the abutments, under 100-year ARI flood conditions.
- (A3.1.1.8) The proposed Manawatū River Bridge must not cause an increase in water surface elevation, measured from downstream to upstream of the bridge, that exceeds 0.06m under exposure to 100-year ARI flood conditions.
- (A3.1.1.12) Debris accumulation on piers shall be based on a rectangular raft, with the thickness determined in accordance with NZTA Bridge Manual Section 2.3.5 and the width based on an estimated maximum tree height of 30m.

1.3 Purpose

The purpose of this report is to describe the updates of the supplied 2D HEC-RAS hydraulic computational model, the impact of the proposed bridge, scour calculations and scour protection design.

2 Hydraulic Model

2.1 Introduction

A hydraulic model was provided by NZTA to assist in the development of design proposals. The hydraulic model files and model report was received under NTT 11 dated 11 February 2019 and included the following:

- HEC-RAS 2D model files; and
- Model Report (BBO, 2019)

The model report states *“The hydraulics of the bridge location are complex and influenced by rapid flow expansion, braiding/anabranching, a confluence with the Pohangina River, and the Ashhurst Bridge [i.e. the existing SH3 Bridge]. Due to this hydraulic complexity and project programme contains, a 2D hydraulic model of the affected reach of the Manawatū River has been developed for bridge hydraulics, assessment of scour, design of scour countermeasures, estimation of debris loading, and freeboard of the bridge over the design flood.”*

The model is representative of the current landscape near the proposed bridge site (Figure 2-1). The model includes a reach of the Manawatū River from approximately 900m upstream of the proposed bridge site to approximately 185m upstream of the existing SH3 Bridge as well as the Pohangina River from the existing railway bridge to the confluence with the Manawatū River. Included were boundary conditions representing the existing climate.

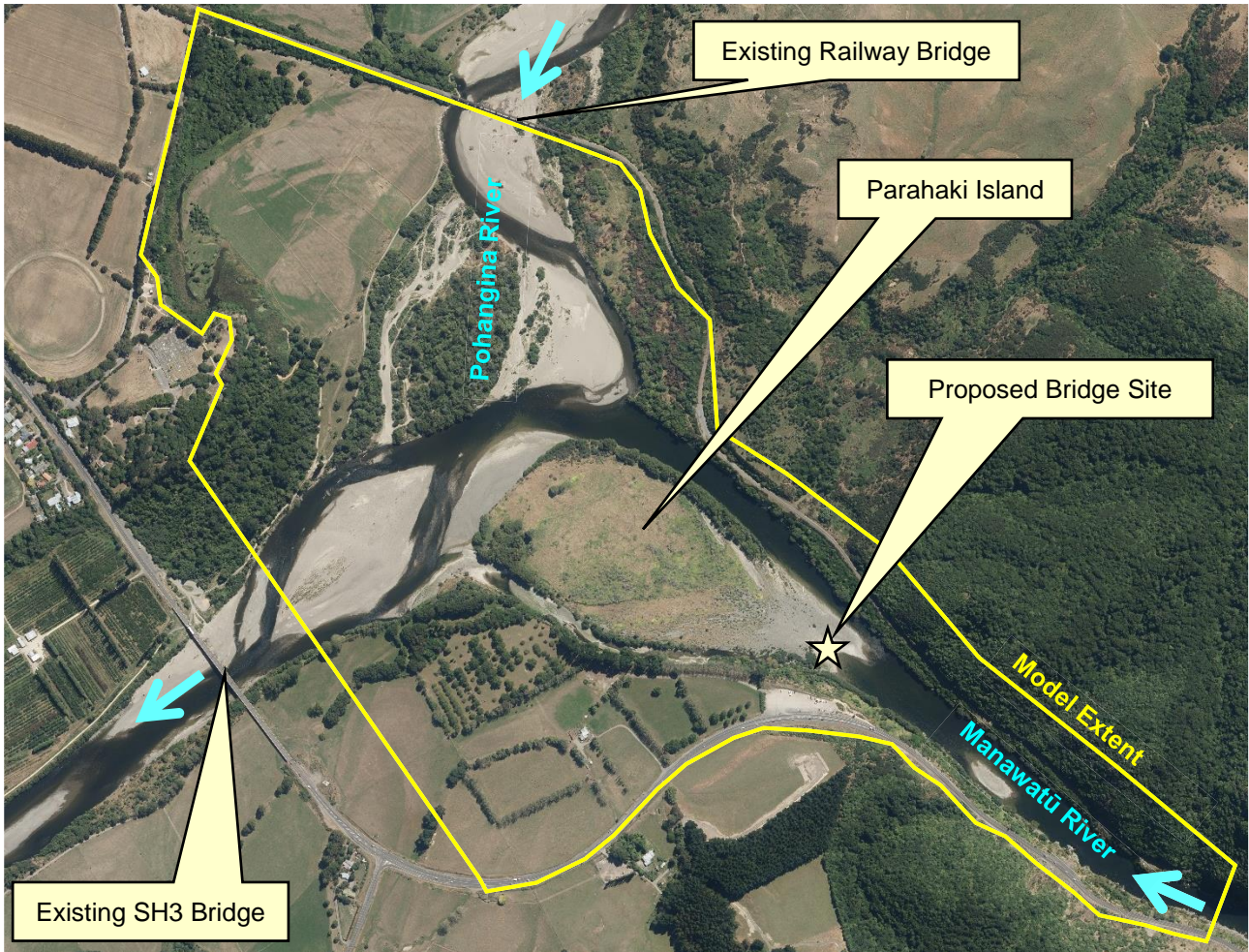


Figure 2-1 Approximate outline of 2D HEC-RAS model.

2.2 Levels and Projection

The coordinates in the supplied model are in terms of Wanganui 2000 projection and the levels are in terms of Moturiki Vertical Datum 1953 (MVD53). All reduced levels (RLs) specified in this report are also in terms of MVD53.

2.3 Changes to Model

This section details the changes made to the model to assist in the design of the proposed bridge.

2.3.1 Manawatū River inflows

The original model only included inflows for the current climate that were vetted by Horizons Regional Council. To ensure that the proposed bridge is suitable for use for its entire life the Manawatū River inflows were adjusted for climate change (As specified in Appendix A3 of NZTA (2019a) and modified by NZTA (2019b)). Table 2-1 details the Manawatū River peak design flows for the existing and future climate used in the modelling and the shape of the hydrographs used for those events are shown in Figure 2-1.

Table 2-1 Peak design flows for the Manawatū River.

Design Event		Design Flows (m ³ /s)	
ARI ¹ (year)	AEP ²	Existing Climate	Adjusted for Climate Change
2	50%	1,169	1,403
100 (SLS)	1%	2,994	3,593
2500 (ULS)	0.04%	4,759	5,711

An additional clarification was sent (TC024) regarding the boundary conditions within the model and the climate change scenario's and clarification received in NTT 26 that "The climate change adjusted flows in the Minimum Requirements will need to be entered as boundary conditions for the bridge design. No other inputs into the model, other than the bridge, highway and countermeasure (if applicable) design should be required."

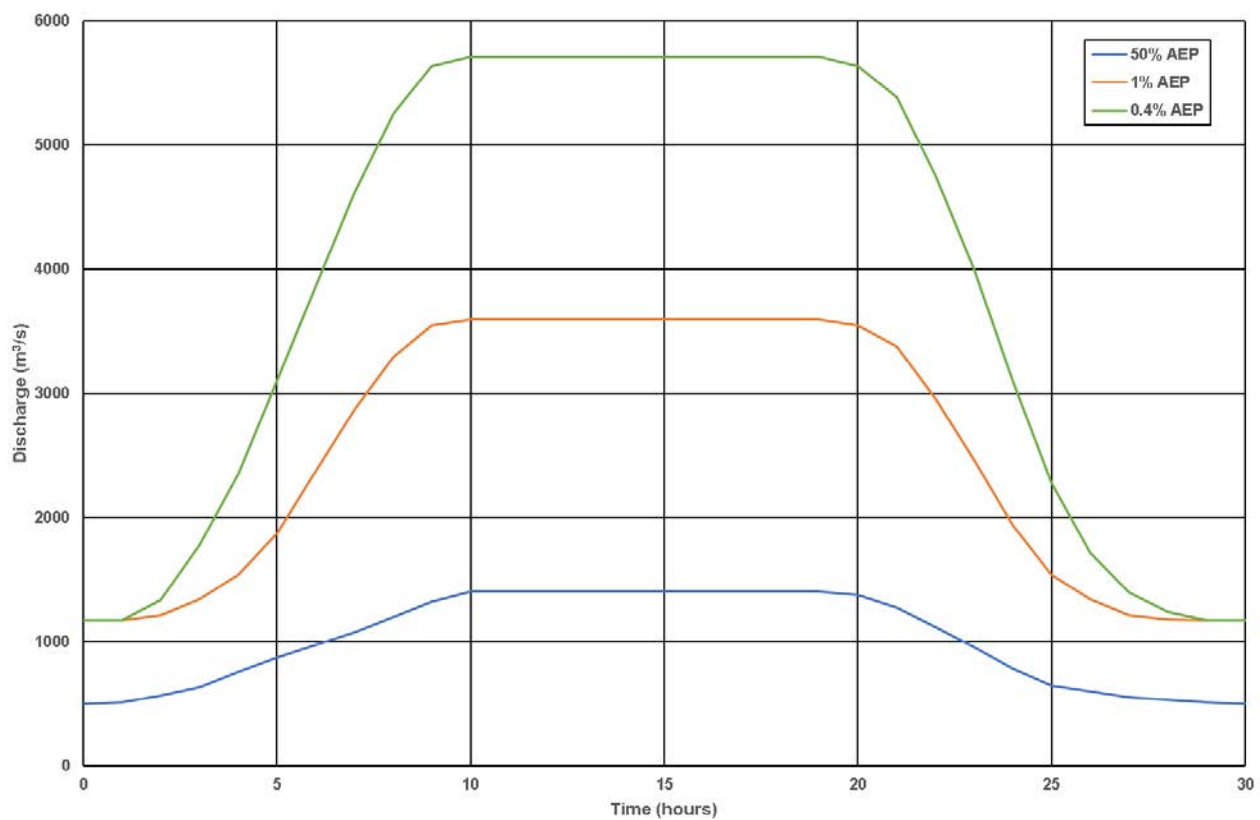


Figure 2-2 Hydrographs of design events adjusted for climate change.

2.3.2 Terrain

The first design iteration of the bridge included piers formed by four 3m diameter cylindrical in-line columns. These were inserted into the landscape by locally raising the landscape to RL100m (Figure 2-3). The diameter of the first column was increased to approximately 5m to simulate the presence of debris.

¹ ARI: Average Recurrence Interval

² AEP: Annual Exceedance Probability

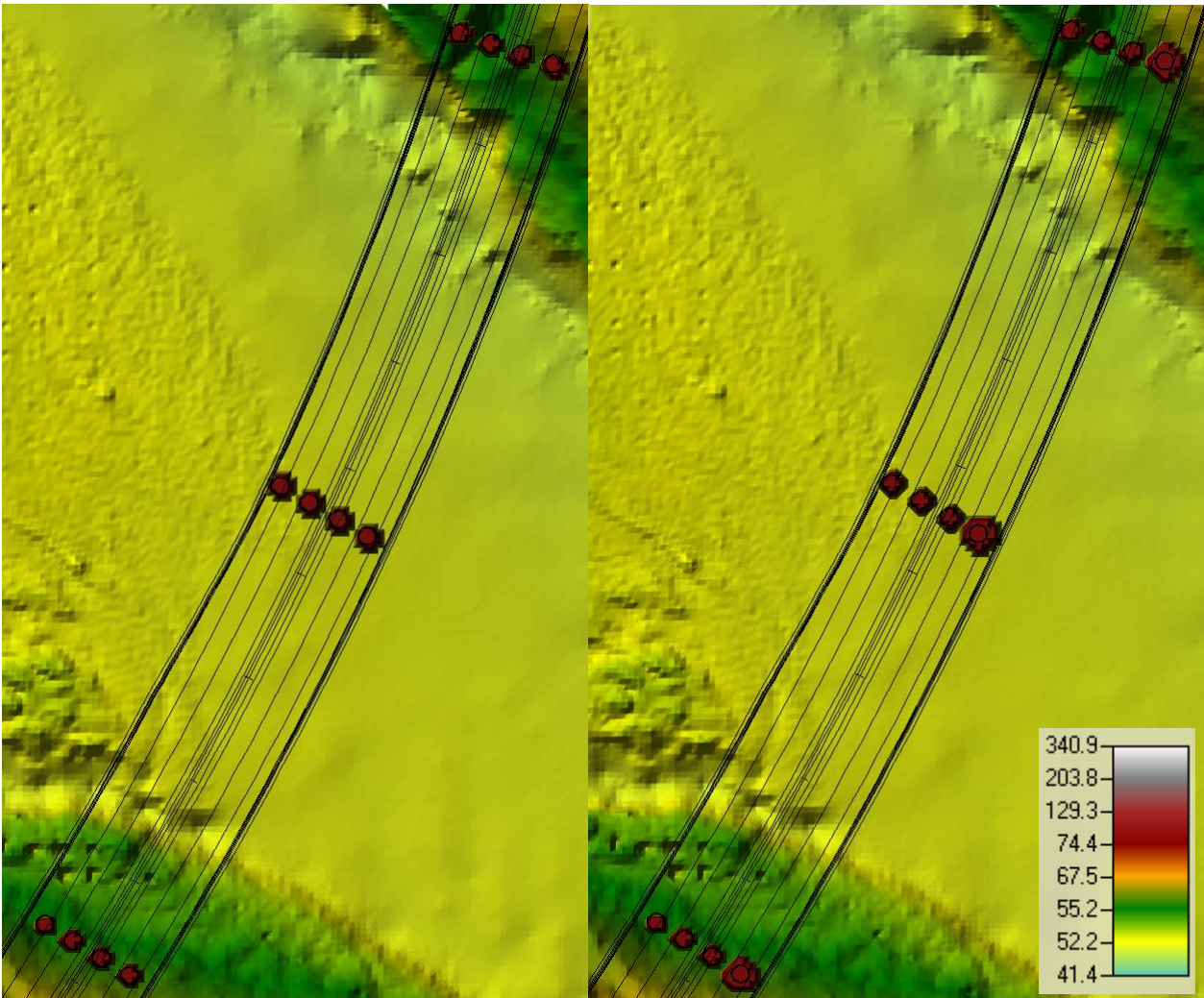


Figure 2-3 Representation of piers columns in the terrain without (left) and with debris (right).

The final design iteration of the bridge includes a 10m-long pier that is 4m-wide instead of the modelled four 3m diameter cylindrical columns. The effect of the modelled bridge is expected to be a good representation of the selected bridge design.

3 Results

3.1 Introduction

The hydraulic computational model has been run for the three climate adjusted events listed in Table 2-1 for the no bridge scenario as well as with the bridge with and without debris on the first column. This discussion of the results will primarily focus on the latter (i.e. with debris on the first column).

3.2 Water Levels & Extent

Figure A-1 to Figure A-3 show the water level and extent during the flood flows of the three design events for the proposed bridge with debris on the pier. Table 3-1 details the cross-sectional peak water levels for these scenarios.

Table 3-1 Summary of cross-sectional averaged peak water levels.

Design Event	Peak Discharge (m ³ /s)	Cross-section Averaged Peak Water Level (m MVD53)
50% AEP	1,403	55.38
1% AEP (SLS)	3,593	57.48
0.04% AEP (ULS)	5,711	59.15

Figure A-1 shows that during a 50% AEP flood flow only the central pier will be in the flood flow and thus the abutments of the proposed bridge are predicted to be well clear of this flood extent as specified by MR A3.1.1.1.

Figure A-4 compares the water levels along a long section in the 1% AEP flood flow that passes through the central pier of the bridge. This shows that:

- The bridge locally raises the water level by up to 1.75m upstream of the bridge due to the “bow wave” of the pier. This effect reduces to 0.06m or less approximately 50 to 60m upstream of the bridge pier.
- Downstream the water levels reduce by up to 0.2m.

Between the piers in the middle of the spans the increase in water level is likely to be significantly less than the above value.

3.3 Flow Velocity

Figure A-5 to Figure A-7 Figure A-3 show the water level and extent during the flood flows of the three design events for the proposed bridge with debris on the pier. These results show that while Pier 2 (in the middle of the flow) is in a high velocity environment, the other two piers are in very low velocity environments. Furthermore, Pier 3 is on the edge of the flow and falls outside the likely failure plane as a result of the scour considered. Hence, no significant scour is likely at Pier 3.

Table 3-2 details the cross-sectional averaged flow velocities for the SLS and ULS design events.

Table 3-2 Summary of cross-sectional averaged peak water levels.

Design Event	Peak Discharge (m ³ /s)	Cross-section Averaged flow velocities (m/s)
1% AEP (SLS)	3,593	3.86
0.04% AEP (ULS)	5,711	4.77

Figure 3-1 shows that even during the ULS design event, the flow velocities near Pier 1 on the south bank are less than 1m/s. Nevertheless, there is considerable uncertainty regarding the behaviour of the flow and its interaction with Pier 1. Hence, the design parameters detailed in Table 3-3 have been adopted for Pier 1, with the flow velocities taken at the edge of the main channel. This is likely to be a conservative assumption. The values in Table 3-2 have been used for the scour analysis and the design of scour protection for Pier 2 only.

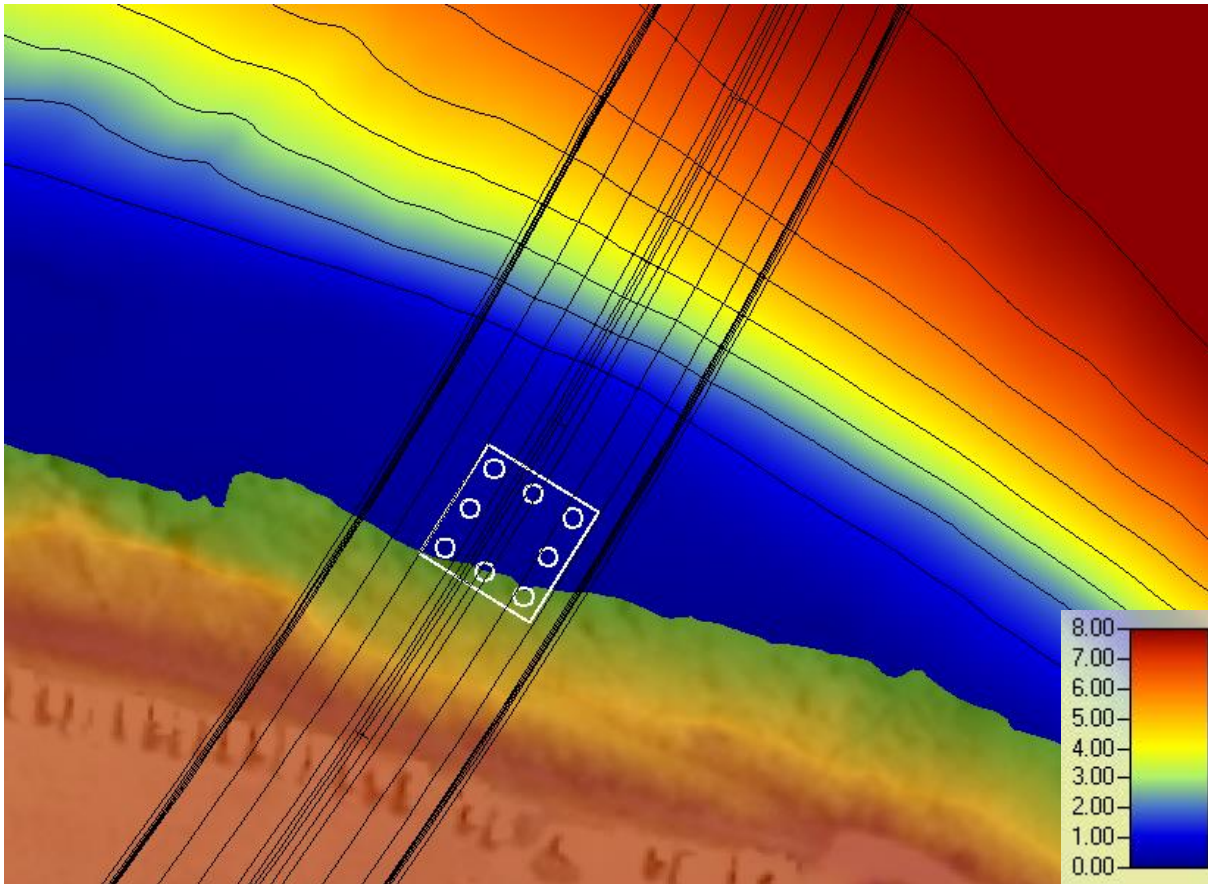


Figure 3-1 ULS (0.04% AEP adjusted for the potential effects of climate change to 2090) design event flow velocities (with 1m/s contours) near Pier 1.

Table 3-3 Pier 1 hydraulic scour analysis and protection design parameters for the design events considered.

Design Event	Design flows adjusted for climate change to 2090 (m ³ /s)	Cross-section averaged peak water level (m MVD53)	Cross-section averaged flow velocity (m/s)
1% AEP (SLS)	3,593	57.5	1.5
0.04% AEP (ULS)	5,711	59.2	1.8

3.4 Adopted Design Parameters

The key parameters used in the hydraulic analysis and design of a bridge are the cross-section averaged peak water level and velocity for the event that a bridge is designed to withstand. These can be obtained from the 2D HEC-RAS model from a cross-section at, or near, the proposed bridge. The river channel widens near the proposed bridge and consequently these parameters have been extracted approximately 10m upstream of the proposed bridge. Table 3-4 Summarises these parameters for the two design events.

Table 3-4 Key hydraulic design parameters for the proposed bridge.

Design Event	Peak Discharge (m ³ /s)	Cross-section Averaged Peak Water Level (m MVD53)	Cross-section Averaged Flow Velocity (m/s)		
			Pier 1	Pier 2	Pier 3
1% AEP (SLS)	3,593	57.48	1.5	3.86	0.0
0.04% AEP (ULS)	5,711	59.15	1.8	4.77	0.0

4 Scour Analysis

4.1 Introduction

In accordance with the MRs the method of scour assessment followed the approach outlined in Melville and Coleman (2000) and Coleman and Melville (2001) with reference to HEC-18 (FHWA, 2012).

4.2 Assumptions

This section summarises the assumptions that had to make with respect to the bridge, the river channel and bed material to be able to complete the bed scour analysis.

4.2.1 Proposed Bridge

The preliminary structural design of the bridge (Figure 4-1) showed that it is proposed to consist of a single cell box girder supported by 2 abutments and 3 piers with only Pier 2, the central pier, likely to be in the main flood flow and thus subject to local pier scour. This design, including the alignment, has been entirely driven by road geometrics and terrain. However, the design would not be appreciably different if it had been driven by hydraulic considerations.

Both abutment will be constructed well above the likely flood levels. They will therefore not be subject to local scour effects.

The preliminary design has now been refined and the single cell box girder has been replaced with a variable depth balanced cantilever. However, there has been no significant change in the location and number of piers or the pier geometry.

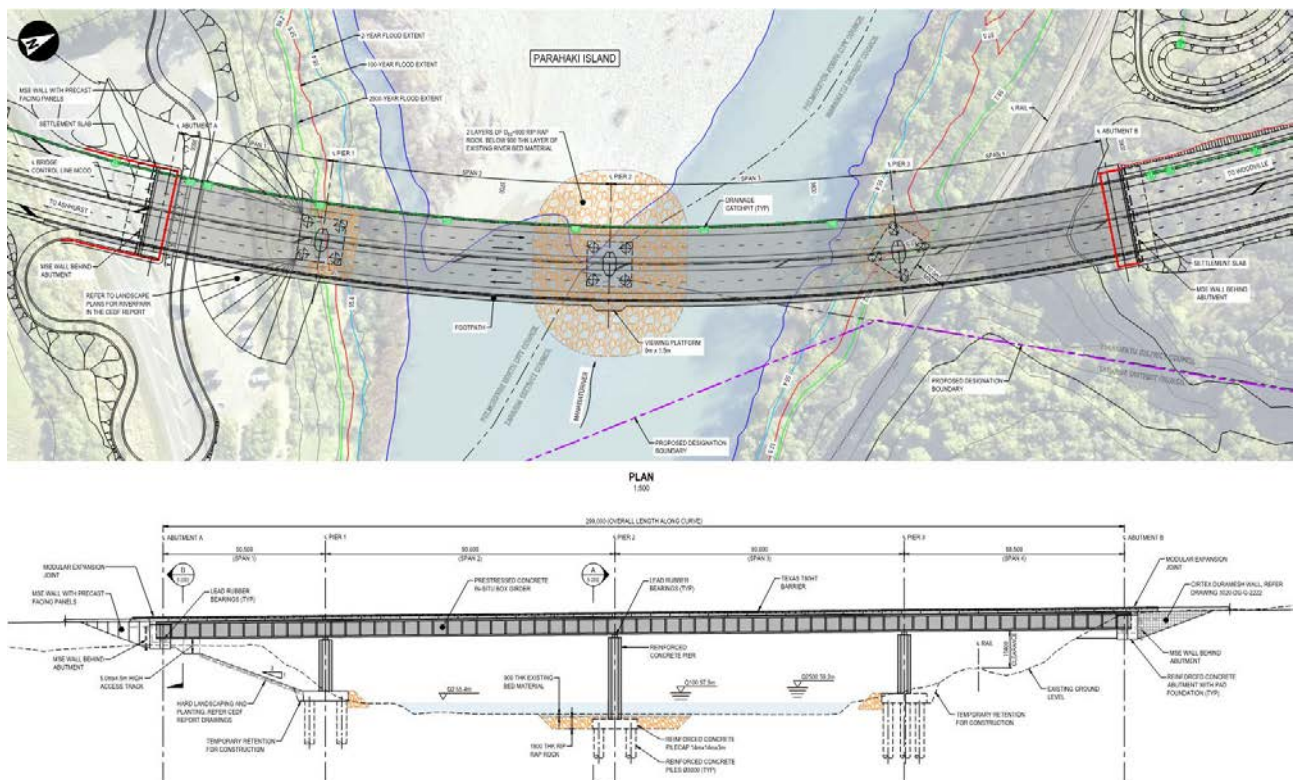


Figure 4-1 Plan and elevation of proposed bridge (Advance, 2019).

4.2.2 Pier Geometry

Table 4-1 summarises the pier geometry for the proposed bridge relevant to the scour analysis.

Table 4-1 Pier geometry data.

Parameter	Dimension / Value
Pier cross-section	4m wide and 10m long, refer Figure 4-2
Equivalent pier width (without debris raft) 0.04% AEP flood level	10.16m
Debris raft width (rectangular cross-section) ³	30m
Debris raft thickness 0.1% AEP flood level ³	3m
Equivalent pier width (with debris raft) 0.04% AEP flood level	11.10m

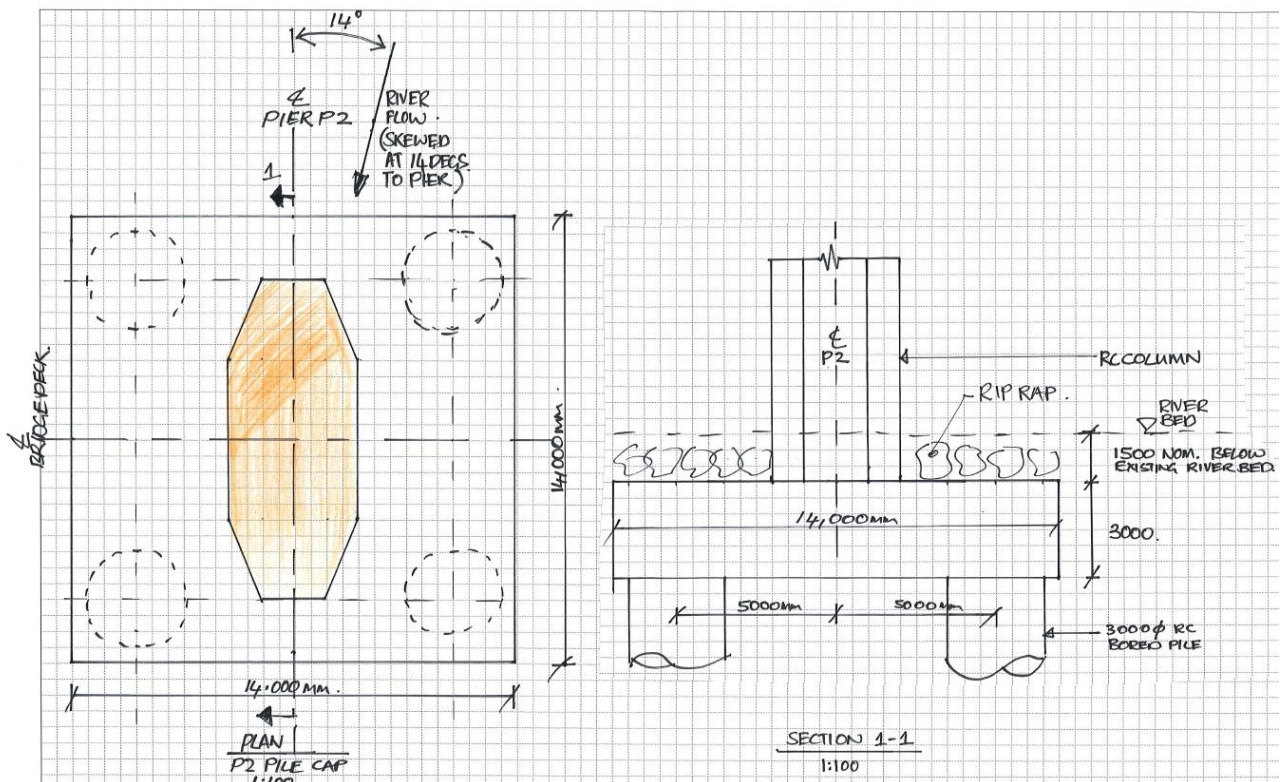


Figure 4-2 Details of pier including foundations.

4.2.3 River Channel Alignment and cross-section

The Manawatū River is a gravel bed river that at the bridge site and upstream is constrained by the bed rock of a narrow gorge (Figure 4-3). The river channel near the site of the proposed bridge widens significantly and is influenced by Parahaki Island and the confluence with the Pohangina River and the bend that the river makes at the confluence. Further downstream the river is much wider and becomes an alternating bar gravel bed river. The thalweg of the river at the bridge site is likely to be relatively stable and located along the right (north) side of the river bed because of the bend in the river at the confluence.

³ Maximum dimensions of a woody debris raft with a rectangular cross-section as specified by MR A3.1.1.12.

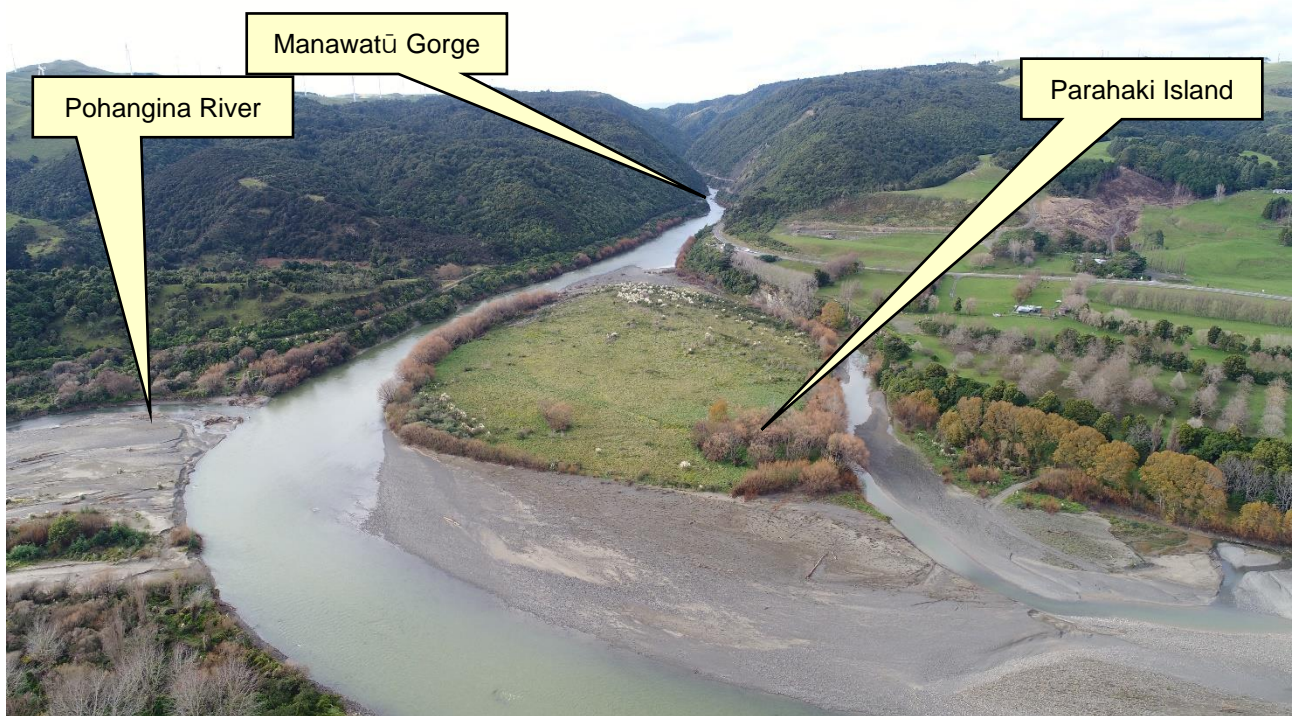


Figure 4-3 Manawatū River looking upstream from the confluence with the Pohangina River and Parahaki Island in the foreground to the Manawatū Gorge.

The proposed bridge will be situated on a relatively straight reach in the river. Hence, it is unlikely that bend scour and contraction scour effects will be significant when determining total scoured bed levels. Thalweg scour may be significant depending on the location of the piers with respect to the thalweg and whether the thalweg moves during a flood event. The latter is unlikely given the relatively straight alignment immediately upstream of a bend in the river near the proposed bridge. Local pier scour effects will be the dominant contributor to the total scoured bed level.

The scour analysis is based on a cross-section taken from the 2D HEC-RAS model bathymetry approximately 10m upstream of the proposed bridge (Figure 4-4). This cross-section shows that the thalweg of the river is on the right (north) side of the river channel.

The terrain in the model represents the existing terrain with the proposed piers and does not include any of the proposed modifications between the south abutment and Pier 1.

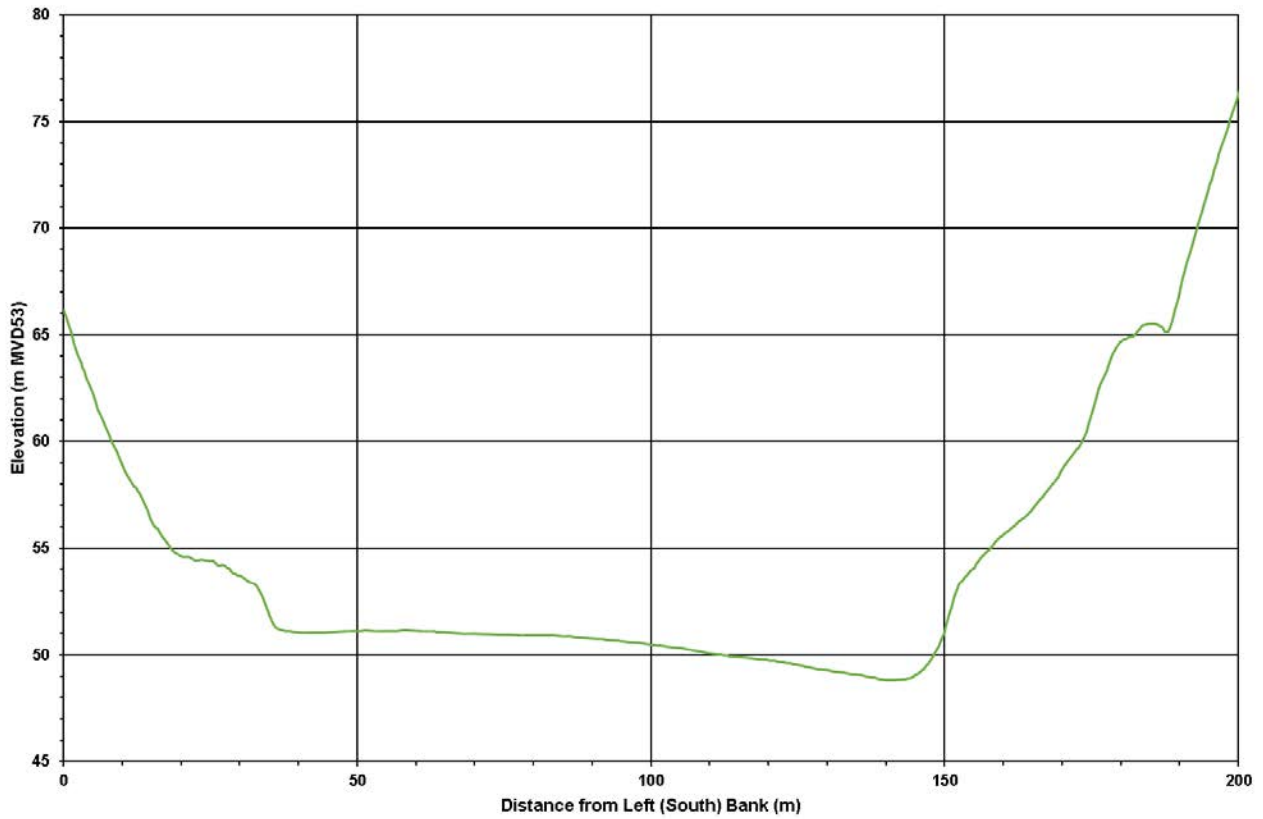


Figure 4-4 Cross-section from the 2D HEC-RAS model bathymetry used for the scour calculations.

4.2.4 Bed material

From photos of the bed material (Figure 4-5) and river channel (Figure 4-6) as well as site visit observations we infer that the bed material predominantly consists of gravelly material with cobbles. In the absence of any more specific information we assume that the bed material has a median particle size of approximately 150mm.

There are no borehole logs available to indicate whether this particle size is representative for all the bed material to the bottom of the piles supporting the bridge piers.



Figure 4-5 Manawatū River bed material near the proposed location of Pier 2.



Figure 4-6 Manawatū River bed material at the upstream end of Parahaki Island.

4.3 Bed Scour

Bed scour consists of the effects of general scour and thalweg on the unscoured channel. The key parameters describing the unscoured cross-section of the channel at the bridge are as follows:

- average unscoured bed level: RL 50.2m MVD53
- minimum unscoured (thalweg) level: RL 48.8m MVD53

Table 4-2 summarises the effect of these components on the channel during the key design events considered.

Table 4-2 Effect of the components of bed scour on the bed level.

Bed Scour Component(s)	Design Event	
	SLS (3,593m ³ /s)	ULS (5,711m ³ /s)
Average unscoured bed level (m RL)	50.2	50.2
Bed level with general scour (m RL)	49.3	48.4
Bed level with general and thalweg scour (m RL)	47.1	45.5

The above calculations assume that the thalweg is free to migrate across the channel and could coincide with any pier.

4.4 Local Scour at Piers

Local scour at piers can be considered with or without a debris raft (as defined in Table 4-1). These effects occur locally near the pier during a flood event and will result in local scour holes in the bed round the piers. Another factor influencing the local scour hole is whether the pier coincides with the thalweg of the river.

4.4.1 Piers outside the thalweg

This section deals with the effect of local pier scour of piers where they do not coincide with the thalweg. Table 4-3 gives a summary of the local scour effects without a debris raft, while Table 4-4 gives the same summary in the case of local pier scour with a debris raft round the pier at the water surface. Note that Pier 3 is on the edge of the flow and falls outside the likely failure plane as a result of the scour considered. Hence, no significant scour is likely at Pier 3. Furthermore, only Pier 2 is inside the active bed of the river and hence the local scour depth for Pier 1 and Pier 3 are given with respect to the current ground level at each pier.

Table 4-3 Effect of local pier scour at a pier outside the thalweg and without a debris raft.

	Design Event					
	SLS (3,593m ³ /s)			ULS (5,711m ³ /s)		
	Pier 1	Pier 2	Pier 3	Pier 1	Pier 2	Pier 3
Local pier scour level (m MVD53)	51.6	41.5	NA	50.6	39.0	NA
Local pier scour depth below						
• average unscoured level (m)	-	8.7	-	-	11.2	-
• Local ground level (m)	3.4	-	0.0	4.4	-	0.0

Table 4-4 Effect of local pier scour at a pier outside the thalweg with a debris raft.

	Design Event					
	SLS (3,593m ³ /s)			ULS (5,711m ³ /s)		
	Pier 1	Pier 2	Pier 3	Pier 1	Pier 2	Pier 3
Local pier scour level (m MVD53)	51.6	34.2	NA	50.6	27.3	NA
Local pier scour depth below						
• average unscoured level (m)	-	16.0	-	-	22.9	-
• Local ground level (m)	3.4	-	0.0	4.4	-	0.0

4.4.2 Piers coinciding with the thalweg

As discussed in Section 4.2.3 there is only a very low probability that the thalweg of the river will coincide with one of the piers. Only Pier 2 is within the active river bed. Hence, Table 4-5 gives a

summary of the local scour effects at Pier 2 only without a debris raft, while Table 4-6 gives the same summary in the case of local pier scour with a debris raft round the pier at the water surface.

Table 4-5 Effect of local pier scour at Pier 2 coinciding with the thalweg and without a debris raft.

	Design Event	
	SLS (3,593m ³ /s)	ULS (5,711m ³ /s)
	Pier 2	Pier 2
Local pier scour level (m MVD53)	27.7	18.9
Local pier scour depth below average unscoured level (m)	22.5	31.3

Table 4-6 Effect of local pier scour at a pier coinciding with thalweg with a debris raft.

	Design Event	
	SLS (3,593m ³ /s)	ULS (5,711m ³ /s)
	Pier 2	Pier 2
Local pier scour level (m MVD53)	21.4	14.0
Local pier scour depth below average unscoured level (m)	28.8	36.2

4.5 Summary

Table 4-7 summarises the scoured bed levels for all the combinations of scour effects considered in the previous sections. As specified in MR A3.1.1.5, the values for the ULS event with debris rafts round the piers should be used for the structural design of the bridge, though it is unlikely that the piers will coincide with the thalweg. Hence the values highlighted in green should be used for the structural design of the bridge.

Table 4-7 Summary of bed levels under the various combinations of scour effects considered.

Design Event	Flow (m ³ /s)	Scoured bed level (m MVD53)									
		General Bed Scour									
		Pier Scour						Thalweg Scour			
		No Debris			Debris			No Debris		Debris	
		Pier 1	Pier 2	Pier 3	Pier 1	Pier 2	Pier 3	Pier 2	Pier 2		
SLS	3,593	49.3	51.6	41.5	NA	51.6	34.2	NA	47.1	27.7	22.6
ULS	5,711	48.4	50.6	39.0	NA	50.6	27.3	NA	45.5	18.9	15.4

5 Scour Protection

5.1 Introduction

Scour protection can take many forms that include passive (i.e. allowing for scour in the design like extra depth of foundations) or active (e.g. providing rock rip-rap) measures. The scour protection at the proposed bridge has been investigated and designed as appropriate.

In accordance with the MRs, the scour protection followed the approach outlined in Melville and Coleman (2000) as specified by NZTA (2018) with reference to HEC-23 (FHWA, 2009). Only the case with debris on the piers for the SLS (3,593m³/s) flood event was evaluated in accordance with MR A3.1.1.5. Note that at this stage only the median rock sizes required to protect against the effects of scour is provided. The full grading envelopes, layer thicknesses, embedment depths and protection extents will be developed from these rock sizes as part of the detailed design that will follow.

During a ULS design event, the velocities will be higher than those for the SLS design event. Consequently, the bridge structural design must allow for hydrodynamic loading and scour depths for this event detailed in Table 4-7

5.2 Pier 2

Pier 2 is in the centre of the flow and in a high-velocity environment. Melville and Coleman (2000) lists many methods and those based on Austroads (1994), Lauchlan (1999), Parola (1993,1995) and Richardson and Davis (1995) were used as they are the most appropriate in this application. The analysis shows that rock riprap with a median rock size (i.e. D_{50}) of 900mm will be required provided it is buried at least 0.9m below the existing bed level and has a minimum layer thickness of 1.8m.

5.3 Pier 1

An analysis following the same approach as that for Pier 2, with the design parameters in Table 3-3, shows that rock riprap with a median rock size (i.e. D_{50}) of 450mm will be required with a minimum layer thickness of 0.9m. However, given the low velocity environment other approaches, such as vegetation, could be considered.

A design manual published by the Department of Mines and Natural Resources of the Queensland Government (Queensland, 2004) provides guidance for the design of vegetated channels. Table 5-1 gives guidance for the maximum permissible velocities for bare and vegetated channels. This table shows that with adequate vegetation cover it is possible to provide scour protection for flows with velocities of up to 2m/s, depending on the type of vegetation.

The model results show that the water surface slope following the construction of the bridge is approximately 2%. Thus, vegetation could be used instead of rock riprap depending on the type of vegetation chosen and the nature of the bank material. Figure 5-1 shows that the existing vegetation near the proposed location of Pier 1 is quite dense and well established with no evidence of bank scour.

Using vegetation for scour protection, however, will only be effective once the vegetation is fully established, and assuming that it is not disturbed at some stage in the future. Consequently, there will be a residual risk of flood-induced scour prior to vegetation establishment. This risk could potentially be mitigated by using vegetation in combination with geofabric.

It must be noted that extensive ground modification is proposed between the south abutment and Pier 1 (Figure 5-2). This could cause recirculating flow with increased scour potential. This is not included in the current terrain used in the modelling or allowed for in the scour analysis. Care will need to be taken when shaping of the finished ground contours or additional scour protection may have to be provided to ensure that such flows do not exacerbate any scour potential.

Table 5-1 Recommended maximum velocities for bare and vegetated channels (source: Queensland, 2004).

Channel gradient %	Recommended maximum velocities (m/s) related to percentage of anchored surface cover			
	0% cover Bare surfaces which are consolidated but not cultivated	50% cover Tussocky species (includes most native grasses)	75% cover Rhodes grass and creeping species such as couch grass in moderate condition	100% cover Creeping species such as kikuyu that can be maintained as a permanent dense sod
	A. Erosion resistant soils (eg. Krasnozems)			
1	0.7	1.6	2.1	2.8
2	0.6	1.4	1.8	2.5
3	0.5	1.3	1.7	2.4
4		1.3	1.6	2.3
5		1.2	1.6	2.2
6			1.5	2.1
8			1.5	2.0
10			1.4	1.9
15			1.3	1.8
20			1.3	1.7
	B. Easily eroded soils (eg. Black earths, fine surface texture-contrast soils)			
1	0.5	1.2	1.5	2.1
2	0.5	1.1	1.4	1.9
3	0.4	1.0	1.3	1.8
4		1.0	1.2	1.7
5		0.9	1.2	1.6
6			1.1	1.6
8			1.1	1.5
10			1.1	1.5
15			1.0	1.4
20			0.9	1.3



Figure 5-1 Manawatū River channel looking upstream from Parahaki Island with existing vegetation near proposed Pier 1 on the true right bank.

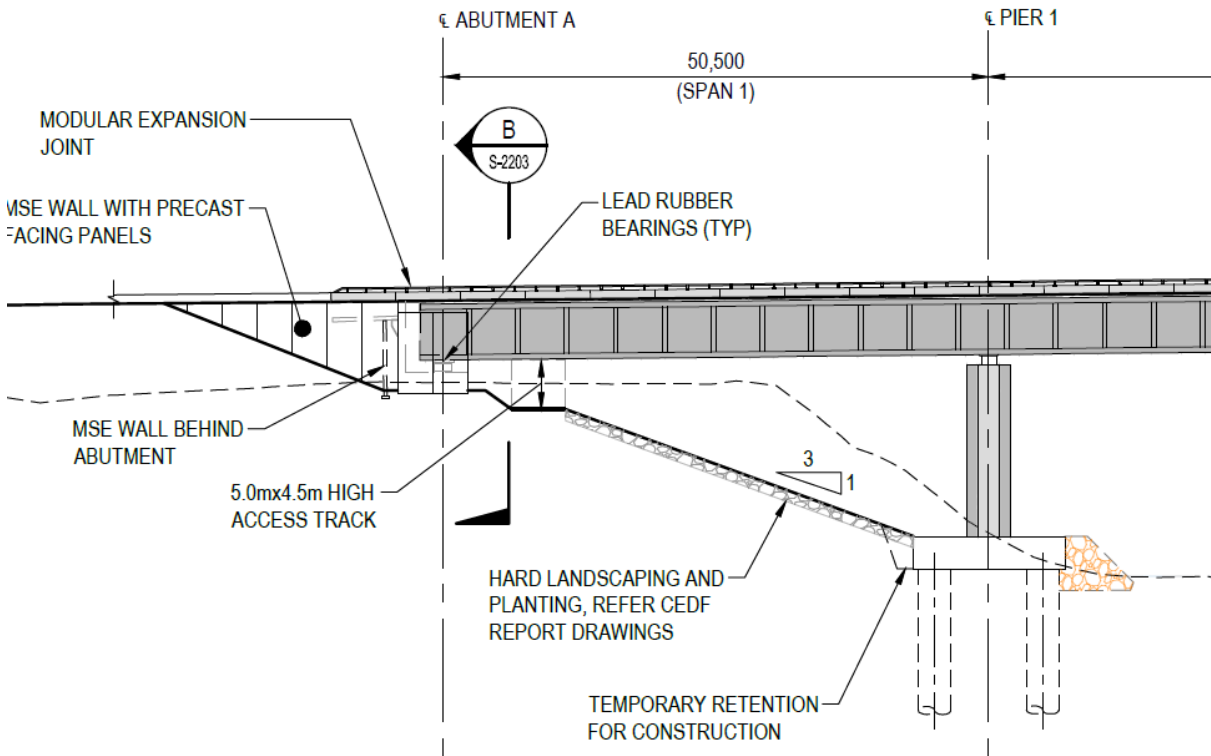


Figure 5-2 Details of the proposed ground modifications between the south abutment and Pier 1 (Advance, 2019).

6 Summary

The proposed Manawatū River Bridge will be part of the new Te Ahu a Turanga Highway that starts from the west at the roundabout intersection with SH57 and crosses the Manawatū River next to the culturally significant Parahaki Island. The proposed bridge will be an Importance Level 3 Bridge in terms of NZTA’s Bridge Manual (NZTA, 2018).

A hydraulic model was provided by NZTA to assist in the development of design proposals. The accompanying model report (BBO, 2019) states “*The hydraulics of the bridge location are complex and influenced by rapid flow expansion, braiding/anabranching, a confluence with the Pohangina River, and the Ashhurst Bridge [i.e. the existing SH3 Bridge]. Due to this hydraulic complexity and project programme contains, a 2D hydraulic model of the affected reach of the Manawatū River has been developed for bridge hydraulics, assessment of scour, design of scour countermeasures, estimation of debris loading, and freeboard of the bridge over the design flood.*” The design flows of the model have been adjusted to account for climate change as specified by the MRs. The model terrain has been modified such that the results reflect the impact of the proposed bridge.

The scour analysis shows that in general the bed level will scour down to RL 49.3m and RL 48.4m respectively for the SLS and ULS events with the thalweg scouring down to RL 47.1m and RL 45.5m respectively for these events. It is unlikely that the thalweg will migrate to coincide with the piers and hence Table 6-1 summarises the results of the final scoured bed levels at the piers as a result of all the components of bed scour considered.

Table 6-1 Summary of final scoured local bed levels for the design events considered.

Design Event	2090 Climate Peak Design Flows (m ³ /s)	Scoured bed levels (m MVD53) allowing for general scour, local scour and debris raft		
		Pier 1	Pier 2	Pier 3
1% AEP (SLS)	3,593	51.6	34.2	NA
0.04% AEP (ULS)	5,711	50.6	27.3	NA

It must be noted that extensive ground modification is proposed between the south abutment and Pier 1. This could cause recirculating flow with increased scour potential. This is not included in the current terrain used in the modelling or allowed for in the scour analysis. Care will need to be taken with shaping of the finished ground contours or additional scour protection may have to be provided to ensure that such flows do not exacerbate any scour potential.

Scour protection can take many forms that include passive (i.e. allowing for scour in the design like extra depth of foundations) or active (e.g. providing rock rip-rap) measures. The scour protection at the proposed bridge has been investigated and designed as appropriate. Table 6-2 summarises the key parameters of the selected scour protection.

Table 6-2 Details of selected scour protection.

Pier	Scour Protection Required
Pier 1	Rock riprap with a median rock size (i.e. D ₅₀) of 450mm with a minimum layer thickness of 0.9m OR Dense vegetation selected in accordance with Queensland (2004); potentially in combination with geofabric to reduce the residual risk of flood-induced scour prior to the vegetation becoming fully established.
Pier 2	Rock riprap with a median rock size (i.e. D ₅₀) of 900mm with a minimum layer thickness of 1.8m and buried at least 0.9m below the existing bed level.
Pier 3	None required

It must be noted that during a ULS design event the velocities will be higher than those for the SLS design event. Consequently, the bridge structural design must allow for hydrodynamic loading and scour depths for this event detailed in Table 6-1.

7 Glossary

- Soffit The soffit of a bridge is the lowest elevation of the underside of the bridge deck structure, including any supporting beams.
- Thalweg The thalweg of a river is a line drawn to join the lowest points along the entire length of a stream bed, defining its deepest channel.

8 References

Advance (2019), Te Ahu a Turanga – Manawatū Tararua Highway – BR02 Manawatū River Bridge plan & elevation”, drawing by Advance Alliance for the New Zealand Transport Agency, drawing number TAT-3020-DG-S-2201, Rev 10, May 2019.

Austrroads (1994), "Waterway design - A guide to the hydraulic design of bridges, culverts and floodways", Austrroads, Australia, 1994.

BBO (2019), "Te Ahu a Turanga - Manawatu River Base Hydraulic Model", a report by Bloxham Burnett & Olliver Ltd for the New Zealand Transport Agency, Reference 145850, February 2019.

Coleman S E and Melville B W (2001), "Case Study; New Zealand Bridge Scour Experiences", ASCE Journal of Hydraulic Engineering, Vol. 127, No. 7, July 2001.

FHWA (2005), "Debris Control Structures - Evaluation and Countermeasures", Hydraulic Engineering Circular No. 9, 3rd edition, Department of Transportation - Federal Highway Administration, Reference FHWA-IF-04-016, October 2005.

FHWA (2009), "Bridge Scour and Stream Instability Countermeasures: Experience, Selection, and Design Guidance", Hydraulic Engineering Circular No. 23, 3rd edition, Department of Transportation - Federal Highway Administration, Reference FHWA-NHI-09-111, September 2009.

FHWA (2012), "Evaluating Scour at Bridges", Hydraulic Engineering Circular No 18, 5th edition, US Department of Transportation - Federal Highway Administration, Reference FHWA-HIF-12-003, April 2012.

Lauchlan, C S (1999), "Countermeasures for pier scour", PhD Thesis, The University of Auckland, New Zealand, 1999.

Melville B W and Coleman S E (2000), "Bridge Scour", Water Resources Publications, 2000.

NZTA (2018), "Bridge Manual", 3rd edition, Amendment 3, a design manual produced by the New Zealand Transport Agency, Document Number SP/M/022, October 2018.

NZTA (2019a), "Te Ahu a Turanga: Manawatū Tararua Highway - Implementation - Minimum Requirements", Version 2, New Zealand Transport Agency, Contract No NZTA 2018576, February 2019.

NZTA (2019b), "Te Ahu a Turanga: Manawatū Tararua Highway - Implementation - Notice to Tenders No 25", New Zealand Transport Agency, Contract No NZTA 2018576, March 2019.

Parola, A C (1993), "Stability of rock riprap at bridge piers", Journal of Hydraulic Engineering, ASCE, 119(10), 1080-1093.

Parola, A C (1995), "Boundary stress and stability of riprap at bridge piers", in "River, Coastal and Shoreline Protection: Erosion Control Using Riprap and Armourstone", edited by C R Thorne et al, John Wiley & Sons, Inc.

Queensland (2004), "Soil Conservation measures - design manual for Queensland", Department of Natural Resources and Mines, Queensland Government, October 2004.

Richardson, E V and Davis, S R (1995), "Evaluating scour at bridges", Report No FHWA-IP-90-017, Hydraulic Engineering Circular 18 (HEC-18), Third Edition, Office of Technology Applications, HTA-22, Federal Highway Administration, US Department of Transportation, November 1995.

Appendix A - Figures

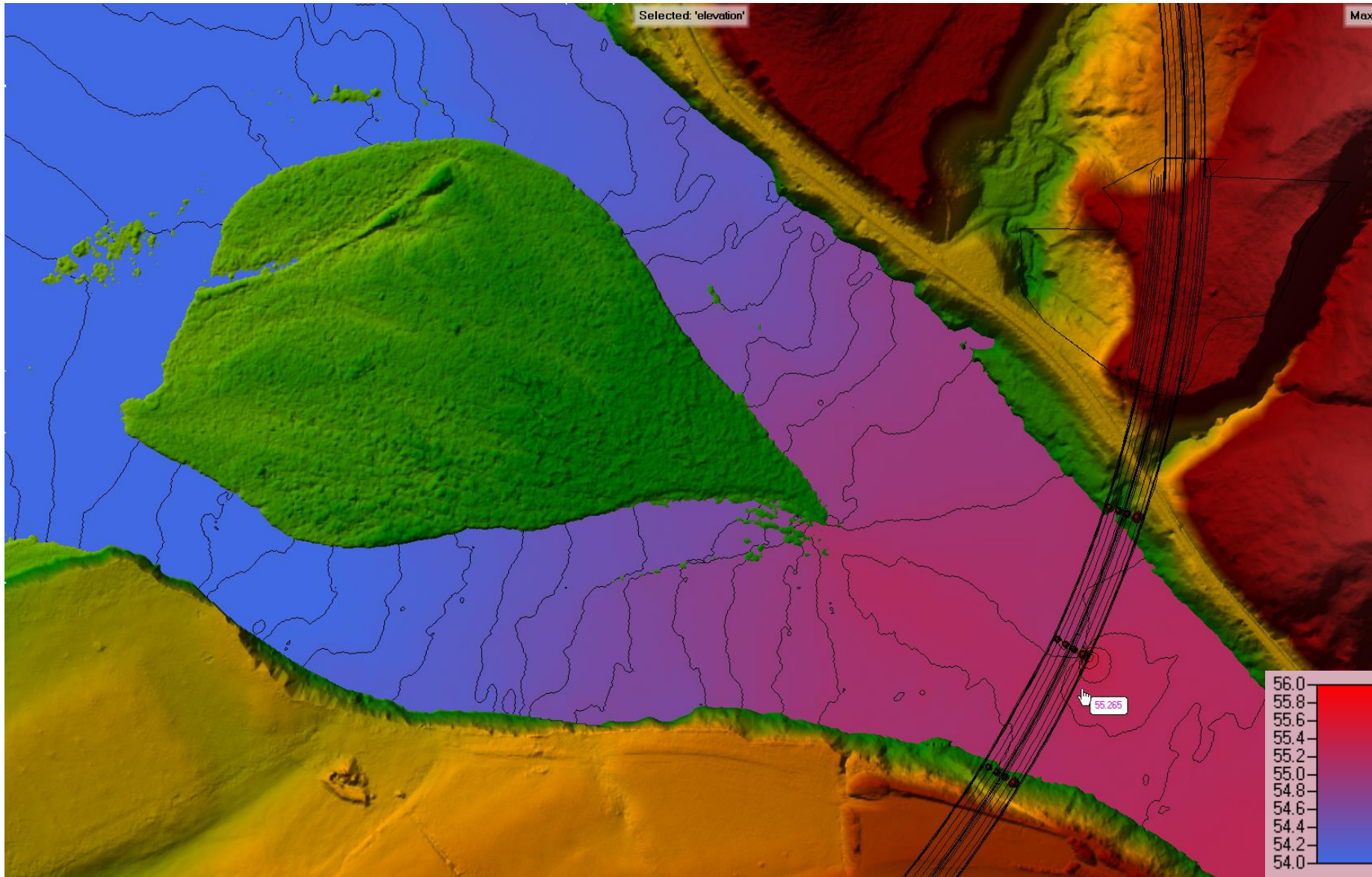


Figure A-1 50% AEP water levels for bridge with debris-laden piers

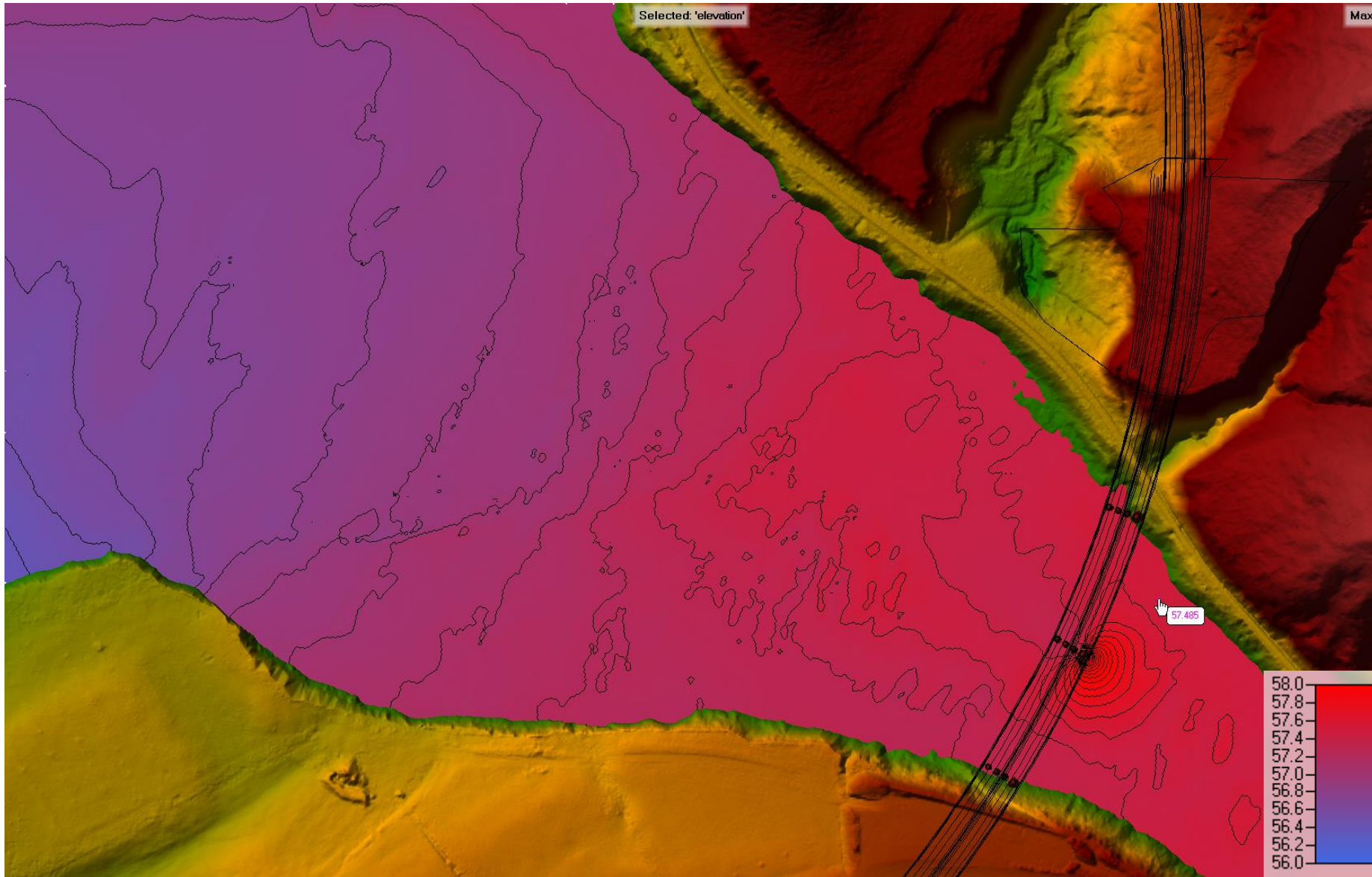


Figure A-2 1% AEP water levels for bridge with debris-laden piers

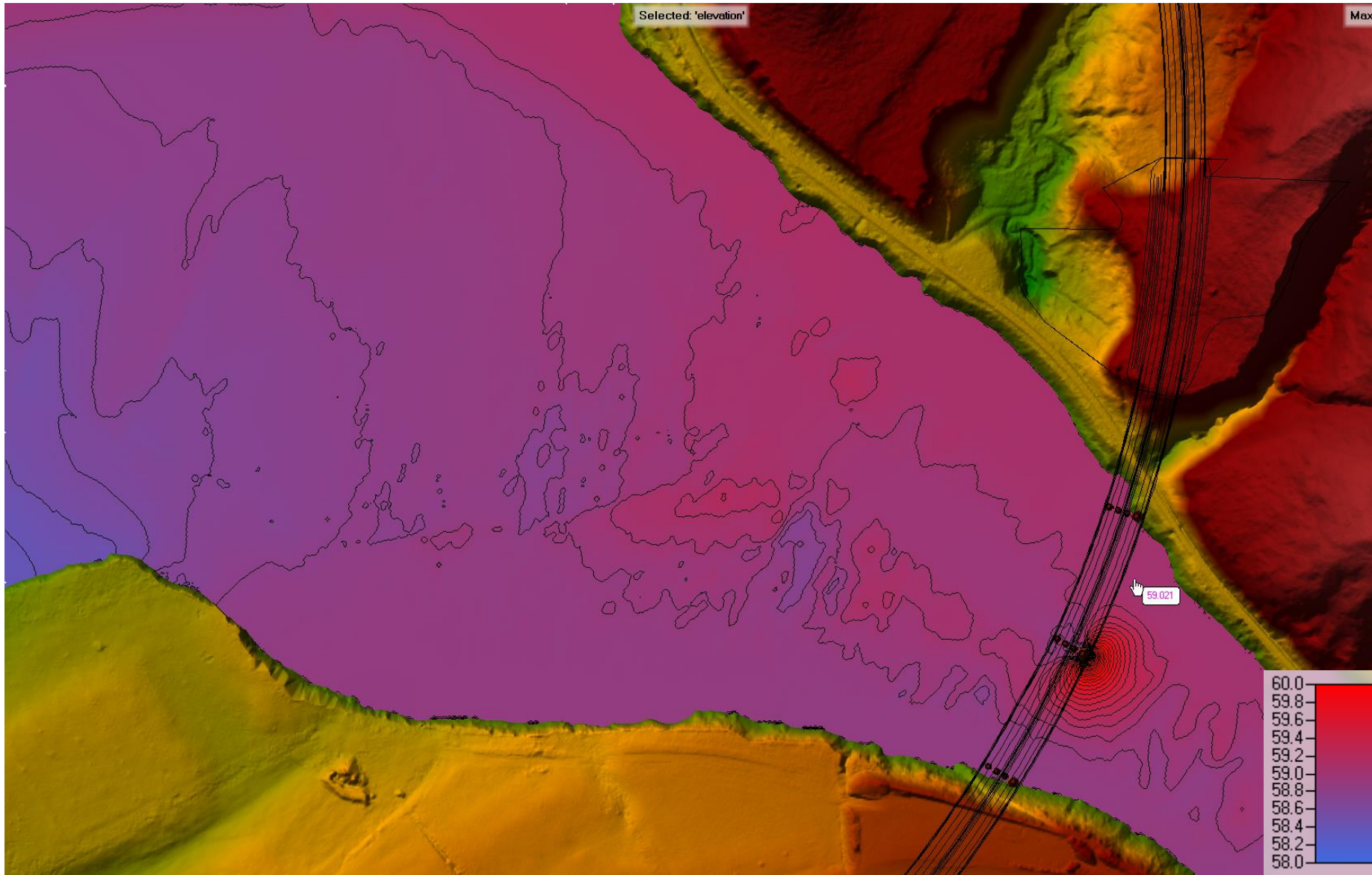


Figure A-3 0.04% AEP water levels for bridge with debris-laden piers

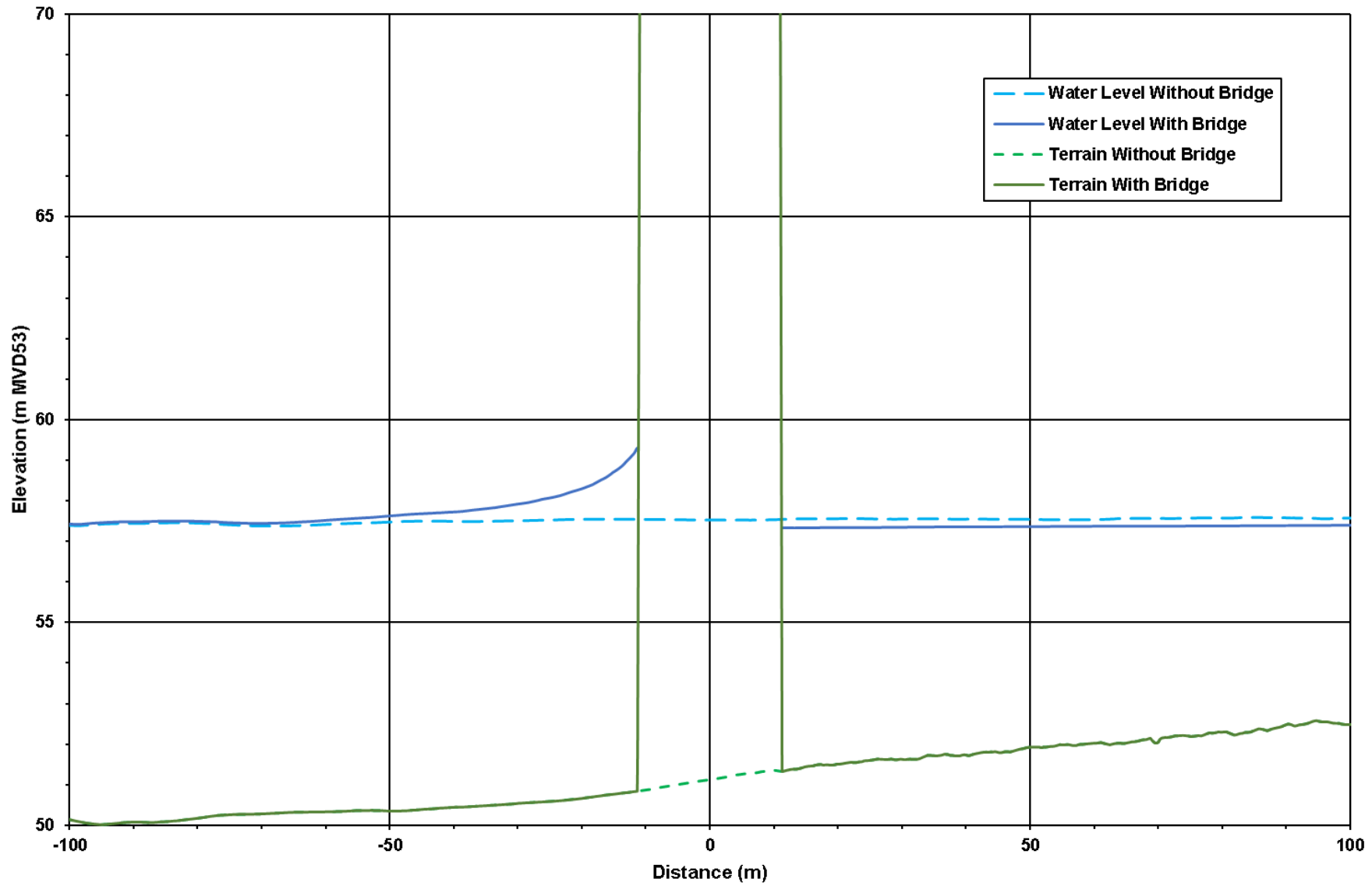


Figure A-4 Long-section through central pier showing impact of bridge on 1% AEP water levels

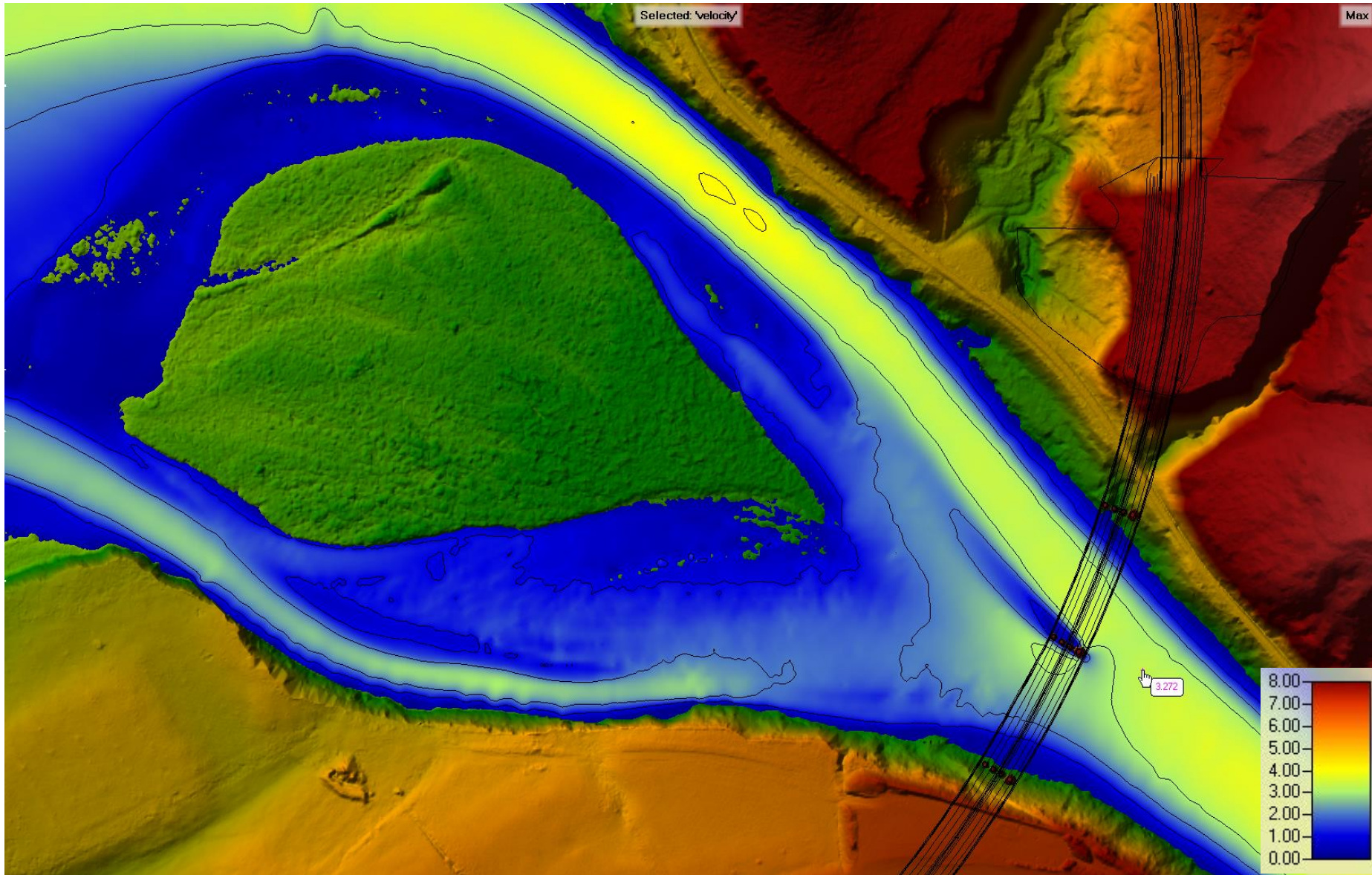


Figure A-5 50% AEP flow velocities for bridge with debris-laden piers

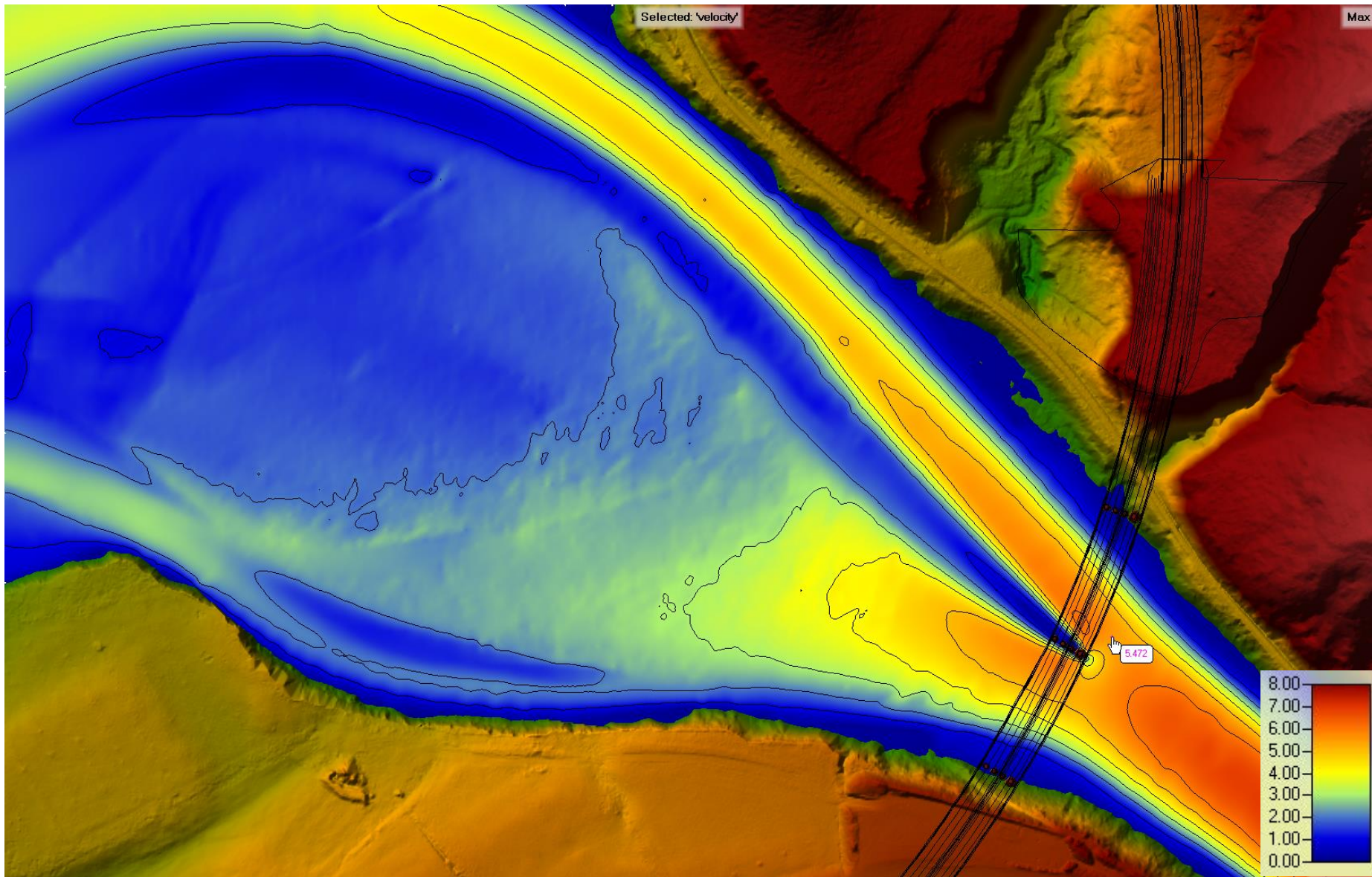


Figure A-6 1% AEP flow velocities for bridge with debris-laden piers

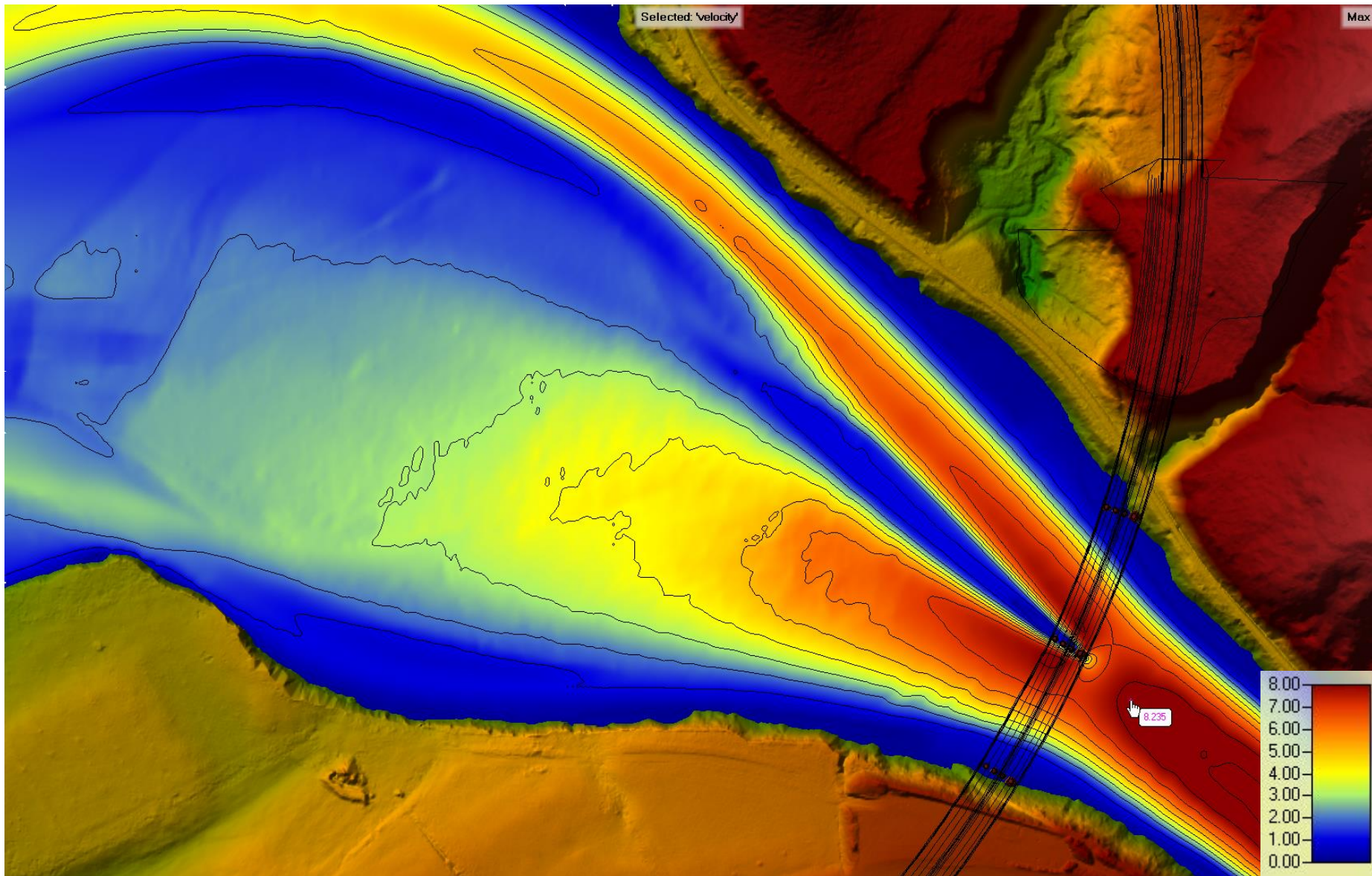


Figure A-7 0.04% AEP flow velocities for bridge with debris-laden piers

Appendix B - Calculations

Te Ahu a Turanga Manawatu Tararua Highway - VE002 (Original 3 piers)

Ref: Melville and Coleman (2000)

Pier

-Pier foundation 10.00 m MSL <- Complete guess as no information is available

Design Event	ARI (yrs)	AEP	Flow (m3/s)	Stage (m MSL)	Scoured bed level (m MVD53)											
					General						Pier 1			Pier 3		
					Pier 2		Thalweg		Pier 2		General		General + Thalweg			
					No Debris	Debris	No Debris	Debris	No Debris	Debris	No Debris	Debris	No Debris	Debris		
SLS	100 + CC	1%	3593	57.48	49.3	41.5	34.2	47.1	27.7	21.4	55.0	51.6	51.6	58.1	58.1	58.1
ULS	2500+CC	0.04%	5711	59.15	48.4	39.0	27.3	45.5	18.9	14.0	55.0	50.6	50.6	58.1	58.1	58.1

Te Ahu a Turanga Manawatu Tararua Highway - General Scour

Ref: Melville and Coleman (2000)

channel width W 113.77 Measured at 9m upstream of piers
 ave unscoured bed level 50.23 m calculated by integration of measured 2018 bottom levels
 min unscoured bed level 48.82 m
 ave normal river level 50.98 m based on LiDAR data
 median bed material size d50 150 mm From geotech observations

floodplain dimensions ignore - assume all goes through bridge, none over floodplain
 left bank width m
 left bank level m
 right bank width m
 right bank level m

floodplain velocity factor not used in this case

main channel dimensions
 effective channel width 113.77 m

NZR after Holmes

ARI	Flow	Stage	ave vel	area	mc area	fp area	mc vel	ave depth	ave bed lev	mc flow	C	V ₁	K	Y _r	Y _{s=f(yr,V1,K)}	ys>ave depth?	yms
(years)	(m3/s)	(m)	(m/s)	(m2)	(m2)	(m2)	(m/s)	(m)	(m)	(m3/s)		(m/s)		(m)	(m)		(m)
100 + CC	3593	57.48			930		3.86	8.17	49.31	3593	1	3.86	0.627	6.50	5.51	No	8.17
2500+CC	5711	59.15			1196		4.77	10.52	48.63	5711	1	4.77	0.558	8.17	6.72	No	10.52
average								48.97									

Maza & Echavaria Only applicable for d75<6mm

ARI	Flow	Stage	ave vel	area	mc area	fp area	mc vel	ave depth	ave bed lev	mc flow	d50	y0	y0/ym0	ys	ys>ave depth?	yms	factored ys
(years)	(m3/s)	(m)	(m/s)	(m2)	(m2)	(m2)	(m/s)	(m)	(m)	(m3/s)	(m)	(m)	(m)	(m)		(m)	
100 + CC	3593	57.48			930		3.86	8.17	49.31	3593	0.1500	8.66	1.06	7.37	no	8.17	7.80
2500+CC	5711	59.15			1196		4.77	10.52	48.63	5711	0.1500	10.33	0.98	10.59	yes	10.59	10.41
average								48.97									

Blench

ARI	Flow	Stage	ave vel	area	mc area	fp area	mc vel	ave depth	ave bed lev	mc flow	d50	q	ys	ys>ave depth?	yms
8-	(m3/s)	(m)	(m/s)	(m2)	(m2)	(m2)	(m/s)	(m)	(m)	(m3/s)	(mm)	(m2/s)	(m)		(m)
100 + CC	3593	57.48			930		3.86	8.17	49.31	3593	150.0	31.6	8.09	no	8.17
2500+CC	5711	59.15			1196		4.77	10.52	48.63	5711	150.0	50.2	11.02	yes	11.02
average								48.97							

Summary

ARI	Flow	Stage	ave vel	area	ave depth	ave bed lev	Holmes yms	M & E yms	Blench yms	ave ys	ave scour level
(years)	(m3/s)	(m)	(m/s)	(m2)	(m)	(m)	(m)	(m)	(m)	(m)	(m)
100 + CC	3593	57.48	3.86	929.8	8.17	49.31	8.17		8.17	8.17	49.31
2500+CC	5711	59.15	4.77	1196.3	10.52	48.63	10.52		11.02	10.77	48.38

Te Ahu a Turanga Manawatu Tararua Highway - Thalweg Scour

Ref: Melville and Coleman (2000)

channel width W	113.77	Measured at 9m upstream of piers
ave unscoured bed level	50.23 m	calculated by integration of measured 2018 bottom levels
min unscoured bed level	48.82 m	
ave normal river level	50.98 m	based on LiDAR data
median bed material size d50	150 mm	From geotech observations

<i>floodplain dimensions</i>		ignore - assume all goes through bridge, none over floodplain
left bank width	m	
left bank level	m	
right bank width	m	
right bank level	m	

floodplain velocity factor not used in this case

main channel dimensions

effective channel width 113.77 m

Thalweg Effects - from general and bend scour

yts = 1.27 yms Eq 4.25 Melville and Coleman
factor 1.27

ARI	Flow (m3/s)	from general scour calcs			factored eq 4.25 M & C			ave yts (m)	from contraction scour calcs		assume yts (m)	Stage (m)	scour level (m)
		Holmes yms (m)	M & E yms (m)	Blench yms (m)	Holmes yts (m)	M & E yts (m)	Blench yts (m)		contraction scour yts (m)	factored yts (m)			
100 + CC	3593	8.17		8.17	10.38		10.38	10.38	no contraction scour in this case		10.38	57.48	47.10
2500+CC	5711	10.52		11.02	13.35		14.00	13.68	no contraction scour in this case		13.68	59.15	45.47

Factor general scour based on 2018 cross-section data

ARI	Flow (m3/s)	Stage (m)	from general scour calcs			from 2018 x-section y0/ym0	factored y0/ym0			ave yts (m)	scour level (m)
			Holmes yms (m)	M & E yms (m)	Blench yms (m)		Holmes yts (m)	M & E yts (m)	Blench yts (m)		
100 + CC	3593	57.44	8.17		8.17	1.06	8.66		8.66	8.66	48.78
2500+CC	5711	59.06	10.52		11.02	0.98	10.33		10.83	10.58	48.48

Te Ahu a Turanga Manawatu Tararua Highway - VE002 Pier 1 Scour

Ref: Melville and Coleman (2000)

channel width W 113.77 Measured at 9m upstream of piers
 ave unscoured bed level 50.23 m calculated by integration of measured 2018 bottom levels
 min unscoured bed level 48.82 m
 ave normal river level 50.98 m based on LiDAR data
 median bed material size d50 150 mm From geotech observations
 median bed material size d50a 450 mm assuming d50 = d50a /3 based on Hutt River samples as a rough guide

floodplain dimensions ignore - assume all goes through bridge, none over floodplain
 left bank width m
 left bank level m
 right bank width m
 right bank level m

floodplain velocity factor not used in this case

main channel dimensions
 effective channel width 113.77 m

pier dimensions
 piers supported on 3m diameter concrete reinforced cylinder
 pile cap foundation level 55 m
 pile cap top level 58 m
 pier width b 4.00 m
 pile cap width b* 14.00 m

pier length l 10.00 m
 pile dia Dp 3 m One 14m x 14m pile cap supported by four 3m dia piers at 10m centres
 pile spacing Sp 10.00 m Sp/Dp 3.333333

Local Pier Scour - reduced general scour

Theta = 0 °

ARI (years)	Flow (m3/s)	ave yms (m)	Stage (m MSL)	gen sc lev	local scour case Fig 6.15	Fig 6.15 Y (m)	Eq 6.8 bequiv (m)	bequiv / y	Eq 6.4 depth size factor Kyb	Fig 6.6 Eq 6.6 flow intens factor Ki	be/d50	Eq 6.7 sed size factor Kd	Table 6.3 shape factor Ks	Eq 6.10 alignment factor Ktheta	time factor Kt	ds (m)	yts + ds (m)	Stage (m MSL)	loc sc lev (m MSL)
100 + CC	3593	2.48	57.48	55.00	III	-3.00	14.32	5.772	11.16	0.308	95.44	1.000	1.00	0.98	1.00	3.37	5.85	57.48	51.63
2500+CC	5711	4.15	59.15	55.00	III	-3.00	13.37	3.221	14.90	0.301	89.11	1.000	1.00	0.98	1.00	4.39	8.54	59.15	50.61

flow intensity factor calculations

time scale factor calculations

ARI (years)	d50	dmax	d50a	Fig 3.5 u*c	= yts y	y/d50	Vc	Fig 3.5 u*ca	y/d50a	Vca	Va	V	vel para	Ki	V/Vc	bequiv/V	y/bequiv	Eq 6.14 te (days)	t (days)	t/te	Kt
100 + CC	150		450	0.374	2.48	16.5	4.212	0.647	5.5	5.521	4.416	1.500	0.308	0.308	0.356	9.544	0.17	-8.34	1	-0.120	#NUM!
2500+CC	150		450	0.374	4.15	27.7	4.692	0.647	9.2	6.352	5.082	1.800	0.301	0.301	0.384	7.426	0.31	-2.80	1	-0.357	#NUM!

Note: Used max V at left edge of main channel instead of average approach flow velocity for calc

Te Ahu a Turanga Manawatu Tararua Highway - VE002 Pier 2 Scour

Ref: Melville and Coleman (2000)

channel width W 113.77 Measured at 9m upstream of piers
 ave unscoured bed level 50.23 m calculated by integration of measured 2018 bottom levels
 min unscoured bed level 48.82 m
 ave normal river level 50.98 m based on LiDAR data
 median bed material size d50 150 mm From geotech observations
 median bed material size d50a 450 mm assuming d50 = d50a /3 based on Hutt River samples as a rough guide

floodplain dimensions ignore - assume all goes through bridge, none over floodplain
 left bank width m
 left bank level m
 right bank width m
 right bank level m

floodplain velocity factor not used in this case

main channel dimensions
 effective channel width 113.77 m

pier dimensions
 piers supported on 3m diameter concrete reinforced cylinder
 pile cap foundation level 45 m
 pile cap top level 48 m
 pier width b 4.00 m
 pile cap width b* 14.00 m

pier length l 10.00 m
 pile dia Dp 3 m One 14m x 14m pile cap supported by four 3m dia piers at 10m centres
 pile spacing Sp 10.00 m Sp/Dp 3.333333

Local Pier Scour - from general scour

Theta = 14 °

ARI (years)	Flow (m3/s)	ave yms (m)	Stage (m MSL)	gen sc lev	local scour case Fig 6.15	Fig 6.15 Y (m)	Eq 6.8 bequiv (m)	bequiv / y	Eq 6.4 depth size factor Kyb	Fig 6.6 Eq 6.6 flow intens factor Ki	be/d50	Eq 6.7 sed size factor Kd	Table 6.3 shape factor Ks	Eq 6.10 alignment factor Ktheta	time factor Kt	ds (m)	yts + ds (m)	Stage (m MSL)	loc sc lev (m MSL)
100 + CC	3593	8.17	57.48	49.31	II	1.31	4.00	0.489	9.60	0.607	26.67	1.000	1.00	1.34	1.00	7.83	16.00	57.48	41.48
2500+CC	5711	10.77	59.15	48.38	II	0.38	4.00	0.371	9.60	0.724	26.67	1.000	1.00	1.34	1.00	9.34	20.11	59.15	39.04

flow intensity factor calculations

ARI (years)	d50	dmax	d50a	Fig 3.5 u*c	= yts y	y/d50	Vc	Fig 3.5 u*ca	y/d50a	Vca	Va	V	vel para	Ki	V/Vc	bequiv/V	y/bequiv	Eq 6.14 te (days)	t (days)	t/te	Kt
100 + CC	150		450	0.374	8.17	54.5	5.324	0.647	18.2	7.447	5.958	3.864	0.607	0.607	0.726	1.035	2.04	12.46	1	0.080	0.80
2500+CC	150		450	0.374	10.77	71.8	5.581	0.647	23.9	7.893	6.315	4.774	0.724	0.724	0.855	0.838	2.69	15.10	1	0.066	0.83

Local Pier Scour - from thalweg scour

Theta = 14 °

ARI (years)	Flow (m3/s)	ave yts (m)	Stage (m MSL)	gen sc lev	local scour case Fig 6.15	Fig 6.15 Y (m)	Eq 6.8 bequiv (m)	bequiv / y	Eq 6.4 depth size factor Kyb	Fig 6.6 Eq 6.6 flow intens factor Ki	be/d50	Eq 6.7 sed size factor Kd	Table 6.3 shape factor Ks	Eq 6.10 alignment factor Ktheta	time factor Kt	ds (m)	yts + ds (m)	Stage (m MSL)	loc sc lev (m MSL)
100 + CC	3593	10.38	57.48	47.10	III	-0.90	10.11	0.974	20.49	0.706	67.41	1.000	1.00	1.34	1.00	19.44	29.82	57.48	27.66
2500+CC	5711	13.68	59.15	45.47	III	-2.53	9.97	0.729	23.36	0.846	66.48	1.000	1.00	1.34	1.00	26.54	40.22	59.15	18.93

flow intensity factor calculations

ARI (years)	d50	dmax	d50a	Fig 3.5 u*c	= yts y	y/d50	Vc	Fig 3.5 u*ca	y/d50a	Vca	Va	V	vel para	Ki	V/Vc	bequiv/V	y/bequiv	Eq 6.14 te (days)	t (days)	t/te	Kt
100 + CC	150		450	0.374	10.38	69.2	5.547	0.647	23.1	7.834	6.267	4.637	0.706	0.706	0.836	2.181	1.03	29.56	1	0.034	0.75
2500+CC	150		450	0.374	13.68	91.2	5.804	0.647	30.4	8.279	6.623	5.729	0.846	0.846	0.987	1.741	1.37	34.15	1	0.029	0.79

Note: V increased by 20% to account for higher local velocities at thalweg location

Te Ahu a Turanga Manawatu Tararua Highway - VE002 Pier 3 Scour

Ref: Melville and Coleman (2000)

channel width W 113.77 Measured at 9m upstream of piers
 ave unscoured bed level 50.23 m calculated by integration of measured 2018 bottom levels
 min unscoured bed level 48.82 m
 ave normal river level 50.98 m based on LiDAR data
 median bed material size d50 150 mm From geotech observations
 median bed material size d50a 450 mm assuming d50 = d50a /3 based on Hutt River samples as a rough guide

floodplain dimensions ignore - assume all goes through bridge, none over floodplain
 left bank width m
 left bank level m
 right bank width m
 right bank level m

floodplain velocity factor not used in this case

main channel dimensions
 effective channel width 113.77 m

pier dimensions
 piers supported on 3m diameter concrete reinforced cylinder
 pile cap foundation level 55 m
 pile cap top level 58 m
 pier width b 4.00 m
 pile cap width b* 14.00 m

pier length l 10.00 m
 pile dia Dp 3 m One 14m x 14m pile cap supported by four 3m dia piers at 10m centres
 pile spacing Sp 10.00 m Sp/Dp 3.333333

Local Pier Scour - reduced general scour

Theta = 0 °

ARI (years)	Flow (m3/s)	ave yms (m)	Stage (m MSL)	gen sc lev	local scour case Fig 6.15	Fig 6.15 Y (m)	Eq 6.8 bequiv (m)	bequiv / y	Eq 6.4 depth size factor Kyb	Eq 6.6 flow intens factor Ki	be/d50	Eq 6.7 sed size factor Kd	Table 6.3 shape factor Ks	Eq 6.10 alignment factor Ktheta	time factor Kt	ds (m)	yts + ds (m)	Stage (m MSL)	loc sc lev (m MSL)
100 + CC	3593	-0.62	57.48	58.10	Outside flow area & failure plane -> NO PIER SCOUR										0.00	-0.62	57.48	58.10	
2500+CC	5711	1.05	59.15	58.10	Outside flow area & failure plane -> NO PIER SCOUR										0.00	1.05	59.15	58.10	

flow intensity factor calculations

ARI (years)	d50	dmax	d50a	Fig 3.5 u*c	= yts y	y/d50	Vc	Fig 3.5 u*ca	y/d50a	Vca	Va	V	vel para	Ki	V/Vc	bequiv/V	y/bequiv	Eq 6.14 te (days)	t (days)	t/te	Kt
100 + CC	150		450	0.374	-0.62	-4.1	#NUM!	0.647	-1.4	#NUM!	#NUM!	1.500	#NUM!	#NUM!	#NUM!	0.000	#DIV/0!	#DIV/0!	1	#DIV/0!	#NUM!
2500+CC	150		450	0.374	1.05	7.0	3.410	0.647	2.3	4.132	3.306	1.800	0.558	0.558	0.528	0.000	#DIV/0!	#DIV/0!	1	#DIV/0!	#DIV/0!

Note: Used max V at right edge of main channel instead of average approach flow velocity for calc

Te Ahu a Turanga Manawatu Tararua Highway - VE002 Pier 1 Debris Scour

Ref: Melville and Coleman (2000)

channel width W 113.77 Measured at 9m upstream of piers
 ave unscoured bed level 50.23 m calculated by integration of measured 2018 bottom levels
 min unscoured bed level 48.82 m
 ave normal river level 50.98 m based on LiDAR data
 median bed material size d50 150 mm From geotech observations
 median bed material size d50a 450 mm assuming d50 = d50a /3 based on Hutt River samples as a rough guide

floodplain dimensions
 left bank width m ignore - assume all goes through bridge, none over floodplain
 left bank level m
 right bank width m
 right bank level m

floodplain velocity factor not used in this case

main channel dimensions
 effective channel width 113.77 m

pier dimensions
 piers supported on 3m diameter concrete reinforced cylinder
 pile cap foundation level 55 m
 pile cap top level 58 m
 pier width b 4.00 m
 pile cap width b* 14.00 m

pier length l 10.00 m Treat set of piers as one supported by four 3m piles at 6.0m centres
 pile dia Dp 3 m
 pile spacing Sp 10.00 m Sp/Dp 3.333333

debris raft information (refer Section 2.3.5 in NZTA's "Bridge Manual")
 max raft thickness (T) 3 m
 length of raft upstream of pier (L) 30 m
 raft width (W) 30 m
 Kd1 0.79
 Kd2 -0.79

Local Pier Debris Scour - from general scour

ARI (years)	Flow (m3/s)	ave yms (m)	Stage (m MSL)	gen sc lev	local scour case	Fig 6.15 Y (m)	Eq 6.8 bequiv (m)	Sect 2.3.5 NZTA BM bequiv (m)	Eq 6.4 bequiv / y	Fig 6.6 Eq 6.6 depth size factor Kyb	flow intens factor Ki	Eq 6.7 be/d50	Table 6.3 sed size factor Kd	Eq 6.10 shape factor Ks	alignment factor Ktheta	time factor Kt	ds (m)	yts + ds (m)	Stage (m MSL)	loc sc lev (m MSL)
100 + CC	3593	2.48	57.48	55.00	III	-3.00	14.31	4.07	5.771	11.16	0.308	95.42	1.000	1.00	0.98	1.00	3.37	5.85	57.48	51.63
2500+CC	5711	4.15	59.15	55.00	III	-3.00	13.42	4.90	3.235	14.93	0.301	89.49	1.000	1.00	0.98	1.00	4.40	8.55	59.15	50.60

Note: Used bequiv from Eq 6.8 instead of pier width to account for complex foundation in Section 2.3.5 NZTA BM

flow intensity factor calculations

ARI (years)	d50	dmax	d50a	Fig 3.5 u*c	= yts y	y/d50	Vc	Fig 3.5 u*ca	y/d50a	Vca	Va	V	vel para	Ki	V/Vc	bequiv/V	y/bequiv	Eq 6.14 te (days)	t (days)	t/te	Kt
100 + CC	150		450	0.374	2.48	16.5	4.212	0.647	5.5	5.521	4.416	1.500	0.308	0.308	0.356	9.542	0.17	-8.34	1	-0.120	#NUM!
2500+CC	150		450	0.374	4.15	27.7	4.692	0.647	9.2	6.352	5.082	1.800	0.301	0.301	0.384	7.458	0.31	-2.81	1	-0.356	#NUM!

Note: Used max V at left edge of main channel instead of average approach flow velocity for calc

Te Ahu a Turanga Manawatu Tararua Highway - VE002 Pier 2 Debris Scour

Ref: Melville and Coleman (2000)

channel width W 113.77 Measured at 9m upstream of piers
 ave unscoured bed level 50.23 m calculated by integration of measured 2018 bottom levels
 min unscoured bed level 48.82 m
 ave normal river level 50.98 m based on LiDAR data
 median bed material size d50 150 mm From geotech observations
 median bed material size d50a 450 mm assuming d50 = d50a /3 based on Hutt River samples as a rough guide

floodplain dimensions
 left bank width m ignore - assume all goes through bridge, none over floodplain
 left bank level m
 right bank width m
 right bank level m

floodplain velocity factor not used in this case

main channel dimensions
 effective channel width 113.77 m

pier dimensions
 piers supported on 3m diameter concrete reinforced cylinder
 pile cap foundation level 46.64 m
 pile cap top level 49.64 m
 pier width b 4.00 m
 pile cap width b* 14.00 m

pier length l 10.00 m Treat set of piers as one supported by four 3m piles at 6.0m centres
 pile dia Dp 3 m
 pile spacing Sp 10.00 m Sp/Dp 3.333333

debris raft information (refer Section 2.3.5 in NZTA's "Bridge Manual")
 max raft thickness (T) 3 m
 length of raft upstream of pier (L) 30 m
 raft width (W) 30 m
 Kd1 0.79
 Kd2 -0.79

Local Pier Debris Scour - from general scour

Theta = 14 °

ARI (years)	Flow (m3/s)	ave yms (m)	Stage (m)	gen sc lev	local scour case Fig 6.15	Fig 6.15 Y (m)	Eq 6.8 bequiv (m)	Sect 2.3.5 NZTA BM bequiv (m)	bequiv / y	Eq 6.4 depth size factor Kyb	Fig 6.6 Eq 6.6 flow intens factor Ki	be/d50	Eq 6.7 sed size factor Kd	Table 6.3 shape factor Ks	Eq 6.10 alignment factor Ktheta	time factor Kt	ds (m)	yts + ds (m)	Stage (m)	loc sc lev (m)
100 + CC	3593	8.17	57.48	49.31	III	-0.33	10.46	10.54	1.290	18.57	0.607	70.29	1.000	1.00	1.34	1.00	15.13	23.31	57.48	34.17
2500+CC	5711	10.77	59.15	48.38	III	-1.26	10.16	10.86	1.009	21.63	0.724	72.42	1.000	1.00	1.34	1.00	21.04	31.81	59.15	27.34

Note: Used bequiv from Eq 6.8 instead of pier width to account for complex foundation in Section 2.3.5 NZTA BM

flow intensity factor calculations

ARI (years)	d50	dmax	d50a	Fig 3.5 u*c	= yts y	y/d50	Vc	Fig 3.5 u*ca	y/d50a	Vca	Va	V	vel para	Ki	V/Vc	bequiv/V	y/bequiv	Eq 6.14 te (days)	t (days)	t/te	Kt
100 + CC	150		450	0.374	8.17	54.5	5.324	0.647	18.2	7.447	5.958	3.864	0.607	0.607	0.726	2.729	0.78	25.77	1	0.039	0.72
2500+CC	150		450	0.374	10.77	71.8	5.581	0.647	23.9	7.893	6.315	4.774	0.724	0.724	0.855	2.276	0.99	31.94	1	0.031	0.75

Local Pier Debris Scour - from thalweg scour

Theta = 14 °

ARI (years)	Flow (m3/s)	ave yts (m)	Stage (m)	gen sc lev	local scour case Fig 6.15	Fig 6.15 Y (m)	Eq 6.8 bequiv (m)	Sect 2.3.5 NZTA BM bequiv (m)	bequiv / y	Eq 6.4 depth size factor Kyb	Fig 6.6 Eq 6.6 flow intens factor Ki	be/d50	Eq 6.7 sed size factor Kd	Table 6.3 shape factor Ks	Eq 6.10 alignment factor Ktheta	time factor Kt	ds (m)	yts + ds (m)	Stage (m)	loc sc lev (m)
100 + CC	3593	10.38	57.480	47.10	III	-2.54	10.78	11.28	1.087	27.08	0.706	75.22	1.000	1.00	1.34	1.00	25.69	36.07	57.48	21.41
2500+CC	5711	13.68	59.150	45.47	III	-4.17	10.56	11.53	0.843	27.67	0.846	76.86	1.000	1.00	1.34	1.00	31.44	45.12	59.15	14.03

Note: Used bequiv from Eq 6.8 instead of pier width to account for complex foundation in Section 2.3.5 NZTA BM

flow intensity factor calculations

ARI (years)	d50	dmax	d50a	Fig 3.5 u*c	= yts y	y/d50	Vc	Fig 3.5 u*ca	y/d50a	Vca	Va	V	vel para	Ki	V/Vc	bequiv/V	y/bequiv	Eq 6.14 te (days)	t (days)	t/te	Kt
100 + CC	150		450	0.374	10.38	69.2	5.547	0.647	23.1	7.834	6.267	4.637	0.706	0.706	0.836	2.433	0.92	32.09	1	0.031	0.75
2500+CC	150		450	0.374	13.68	91.2	5.804	0.647	30.4	8.279	6.623	5.729	0.846	0.846	0.987	2.012	1.19	38.08	1	0.026	0.78

Note: V increased by 20% to account for higher local velocities at thalweg location

Te Ahu a Turanga Manawatu Tararua Highway - VE002 Pier 3 Debris Scour

Ref: Melville and Coleman (2000)

channel width W 113.77 Measured at 9m upstream of piers
 ave unscoured bed level 50.23 m calculated by integration of measured 2018 bottom levels
 min unscoured bed level 48.82 m
 ave normal river level 50.98 m based on LiDAR data
 median bed material size d50 150 mm From geotech observations
 median bed material size d50a 450 mm assuming d50 = d50a /3 based on Hutt River samples as a rough guide

floodplain dimensions
 left bank width m ignore - assume all goes through bridge, none over floodplain
 left bank level m
 right bank width m
 right bank level m

floodplain velocity factor not used in this case

main channel dimensions
 effective channel width 113.77 m

pier dimensions
 piers supported on 3m diameter concrete reinforced cylinder
 pile cap foundation level 55 m
 pile cap top level 58 m
 pier width b 4.00 m
 pile cap width b* 14.00 m

pier length l 10.00 m Treat set of piers as one supported by four 3m piles at 6.0m centres
 pile dia Dp 3 m
 pile spacing Sp 10.00 m Sp/Dp 3.333333

debris raft information (refer Section 2.3.5 in NZTA's "Bridge Manual")
 max raft thickness (T) 3 m
 length of raft upstream of pier (L) 30 m
 raft width (W) 30 m
 Kd1 0.79
 Kd2 -0.79

Local Pier Debris Scour - from general scour

ARI (years)	Flow (m3/s)	ave yms (m)	Stage (m)	gen sc lev	local scour case	Fig 6.15 Y (m)	Eq 6.8 bequiv (m)	Sect 2.3.5 NZTA BM bequiv (m)	Eq 6.4 bequiv / y	Fig 6.6 Eq 6.6 depth factor Kyb	Fig 6.6 Eq 6.6 flow intens factor Ki	Eq 6.7 be/d50	Table 6.3 sed size factor Kd	Eq 6.10 shape factor Ks	alignment factor Ktheta	time factor Kt	ds (m)	yts + ds (m)	Stage (m)	loc sc lev (m)
100 + CC	3593	-0.62	57.48	58.10	Outside flow area & failure plane -> NO PIER SCOUR												0.00	-0.62	57.48	58.10
2500+CC	5711	1.05	59.15	58.10	Outside flow area & failure plane -> NO PIER SCOUR												0.00	1.05	59.15	58.10

Note: Used bequiv from Eq 6.8 instead of pier width to account for complex foundation in Section 2.3.5 NZTA BM

flow intensity factor calculations

ARI (years)	d50	dmax	d50a	Fig 3.5 u*c	= yts y	y/d50	Vc	Fig 3.5 u*ca	y/d50a	Vca	Va	V	vel para	Ki	V/Vc	bequiv/V	y/bequiv	Eq 6.14 te (days)	t (days)	t/te	Kt
100 + CC	150		450	0.374	-0.62	-4.1	#NUM!	0.647	-1.4	#NUM!	#NUM!	1.500	#NUM!	#NUM!	#NUM!	0.000	#DIV/0!	#DIV/0!	1	#DIV/0!	#NUM!
2500+CC	150		450	0.374	1.05	7.0	3.410	0.647	2.3	4.132	3.306	1.800	0.558	0.558	0.528	0.000	#DIV/0!	#DIV/0!	1	#DIV/0!	#DIV/0!

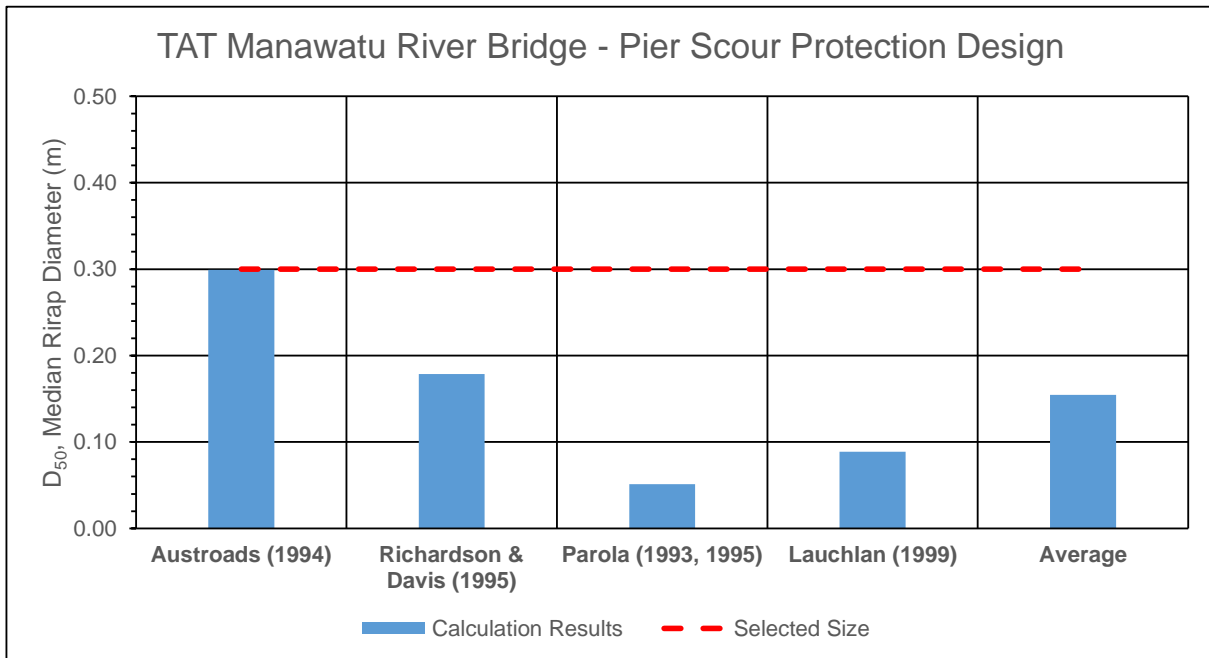
Note: Used max V at left edge of main channel instead of average approach flow velocity for calc

Project: Te Ahu a Turanga Manawatu Tararua Highway - Pier 1
 Project No: 5-C3567.00 / 3000

Date: 9/10/2019

Created by Franciscus Maas

d _{r50} , Median Riprap Diameter (m)				
Austrroads (1994)	Richardson & Davis (1995)	Parola (1993, 1995)	Lauchlan (1999)	Average
0.299	0.179	0.051	0.089	0.154



Project: Te Ahu a Turanga Manawatu Tararua Highway - Pier 1
 Project No: 5-C3567.00 / 3000

Date 9/10/2019

Created by Franciscus Maas
 Method: Austroads (1994)

Input data: SDF (1100m3/s)

g 9.81 m/s²
 S_s 2.65 Specific gravity of rock
 V_{approach} 1.00 m/s

$$\frac{d_{r50}}{y} = \frac{0.58K_p K_v}{(S_s - 1)} Fr^2$$

y 4.30 m Water Depth

K_p 2.89 Rectangular pier

K_v 2.89 Pier in the middle of a straight diverging flow

Output data:

Safety factor	Fr	d _{r50}
1	0.154	0.299
1.2	0.154	0.359

K_p = factor for pier shape; K_p = 2.25 (round-nose), 2.89 (rectangular)

K_v = velocity factor, varying from 0.81 for a pier near the bank of a straight channel to 2.89 for a pier at the outside of a bend in the main channel

Project: Te Ahu a Turanga Manawatu Tararua Highway - Pier 1 Date 9/10/2019
 Project No: 5-C3567.00 / 3000
 Created by Franciscus Maas
 Method: Richardson & Davis (1995)

Input data: SDF (1100m3/s)

g	9.81 m/s ²		$\frac{d_{r50}}{y} = \frac{0.346 f_1^2 f_2^2}{(S_s - 1)} Fr^2$
S _s	2.65	Specific gravity of rock	
V _{approach}	1.00 m/s	Velocity in thalweg	
y	4.30 m	Water Depth	
f ₁	1.7	Rectangular pier	
f ₂	1.7	Pier in the middle of a straight diverging flow	

Output data:

Safety factor	Fr	dr ₅₀	<i>f</i> ₁ = factor for pier shape; <i>f</i> ₁ = 1.5 (round-nose), 1.7 (rectangular) <i>f</i> ₂ = factor ranging from 0.9 for a pier near the bank in a straight reach to 1.7 for a pier in the main current at a bend
1	0.154	0.179	
1.2	0.154	0.214	

Project: Te Ahu a Turanga Manawatu Tararua Highway - Pier 1
 Project No: 5-C3567.00 / 3000

Date 9/10/2019

Created by Franciscus Maas
 Method: Parola (1993, 1995)

Input data: SDF (1100m3/s)

g	9.81 m/s ²	
S _s	2.65	Specific gravity of rock
V _{approach}	1.00 m/s	Velocity in thalweg
y	4.30 m	Water Depth
b _p	4.00 m	
f ₁	1.00	
f ₃	0.83	

$$\frac{d_{r50}}{y} = \frac{f_1 f_3}{(S_s - 1)} Fr^2$$

b_p = projected width of pier
 f₁ = pier shape factor; f₁ = 1.0 (rectangular), 0.71 (round-nose if aligned)

f₃ = pier size factor = f(b_p/d_{r50}):

$$f_3 = 0.83 \quad 4 < \frac{b_p}{d_{r50}} < 7$$

$$f_3 = 1.0 \quad 7 < \frac{b_p}{d_{r50}} < 14$$

$$f_3 = 1.25 \quad 20 < \frac{b_p}{d_{r50}} < 33$$

Output data:

Safety factor	Fr	dr ₅₀
1	0.154	0.051
1.2	0.154	0.062
1.5	0.154	0.077
2	0.154	0.103

Project: Te Ahu a Turanga Manawatu Tararua Highway - Pier 1
 Project No: 5-C3567.00 / 3000

Date: 9/10/2019

Created by Franciscus Maas
 Method: Lauchlan (1999)

Input data: SDF (1100m3/s)

g 9.81 m/s²
 S_s 2.65 Specific gravity of rock
 V_{approach} 1.00 m/s Velocity in thalweg

$$\frac{d_{r50}}{y} = 0.3S_f \left(1 - \frac{Y_r}{y}\right)^{2.75} Fr^{1.2}$$

y 4.30 m Water Depth

S_f = safety factor, with a minimum recommended value = 1.1
 Y_r = placement depth below bed level

Output data:

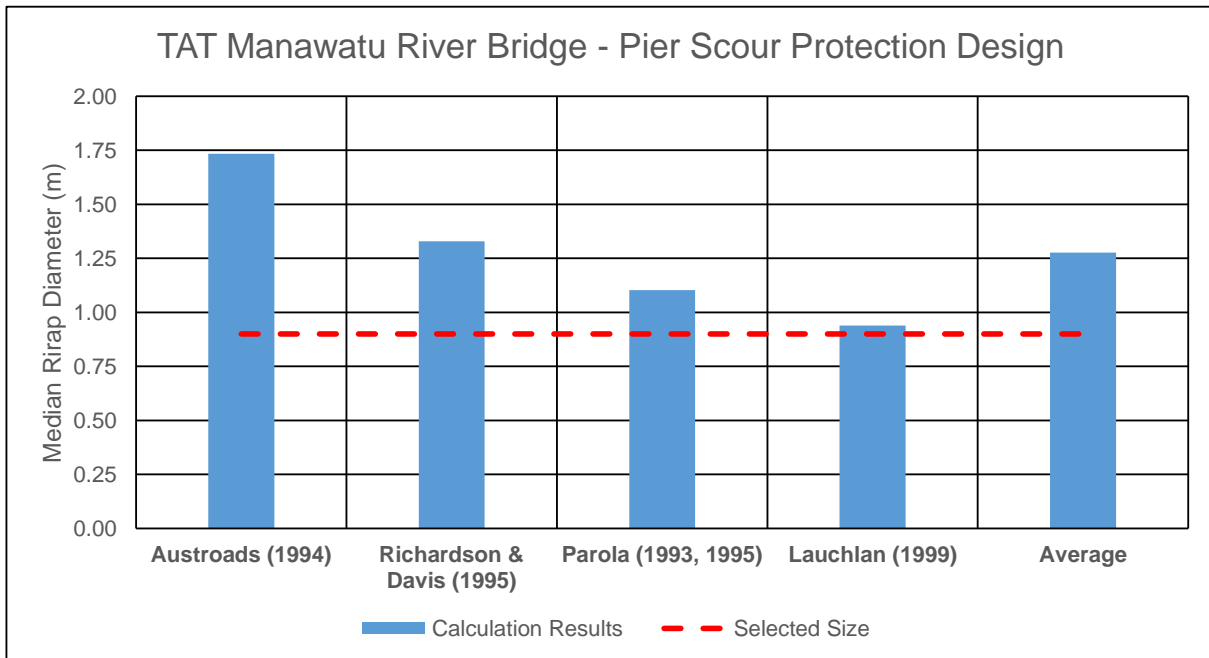
Safety Factor	Y_r (m)	Fr	d_{r50}
1.1	0	0.154	0.150
1.2	0	0.154	0.164
1.1	0.25	0.154	0.127
1.2	0.25	0.154	0.139
1.1	0.5	0.154	0.107
1.2	0.5	0.154	0.117
1.1	0.75	0.154	0.089
1.2	0.75	0.154	0.097
1.1	1	0.154	0.073
1.2	1	0.154	0.079
1.1	1.25	0.154	0.058
1.2	1.25	0.154	0.064
1.1	1.5	0.154	0.046
1.2	1.5	0.154	0.050
1.1	1.75	0.154	0.036
1.2	1.75	0.154	0.039
1.1	2	0.154	0.027
1.2	2	0.154	0.029

Project: Te Ahu a Turanga Manawatu Tararua Highway - Pier 2
 Project No: 5-C3567.00 / 2000

Date: 2/04/2019

Created by Franciscus Maas

d _{r50} , Median Riprap Diameter (m)				
Austrroads (1994)	Richardson & Davis (1995)	Parola (1993, 1995)	Lauchlan (1999)	Average
1.734	1.328	1.103	0.940	1.276



Project: Te Ahu a Turanga Manawatu Tararua Highway - Pier 2
 Project No: 5-C3567.00 / 2000

Date 2/04/2019

Created by Franciscus Maas
 Method: Austroads (1994)

Input data: SDF (1100m3/s)

g 9.81 m/s²
 S_s 2.65 Specific gravity of rock
 V_{approach} 4.64 m/s Velocity in thalweg

$$\frac{d_{r50}}{y} = \frac{0.58K_p K_v}{(S_s - 1)} Fr^2$$

y 8.17 m Water Depth

K_p 2.25 Cylindrical piers

K_v 1 Pier in the middle of a straight diverging flow

Output data:

Safety factor	Fr	d _{r50}
1	0.518	1.734
1.2	0.518	2.080

K_p = factor for pier shape; K_p = 2.25 (round-nose), 2.89 (rectangular)

K_v = velocity factor, varying from 0.81 for a pier near the bank of a straight channel to 2.89 for a pier at the outside of a bend in the main channel

Project: Te Ahu a Turanga Manawatu Tararua Highway - Pier 2 Date 2/04/2019
 Project No: 5-C3567.00 / 2000
 Created by Franciscus Maas
 Method: Richardson & Davis (1995)

Input data: SDF (1100m3/s)

g 9.81 m/s²
 S_s 2.65 Specific gravity of rock
 V_{approach} 4.64 m/s Velocity in thalweg
 y 8.17 m Water Depth
 f₁ 1.7 Cylindrical pier
 f₂ 1 Pier in the middle of a straight diverging flow

$$\frac{d_{r50}}{y} = \frac{0.346 f_1^2 f_2^2}{(S_s - 1)} Fr^2$$

Output data:

Safety factor	Fr	dr ₅₀
1	0.518	1.328
1.2	0.518	1.594

f₁ = factor for pier shape; f₁ = 1.5 (round-nose), 1.7 (rectangular)
 f₂ = factor ranging from 0.9 for a pier near the bank in a straight reach to 1.7 for a pier in the main current at a bend

Project: Te Ahu a Turanga Manawatu Tararua Highway - Pier 2
 Project No: 5-C3567.00 / 2000

Date 2/04/2019

Created by Franciscus Maas
 Method: Parola (1993, 1995)

Input data: SDF (1100m³/s)

g	9.81 m/s ²	
S _s	2.65	Specific gravity of rock
V _{approach}	4.64 m/s	Velocity in thalweg
y	8.17 m	Water Depth
b _p	1.00 m	
f ₁	1.00	
f ₃	0.83	

$$\frac{d_{r50}}{y} = \frac{f_1 f_3}{(S_s - 1)} Fr^2$$

b_p = projected width of pier
 f₁ = pier shape factor; f₁ = 1.0 (rectangular), 0.71 (round-nose if aligned)

f₃ = pier size factor = f(b_p/d_{r50}):

$$f_3 = 0.83 \quad 4 < \frac{b_p}{d_{r50}} < 7$$

$$f_3 = 1.0 \quad 7 < \frac{b_p}{d_{r50}} < 14$$

$$f_3 = 1.25 \quad 20 < \frac{b_p}{d_{r50}} < 33$$

Output data:

Safety factor	Fr	d _{r50}
1	0.518	1.103
1.2	0.518	1.323
1.5	0.518	1.654
2	0.518	2.205

Project: Te Ahu a Turanga Manawatu Tararua Highway - Pier 2
 Project No: 5-C3567.00 / 2000

Date: 2/04/2019

Created by Franciscus Maas
 Method: Lauchlan (1999)

Input data: SDF (1100m3/s)

g 9.81 m/s²
 S_s 2.65 Specific gravity of rock
 V_{approach} 4.64 m/s Velocity in thalweg

$$\frac{d_{r50}}{y} = 0.3S_f \left(1 - \frac{Y_r}{y}\right)^{2.75} Fr^{1.2}$$

y 8.17 m Water Depth

S_f = safety factor, with a minimum recommended value = 1.1
 Y_r = placement depth below bed level

Output data:

Safety Factor	Y_r (m)	Fr	dr_{50}
1.1	0	0.518	1.224
1.2	0	0.518	1.336
1.1	0.25	0.518	1.124
1.2	0.25	0.518	1.226
1.1	0.5	0.518	1.029
1.2	0.5	0.518	1.123
1.1	0.75	0.518	0.940
1.2	0.75	0.518	1.025
1.1	1	0.518	0.855
1.2	1	0.518	0.933
1.1	1.25	0.518	0.776
1.2	1.25	0.518	0.846
1.1	1.5	0.518	0.701
1.2	1.5	0.518	0.765
1.1	1.75	0.518	0.631
1.2	1.75	0.518	0.689
1.1	2	0.518	0.566
1.2	2	0.518	0.617

WSP | OPUS

www.wsp-opus.co.nz

Appendix D.4:

*Te Ahu a Turanga - Manawatū Tararua Highway: Mangamanaia
Bridge 2D hydraulic analysis.*

Project Number: 5-C3567.26

Te Ahu a Turanga - Manawatū Tararua Highway

28 February 2020

CONFIDENTIAL



Mangamanaia Bridge 2D Hydraulic Analysis





Contact Details

Courtenay Giles

WSP
L9 Majestic Centre
100 Willis Street
Wellington 6011
+64 4 471 7000

courtenay.giles@wsp.com

Document Details:

Date: November 2019
Reference: 5-C3567.26
Status: DRAFT

Prepared by
Courtenay Giles

Reviewed by
Franciscus Maas

Approved for release by



Document History and Status

Revision	Date	Author	Reviewed by	Approved by	Status
1	17/12/19	C. Giles	F. Maas		DRAFT

Revision Details

Revision	Details





Contents

1	Introduction	1
1.1	Background	1
2	Bridge Design Standards.....	2
2.1	Design Requirements.....	2
2.2	Design Flows.....	2
3	Model Built.....	3
3.1	Software.....	3
3.2	Assumptions.....	3
3.3	Model Extent	3
3.4	Survey.....	4
3.5	Boundary Conditions.....	4
3.6	Roughness	5
3.7	Time Step & Computational Mesh.....	5
4	Comparison to 1D Model.....	6
5	Sensitivity Analysis.....	6
5.1	Existing Situation	6
5.2	Sensitivity Testing.....	9
6	Impact of Proposed Bridge.....	9
6.1	Proposed Bridge Schematisation.....	9
6.2	Bridge Terrain.....	11
7	Results.....	12
7.1	Predicted Peak Water Levels	12
7.2	Predicted Flow Velocities.....	15
8	Summary	18
9	References.....	18
	Appendix A - Roughness Estimation.....	19
	Appendix B - Result Maps (10-year and 2500-year ARI)	20



1 Introduction

1.1 Background

The New Zealand Transport Agency (NZTA) identified a preferred option for a new State Highway 3 (SH3) to connect the Manawatū, Tararua District, Hawke's Bay and northern Wairarapa, to replace the closed SH3 Manawatū Gorge route. WSP has been commissioned to undertake a hydraulic analysis of the new Te Ahu a Turanga: Manawatū, Tararua Highway where it crosses the Mangamanaia Stream. The location of this hydraulic analysis is shown in Figure 1-1.

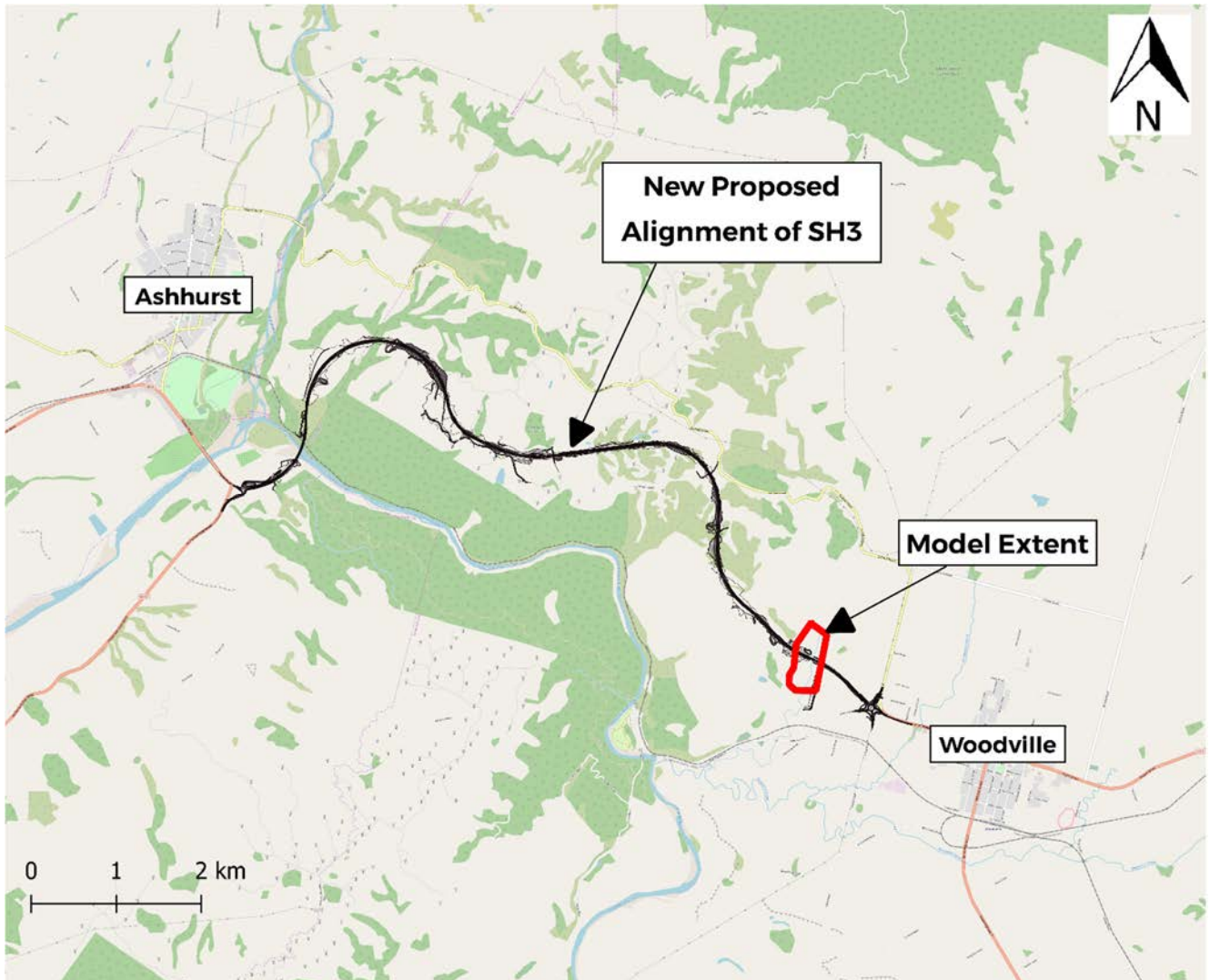


Figure 1-1: Mangamanaia model location

A one-dimensional (1D) HEC-RAS model of the site was built for the initial analysis of the proposed bridge. However, this was deemed to not provide enough detail of the flooding in the floodplain, so a two-dimensional (2D) HEC-RAS model was built. This report details the development of the 2D hydraulic model to be able to assess the location of the bridge and the impacts it will potentially have on the Mangamanaia Stream including its floodplain. The main factors to be estimated are the peak water surface elevations and flow velocities. These will help to understand the likely impact the bridge will have on stream flows. Furthermore, it will provide information to assess if the bridge will meet relevant criteria.

2 Bridge Design Standards

2.1 Design Requirements

The proposed bridge will be designed in accordance with the New Zealand Transport Agency (NZ Transport Agency, 2019) design requirements. This bridge is an importance level 4 with the serviceability limit state (SLS) event being the 100-year annual recurrence interval (ARI) design event and the ultimate limit state (ULS) event being the 2500-year ARI event.

Relevant design criteria provided by NZTA (NZ Transport Agency, 2019) include:

- The detail of all abutment structures and approach embankment shall be acceptable to the Horizons Regional Council;
- It must be demonstrated that the bridge will survive the ULS condition;
- Bridge abutments shall be located a minimum of 5 m outside of the 10-year ARI flood limits or 3 m outside of the top of the gully, whichever is greater;
- Piers shall not be located in the bed of the stream or within 3 m of the streambanks;
- The streambanks are defined as the portion of the channel that confine the winter time low to normal flow. The streambed is defined as the portion of the channel between the banks where terrestrial vegetation is not established;
- The model shall cover a minimum of 200 m of the reach, centred upstream and downstream on the proposed bridge;
- The model shall provide the basis for bridge scour estimates, the design of scour countermeasures, and debris load calculations;
- Debris accumulation and loading shall be accounted for on the Mangamanaia Stream Bridge; and
- The clearance height required between the 10-year water level and the bridge soffit is 4.5 m.

2.2 Design Flows

Design flows were derived for the Mangamanaia Stream (J.A. McConchie, 2019). The design hydrographs produced were used as inputs for the hydraulic model. The peak flow for each of the design events is shown in Table 2-1. These flows are adjusted for climate change up to 2120. The peak flows used for this analysis are significantly larger than the flows provided in the minimum requirements. The 10-year ARI design flow provided by NZ Transport Agency largely remains within the channel, with limited overbank flooding. This is considered unrealistic in New Zealand as bankfull discharge, when the channel reaches capacity and overbank flow occurs, are about a 2.3-year ARI event. This suggests that the NZ Transport Agency design flows are too low. The flows used in this analysis are considered more realistic, although possibly a little high (WSP, 2019).

Table 2-1: Design flows for Mangamanaia Stream accounting for climate change

Design Event (ARI)	NZTA flows adjusted for climate change up to 2090 (m ³ /s)	WSP flows adjusted for climate change up to 2120 (m ³ /s)
2-year	12.0	42.2
10-year	32.0	67.1
50-year	56.0	82.7
100-year (SLS)	68.0	88.4
2500-year (ULS)	93.0	127.0

3 Model Built

3.1 Software

The hydraulic assessment was carried out using HEC-RAS version 5.0.7 a computational hydraulic modelling software package developed by the United States Army Corps of Engineers (USACE). HEC-RAS is designed to perform one and two-dimensional computational modelling of flow. HEC-RAS is used worldwide for modelling open-channel flow and hydraulic structures through rivers.

3.2 Assumptions

This hydraulic analysis includes the following assumptions:

- LiDAR resolutions provides adequate representation of the terrain;
- The extent of the model provides enough detail of flooding effects in the floodplain;
- The water depth in the channel was insignificant when the LiDAR was flown so no additional surveyed cross-sections were required; and
- As there is minimal calibration data for the Mangamanaia Stream the model will be the best representation of data available

3.3 Model Extent

Figure 3-1 depicts the extents of the HEC-RAS model. The model covers approximately 700 m of the Mangamanaia stream. The model extends approximately 350 m upstream of the bridge and 350 m downstream of the bridge.

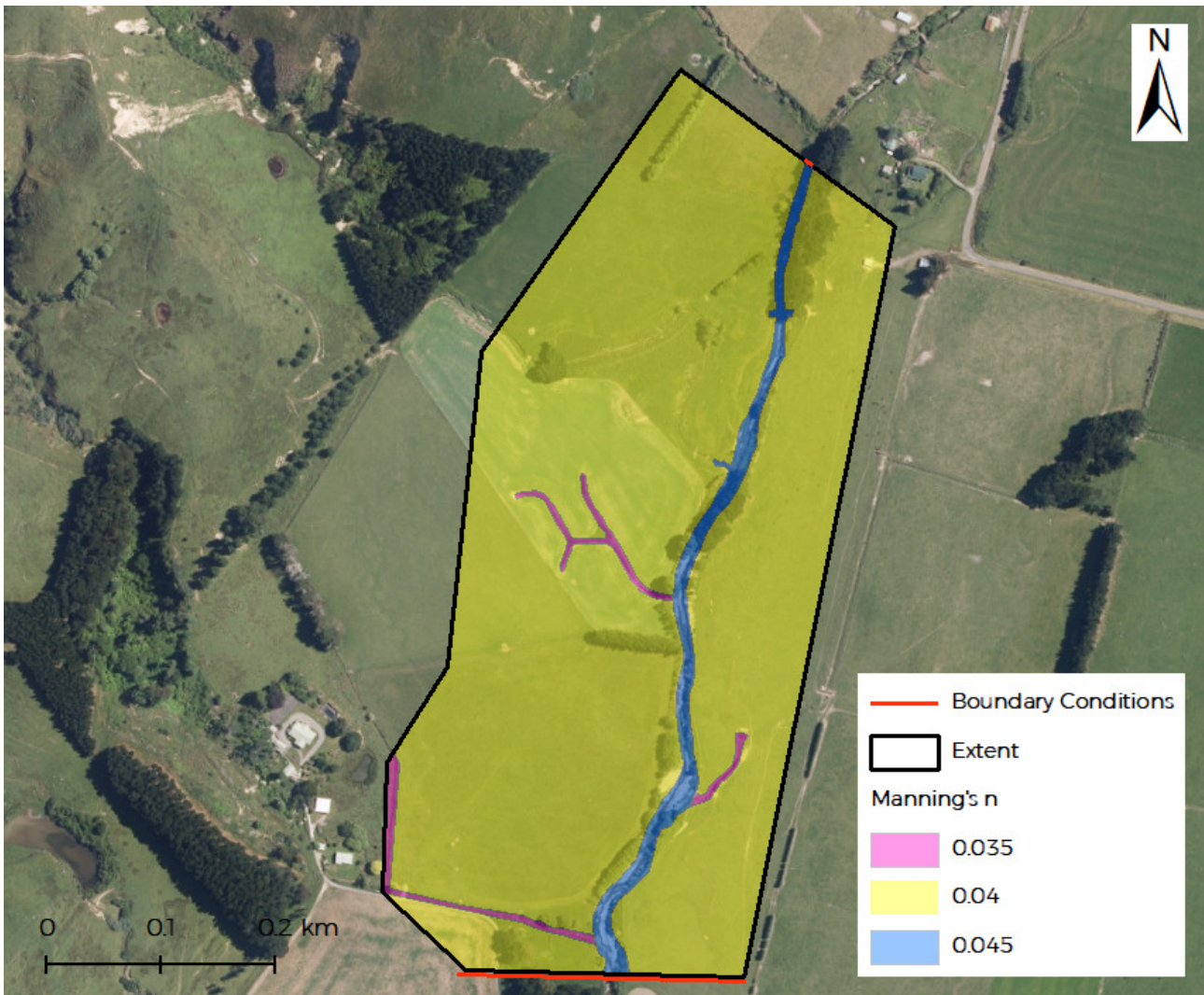


Figure 3-1: Model extent, boundary condition locations and Manning's roughness values

3.4 Survey

LiDAR data was provided by the client. This data includes approximately 1km of the Mangamanaia stream. Therefore, the LiDAR data covers enough distance upstream and downstream of the bridge location to assess the potential impact of the bridge on the stream. A shape file of the current proposed road and bridge location were also provided.

The surveyed data was captured in the following projection and datum:

- NZGD2000 / Wanganui 2000 Projection
- New Zealand Vertical Datum 2016

The bridge design, and therefore the hydraulic computational model and its result are in the same projection and datum.

3.5 Boundary Conditions

The upstream boundary condition used was a flow hydrograph with the peaks for the different design events shown in Table 2-1.

The downstream boundary condition was assumed to be flow at normal depth with a friction slope of 0.7% based on the average channel slope.

3.6 Roughness

A section of the Mangamanaia stream is shown in Figure 3-2. The banks of the Mangamanaia stream are covered in long grasses. The bank appears to be unstable and has collapsed into the stream in some places. Trees are widely spaced along the banks. The river bed is mainly composed of stones and sand.



Figure 3-2: Mangamanaia Stream Bed

The Manning's roughness coefficient (n) was determined with the use of Hicks & Mason (1998) and Chow (1959). The page used from Hicks & Mason is shown in Appendix A – Roughness Estimation. It was deemed that the roughness value in the Mangamanaia would be slightly higher than the river depicted in. This was because of the differences in bed material, size of the channel, slope of the channel and what plant material the banks are composed of. The Manning's value used for the different land covers in the model is shown in Table 3-1 and graphically in Figure 3-1.

Table 3-1: Model Manning's n values based on land cover

Land Cover	Manning's n
Floodplain (Short grass)	0.040
Stream Channel	0.045
Tributary Drain	0.035
Proposed Bridge	0.02

3.7 Time Step & Computational Mesh

Due to instabilities in the model a warm-up period of 16 hours was used. The full momentum (Saint-Venant) equation was used with the time step based on Courant. The minimum Courant is 0.5 and the maximum Courant is 3 (this is the maximum number recommended by HEC-RAS for the full momentum equation). This method allows for the computational time-step to be adjusted based on the cell size and velocity.

For HEC-RAS 2D each cell is a detailed elevation volume/area relationship that represents the details of the underlying terrain. This approach allows larger cell sizes to be used while still accurately representing the terrain (US Army Corps of Engineers, 2016). A single water surface elevation is computed in the centre of each cell. Therefore, as the modelled area is relatively flat, and the water surface slope does not change rapidly a mesh size of 3m x 3m was deemed as appropriate.

4 Comparison to 1D Model

The details of the 1D model build can be found in WSP, 2019.

Differences are to be expected between the 1D and 2D model as the 1D is based off of cross-sections extracted from the terrain. It then interpolates between these cross-sections based on downstream reach lengths. Therefore, this model is less detailed than the 2D model. A long-section comparing the NZTA 100-year ARI + CC for the 1D and 2D model is shown in Figure 4-1. It can be seen that the water level results follow similar trends. However, the main difference in water level between the models happens near the location of the bridge. The 2D model's water level is approximately 0.6m higher than the 1D model.

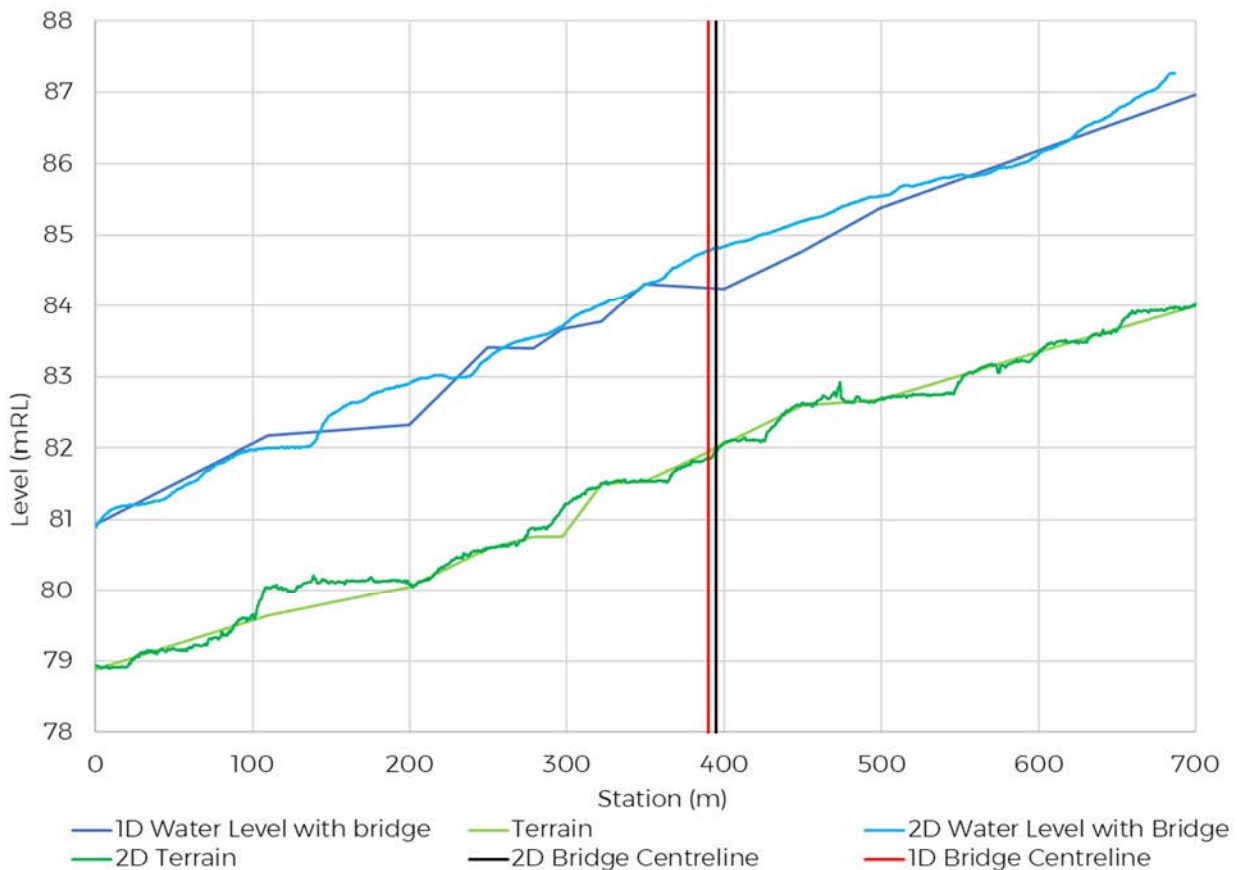


Figure 4-1: Comparison of 1D results to 2D results for NZ Transport Agency, 2019 100-year ARI design flow

5 Sensitivity Analysis

5.1 Existing Situation

This model will provide understanding of how the stream responds to the design flow events with and without the bridge to see the impact of the bridge on stream flow hydraulics. The simulations

that were analysed are the 10-year ARI, 100-year ARI and 2500-year ARI with allowance for climate change to 2120.

The model was first created without the proposed bridge. This was used to analyse the current state of the Mangamanaia Stream. Figure 5-1, shows the water surface elevation results for the 10-year ARI existing scenario and Figure 5-2 shows the stream velocity results for the 10-year ARI existing scenario. The result maps for 100-year ARI and 2500-year ARI can be found in Appendix B.

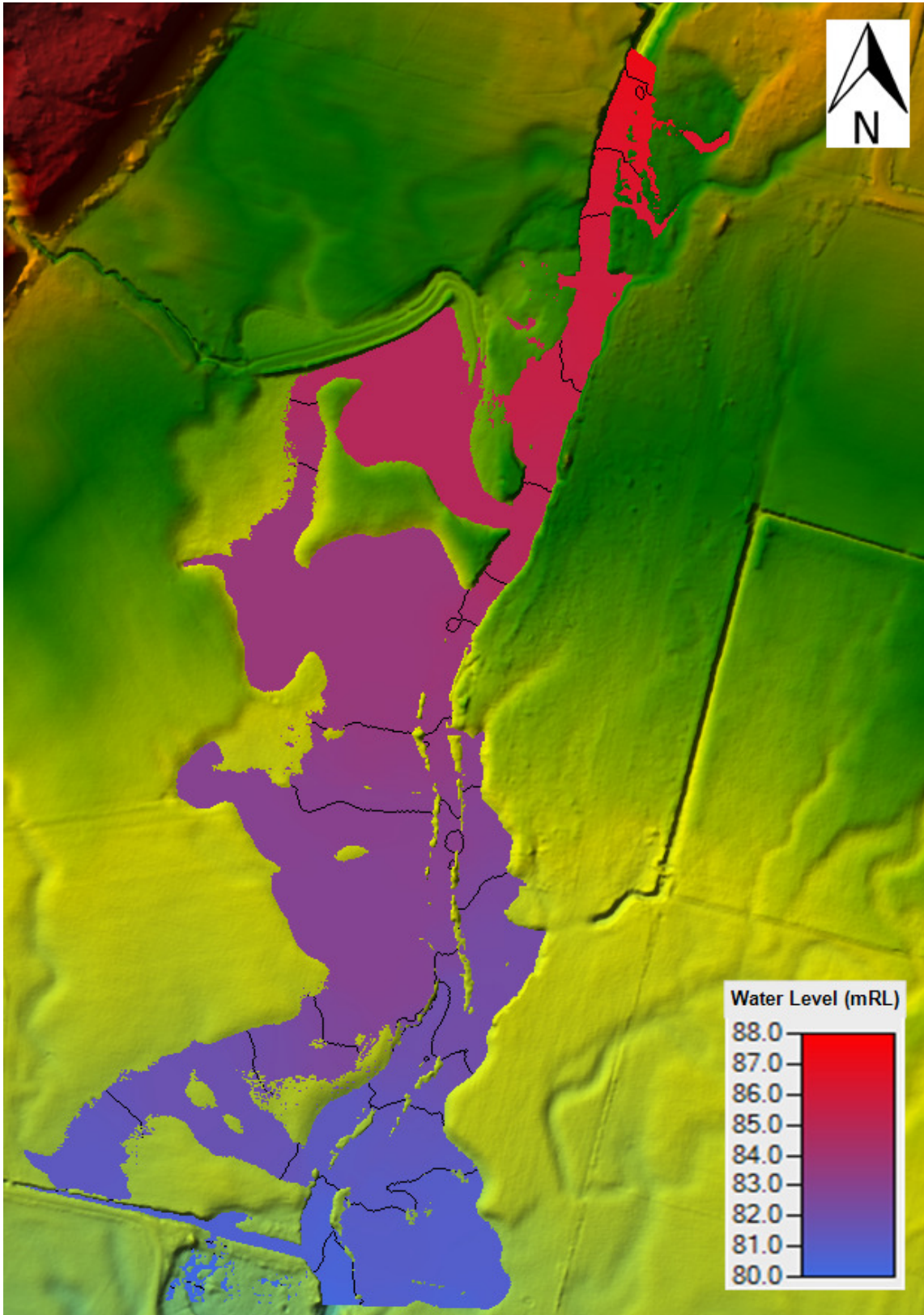


Figure 5-1: 10-year ARI 2120 climate, existing scenario water level results with 0.5 m contours

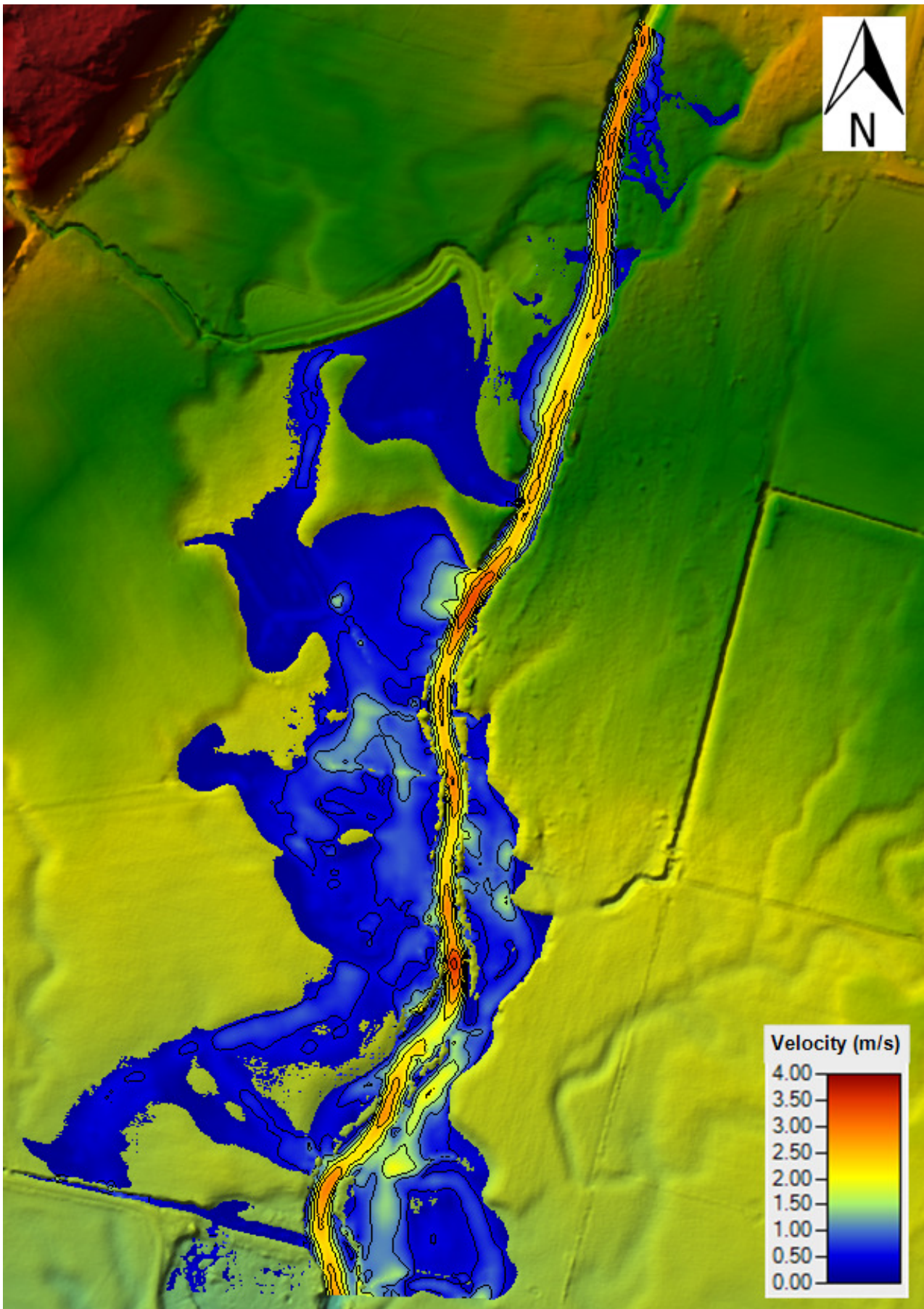


Figure 5-2: 10-year ARI 2120 climate, existing scenario velocity results with 0.5 m/s contours

5.2 Sensitivity Testing

The results in Section 5.1 were used as a baseline to determine the model's sensitivity to Manning's roughness and downstream slope.

The Manning's n used for the model are shown in Table 3-1. To test the model's sensitivity to Manning's these values were increased by 0.005 and decreased by 0.005. Table 5-1 shows the results for running the 100-year ARI flow with different Manning's values. The water depths are taken at the centre-line of the proposed bridge location.

Table 5-1: Manning's n sensitivity analysis

Manning's n	Depth (m)	Difference from Original (m)	% Difference from Original
+0.005	2.50	+0.03	+1.2%
Original	2.47	-	-
-0.005	2.44	-0.03	-1.2%

Therefore, as the difference is minimal it was determined that the roughness of the channel appears to have no significant effect on the results, so the estimation of Manning's values provided in Table 3-1 are adequate.

The friction slope used for the downstream normal depth boundary condition was 0.007. Table 5-2 shows the results for running the 100-year ARI flow with different slopes. The water depths are taken at the proposed bridge centre-line location.

Table 5-2: Slope sensitivity analysis

Slope	Depth (m)	Difference from 0.007 (m)	% Difference from 0.007
0.008	2.47	0.00	0%
0.007	2.47	-	-
0.006	2.47	0.00	0%

Changing the friction slope of the channel resulted in no change to the depth. Therefore, the choice of channel slope at the downstream boundary appears to have no significant effect on the model results, so the estimation of 0.007 is adequate.

6 Impact of Proposed Bridge

6.1 Proposed Bridge Schematisation

The proposed bridge is shown in Figure 6-1 and Figure 6-2.

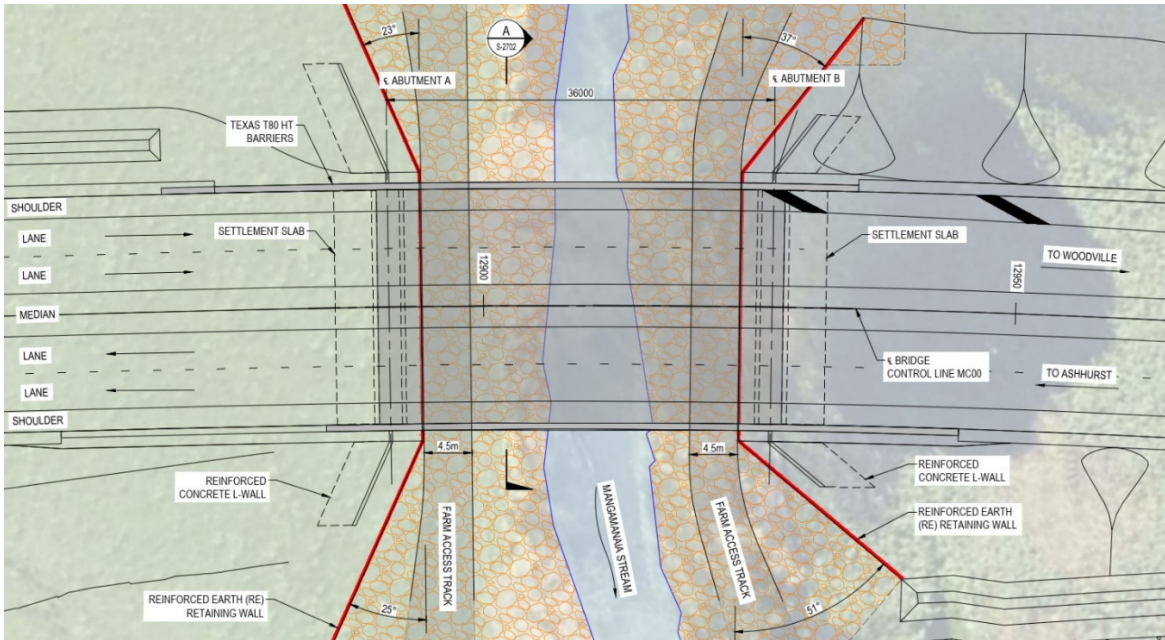


Figure 6-1: Bridge crossing plan

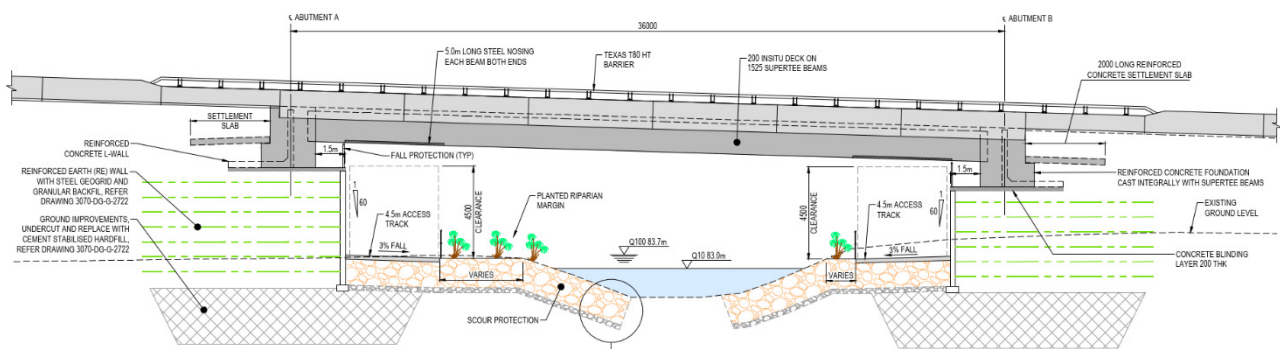


Figure 6-2: Bridge cross-section looking upstream

The defined bridge characteristics are shown in Table 6-1.

Table 6-1: Bridge characteristics

Bridge Characteristics	Value
Required clear width	30.0m
Minimum width of access tracks	4.5m
Buffer strip (between track and stream edge)	Not defined
Minimum clearance (between water level and soffit in 10-year ARI flow)	4.5m
Width	23.0m
Lowest soffit point (left/east abutment)	87.9 m RL
Slope of bridge	3.0%

6.2 Bridge Terrain

It was deemed that the best way to represent the bridge abutments and proposed wetland (located north of the west abutment) in the model was to include them in the terrain. This was done by using the provided shape file of the bridge alignment and bridge levels.

A digital elevation model (DEM) was interpolated using ArcGIS and contours. This DEM was then used in HEC-RAS with the base terrain to generate the bridge terrain shown in Figure 6-3. The bridge soffit level was not included in the model. The terrain between the bridge abutments also had to be adjusted to represent the cross-section shown in Figure 6-2. This was done in a similar way to the abutments and wetland and was also incorporated into the HEC-RAS terrain.

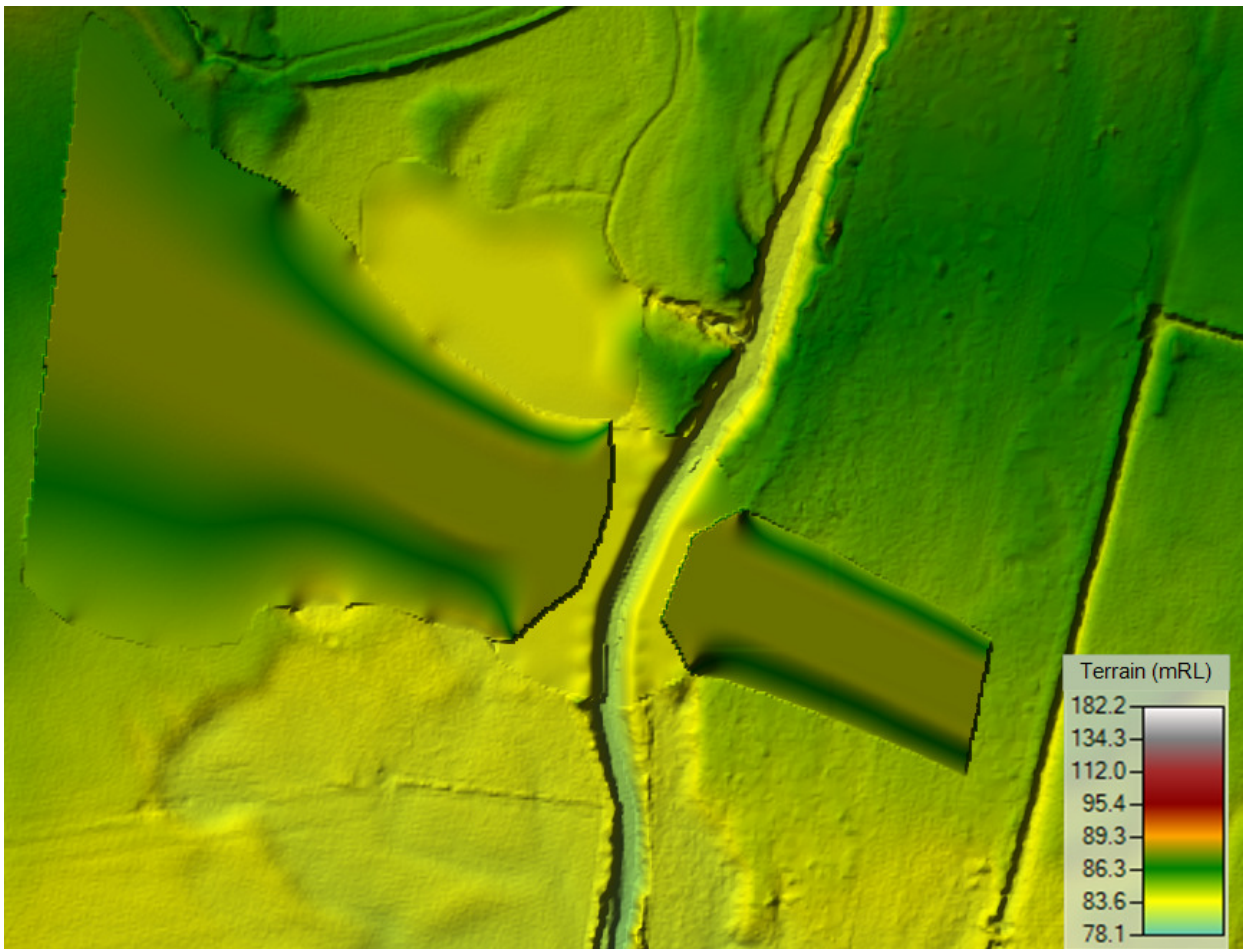


Figure 6-3: Final altered Terrain in HEC-RAS

The Manning's n regions had to be updated for the bridge terrain to account for the new surface type (road). The updated Manning's n values are shown in Figure 6-4.



Figure 6-4: Manning's n regions for bridge terrain

7 Results

7.1 Predicted Peak Water Levels

The predicted peak water levels after the construction of the bridge are shown in Figure 7-1. These results can be compared to Figure 5-1 to see the theoretical impact the bridge will have on water levels in the stream. Figure 7-1 shows that with WSP's higher design flows the design does not meet the minimum requirement of bridge abutments being a minimum of 5 m outside of the 10-year ARI flood extent. However, as stated in Section 2.2, this is considered unrealistic in New Zealand as bankfull discharge, when the channel reaches capacity and overbank flow occurs, is at about a 2.3-year ARI event.

The difference in water level between the existing and the bridge scenario for the 10-year ARI 2120 climate is shown in Figure 7-2. Increases in water level as a result of the construction of the road and bridge are shown in red and pink, whereas decreases are shown in green.

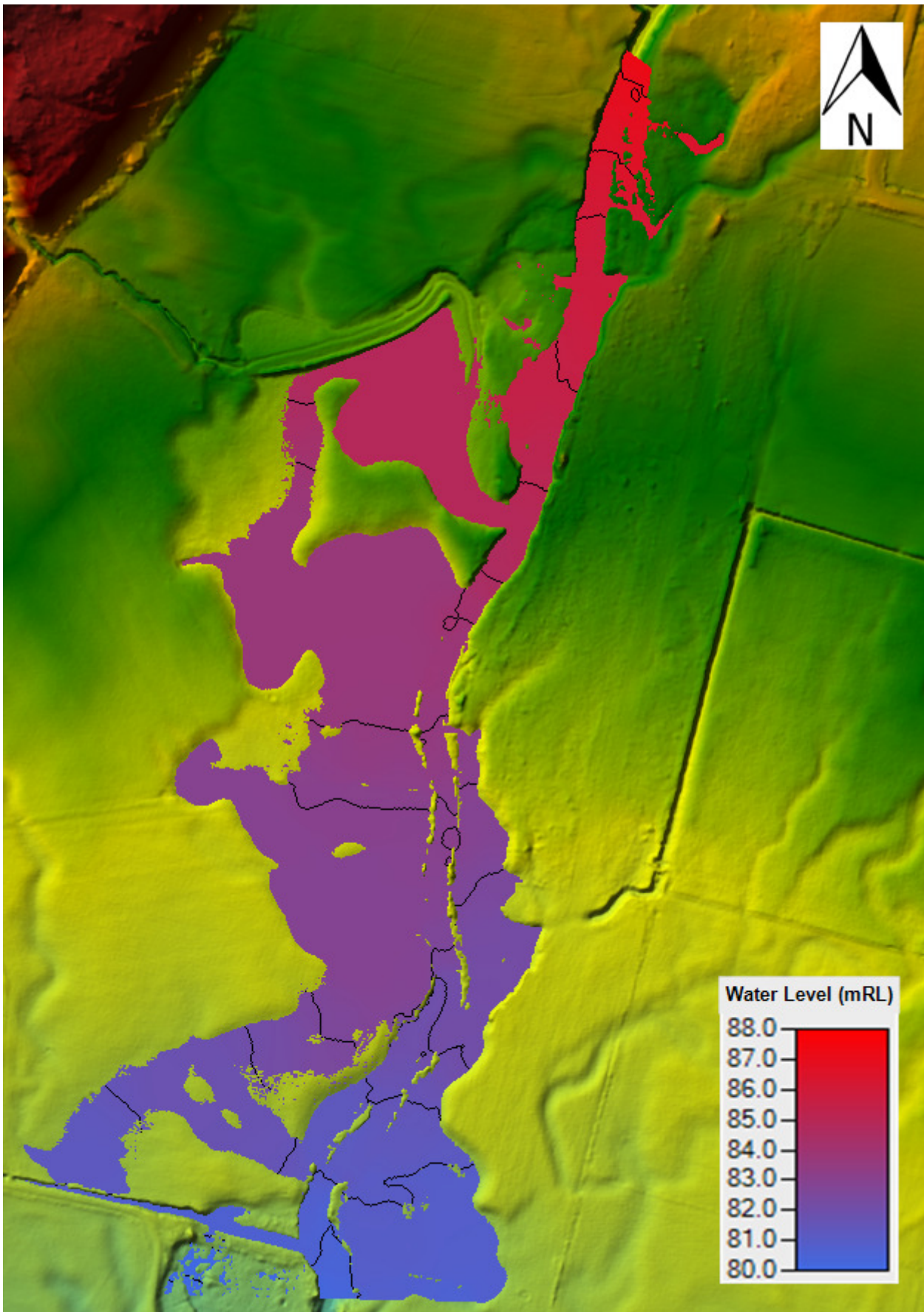


Figure 7-1: 10-year ARI proposed bridge water level results with 0.5 m contours

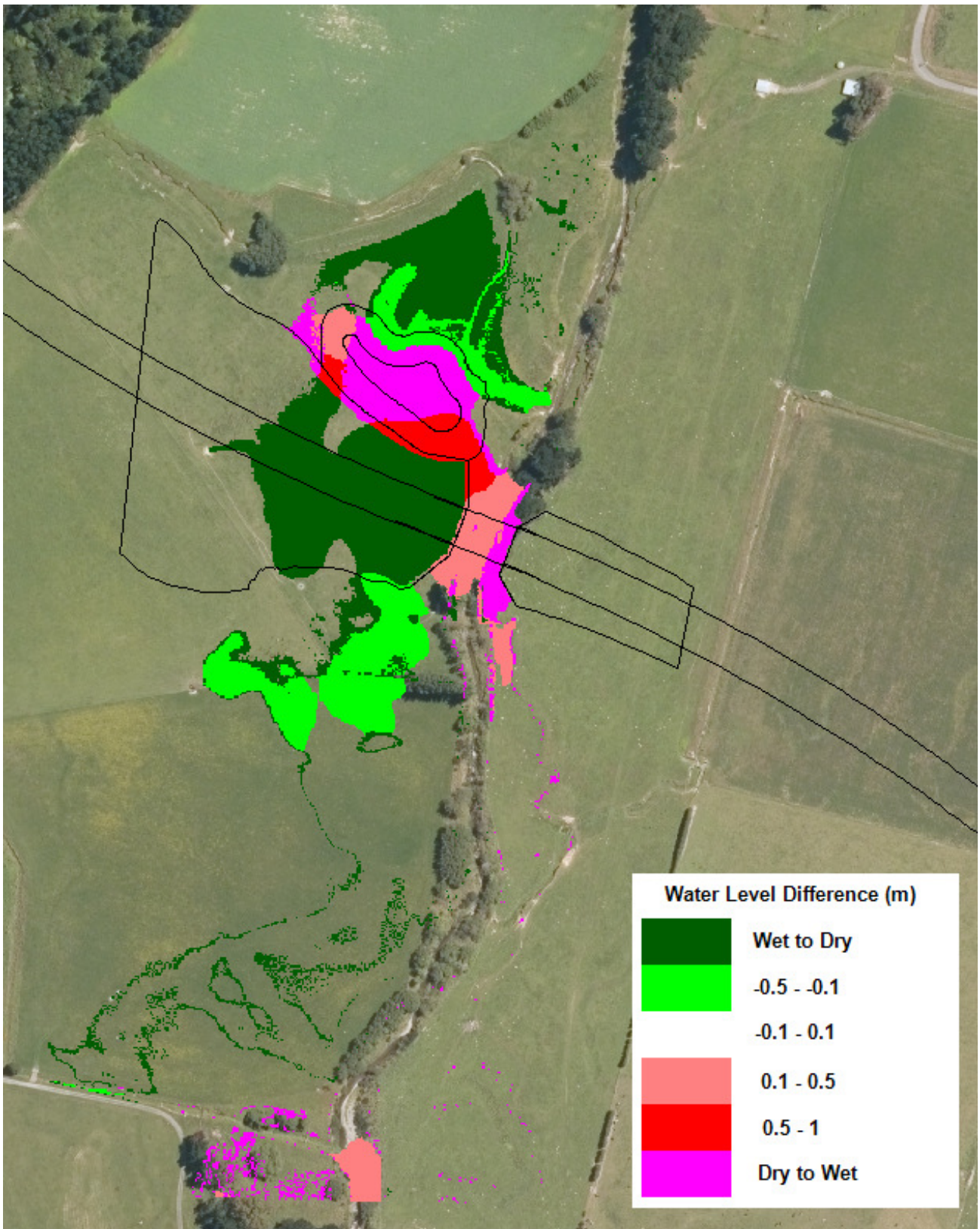


Figure 7-2: 10-year ARI 2120 climate, water level difference

The increases in water level are mainly on the true right bank upstream of the embankment of the proposed bridge. However, most of this change in water level is around the immediate vicinity of the bridge and proposed wetland which is approximately 1.5 m deep. The rest of the increase in water level are down the stream channel, where the introduction of the bridge causes water to be directed down the 30 m wide gap between the bridge abutments. The addition of the bridge greatly reduces the extent of the flooding in the floodplain. Water level changes between -0.1 m to

0.1 m have been made transparent as these changes are deemed to be insignificant. Overall, these changes in water level due to the proposed bridge are relatively small.

The water level results in the main channel at the bridge centreline for the three design scenarios are shown in Table 7-1.

Table 7-1: Peak water levels in stream channel at bridge centreline for existing scenario and bridge scenario

Design Event (ARI)	Existing Scenario Water Level (mRL)	Proposed Bridge Scenario Water Level (mRL)	Difference (m)
10	83.78	84.21	+0.43
100 (SLS)	83.85	84.38	+0.53
2500 (ULS)	83.97	84.69	+0.72

The clearance height required between the 10-year ARI water level and the bridge soffit level is 4.5m. This means that for the 10-year with bridge scenario the water level will need to be 88.71 mRL to meet minimum requirements. This is 0.8m higher than the current proposed bridge soffit level.

7.2 Predicted Flow Velocities

The predicted peak flow velocities after the construction of the road and bridge are shown in Figure 7-3. These results can be compared to Figure 5-2 to see the impact the bridge will have on channel velocities.

The difference in channel velocity between the existing scenario and the bridge scenario is shown in Figure 7-4. The increases in velocity are mainly down the main stream channel and on the true right bank before the proposed bridge. These increases in velocity are mainly in the range of 0.1 – 0.5 m/s with a few areas that increase to a maximum of 1.4 m/s. The bridge results in reductions in flow velocities in the floodplain to the south of the bridge. Overall, the changes in velocity due to the proposed bridge are relatively small. Velocity changes between -0.1 m/s to 0.1 m/s have been made transparent as these changes are deemed to be insignificant.

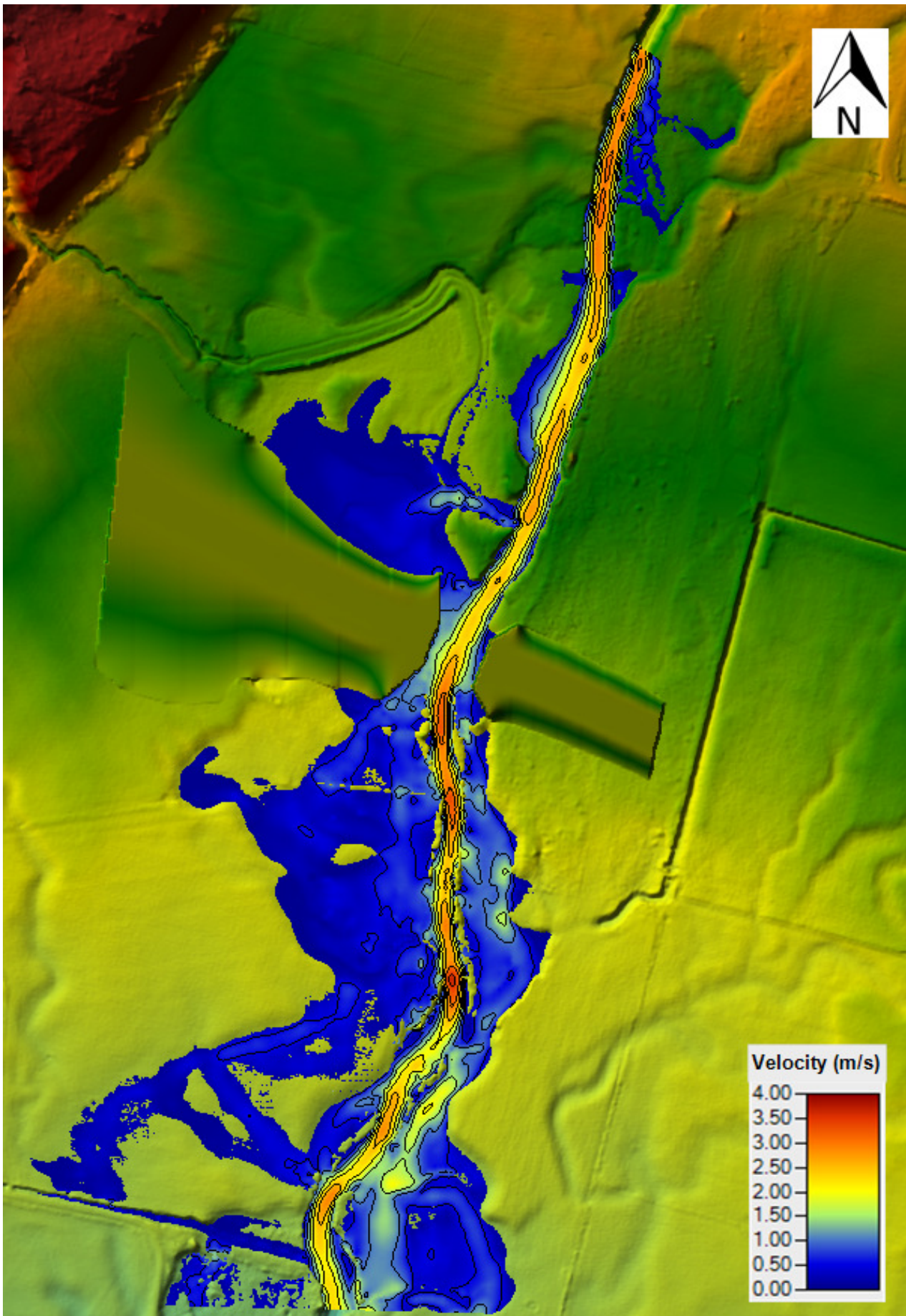


Figure 7-3: 10-year ARI 2120 climate, proposed bridge velocity results with 0.5 m/s contours

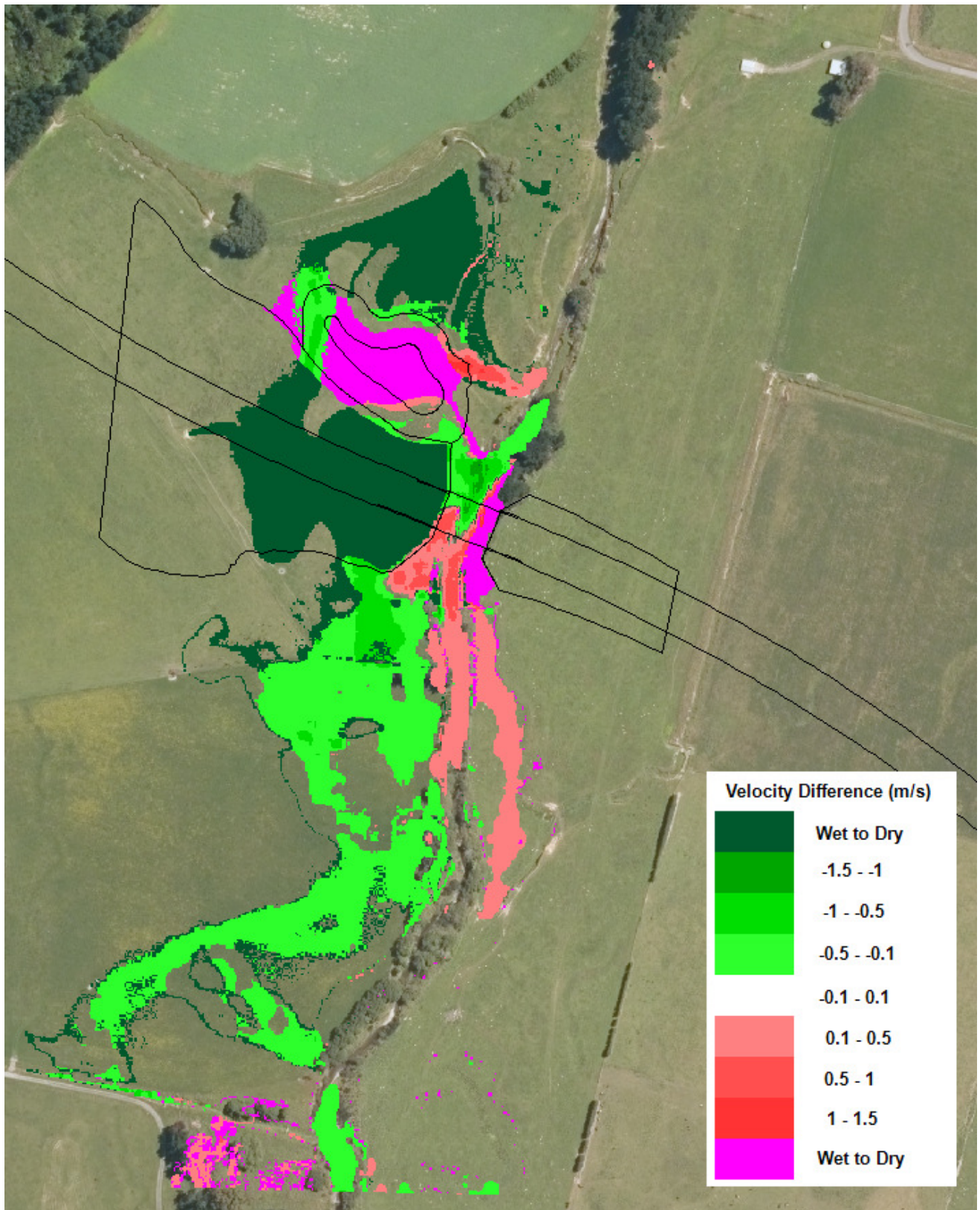


Figure 7-4: 10-year ARI 2120 climate, velocity difference

The velocity results in the main channel at the bridge centreline for the three design scenarios are shown in Table 7-2. The velocity decreases compared to the existing scenario at the centreline of the bridge, this can be seen in Figure 7-4Figure 9-4.

Table 7-2: Peak velocities in stream channel at the bridge centreline for existing scenario and with bridge scenario

Design Event (ARI) with 2120 climate	Existing Scenario Velocity (m/s)	Proposed Bridge Scenario Velocity (m/s)	Difference
10	2.98	2.42	-0.56
100 (SLS)	3.39	2.70	-0.69
2500 (ULS)	3.69	3.07	-0.62

8 Summary

To assist in the design of the proposed bridge for the Te Ahu a Turanga Highway across the Mangamanaia Stream a hydraulic analysis was undertaken. The outputs of this work are valuable for determining the structural design of the bridge and the suitability of proposed location.

The proposed bridge has the following design standards:

- The SLS event is the 100-year ARI;
- The ULS event is the 2500-year ARI; and
- The abutments shall be located a minimum of 5m outside the limits of the 10-year ARI flood limits.
- The clearance height required between the 10-year water level and the bridge soffit is 4.5 m.

With the updated hydrology (higher design flows) the proposed bridge no longer meets the minimum requirements for the abutments being located a minimum of 5m outside the limits of the 10-year ARI flood limits. However, with the higher flows used in this analysis the results are deemed to be more realistic. For the 10-year ARI flow the proposed bridge will result in the velocity at the bridge centreline reducing by about 0.56 m/s. The water level at the bridge centreline will increase by about 0.43 m with the proposed bridge. Overall, the effects of constructing the proposed bridge over the Mangamanaia Stream are likely to be positive.

9 References

Chow, V. T. (1959). *Open-Channel Hydraulics*.

Mason, D. M. (1998). *Roughness Characteristics of New Zealand Rivers*. NIWA.

NZ Transport Agency. (2019). *Te Ahu a Turanga: Manawatu Tararua Highway - Implementation*. In *Minimum Requirements Appendix A3 River and Bridge Hydraulics, February 2019*.

US Army Corps of Engineers. (2016). *HEC-RAS River Analysis System 2D Modeling User's Manual*. Version 5.0.

WSP. (2019). *Te Ahu a Turanga Technical Assessment: Hydrology and Hydraulics*.

McConchie, J.A. 2019: *Hydrological & Hydraulic Assessment* contained in Volume V Technical Assessment F of the Assessment of Environmental Effects submitted in support of an application for resource consents to construct and operation the Te Ahu a Turanga Manawatu Tararua Highway on behalf of the New Zealand Transport Agency.

Appendix A – Roughness Estimation

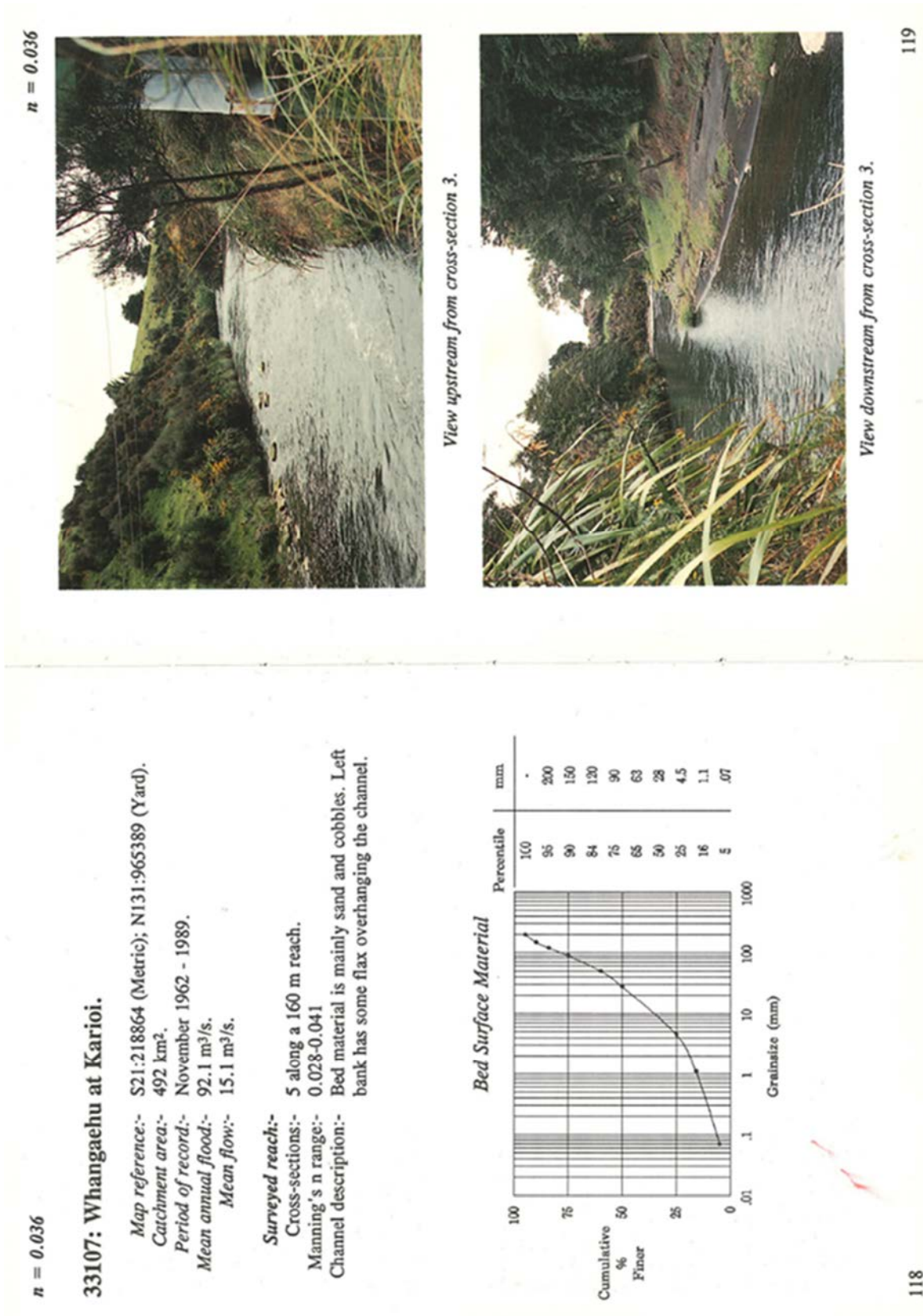


Figure 9-1: Manning's roughness estimation (Mason, 1998)

Appendix B – Result Maps (10-year and 2500-year ARI)

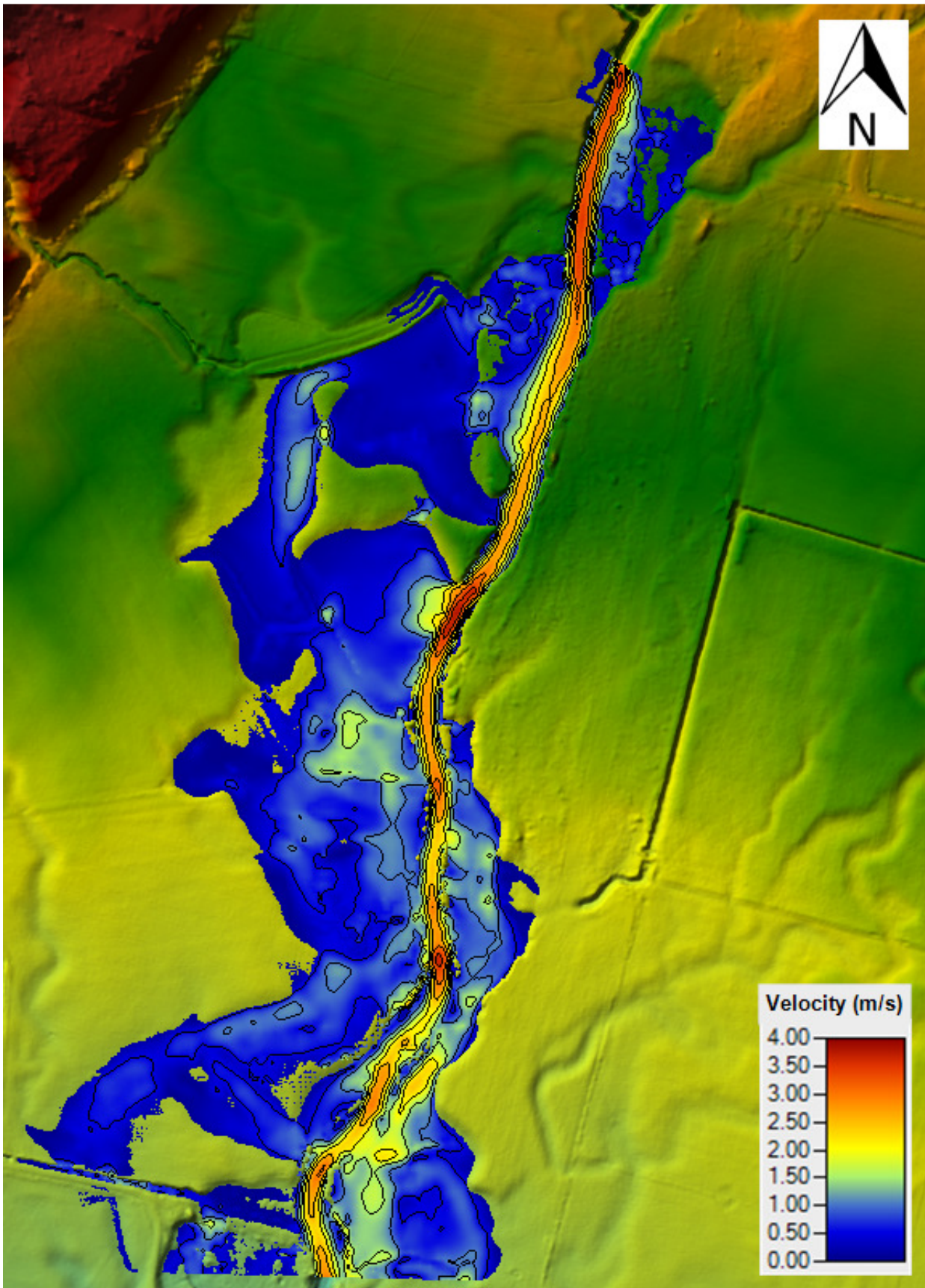


Figure 9-2: 100-year ARI 2120 climate, velocity results for existing scenario with 0.5 m/s contours.

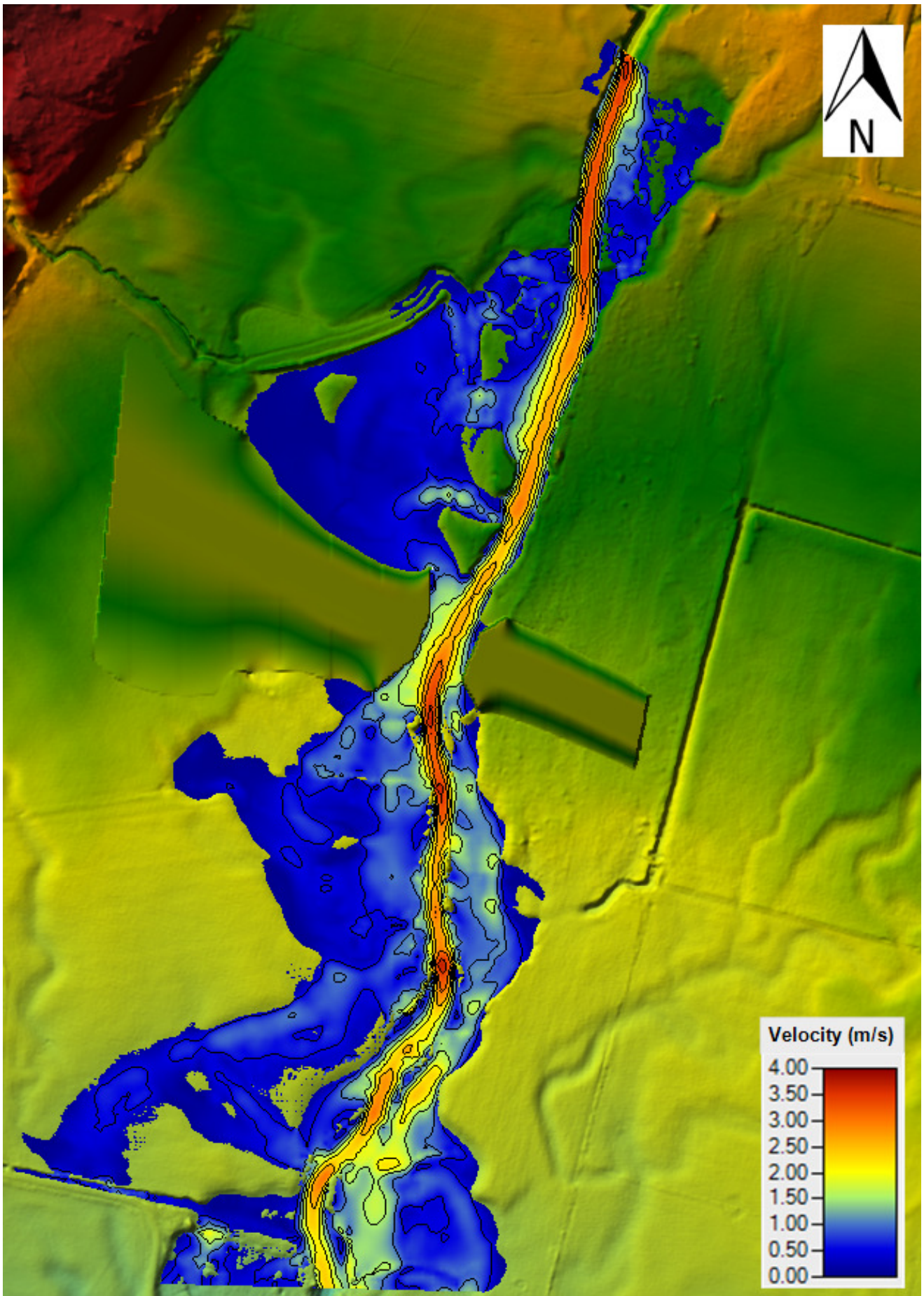


Figure 9-3: 100-year ARI 2120 climate, velocity results for bridge scenario with 0.5 m/s contours

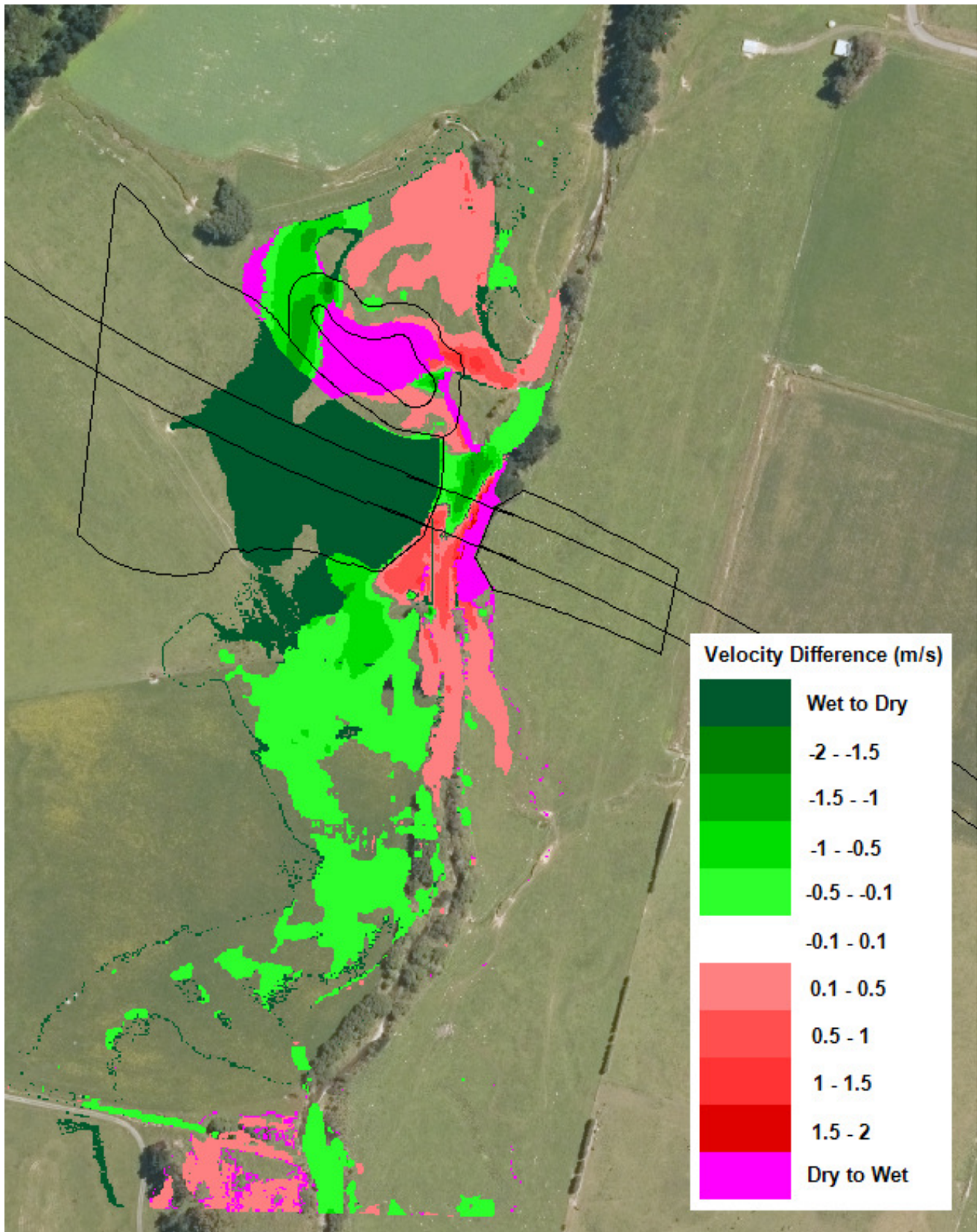


Figure 9-4: 100-year ARI 2120 climate, velocity difference

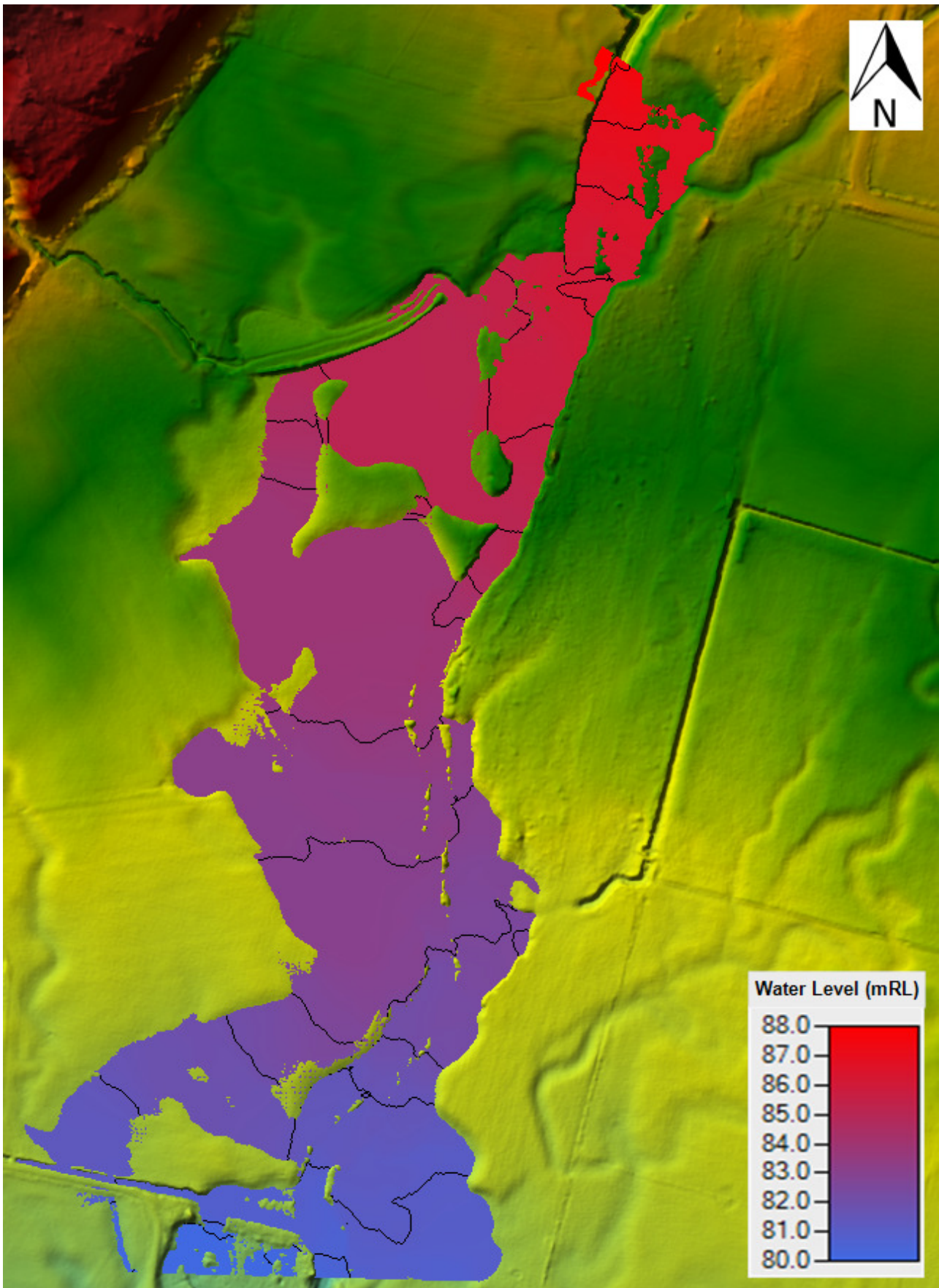


Figure 9-5: 100-year ARI 2120 climate, water surface elevation results for existing scenario with 0.5 m contours

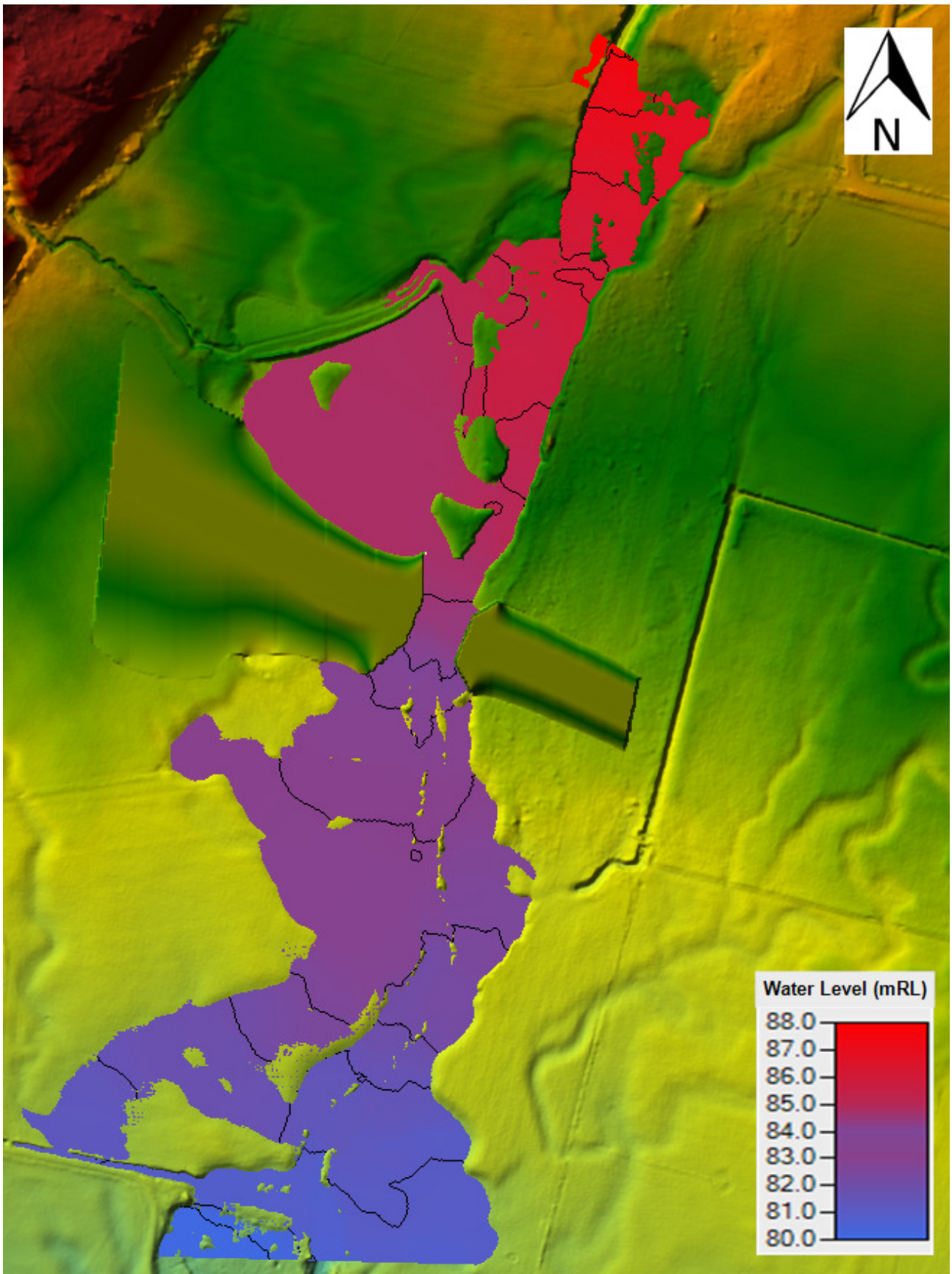


Figure 9-6: 100-year ARI 2120 climate, water surface elevation results for bridge scenario with 0.5 m contours

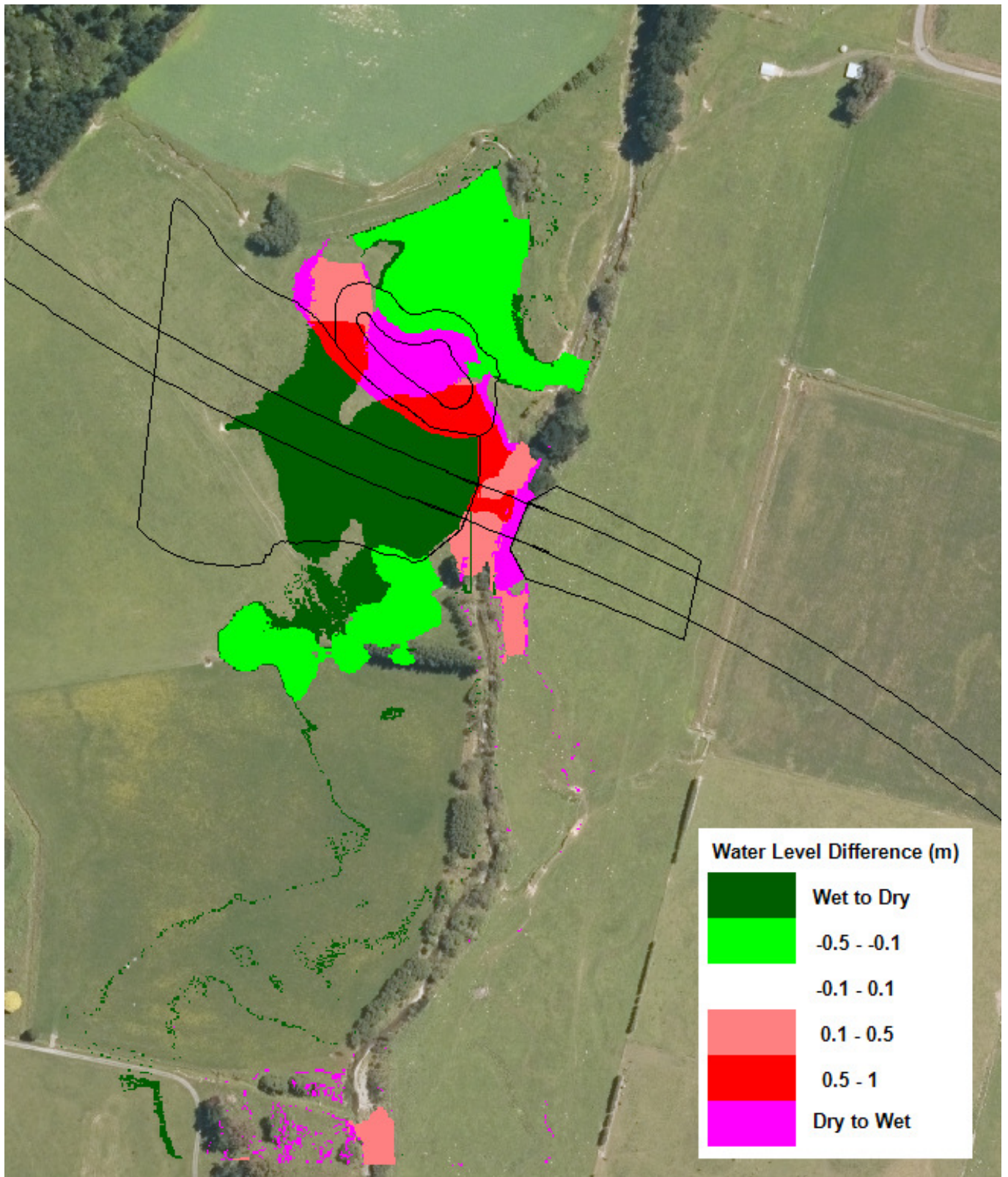


Figure 9-7: 100-year ARI 2120 climate, water level difference

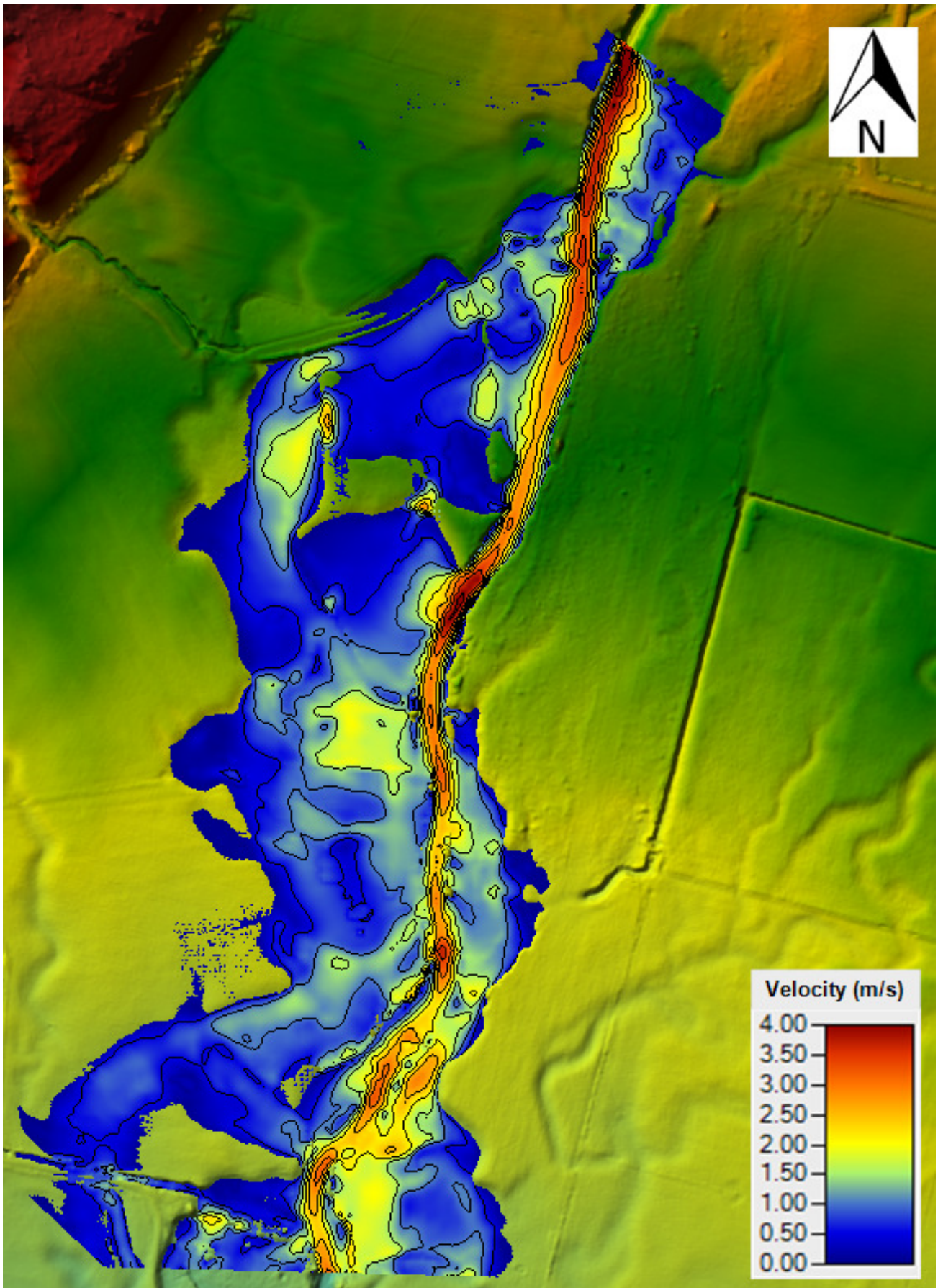


Figure 9-8: 2500-year ARI 2120 climate, existing scenario velocity results with 0.5 m/s contours

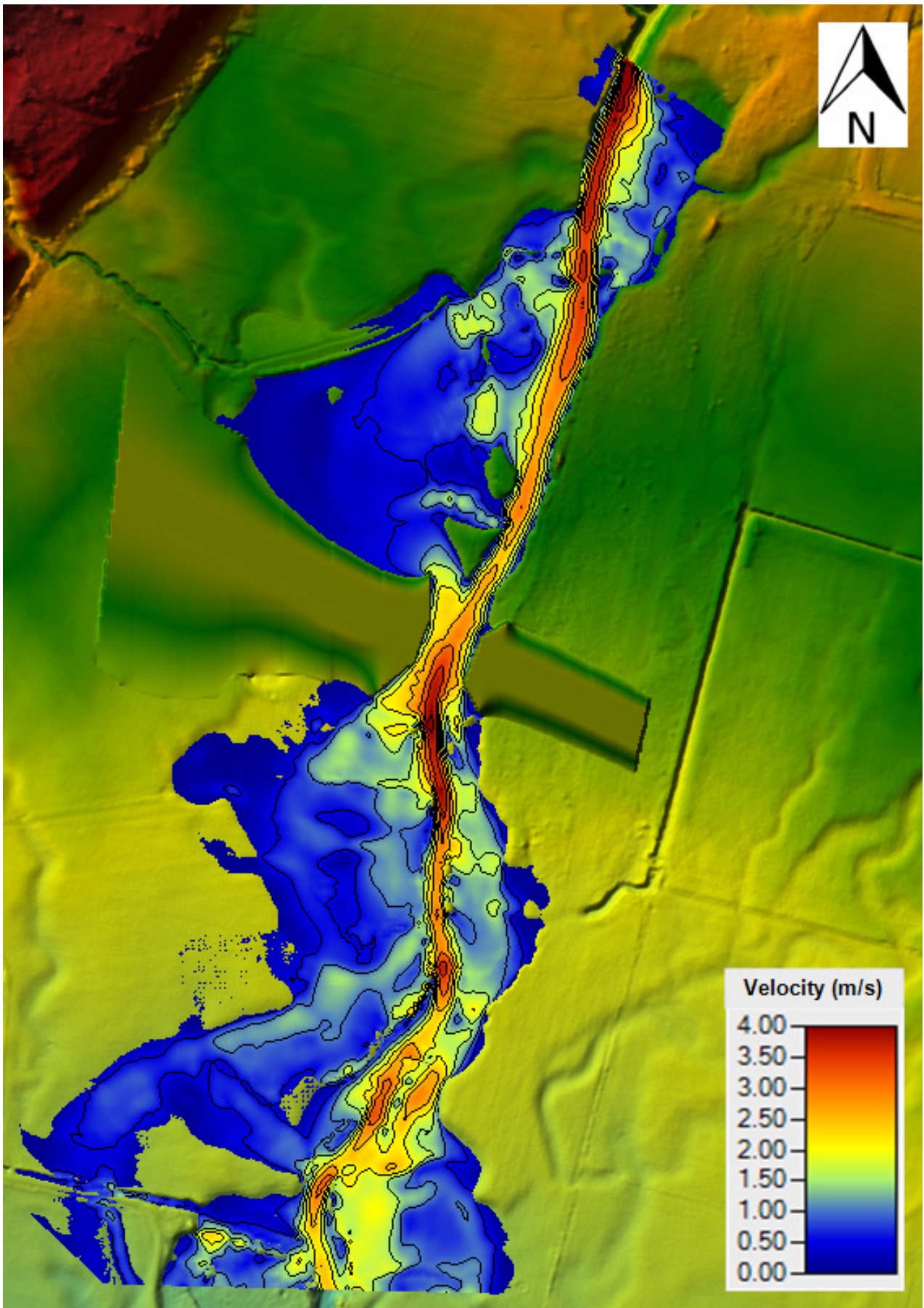


Figure 9-9: 2500-year ARI 2120 climate, proposed bridge scenario velocity results with 0.5 m/s contours

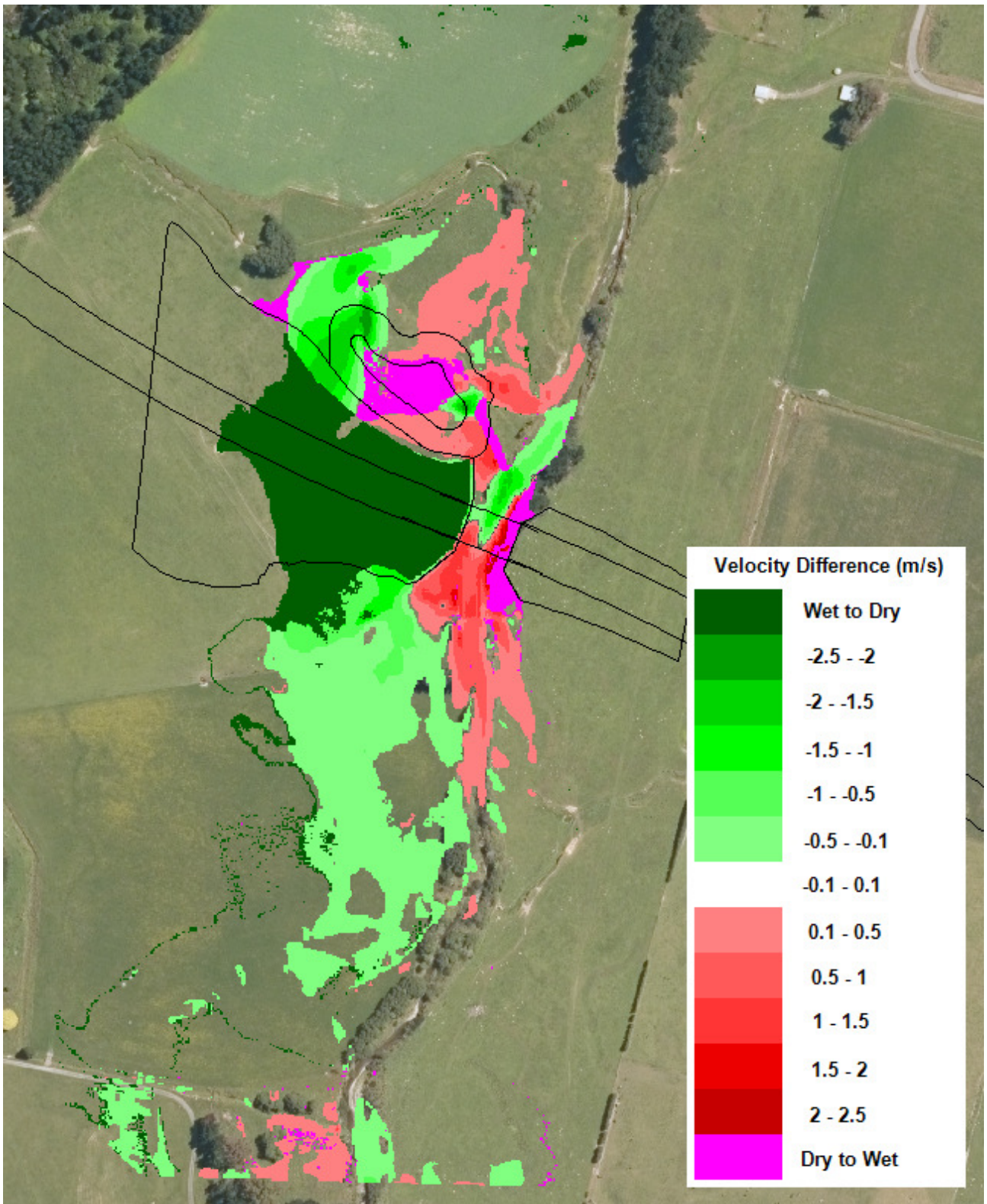


Figure 9-10: 2500-year 2120 climate, velocity difference

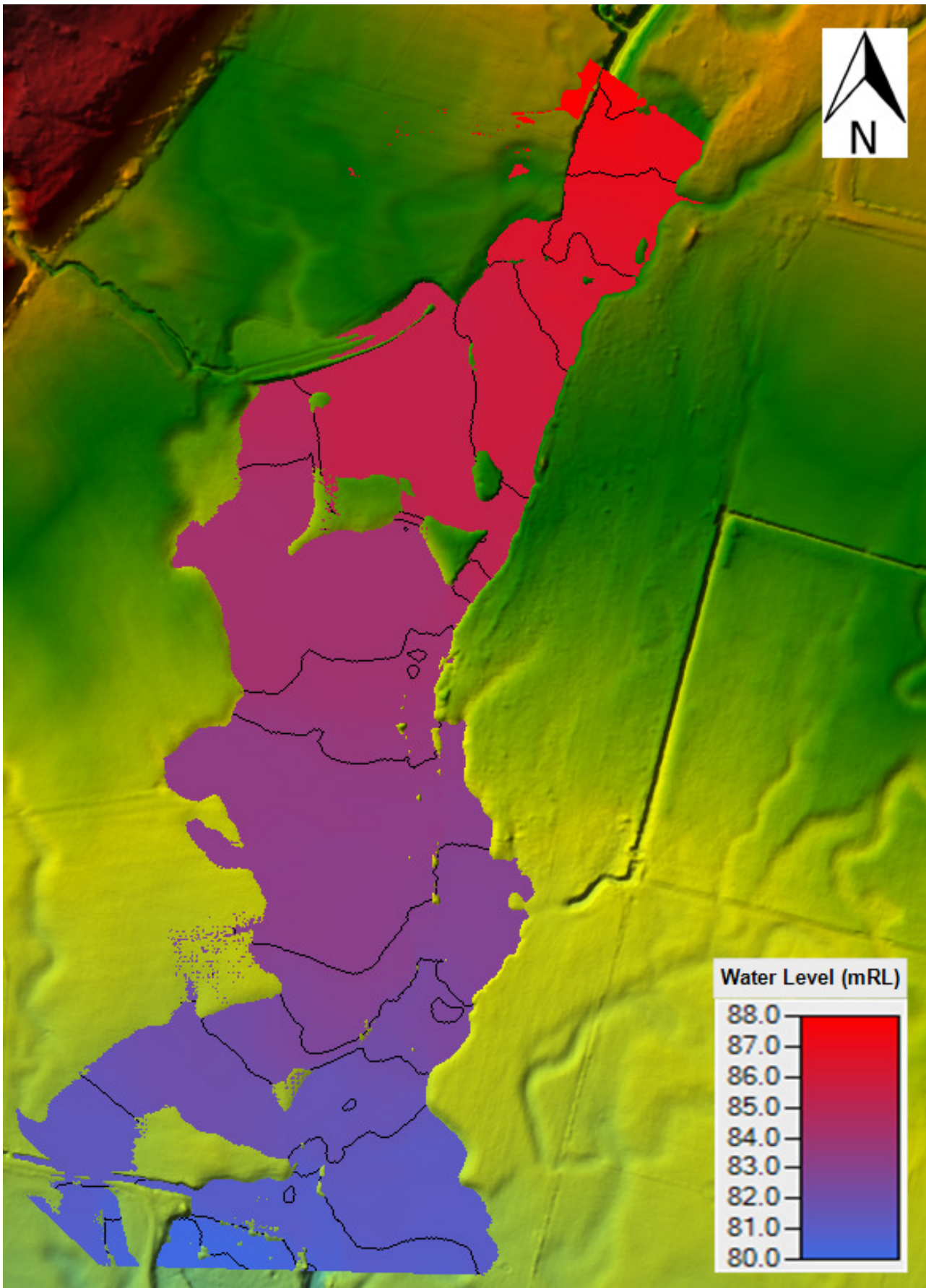


Figure 9-11: 2500-year ARI 2120 climate, existing scenario water level results with 0.5 m contours

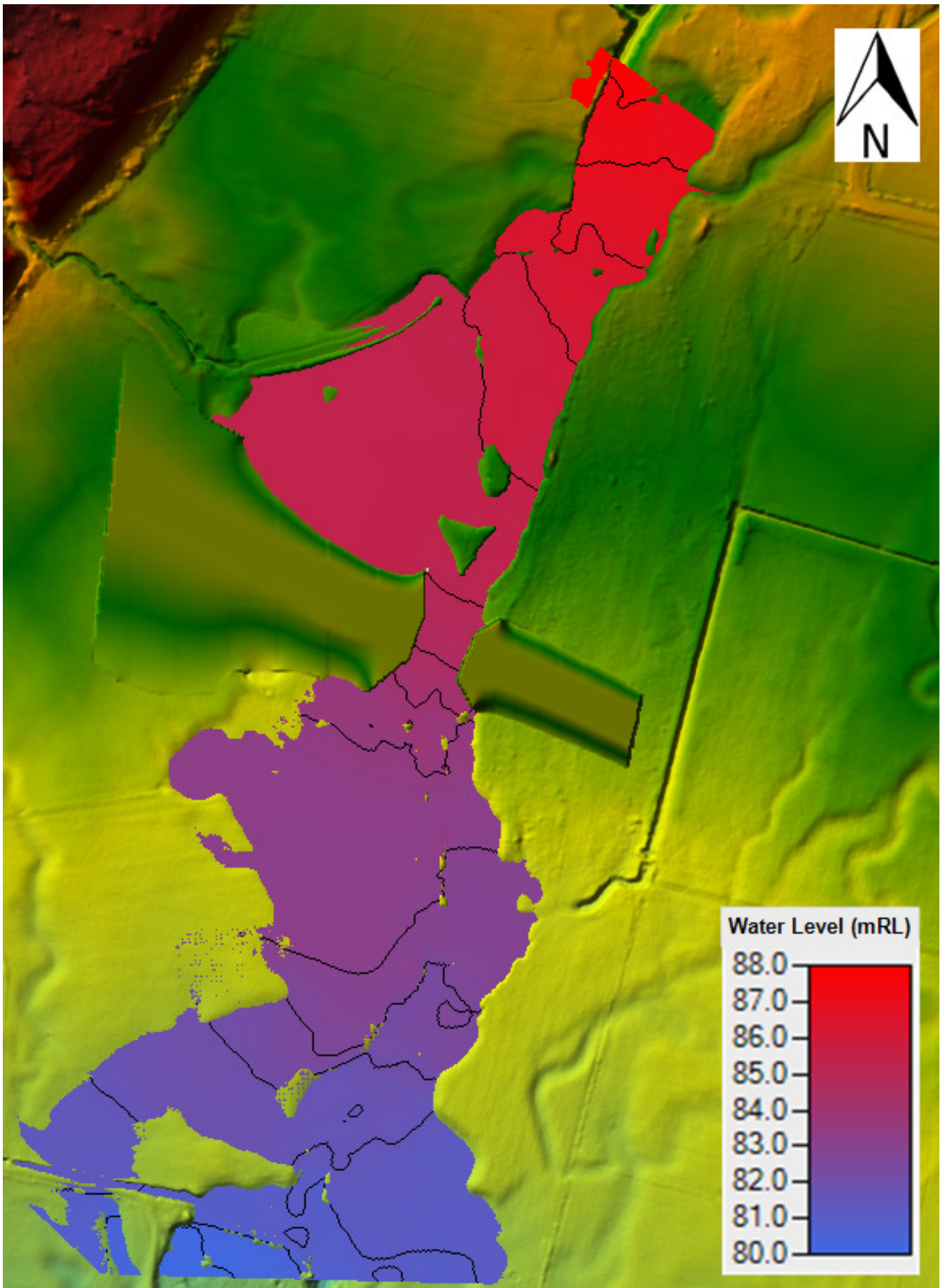


Figure 9-12: 2500-year ARI 2120 climate, proposed bridge scenario water level results with 0.5 m contours

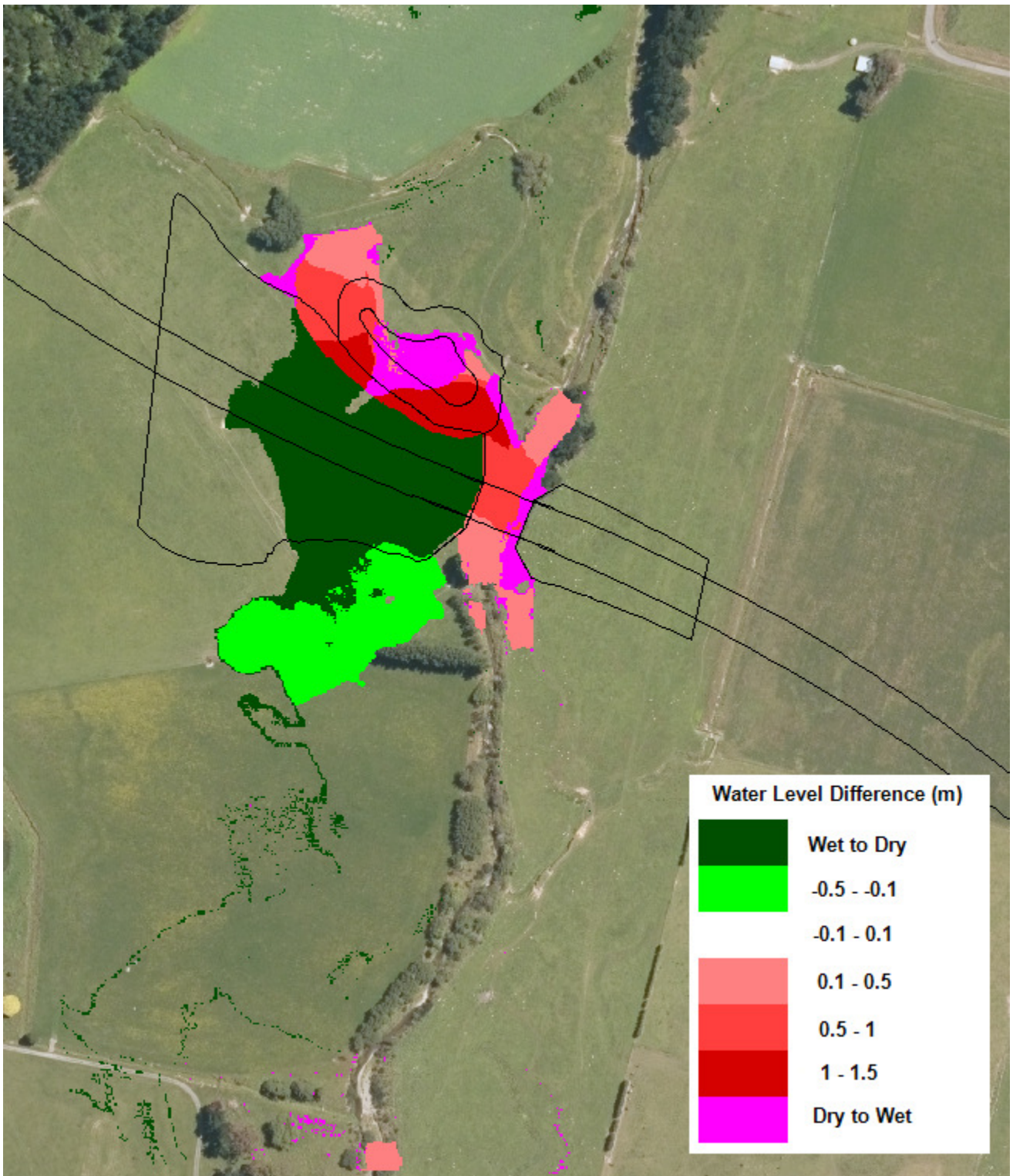


Figure 9-13: 2500-year ARI 2120 climate, water level difference

wsp

wsp.com/nz

Appendix D.5: *Te Ahu a Turanga - Manawatū Tararua Highway: Flood risk analysis
– Eastern Roundabout.*

Te Ahu a Tūranga: Manawatū Tararua Highway Project

Memorandum

To Dr. Jack McConchie

Copy Josh Irvine, David Hughes

From Louise Algeo, Kirsty Duff

Date 29 November 2019

Subject Te Ahu a Turanga: Flood risk analysis – Eastern Roundabout



1 Introduction

The proposed changes to the road alignment of SH3 for Te Ahu a Turanga includes construction of a roundabout to the west of Woodville that will join the existing road network to the new road. This is known as the Eastern Roundabout.

This section of the road is planned to be at a greater elevation than the existing ground level and therefore there is the potential that it will disrupt overland flow paths on this flatter terrain. Disrupting overland flow paths has the potential to increase the flooding risk and therefore an assessment is required to ascertain the extent and magnitude of the impact.

Overland flow is generated when rainfall depths exceed the storage capacity within the catchment and the surface runoff that occurs begins to make its way to natural streams, manmade channels, and pipe networks; or when streams and channels cannot completely contain the flow and overbank flooding occurs.

Overland flow as a result of excess rainfall conveyed across the floodplain and as a result of spilling from open channels and drains has been considered for this study. A 2-dimensional (2-D) hydraulic model was constructed in Tuflow™ using the information available for the catchment to represent the existing situation including land use, ground elevations, catchment extent, and temporally varying rainfall.

The catchment is shown in Figure 1.

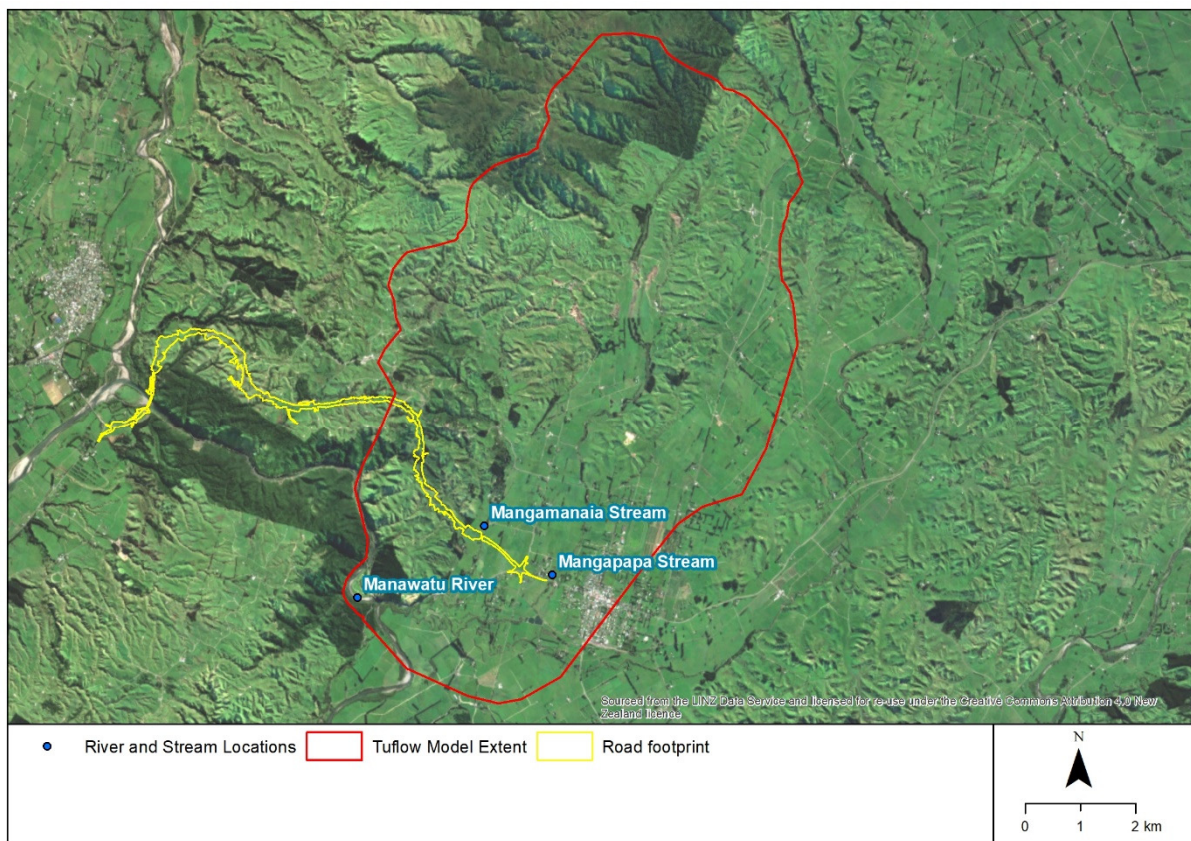


Figure 1: Location map.

2 Flooding analysis

2.1 Methodology

The following methodology was undertaken to determine the impact of the proposed changes to the road network on the existing flood hazard near Woodville. This scope of work was developed to investigate the difference in water level predicted between the existing situation and the future changes to the road alignment, elevation and culvert installation. It included the following tasks:

1. Review of available data and confirmation of inputs including spatially and temporally varying rainfall, catchment extents, land use and roughness, terrain (before and after road construction).
2. Development of a 2-dimensional (2-d) Tuflow model of the existing situation of the catchment and road drainage using a 'Rain on Grid' approach to define overland flow routes that may be affected or disrupted by the proposed road.
3. Modification of the Tuflow model to represent the proposed road alignment and elevations, the relevant cross drainage connections included in the design, and changes to the land use as a result of the construction of the road.
4. Application the 1% AEP rainfall event (with allowances for climate change to 2120) to the two versions of the model and simulation of the routing of the flow.
5. Extraction and analysis of results, and comparison of water levels within the vicinity of the proposed road.
6. Undertake a sensitivity analysis on different culvert designs.

2.2 Available data

To assess the flooding impact, a 2-dimensional (2-D) hydraulic model was developed in Tuflow using available data. Two versions of this model have been developed: one to represent the existing catchment; and one to represent the proposed post-construction catchment. A review of the suitability of the data available to develop this model is shown in Table 1.

A catchment area was defined using the existing Digital Elevation Model (DEM). Changes to the road alignment and levels do not impact the extent of the catchment.

A 10m gridded representation of the terrain within the entire catchment under the existing and proposed scenarios has been developed using the ground elevations in the two variations of DEM.

A hydraulic roughness has been applied to all parts of the catchment based on an estimate of the resistance to flow for the representative land use for that area. This varies spatially across the catchment and is represented as a Manning's n value. The land use and corresponding Manning's n value is shown in the Appendix.

The existing version of the model included four existing road drainage culverts. One (EXCU09) could not be included as it was installed following changes to the road which are not present in the DEM.

The Tuflow model was adapted to represent the catchment following the proposed construction of the new road which included amendments to land use, ground elevation and inclusion of proposed culverts to convey overland flow where they have been proposed. No changes to the rainfall were made between the existing and proposed version of the model.

Table 1: Data availability and suitability review

Dataset	Origin and details	Pre-processing	Suitability
Digital Elevation Model (DEM) for existing catchment combined from 2 sources.	Horizons Regional Council (HRC). Datum: Wellington 1953 Projection: New Zealand Transverse Mercator 2000 (NZTM2000).	An elevation conversion of 0.1855m was applied to the HRC DEM to change the elevation from Wellington 1953 datum to Moturiki 1953.	Provides ground elevations for the model grid. Extent of model derived from this dataset. Outputs can be converted to other projections as required.
	New Zealand Transport Agency (NZTA). Datum: Moturiki 1953 Projection: New Zealand Transverse Mercator Whanganui 2000 (NZTM Whanganui 2000).	The spatial projection was adjusted to NZTM 2000 for use in the model.	The final DEM was a good approximation of the existing catchment area and the overall model extent. The LiDAR was flown in 2018 and does not include the current road layout at this junction.
Digital Elevation Model (DEM) for catchment in proposed scenario	DEM for existing catchment developed by Te Ahu a Turanga Alliance (2019) Datum: Wellington 1953 Projection: New Zealand Transverse Mercator 2000 (NZTM2000).	Combined with the proposed road elevations.	Provides updated ground elevations for the model grid. No changes to the extent. Both existing and proposed datasets will be in this datum and projection and therefore are directly comparable with each other.
	Proposed road elevations developed by Te Ahu a Turanga Alliance (2019)	The spatial projection was adjusted to NZTM 2000 for use in the model. Projection of this dataset was converted to NZTM2000 and merged with the HRC elevation data to create a proposed future elevation for the catchment.	In the DEM processing the edges to the road were feathered slightly to smooth the spatial warping that occurs when re-projecting raster data. Outputs can be converted to other projections as required. The final DEM was a good approximation of the catchment area and proposed road elevations and the overall model extent.
Spatially and temporally varying rainfall depths	Developed by Te Ahu a Turanga Alliance (2019)	Developed using HIRDS v4 (NIWA, 2018). 6-hour duration assumed to be critical duration. Areal reduction factor (ARF) of 95% using (NIWA, 2018). 40% losses for infiltration.	Suitable for comparison purposes. No validation data available to confirm the rainfall induced flows. ARF based on an upstream catchment area of 32km ² . Losses reasonable for an impervious catchment with a large area of flatter terrain.
Hydraulic roughness	Derived from land use Landcare's land cover database version 4.1 (LCDBv4)	Land use has been used to determine a hydraulic roughness value for each part of the catchment based on the resistance to flow that the land use presents.	The combined dataset included a representation of the resistance to flow based on roughness.
	Aerial photography (LINZ)	Roads were digitised using this information and assigned a roughness value.	
Cross drainage culverts	Developed by Te Ahu a Turanga Alliance (2019) Invert levels Moturiki 1953 datum.	Culverts were only included in the model in the proposed scenario.	The number and size of culverts maybe subject to change as the road design progresses, this will affect the validity of these modelled results.

2.3 Boundary conditions

Derived rainfall for the 1% AEP event (with an allowance for climate change to 2120) has been applied to a gridded representation of the terrain within the entire catchment, with the resulting overland flow routed through the catchment overland. An aerial reduction factor of 95% was factored into the derivation of the rainfall to account for the size of the catchment modelled (approximately 32km²); and a reduction of 40% was applied to the derived rainfall to account for the losses due to infiltration across the catchment. A temporally varying profile was developed for the 6-hour duration.

No downstream water level boundary has been applied and therefore flow can leave the study area overland without restrictions other than surface resistance, physical features in the terrain and cross drainage network, and any downstream water levels as a result of the flow from the catchment. The water levels in the Manawatu River was not considered in this study.

2.4 Results

The results provided overland flow direction for the upstream catchment, highlighting those that have the potential to be impacted by construction of the roundabout within the study area. The predicted water levels for the existing and proposed scenarios are shown in Figure 2 and Figure 3 respectively.

To account for the inherent uncertainty in the hydraulic modelling process, which was not been to include model calibration, the results do not show water depths less than 100mm. Flooding below this level is deemed to be minor and would pose no risk to life or property. These outputs show the spill locations for the open channels and the resulting overland flow directions.

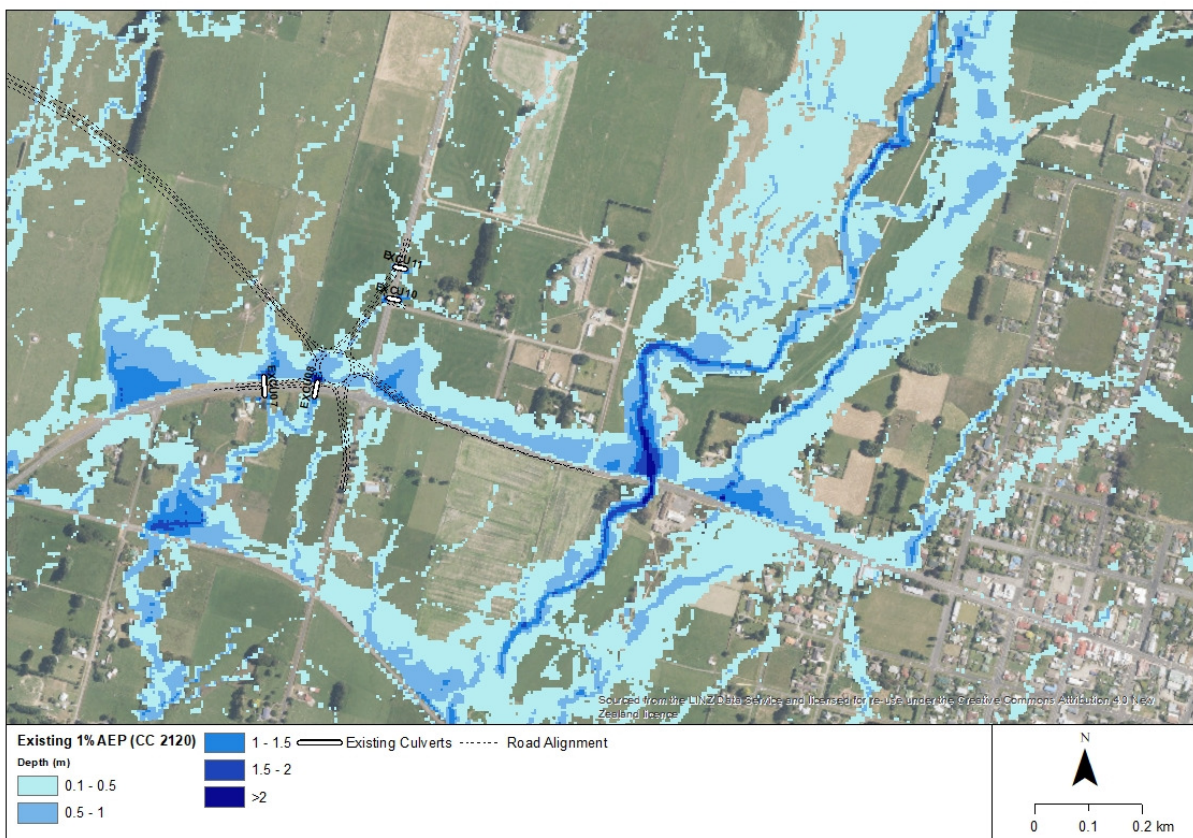


Figure 2: Predicted depth of water resulting from a 1% AEP rainfall event (with allowances for climate change to 2120) with the existing road layout and terrain. Proposed road layout also shown for reference.

Flow arrives at the proposed roundabout location conveyed by small overland flow routes; and from spill locations on the Mangapapa Stream immediately to the north of the SH3 Bridge crossing. All flow is restricted and maintained on the north side of the existing SH3 road and is shown to flow from east to west. It should be noted that there may be unknown cross drainage located along this section of road that is not included in the model. Four culverts have been included (Figure 2); however, culvert EXCU09 was omitted as the DEM does not include subsurface features. The model may therefore over-predict flood depths upstream and under-predict flood depths downstream of the existing SH3 road if hydraulic connectivity is not included in the model.

In the proposed scenario (Figure 3), the roundabout is predicted to prevent the conveyance of water along the preferential flow path from east to west along the north of the SH3. This flow is predicted to be conveyed through culverts with water diverted via Culverts 20 and 18 to join the flow path to the west of the roundabout; however, these water depths are predicted to be at a lower level in the 1% AEP event as water backs up behind the roundabout. Additionally, Culvert 19 conveys additional flow towards the south which eventually meets the Mangapapa Stream approximately 600m to the south.

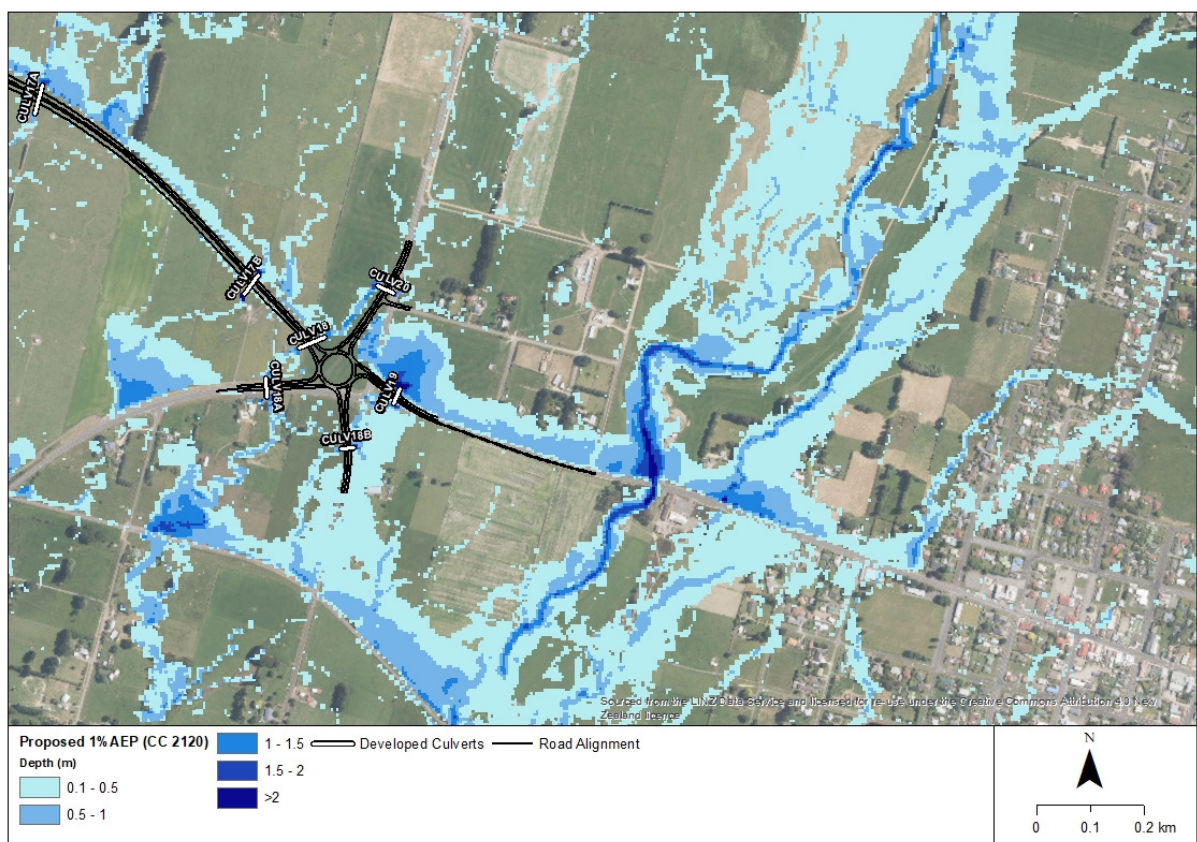


Figure 3: Predicted depth of water resulting from a 1% AEP rainfall event (with allowances for climate change to 2120) with the proposed road layout and terrain.

Upstream of Culvert 19, the water depth is the greatest. Figure 4 shows a point upstream of this culvert and the predicted temporally varying water depth output from the model. It shows that the water level is greater than 0.5m for approximately 3.5 hours in a 1% AEP (with climate change allowances to 2120) 6-hour duration rainfall event.

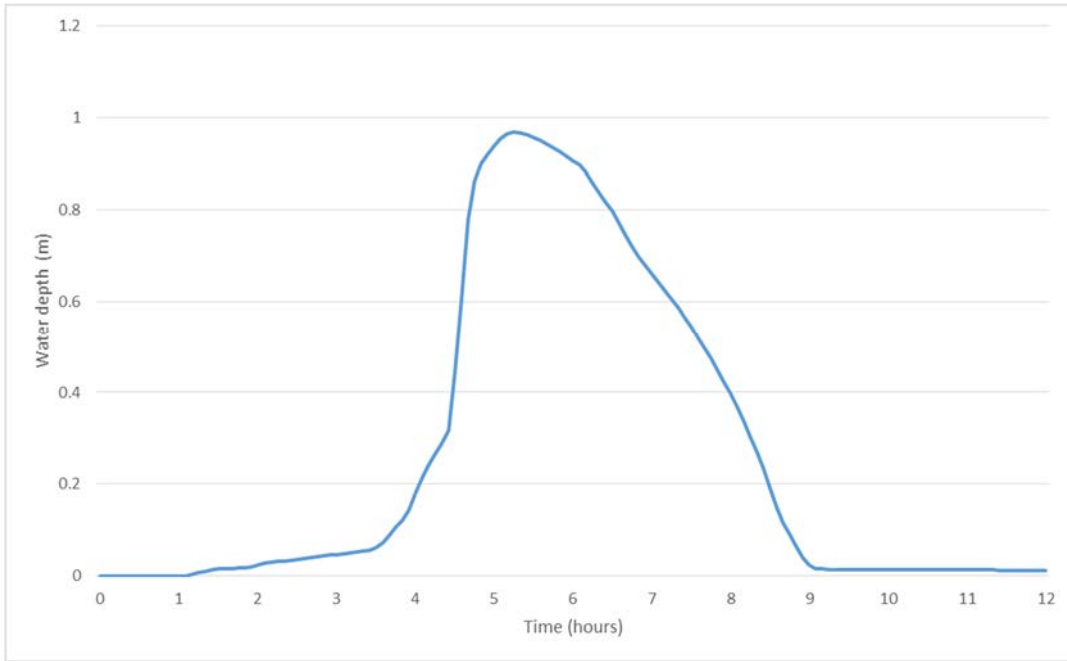


Figure 4: Predicted temporally varying water depth upstream of the roundabout, north of Culvert 19.

2.5 Sensitivity testing

The assessment has also investigated the sensitivity to design changes on the flooding depth in the catchment. Culverts 18 and 18A in the proposed scenario were changed from box culverts to circular culverts to analyse if there were any effects. Figure 5 shows that the differences are negligible and between $\pm 100\text{mm}$.



Figure 5: Differences between installing box culverts and circular culverts for Culverts 18 and 18A.

3 Conclusions

Water levels resulting from a 1% AEP rainfall event (including an allowance for climate change to 2120) have been reviewed both in the existing situation and the proposed scenario. Changes in water level provide information about the impact of the proposed road on the flow paths and indicate areas where greater conveyance may be required.

The modelling analysis shows that there is little impact on water levels predicted as a result of this design rainfall event falling on the catchment upstream of the proposed roundabout and road that connects the new SH3 to the existing road network near Woodville.

No validation of these results have been undertaken and therefore while due care has been taken to develop this model and its outputs, the results should not be taken as absolute and used for comparison purposes only. There is no impact of backwater effects from the Manawatu considered as this assessment was to ascertain the impact on the overland flow from the upstream catchment in isolation. The outputs are not suitable for use in detailed design stages in their current format.

Figure 6 shows the differences in water level for those areas predicted to be inundated. The outline of the area where ground elevation changes have been made and aerial photography to show the location of Woodville are also shown. The results show that the proposed roundabout has negligible impact on the town of Woodville with increases in water level greater than 100mm only shown immediately upstream of the proposed roundabout and to the south. Differences in water level less than ± 100 mm are assumed to be minor.

While flooding is predicted in Woodville in the existing and proposed scenario (Figure 2 & Figure 3 respectively), the change of water level and therefore impact is localised to the proposed changes to the road.

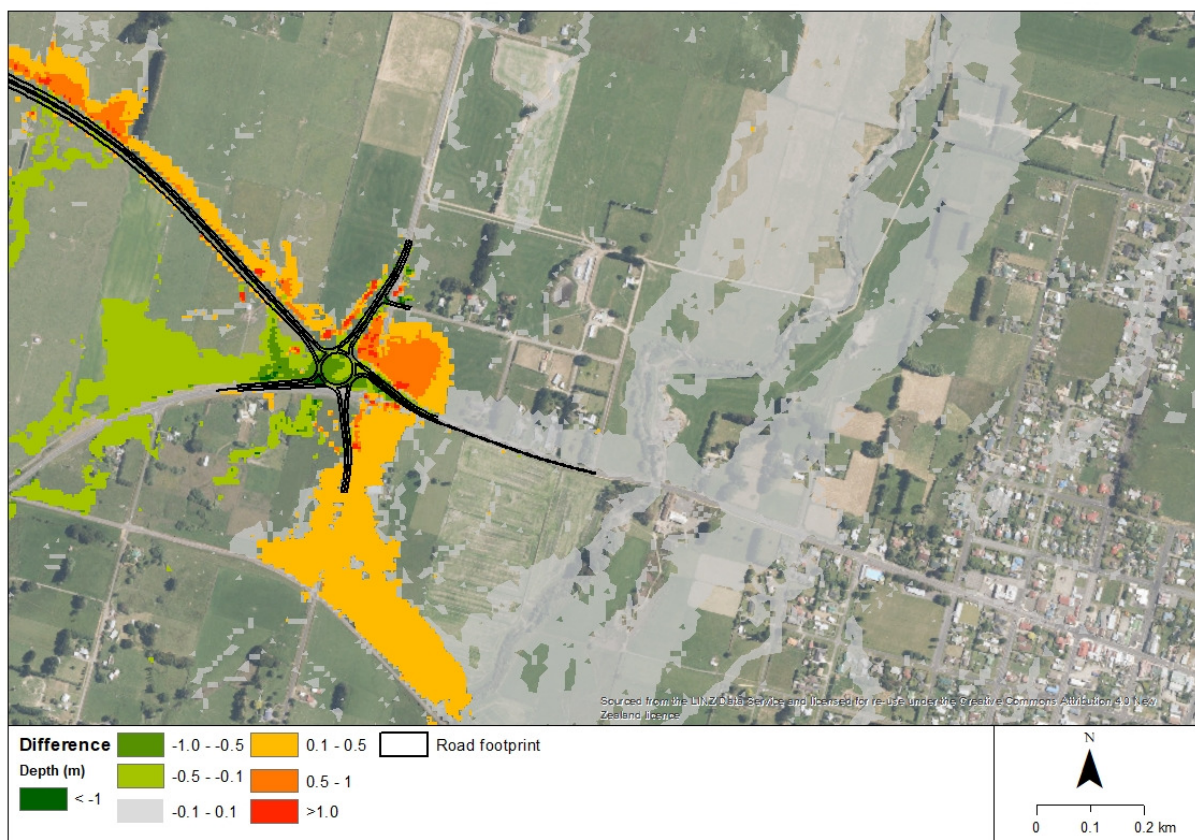


Figure 6: Differences in water depth (m) between the existing situation and proposed road scenario.

3.1 Assumptions and limitations

A number of assumptions have been made in order to simplify the complex natural processes that occur within the catchment and create this 2-D hydraulic model. The assumptions include:

- The critical duration (the duration of rainfall that results in the highest water levels at the roundabout) has been assumed to be 6-hours. The actual critical duration may vary from this; however, a 6-hour duration is considered realistic.
- A design rainfall profile has been derived based on historical rainfall analysis and may not be representative to rainfall actually experienced in the catchment in the future.
- The rainfall has been assumed to fall on every part of the catchment simultaneously. An areal reduction factor has been applied, assuming an upstream catchment area of approximately 32km². This catchment area includes some neighbouring catchments e.g. Mangapapa Stream, that contribute to flow during extreme events such as that modelled.
- The catchment upstream of the proposed roundabout is pervious and losses due to infiltration have been assumed to be 40% of the rainfall.
- The model has been developed assuming the water can freely runoff into the Manawatu River. The model does not account for any backwater effects. Any tailwater conditions are solely the result of rainfall in the catchment.
- No flow gauging or validation data is available. The study assumes a 1% AEP rainfall event generates a 1% flow in the streams which may not be accurate.

The result of these assumptions is that the model only allows for a comparison of the likely differences in water level during a 1% AEP rainfall event (with allowances for climate change). The model has produced flows, flood extents, depths and velocities that have not been verified against real world conditions.

Information for detailed design such as levels cannot therefore be confirmed using this approach. If this is required, this model should be adapted to include more detailed information to create a 2-D hydraulic model and validation should be undertaken to provide confidence in the results.

Appendix

Table 2: Land use and roughness

Land use	Manning's n
Grass floodplain	0.045
Native bush	0.06
Road and paved areas	0.022
Pine forest	0.075
Scrub	0.05
Bare ground	0.03
Crops	0.04
Urban	0.1